

**Tracking of bacterial metabolism with
azidated precursors and
click-chemistry**

Dissertation

zur Erlangung des Doktorgrades
der Naturwissenschaften

vorgelegt beim Fachbereich für Biowissenschaften (15)
der Johann Wolfgang Goethe Universität
in Frankfurt am Main

von Alexander J. Pérez
aus Nürnberg

Frankfurt am Main 2015

Dekanin: Prof. Dr. Meike Piepenbring

Gutachter: Prof. Dr. Helge B. Bode

Zweitgutachter: Prof. Dr. Joachim W. Engels

Datum der Disputation:

Danksagung

Ich danke meinen Eltern für die stete und vielseitige Unterstützung, deren Umfang ich sehr zu schätzen weiß.

Herrn Professor Dr. Helge B. Bode gilt mein besonderer Dank für die Übernahme als Doktorand und für die Gelegenheit meinen Horizont in diesen mich stets faszinierenden Themenbereich in dieser Tiefe erweitern zu lassen. Seine persönliche und fachliche Unterstützung bei der Projektwahl und der entsprechenden Umsetzung ist in dieser Form eine Seltenheit und ich bin mir dieser Tatsache voll bewusst.

Gerade die zusätzlich erworbenen Kenntnisse im Bereich der Biologie, sowie der Wert interdisziplinärer Zusammenarbeit ist mir durch zahlreiche freundliche und wertvolle Mitglieder der Arbeitsgruppe bewusst geworden und viele zündenden Ideen wären ohne sie womöglich nie aufgekommen. Einen besonderen Dank möchte ich in diesem Kontext Wolfram Lorenzen und Sebastian Fuchs, die gerade in der Anfangszeit eine große Hilfe waren, ausdrücken.

Dies gilt ebenso für die „N100-Crew“ und sämtliche Freunde, die in dieser Zeit zu mir standen und diesen Lebensabschnitt unvergesslich gemacht haben.

Table of contents

Danksagung	I
Table of contents	II
Table of abbreviations	IV
Summary	VI
Zusammenfassung	VIII
1 Introduction	1
1.1 Bacterial metabolism – The entry-door to understanding life	1
1.2 The membrane – More than just a barrier	2
1.2.1 Building a bacterial membrane	3
1.2.2 Fatty acid biosynthesis and degradation.....	5
1.2.3 Fatty acids as an exogenic energy source.....	9
1.3 Secondary metabolites – A world of infinite possibilities	11
1.3.1 From primary to secondary metabolism – The metabolism of phenylalanine.....	11
1.3.2 Non-ribosomal peptides.....	15
1.3.3 Fatty acids in secondary metabolism.....	18
1.3.4 Small molecules with a strong effect.....	21
1.4 Click-Chemistry – Azides as silent intruders	22
1.4.1 The evolution of cyclooctynes for bioorthogonal applications ...	23
1.5 Aims of this work	25
2 Manuscripts and publications.....	28
2.1 Publication: “ ω -Azido fatty acids as probes to detect fatty acid biosynthesis, degradation, and modification“	28
2.2 Publication: “Click Chemistry for the Simple Determination of Fatty Acid Uptake and Degradation: Revising the Role of Fatty Acid Transporters”	

2.3	Manuscript: “Solid phase enrichment and analysis of azide labeled secondary metabolites – fishing downstream of biochemical pathways”.	30
3	Additional results.....	32
4	Discussion.....	36
4.1	The true nature of the lipid bilayer – From static to dynamic	36
4.2	Click-Chemistry for metabolic analysis – Does it compete?	38
4.3	New discoveries through innovative searching tools	42
5	Concluding remarks	45
6	References.....	46
7	Attachments	56
7.1	Publication: “ ω -Azido fatty acids as probes to detect fatty acid biosynthesis, degradation, and modification“	56
7.2	Publication: “Click Chemistry for the Simple Determination of Fatty Acid Uptake and Degradation: Revising the Role of Fatty Acid Transporters” 102	
7.3	Manuscript: “Solid phase enrichment and analysis of azide labeled secondary metabolites – fishing downstream of biochemical pathways”	122
8	Curriculum vitae	174
9	List of Publications	175
10	Record of conferences.....	176
11	Versicherung.....	177

Table of abbreviations

ACP	acyl carrier protein
AFA	azido fatty acid
ATP	adenosine triphosphate
BCN	bicyclononyne
CARR	cleavable azide-reactive resin
CoA	Coenzyme A
DNA	desoxy-ribonucleic acid
DNS	Desoxyribonucleinsäure
FAD	flavin adenine dinucleotide
FAME	fatty acid methyl ester
FRET	Förster resonance energy transfer
HOMO	highest occupied molecular orbital
HPLC-MS	high performance liquid chromatography coupled to mass spectrometry
IM	inner membrane
LPS	lipopolysaccharide
LD ₅₀	Lethal dose at which 50% of tested cells perish
LUMO	lowest unoccupied molecular orbital
MRSA	multi-resistant <i>Staphylococcus aureus</i>
NADP	nicotinamide adenine dinucleotide phosphate
NRP	non-ribosomal peptide
NRPS	non-ribosomal peptide synthetase
OM	outer membrane
PKS	polyketide synthase
RNA	ribonucleic acid
RNS	Ribonucleinsäure

SILAC	stable isotope labeling with amino acids
SPAAC	strain-promoted azide-alkyne cycloaddition
tRNA	transfer ribonucleic acid
UPLC-MS	ultra performance liquid chromatography coupled to mass spectrometry
UV	ultraviolet

Summary

The metabolome of any live cell consists of several hundred, if not thousands of different molecules at any given moment, be it a relatively small bacterial cell or a whole multicellular organism. Although there are continuous attempts to differentiate between primary and secondary metabolites, the borders often blur in the eye of almost perfect interconvertability of all such matter. With chemistry and physics dominating this domain of biology it is an interdisciplinary endeavor to tackle the questions surrounding the workings of the metabolic pathways involved, searching for answers that ultimately help us to better understand life and find solutions to problems that affect us humans. One area of biochemistry that serves as a formidable example of the intertwined primary and secondary metabolic pathways are fatty acids, essential components of bacterial membranes, sources of energy and carbon but also important building blocks of several natural products. The second area to be mentioned is the metabolism of amino acids, the basic components of proteins and enzymes, which also serve as precursors to a diverse set of metabolites with many biological purposes.

This work focuses on these two areas of biochemistry, as several intermediates of their metabolism serve as building blocks for complex secondary metabolites whence many interesting and bioactive natural products are derived. The powerful and relatively novel tool of click-chemistry is employed to track azide-labeled precursors of primary and secondary metabolism in various bacterial strains to observe biochemistry at work and adds to the knowledge gained through other methods. The methods presented in this work serve the observation of fatty acid biosynthesis, degradation, modification and transport through direct ligation of azido fatty acids with cyclooctynes on one hand, leading to a revision of fatty acid transport in general. On the other hand a cleavable azide-reactive resin is devised to generally track the fate of azidated compounds through the myriads of metabolic pathways offered by entomopathogenic bacteria possessing a rich secondary metabolism. The resulting findings led to the identification of several antimicrobial peptides, amides and other compounds of which many

had remained so far undetected in the strains that underwent investigation, underlining the worth of this method for future metabolomic research and beyond.

Zusammenfassung

Eine jede lebendige Zelle produziert zu jedem Zeitpunkt hunderte, wenn nicht tausende von verschiedenen Stoffwechselprodukten, welche verschiedensten Aufgaben dienen. Viele dieser Stoffwechselprodukte dienen allseits bekannten Aufgaben wie der Energiegewinnung durch Glykolyse, dem Aufbau der Zellmembran oder der Informationsspeicherung in Form von DNS oder RNS, jedoch sind die Verwendungszwecke vieler der dabei auftretenden Intermediate bei weitem nicht auf diese Aufgaben beschränkt. So wird immer wieder versucht eine Trennung zwischen diesen primären und allen nicht dazu gerechneten, sekundären Stoffwechselwegen (Herstellung von Antibiotika, Botenstoffen, etc.) gemacht, dabei sind diese Stoffwechselwege eng miteinander verwoben und die Unterscheidung spielt aus Sicht des betroffenen Organismus keine Rolle. Die Klärung dieser Stoffwechselwege steht im Zentrum vieler biologischer Fragestellungen und die Tatsache, dass diese Welt der Moleküle von Physik und Chemie beherrscht wird macht deren Erforschung zu einem interdisziplinären Feld, das uns Antworten sowohl über das Leben im allgemeinen, als auch zu Fragen rund um die menschliche Gesundheit und andere praktische Anwendungen erbringt. Wie sich diese verschiedenen Gebiete gegenseitig ergänzen wird klar, wenn man berücksichtigt, dass die meisten Pharmazeutika, die seit frühester Zeit bis heute im Einsatz sind, letztlich auf Naturstoffen basieren. Bioaktive Naturstoffe werden von ihren jeweiligen Produzenten hergestellt, um sich konstruktiv oder destruktiv mit ihrer Umwelt auseinanderzusetzen, und so wie die Umwelt seit Anbeginn der Zeit einem steten Wandel unterliegt, so mussten dies auch die zum Einsatz gebrachten Naturstoffe tun. Das Verständnis der Biosynthese solcher Naturstoffe, sowie die breite Erfassung ihrer Diversität und natürlicher Anwendungsgebiete erlaubt somit einen Einblick in prinzipielle Methoden der Natur zur Erreichung diverser Ziele. Wann immer ein solches Ziel mit einem der von uns gesetzten übereinstimmt, etwa bei der Entwicklung neuer Antibiotika, so wird der Wert des Verständnisses der in diesem Gebiet sehr erfahrenen Natur offensichtlich.

Ein Bereich der Biochemie, der als hervorragendes Beispiel für die enge Verstrickung primärer und sekundärer Stoffwechselwege dient, ist der Fettsäuremetabolismus als essentieller Bestandteil der Membranbiosynthese und als Zugang zu einer ergiebigen Kohlenstoff- und Energiequelle im Herzen des zellulären Stoffwechsels. Ein weiterer Bereich, der hier Erwähnung finden soll, ist der Stoffwechsel der Aminosäuren, welche die Grundbausteine von Proteinen, Enzymen und darüber hinaus von Vorstufen etlicher weiterer Stoffwechselprodukte sind. So findet man zahlreiche nicht-proteinogene Aminosäuren, wie deren *D*-Epimere oder Ornithin, in nicht-ribosomalen Peptiden eingebaut, während verschiedene Aminosäureabbauprodukte auch in Polyketiden oder andern kleinen bioaktiven Substanzen Verwendung finden.

Die Methoden, die der Wissenschaft zur Untersuchung dieser Stoffwechselwege und der ihnen entspringenden Substanzen zur Verfügung stehen sind zahlreich und umfassen radiometrische, chromatographische, spektrometrische, spektroskopische und weitere Methoden, die teils seit langer Zeit im Einsatz sind. Nichtsdestotrotz ist eine jede Methode auch mit Nachteilen behaftet, die erst durch neue Erfindungen oder komplementäre Experimente überwunden werden können. Die Entwicklung der noch relativ jungen und mächtigen Technik der Klick-Chemie feiert dabei große Erfolge, da sie die bestehenden Methoden mit einem hohem Maß an Selektivität und Zuverlässigkeit bereichert, so dass insbesondere der Bereich des Biolabeling jüngst enorme Fortschritte erfahren konnte. Bis dato lag das Hauptaugenmerk dabei auf der Markierung von Proteinen und anderen Makromolekülen zur Sichtbarmachung oder Isolation derselben in teils lebendigen Systemen. Letzteres wurde insbesondere durch den Einsatz ringgespannter Alkine in Verbindung mit Aziden in einer 1,3-dipolaren Cycloaddition, das bekannteste Beispiel der sogenannten bioorthogonalen Klick-Chemie, ermöglicht. Die Vorzüge besonders letzterer Technik wurden bisher allerdings kaum auf die Verfolgung des Schicksals kleiner Moleküle und ebenso kleiner Folgeprodukte angewendet.

In der hier vorliegenden Arbeit wird die Klick-Chemie in Verbindung mit azidmarkierten Vorläuferstufen verschiedenster Naturstoffe eingesetzt um das Repertoire biochemischer Analytik zu erweitern und dabei auch neue Substanzen zu entdecken, die mit klassischen Methoden allzu leicht

übersehen werden konnten. Der erste Teil dieser Arbeit, dem auch die ersten beiden Publikationen entsprangen, widmet sich insofern der Untersuchung des Auf- und -abbaus von Fettsäuren, sowie deren Transport in Bakterien, wozu ω -ständig azidierte Fettsäuren und verschiedene ringgespannte Alkine Verwendung fanden. Die Rückverfolgung dieser modifizierten Fettsäuren fand mittels Massenspektrometrie-gekoppelter Flüssigchromatografie statt, einem Mittel, welches heute bereits in vielen Forschungseinrichtungen zur Grundausstattung gehört. Zudem erwies sich der Einsatz solcher unnatürlichen Stoffe in biologischer Hinsicht als unproblematisch und äußerst effizient, und bietet zudem eine attraktive Alternative zu in der Handhabung der entsprechenden Chemikalien aufwendigen Methoden wie der Radioisotopenmarkierung. Auch erübrigt sich hierdurch der Einsatz von massenspektrometrie-gekoppelter Gaschromatografie, welche eine wichtige Rolle in der Fettsäureanalytik einnimmt. Auf diesem Wege wurden zudem neue Erkenntnisse zum bestehenden Modell des Fettsäuretransports in Gram-negativen Bakterien gewonnen und ein revidiertes Modell dazu wird vorgestellt.

Der zweite Teil dieser Arbeit behandelt die Entwicklung und Anwendung einer Technik zur Anreicherung von azid-markierten Substanzen, mit dem Ziel sämtliche Stoffwechselprodukte einer azidierten Vorstufe zu detektieren und zu identifizieren. Zur Verwirklichung dieser Aufgabe wird ein Harz vorgestellt, welches mit einem selektiv abspaltbarem Bicyclononin funktionalisiert wurde. Nach Inkubation dieses Harzes mit einem zu untersuchenden Extrakt einer vorher mit azidierten Vorstufen gefütterten Bakterienkultur können die zyklisierten Azide abgespalten und mittels Flüssigchromatografie in Verbindung mit Massenspektrometrie charakterisiert werden. Dabei kommen insbesondere kleine azidierte Aromaten wie Azidophenylalanin, aber auch die bereits im ersten Teil verwendeten Azidofettsäuren zum Einsatz. Als zu untersuchende Organismen wurden dabei zahlreiche Stämme der insektenpathogenen Bakterien *Xenorhabdus* und *Photorhabdus* untersucht. Diese Spezies hat sich darauf spezialisiert in Symbiose mit Fadenwürmern Insektenlarven als Nahrungsquelle zu nutzen und diese gegen mikrobiotische Konkurrenten zu verteidigen. Letzteres wird durch die Herstellung einer großen Bandbreite antimikrobiell wirksamer Naturstoffe (vor allem nicht-

ribosomaler Peptide) verschiedener Komplexität erreicht, wodurch sich diese hochspezialisierte Spezies hervorragend für die Prüfung der hier vorgestellten Methode, aber auch zur Entdeckung neuer Pharmazeutika eignen. Die unternommenen Untersuchungen zeigten, dass die Azidgruppe an sich sehr gut geeignet ist um Sonden mit einer, im Vergleich zu ihrem natürlichen Vorbild, minimalen Veränderung auszustatten, da etliche biochemische Modifikationen beobachtet werden konnten, die auch von einem natürlichen Substrat zu erwarten waren. So wurde etwa der Umsatz von Phenylalaninderivaten hin zu den entsprechenden Phenylessigsäure- und Benzaldehydderivaten erfasst. Viel interessanter war jedoch die Beobachtung, dass Phenylalaninderivate wie Azido-phenethylamin auch in größere Moleküle wie Xenortid eingebaut wurden

Darüber hinaus zeigte sich, dass es zwar eine starke Kontrolle der eingesetzten Aminosäuren in der ribosomalen Biosynthese gibt, dies jedoch nur sehr bedingt für nicht-ribosomal hergestellte Peptide gilt. Mehrere dieser Peptide konnten erfolgreich aus den Extrakten verschiedener insektenpathogener Bakterien angereichert und analysiert werden. Auch einige kleinere Metabolite, die bisher nicht in Verbindung mit den jeweiligen Organismen gebracht worden waren, wurden insbesondere im Organismus *Xenorhabdus szentirmaii* entdeckt und unterstreichen damit die Vorzüge der hier vorgestellten Methode Substanzen zu finden, die man im Voraus nicht erwarten konnte, da dafür entweder eine auffällig große Menge produziert werden, oder aber eine Vorahnung bezüglich möglicher komplexer Endprodukte vorliegen müsste.

Es ist somit davon auszugehen, dass bei der Suche nach neuen bioaktiven Substanzen die Nachfrage nach Methoden, die den Einbau beliebiger Vorstufen in bisher unbekannte Endprodukte des sekundären Stoffwechsels verfolgen können, anhand solcher Erfolge steigen wird. Zwar befinden sich einige auf Isotopenmarkierung basierende Techniken zur Metabolitenverfolgung in der Entwicklung, doch hat man sich allzu lange in diesem Feld auf zufällige Entdeckungen verlassen, die dem zunehmenden Druck, unter dem die moderne Medizin durch multiresistente Krankheitserreger steckt, nicht mehr gerecht werden. Die hier vorgestellte Methode, insbesondere die der selektiven Azidanreicherung, hat großes

Potential, welches sicherlich nicht allein auf den Bereich der Mikrobiologie beschränkt bleiben muss, und selbst dort durch die Ausweitung der untersuchten Stämme noch einige Überraschungen verspricht.

1 Introduction

1.1 Bacterial metabolism – The entry-door to understanding life

At the beginning of life, early cells are generally thought to have been rather simple, but were already capable of basic metabolism encompassing DNA and RNA maintenance, energy processing and tackling of structural issues. A true explosion of diversity in the biochemistry however first occurred with the harnessing of amino acids for all kinds of purposes by combining them into peptides of varying length and eventually, into proteins.^[1,2] The advent of proteins increased the versatility of tools available to a cell to modify and synthesize molecules to an enormous degree and led to what we now observe as the huge variety of molecules that are formed by living beings. Although evolution continued on its path to ever increasing complexity, ultimately leading to eukaryotes and then multi-cellular life, the basics of primary metabolism had already been established and remain very similar among all known, non-viral life forms.^[3] For this reason the study of prokaryotes, which are made up of bacteria and archaea, was and still remains immensely useful to study the basic processes of life. This is mostly due to their impressive growth rates and widely found sturdiness which are both useful for cultivation under common lab conditions. The development of analytical procedures can thus often take place in bacterial test systems, while also giving insights into specifics of the tested organisms, which in turn can prove useful for understanding the pathogenicity or other features of interest in certain bacteria.^[4,5] Furthermore, with prokaryotes fighting for resources amongst themselves and against the environment they live in eons before eukaryotes even came into existence, there is much to learn of their solutions to problems that we share with them. The tools to achieve these aims are molecules with specific abilities of which many yet await discovery and evaluation.^[6] With central concepts of the working of proteins, DNA and the membrane being understood better and better, a door opens that allows us to understand and thus manipulate life in a manner most beneficial to us.

In the light of evolution displaying symbiosis and control of one's immediate surroundings as key elements of higher life-forms, it becomes evident to the inclined reader that such understanding and the resulting power are not only by-products of our own evolution, but possibly a necessity for the survival of a complex species like our own.

1.2 The membrane – More than just a barrier

At the very beginning, the first cell that could legitimately be called so already possessed one of the core features of life: a separation from its surroundings. This is what we now call a membrane, a hydrophobic capsule surrounding the vital content of life.^[7] The membrane however is more than just a barrier to fight diffusion, since it serves many of the roles needed to fulfill the definition of life. Although a general definition of life is still heavily debated ^[8] the author would like to suggest the following:

1. Regulation of the influx and efflux of substances
2. Non-arbitrary internal organization and/or compartmentalization
3. Energy production by harnessing of chemical energy
4. Proliferation either by growth or multiplication
5. Adaptability to changing surroundings through stimuli

The membrane actually plays a central role in almost all of these processes, which is exemplified by the separation of the cell from its surroundings and by selective channels and carriers^[9] (1.), the compartmentalization of organelles in eukaryotes or inclusion bodies in bacteria^[10] (2.), the role of components of the membrane as a source of energy^[10] (3.) and finally the adaptability of the membrane to temperature changes^[11] (5.). Obviously, all these examples are true for bacteria as well, simply because their way of functions are similar to all other known cells, especially because they are all made of basically the same components. The general structure of a membrane is a bilayer of lipids, each with a polar head group and a hydrophobic hydrocarbon tail with an altogether thickness of roughly 4 nm.^[12] Together these two sheets form an almost two-dimensional hydrophobic

space with liquid crystal properties^[13] that prevent polar molecules or atoms, such as water or mineral ions, from passing in and out. Since the first condition of life (exchange of substances in and out of the cell) is vital and includes polar as well as unpolar substances, a myriad of ion channels and other proteins are found covering the membrane, facilitating and also directing the passage of a specific range of substances.

The individual function of each of those membrane proteins plays a significant role in understanding and eventually manipulating the way bacteria interact with their environment. Roles fulfilled by membrane proteins in bacteria include, but are not limited to, ion-permeation, energy production, nutrient transport, cell envelope production and signal transduction, either by direct interaction with a stimulus^[14] or by transporting a signal molecule to the interior of the cell.^[9] However the basic membrane itself already fulfills several functions that can be varied according to the requirements imposed by the environment. For example, the psychrophilic bacterium *Psychrobacter urativorans*, formerly called *Micrococcus cryophilus*, is capable of changing the fluidity of its membrane to adapt to temperature changes in cold habitats^[11] while thermophilic archaea possess an especially sturdy membrane to adapt to temperatures above 100°C.^[15] All of these abilities require an enormous versatility of a generally simple principle, and an insight will be given as to how some of these abilities are achieved in Gram-negative bacteria, the main focus of this work.

1.2.1 Building a bacterial membrane

While all bacteria have a membrane, there is more to it than just the lipid bilayer described above. Gram-positive bacteria for example possess an additional cell envelope that extends outwards of the membrane into extracellular space. It features a thick, three-dimensional peptidoglycan layer that is linked to the membrane *via* lipoteichoic acids. The high amount of connections between the polymer and the membrane leads to the rigidity that the envelope has to exhibit in order to serve as a kind of pressure tank for a

cell that usually stands under high osmotic pressure from the high electrolyte content within the cell.

Gram-negative bacteria on the other hand also have a peptidoglycan layer, albeit with much lower density and thickness. Additional protection and rigidity is achieved by the formation of a second membrane beyond the peptidoglycan layer. This leads to the termini of outer (OM) and inner membrane (IM), with the space in between termed the periplasm. The two membranes differ in the composition of the lipids they are made from, with the IM containing mostly phospholipids and the OM containing phospholipids on the periplasmic side and a large portion of lipopolysaccharides (LPS) on the extracellular side (**Figure 1**). The setup of two separate membranes allows energy production *via* a pH-gradient under aerobic conditions, where an increased proton concentration in the periplasm relative to the cytoplasm allows the controlled transduction of protons into the cytoplasm under the formation of ATP by ATPases in the IM (**Figure 2**).^[16–19]

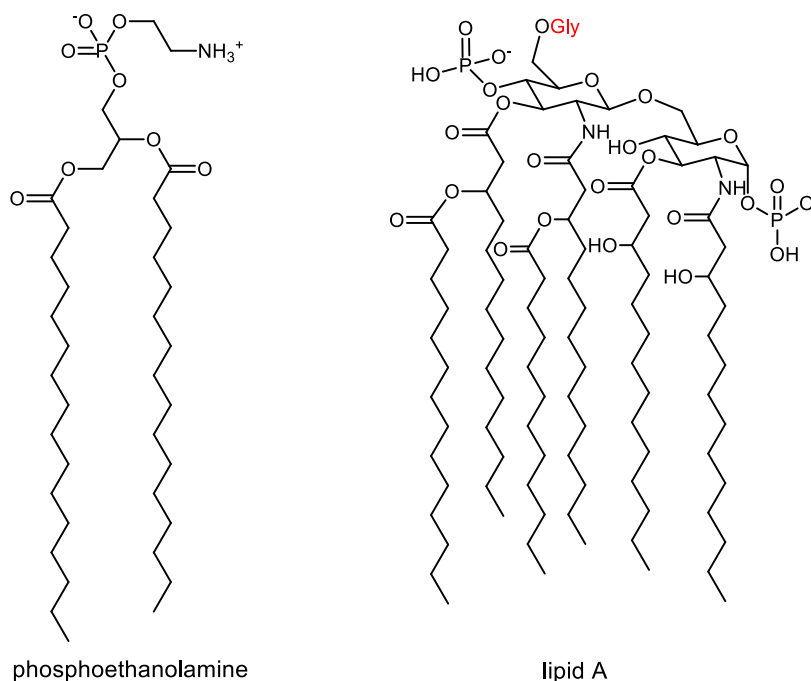


Figure 1. Structures of the main lipid components of the bacterial membrane, showing the most abundant phospholipid of most Gram-negative bacteria phosphoethanolamine and the lipid moiety of the LPS, lipid A. The polyglycosylated part is attached at the oxygen labeled accordingly.

With each membrane differing in its composition and properties, the cell has to produce a variety of lipids and has to be able to transport them to their final destination.^[20] While the precise mechanisms of this transport are not completely understood to this day, it is clear that the process is not trivial, especially for the translocation of LPS to the outer envelope.^[21,22] What all of these lipids do have in common however is that the hydrophobic moiety requires fatty acids for its biosynthesis, a process that differs only marginally between eukaryotes and bacteria.

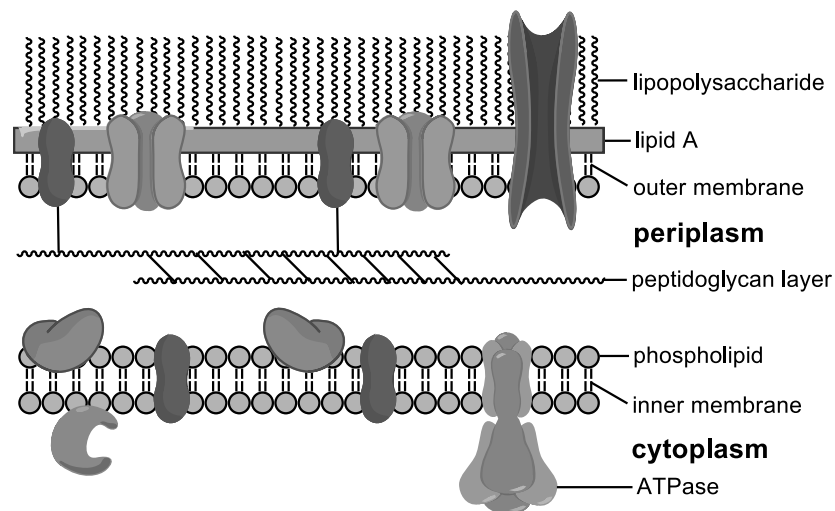


Figure 2. Schematic depiction of the double membrane system of Gram-negative bacteria, showing the different composition of the outer and inner membrane as well as additional structural elements (e.g. the peptidoglycan layer) described in **chapter 1.2.2**. Both membranes are laced with proteins that either serve as anchors for a cytoskeleton, pores for metabolite transfer, ATP-production and many other passive or active roles.

1.2.2 Fatty acid biosynthesis and degradation

As was explained in the introduction of **chapter 1.2**, the membrane fulfills many roles vital for life. This is especially true for the main component of almost all membranes: fatty acids. The term fatty acid itself encompasses a large variety of hydrocarbons with a terminal carboxylic acid function, with the variety being found at the hydrocarbon chain. Although there exist many exotic forms, including structure components such as cyclopropane, cyclohexane, more common modifications such as mono- or polyunsaturated hydrocarbon chains, chains with uneven length or branched fatty acids^[23], a

fatty acid is usually thought of as a simple, saturated hydrocarbon chain, however its biosynthesis involves several different steps (**Figure 3**).

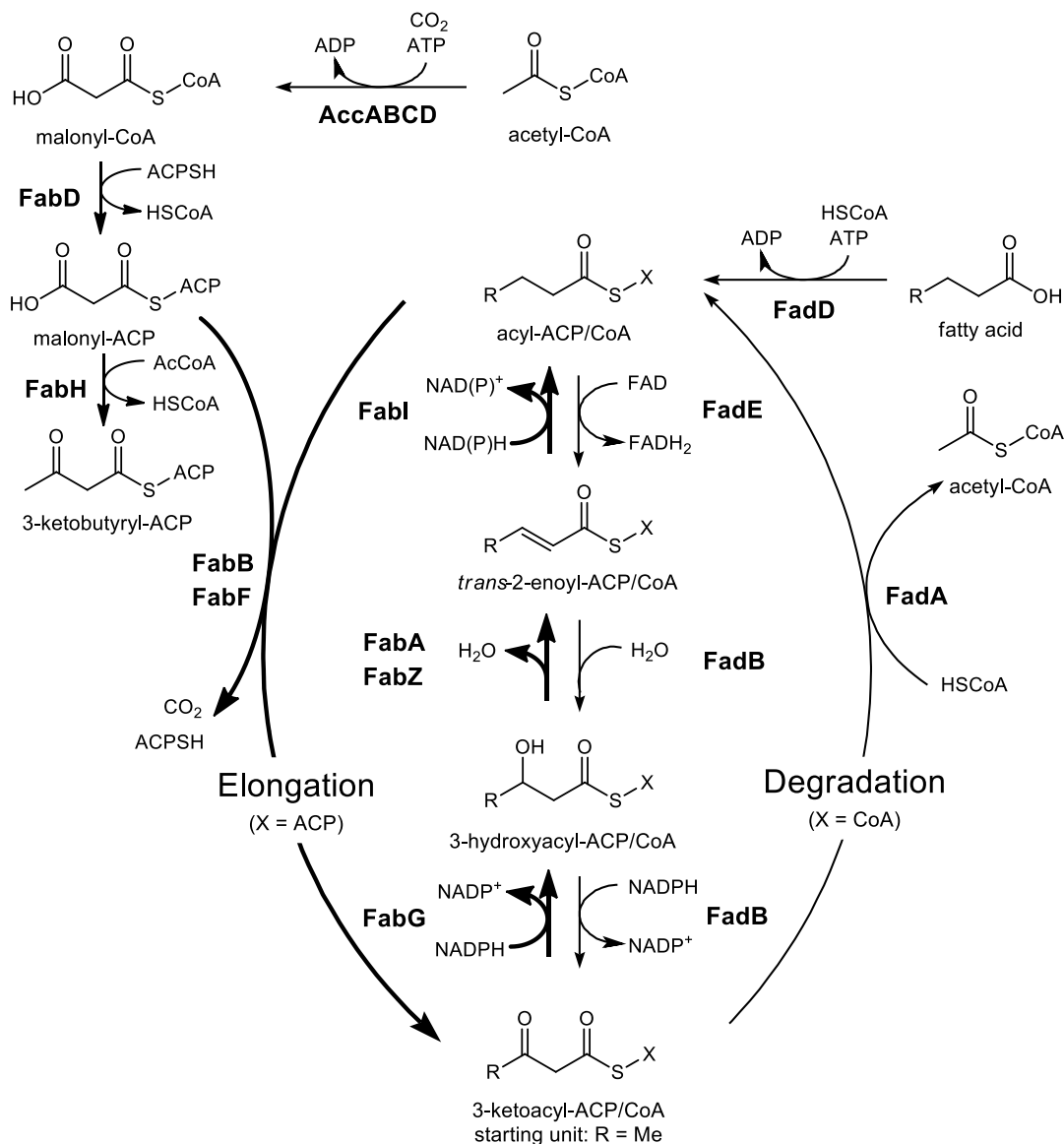


Figure 3. Biosynthetic steps for the elongation and degradation of fatty acids in *E. coli*. As can be seen, Fatty acids are both synthesized from (after carboxylation to malonyl-ACP by AccABCD) and degraded to acetate units, albeit with a specialty in fatty acid biosynthesis, which requires an additional pathway for the formation of the initiation unit β -ketobutyryl-ACP (shown left and bottom) by FabH.^[24] The pathway that acetate units follow is dictated by the thiol they are esterified with, with ACP-ligation leading to elongation and CoA-ligation leading to degradation.^[24–26]

The process of bacterial fatty acid biosynthesis in *Escherichia coli* starts with the ATP-consuming formation of malonyl-CoA from acetyl-CoA by a multienzyme complex (AccABCD) consisting of a biotin carboxylase (AccC), a biotin carboxyl carrier protein (AccB) and a carboxyltransferase

heterotetramer (AccAB). The malonyl function is then transferred to an acyl carrier protein (ACP) by FabD and the resulting thioester can be seen as a spring-loaded molecule ready to form an ACP-bound two-carbon thioenolate that readily performs an aldol-addition with acetyl-CoA, catalyzed by FabH.^[24] The result of this addition is the β -ketobutyryl-ACP starting unit and enters the common fatty acid elongation cycle, which consists of α,β -dehydrogenation (FabG), elimination of water (FabA and Z) and eventually reduction of the double bond of the α -enoate by FabI. From then on FabB and F take over part of the role of FabH and the elongation cycle continues, albeit with acyl-ACPs as the carriers of fatty acid intermediates. This process goes on until a competitive influence of the acyltransferase enzymes in charge of transferring sufficiently elongated fatty acids to their respective recipients (phosphoglycerol derivatives or saccharides as in lipid A) removes the fatty acids needed elsewhere from the pool of elongated fatty acids. In this way acetate units become what largely makes up the bacterial membrane, costing the cell one ATP, one NADPH/H⁺ and one FADH molecule per two carbons of chain length of the fatty acid.^[27] It is because of this process, that formerly the addition of radioactive acetate was used to monitor such incorporation processes.^[28] While more modern and less dangerous methods have been developed, the indisputable findings of that time have shed remarkable light on the basic processes of life.

The degradation of fatty acids follows a very comparable biochemical path to that of fatty acid elongation, except it runs in the opposite direction. Fatty acids available to the cytoplasm need to be activated *via* CoA-ligation, a job performed by FadD (**Figure 5A**). FadD, which is assumed to be membrane-associated^[29], ligates free fatty acids with CoA, forming a thioester more readily available for identification and modification by the respective processing enzymes (see **Scheme 1** in the following chapter for acyl-CoA structure). Once a fatty acid has been thioesterified, FadE performs the first crucial step: dehydrogenation to form the α,β -desaturated fatty enoate. The resulting CoA-thioester is then relocated to the FadA/B heterotetramer,^[30,31] which performs all remaining three tasks of hydratization, oxidization and final thiolysis. The latter steps create one acetyl-CoA for each degradation cycle, a molecule which is able to enter the citric acid cycle and thus

contributes notably to the energy production of the cell with a total energy balance of a stunning 17 ATP molecules for each degradation cycle.^[32]

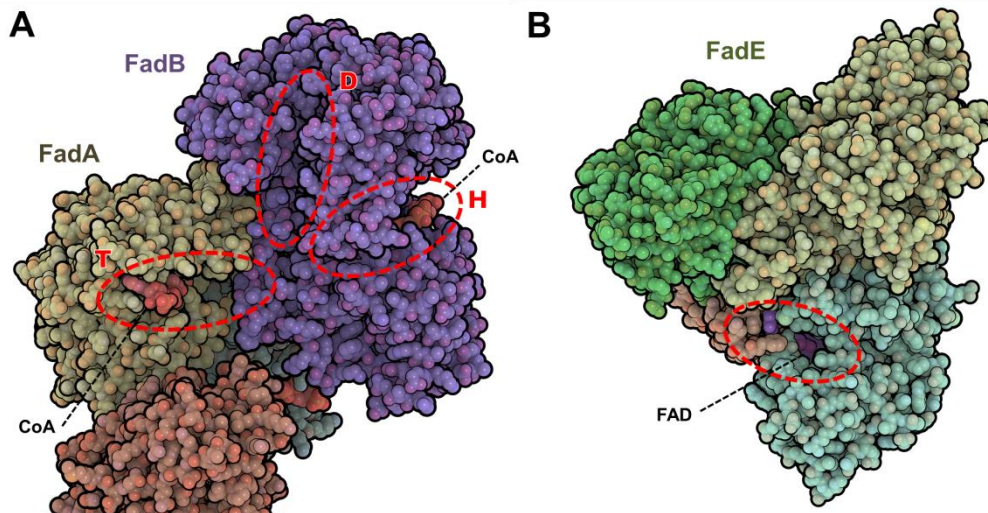


Figure 4. A) Top half of the FadA/B $\alpha^2\beta^2$ heterotetramer of *Mycobacterium tuberculosis*, showing the FadB (brown) and FadA (purple) enzymes at the top. A deep triangular cleft with hydrophobic properties can be seen in the center of the structure where the hydrocarbon chain of acyl-CoA eventually resides (two CoAs are shown in red in their respective binding pockets). At the tips of the triangle exist CoA-binding motives and hydrophobic channels (red circles) that allow the catalysis of the hydratization (H), dehydrogenation (D) and thiolysis (T) steps.^[30] B) FadE homotetramer of *Bukholderia thailandensis*. The active site (red circle) has a FAD-cofactor deeply borrowed inside, with a tunnel allowing access to acyl-CoA. Both images were created using QuteMol^[33] (Version 0.4.1) with crystal structure data from PDB-entry 4B3J^[30] (FadA/B) and 4M9A^[34] (FadE).

The mechanisms of degradation and elongation described above are basically the same for modified fatty acids like branched fatty acids. The biosynthesis of the latter still uses malonyl-CoA for elongation but requires a different starting unit than the β -ketobutyryl-ACP produced by FabH (**Figure 3**).^[24] These starting units are derived from the branched hydrophobic amino acids valine, leucine and isoleucine which undergo transamination and oxidative decarboxylation to form the respective CoA-thioester that can then enter the regular elongation cycle.^[35] As will be shown later (**chapter 1.3.4**), such amino acid-derived thioesters are also used in secondary metabolite biosynthesis and thus contribute to the diverse metabolome that some bacteria exhibit.

1.2.3 Fatty acids as an exogenic energy source

Although nearly every human knows the concept of fat as an energy reservoir, such a mechanism is rare among prokaryotes. Although some exceptions exist,^[10] prokaryotes usually do not produce triglycerides, which mainly serve as energy storage. Nevertheless, the spoils of the energy stored in the main components of fat, fatty acids, have not eluded the attention of basic life. Thus even simple organisms like *E. coli* possess specialized proteins to increase the likelihood of absorbing exogenous fatty acids for energy production (**Figure 5**).

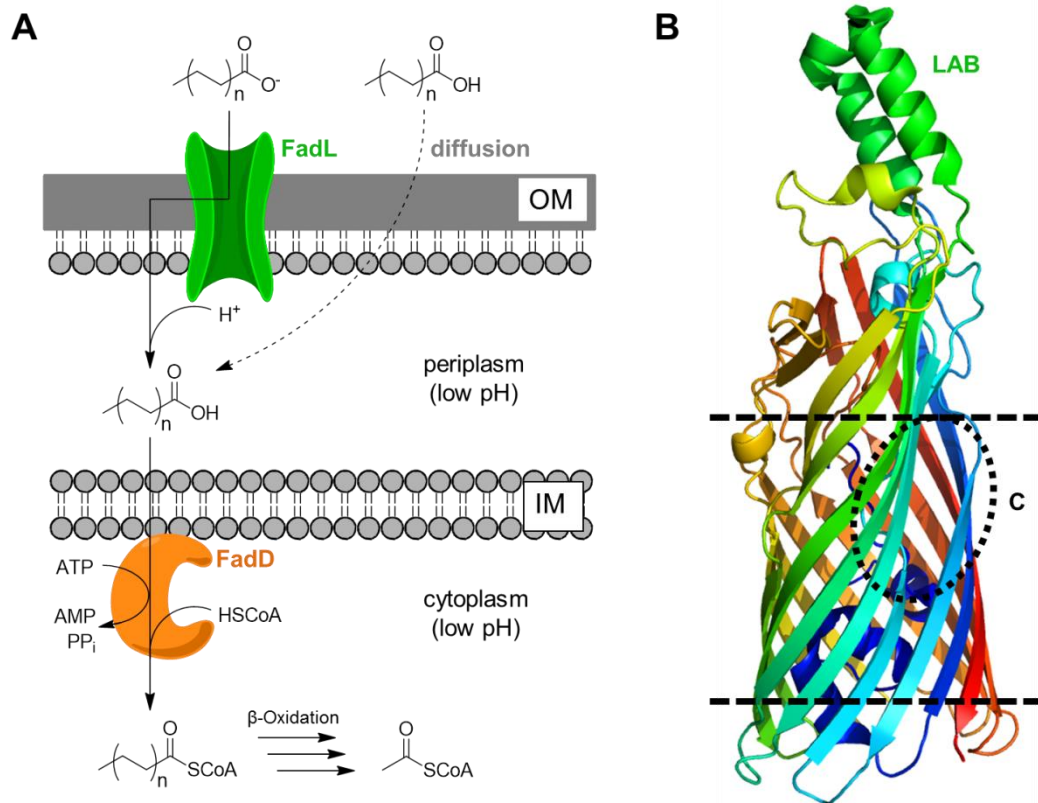
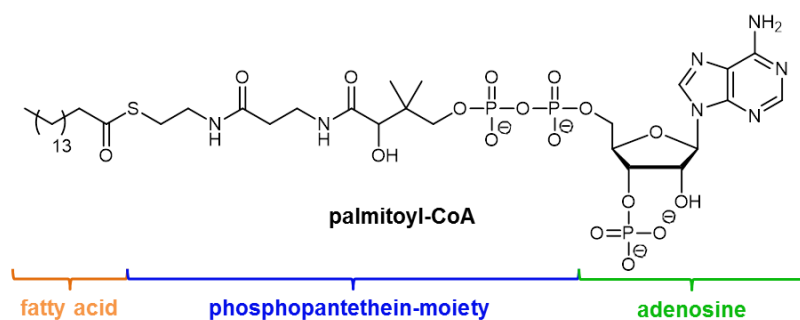


Figure 5. A) Schematic of exogenous fatty acid transport into the cytoplasm either by means of facilitated OM passage *via* FadL or *via* diffusion. Once on the cytoplasmic side of the membrane is reached, FadD causes fatty acyl-CoA formation which traps the fatty acid inside the cell. B) β -Barrel structure of FadL from *E. coli*, showing a low affinity binding domain (LAB) that protrudes from the LPS on top and the lateral cleft through which the fatty acid is released into the membrane (C, dotted circle).^[36] The approximate position of the beginning and end of the outer membrane is shown with dotted lines. The image was created using PyMol (Version 1.5.0.3 Schrödinger, LLC) with crystal structure data from PDB-entry 1T16.^[37]

The protein dominantly attributed with this ability is FadL, a fatty acid transporter located in the OM that was previously acknowledged to be vital for survival under conditions where no other energy and carbon sources but fatty acids were available.^[38] FadL indeed promotes permeability of fatty acids through the OM, the first hurdle on the way to the cytoplasm where the degradation machinery described earlier resides. Fatty acids associated with FadL are then released laterally into the OM^[36,39], after which diffusion and flip-flop mechanisms^[19] allow the movement of fatty acids to the cytoplasm. Once there, FadD causes an irreversible modification by the ligation to CoA (**Scheme 1**), which keeps the fatty acids inside the cell by increasing the polarity of the compound dramatically. This process is irreversible in such way that these thioesters are subsequently activated and ready for degradation. This metabolic gradient is further reinforced by the fact that the pH of the cytoplasm of most cells intends to stay higher than that of its environment. A high pH causes carboxylic acids to spend a longer life-time being deprotonated, and thus less able to penetrate the membranes that enclose them.^[40] Fatty acids thus have a physically and a biologically aided tendency to move towards the cytoplasm of bacteria.

Scheme 1. Structure of palmitoyl-CoA. Under physiological conditions the compound is quadruple-charged negatively, making passage through the phospholipid bilayer practically impossible.



Bacteria can thus thrive on media that contain only fatty acids and some have even specialized in living in lipid-rich environments such as our lung tissue, for which *Pseudomonas aeruginosa* has actually evolved a large set of lipid degradation enzymes, including two FadD-like CoA-ligases with different chain-length specificities to access the energy of its surroundings.^[41] This is just one of the reasons why research on bacterial FA metabolism

remains an area of interest to this day and the toolbox available to researches from all areas keeps expanding.^[42,43]

1.3 Secondary metabolites – A world of infinite possibilities

Another focus of bacterial research consists of finding ways to fight bacteria with their own biochemical weaponry. After all they are the source of many ailments that have plagued humanity and its livestock ever since each came into existence. While one of the first of these natural interspecies weapons, the antibiotic penicillin, was found in a fungus,^[44] we now know that antibiotics are also produced from many bacteria to fight rivals in their respective habitat.^[45,46]

Yet another group of compounds of great interest that are produced by bacteria are natural products that have effects on other pathogens, such as parasites,^[47] insects,^[48,49] fungi or even cancer cells.^[50] Almost all of these compounds have in common that they are produced by pathways associated with the so-called secondary metabolism. This chapter will attempt to explain what secondary metabolism is and why it offers such a wealth of chemical complexity.

1.3.1 From primary to secondary metabolism – The metabolism of phenylalanine

The somewhat not very clearly cut definition of secondary metabolism originates from a rather easily comprehensible definition of what primary metabolism is.^[51] The core aspects of the latter that apply to most organisms encompass the metabolism of:

- fatty acids and lipids
- DNA and RNA
- carbohydrates
- ribosomally produced proteins and the amino acids needed therefore

- energy production (photosynthesis, respiration or lithotrophy)^[52]

All of these intertwined metabolic pathways are central and vital features of a cell and associated enzymatic machinery is thus found in all known cells. Each environment however poses new challenges to its inhabitants, challenges that can often be tackled by the primary metabolism, e.g. *via* the evolution of new proteins or adaptations of the cell membrane(s). Some tasks however are more efficiently confronted by specialized small molecules, which is where the realm of secondary metabolism commences.^[53] Secondary metabolites are thus best understood as being the product of biochemical pathways that are not exclusively produced *via* the primary metabolism. Naturally there exist many connections between the primary and secondary metabolism, since the raw materials used for the biosynthesis of secondary metabolites, such as the well-known penicillin, are usually taken from the pool of primary metabolites and their intermediates.^[54]

As an example, we will take a closer look at some parts of the metabolism of phenylalanine in *E. coli* to demonstrate the smooth transition from primary to secondary metabolism. Phenylalanine is one of the three basic aromatic amino acids together with tyrosine and tryptophan. The biosynthesis and catabolism of phenylalanine and tyrosine share several key enzymes owing to the fact that most intermediates are the same for both amino acids.^[55–57]

Figure 6 shows several intermediates of the catabolism, biosynthesis as well as other metabolites of phenylalanine. First, it is interesting to note that phenylalanine and tyrosine share the common intermediate prephenate which can be turned into the respective α -keto acids by either eliminating water or hydrogen along with carbon dioxide, after which transamination yields the corresponding amino acid.^[57] In eukaryotic cells this interconversion of the two aromatic amino acid is even performed in a single step through an oxygen-dependent phenylalanine-4-hydroxylase.^[58] The biosynthetic pathways from *L*-phenylalanine towards the citric acid cycle then offer several alternative routes that eventually lead to the production of fumaric acid. Fumaric acid is the first component shown in this diagram that, as part of the citric acid cycle, is used by many other metabolic pathways of

the primary metabolism, thus making the basic concept of the flow of metabolites as a kind of recycling mechanism very clear.

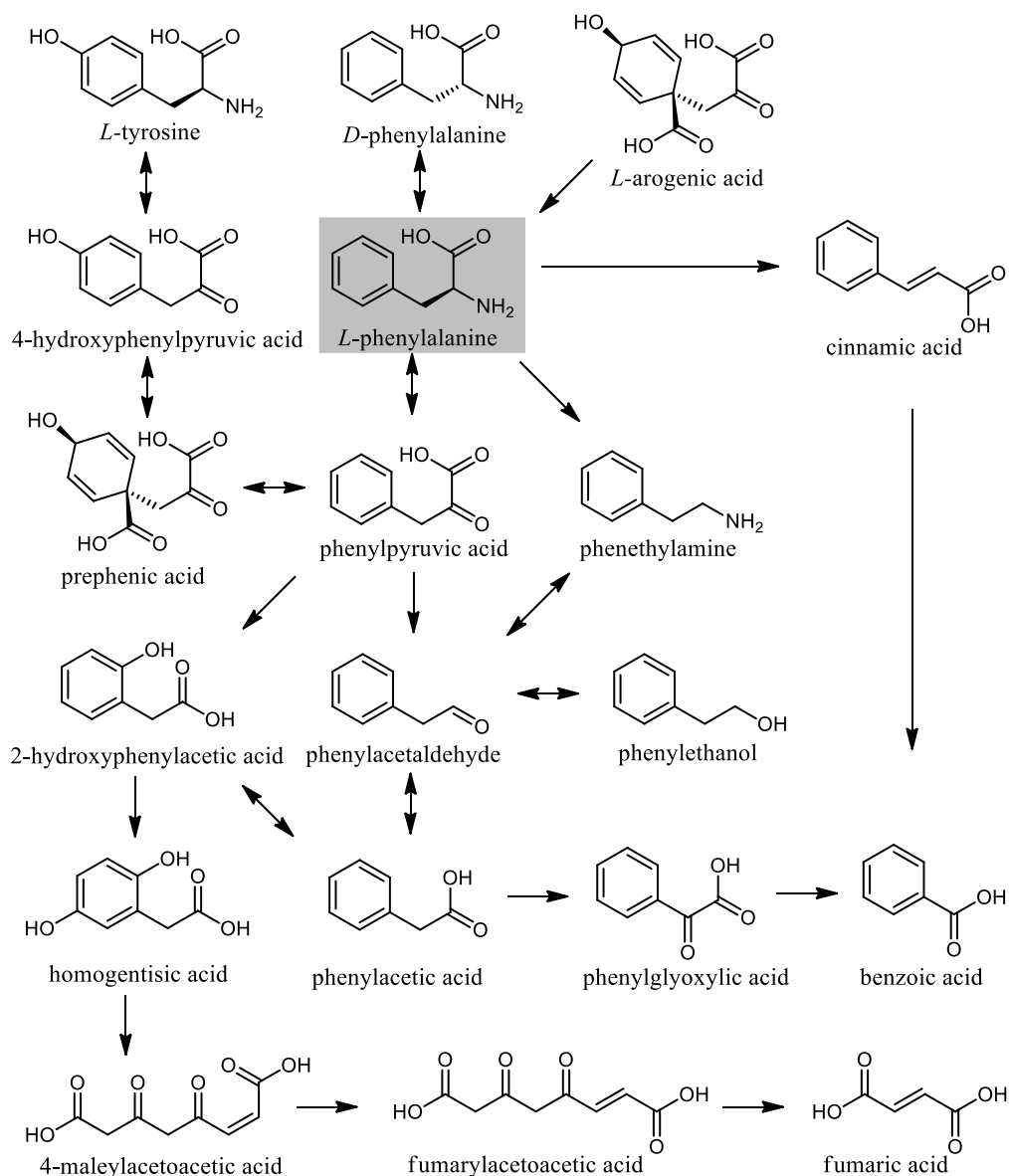


Figure 6. A part of the bacterial metabolism of phenylalanine, focusing on the degradation pathway leading from L-phenylalanine (grey box) to fumaric acid which constitutes this pathway's entry into the citric acid cycle. Additional pathways including the transformation of phenylalanine to tyrosine and some of the precursors of phenylalanine are also shown. The pathways were taken from the Kyoto Encyclopedia of Genes and Genomes (KEGG) database.^[59] Tyrosin biosynthetic pathways were taken from Zhang et al.^[57]

Yet why are there so many ways down this cascade and are there any uses for these many intermediates apart from the recycling of an amino acid? What about apparent dead-ends? Indeed, a small selection of natural products, shown in **Figure 7**, indicates where some of these intermediates can be incorporated in. The bacteriostatic wailupemycin F from *Streptomyces*

maritimus^[60] for example incorporates benzoic acid, whereas Xenortide A^[61] from *Xenorhabdus nematophila* incorporates phenethylamine as well as *L*-phenylalanine, which is connected by the NRPS XndAB.^[61] In xentrivalpeptide A^[62] from *Xenorhabdus stockiae* we then see the incorporation of phenylacetic acid and of *D*-phenylalanine. As a last example there is the antimicrobially active Isopropylstilbene from *Photorhabdus luminescens*, which incorporates cinnamic acid.^[63–65]

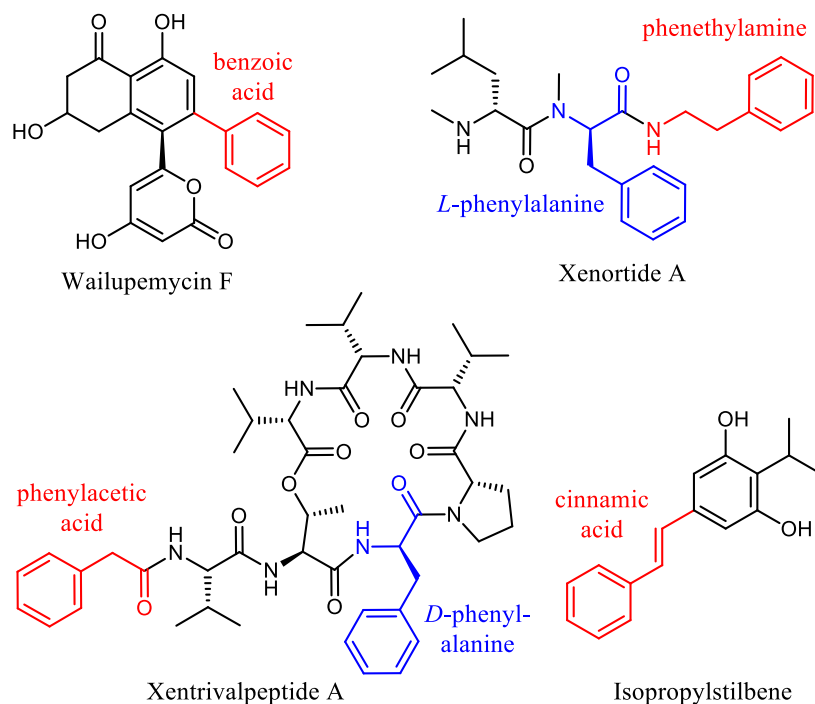


Figure 7. Four bacterial natural products that include phenylalanine derivatives not essential for primary metabolism. The compounds shown are: wailupemycin F from *S. maritimus*, which incorporates benzoic acid;^[60] Xenortide A from *X. nematophila*, which incorporates phenethylamine and *L*-phenylalanine^[61]; xentrivalpeptide A from *X. stockiae*, which incorporates phenylacetic acid and *D*-phenylalanine;^[62] Isopropylstilbene from *P. luminescens*, which incorporates cinnamic acid.^[63–65]

These examples impressively show the many uses of a primary metabolite amino acid for secondary metabolism, increasing the amount of available building blocks for natural compounds enormously. By thus having access to thousands of different small molecules and complex machineries that are able to combine these building blocks into an almost infinite number of compounds, bacteria and other organisms have developed a powerful tool to adapt to the demands of their respective environment. Many of these compounds are produced in an oligo- or polymeric manner that closely

resembles the mode of action of the machinery performing protein or fatty acid assembly from smaller building blocks (amino acids or malonate). Natural products like wailupemycin or isopropylstilbene that possess a carbon backbone and some oxygen are generally produced by polyketide synthases (PKS) that work much like the elongation enzymes in fatty acid biosynthesis but can vary the individual steps in a controlled manner, leading to carbon chains that retain many functional groups (unlike the alkyl chains of fatty acids) for possible cyclization or elimination reactions.^[66] For even more complex molecules, the implementation of amino acids offers additional possibilities that are utilized by non-ribosomal peptide synthetases (NRPS) or hybrids of both (NRPS/PKS hybrids, e.g.: vancomycin^[67]).^[68] Due to the strong focus of this work on NRPS-derived natural products, the latter will be described in more detail in the following chapter.

1.3.2 Non-ribosomal peptides

The ribosomal condensation of amino acids into long peptide chains generally termed proteins evolved near the beginning of life and thus reached an astounding degree of efficiency.^[69] With this high degree of specialization also comes a limitation in substrate specificity: Ribosomes usually only access 20-22 amino acids (20 canonical ones plus hydroxyproline and selenocysteine), which are all incorporated as their *L*-epimers. Although it has recently been shown that posttranslational modifications allow the appearance of *D*-amino acids and uncommon amino acids such as *tert*-leucine,^[70] the ribosome itself sticks to its primary role of classic protein biosynthesis.

In order to have full access to practical building blocks from the primary metabolism however, a distinct machinery has evolved. These non-ribosomal peptide synthetases (NRPS) are proteins that have a modular structure with each module being responsible for adding a single building block to the nascent peptide chain.^[71] The mechanism by which they work differs substantially from ribosomes, since the amino acid sequence is not encoded in m-RNA, but is instead determined by the sequence of modules of the

NRPS. Thus, when looking closer at a single module it becomes evident that several tasks are to be tackled, leading to several active sites called domains. A canonical module consists of three domains: an adenylation (A) domain for the activation of the carboxylic group of an amino acid under ATP-consumption, a thiolation (T) domain responsible for taking over the activated acid and moving it to the next catalytic site, and finally a condensation (C) domain that catalyzes the nucleophilic attack of the amine group of the amino-acyl-CoA thioester on the carbonyl-carbon of the amino-acyl-CoA thioester of the preceding module. Apart from these three central domains, modules can also possess additional domains capable of epimerization (E- or C/E-domains) or methylation (MT-domains) of a loaded amino acid, or also cyclization or hydrolysis (TE-domains) of the final peptide chain.^[68] Several methods for this final cleavage are known, one of which being the condensation through a small amine^[47] or the N-terminus of the peptide chain by a terminal C-domain,^[72] and in other cases a terminal thioesterase (TE-domain) causes the condensation of the peptide chain.^[73] Thioesterases like this work by transesterification of the peptide thioester to a conserved serine residue in the active site of the TE-domain.^[74] This ester can then be catalytically cleaved either through water (leading to linear peptides), an alcohol function within the peptide chain (e.g. from a threonine sidechain, leading to the formation of depsipeptides as in the case of xentrivalpeptide A, **Figure 7**) or by an amine function within the peptide (either from the N-terminus or a lysine residue from the peptide chain^[75]). The whole process is exemplified in **Figure 8** with the NRPS GxpS, which among others produces GameXPeptide A, an antimicrobial cyclic pentapeptide from *P. luminescens*.^[76,77]

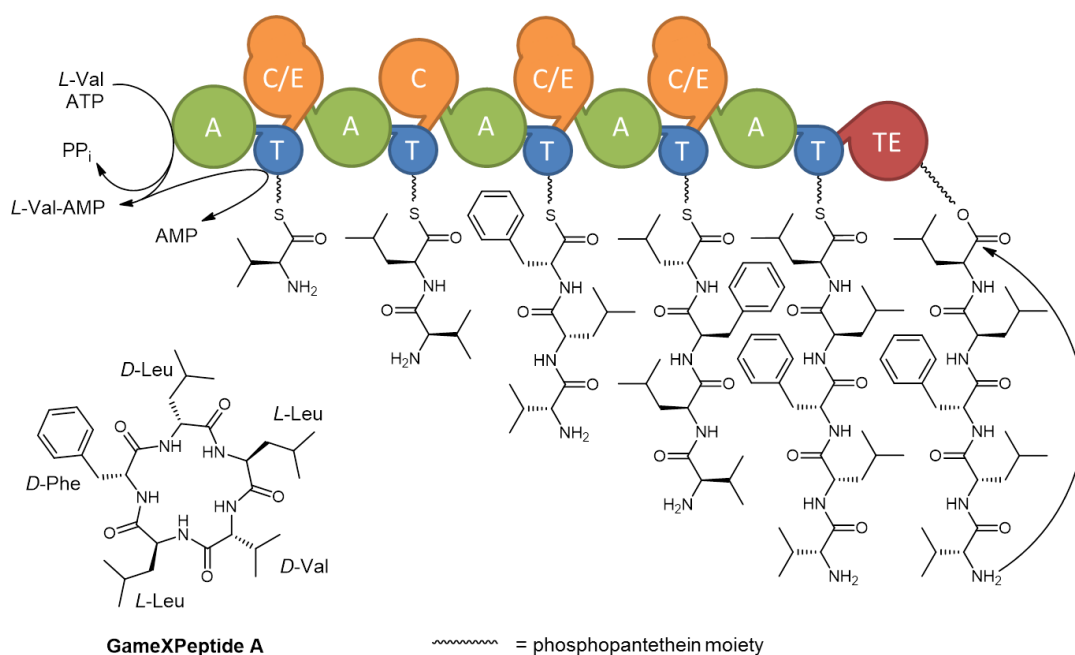


Figure 8. Biosynthesis of GameXPeptide A via the multifunctional protein GxpS.^[76,78] C/E-domains are depicted larger than ordinary C-domains due to their bifunctionality and the flexible phosphopantethein moiety is shown as a wavy line.

The NRP assembly starts with the activation of an *L*-amino acid through adenylation at the A-domain. The adenyated amino acid is then thiolized by a post-transcriptionally added phosphopantethein-moiety (compare with CoA in **Scheme 1**) of the T-domain. This long and flexible prosthetic group allows the amino acid to be moved to the active sites of other domains such as the E-domain, where *L*-valine is epimerized, leading to the appearance of *D*-valine in the second step onwards in the example of GameXPeptide biosynthesis shown above (**Figure 8**). The modified amino acid thioester is then moved to the C-domain, where *D*-valine and the amino group of the *L*-leucine thioester of the next module react through a nucleophilic substitution. The resulting dipeptide is now loaded to the T-domain of the second module and can react with the next activated amino acid at the following C-domain. This process continues until the final module is reached, and the pentapeptide is set free by an attack of the N-terminal amino group on the ester formed at the TE-domain, leading to the cyclic peptide.^[76]

GxpS is also a great example for additional versatility offered by NRPS: While in ribosomal protein biosynthesis a high substrate specificity of aminoacyl tRNA synthetases is desired and achieved, the A- and C-domains

responsible for amino acid recognition and condensation often allow for a higher degree of variation. GxpS thus also readily incorporates valine instead of leucine and vice versa and the phenylalanine residue can also be replaced by *p*-aminophenylalanine,^[77] *p*-azidophenylalanine (**chapter 7.3**) and other aromatic derivatives (Bozhüyük, K. A., unpublished), if available to the cell. This promiscuity is observed in some NRPs and adds to the broad pool of substances produced by a single NRPS, a class of proteins that with a size of up to 1.8 MDa^[79] is in the same league as ribosomes and thus energetically expensive to produce. The already intrinsically vast pool of secondary metabolites thus is increased in an evolutionary beneficial way and also opens up a door for precursor-directed semi-biosynthetic metabolite production (Bozhüyük, K. A., unpublished).

1.3.3 Fatty acids in secondary metabolism

As has been shown in the last two chapters, NRPS are not limited to amino acids to incorporate into their biosynthetic products. A multitude of amines is known to serve as terminal condensation agents in non-ribosomal peptide (NRP) biosynthesis, and it does not come as a surprise that the N-terminus of such a peptide can also be acylated, as is the case in xentrivalpeptides (**Figure 7**). The use of longer acyl chains, as offered by fatty acids in the form of their respective CoA-thioesters,^[80] thus gives acylated compounds a strong and localized hydrophobicity that can induce association with the membrane. One such example is the mode of action of lipopeptide daptomycin (**Figure 9**), a potent antibiotic from *Streptomyces roseosporus* discovered in 1986 that is active against Gram-positive bacteria.^[81,82]

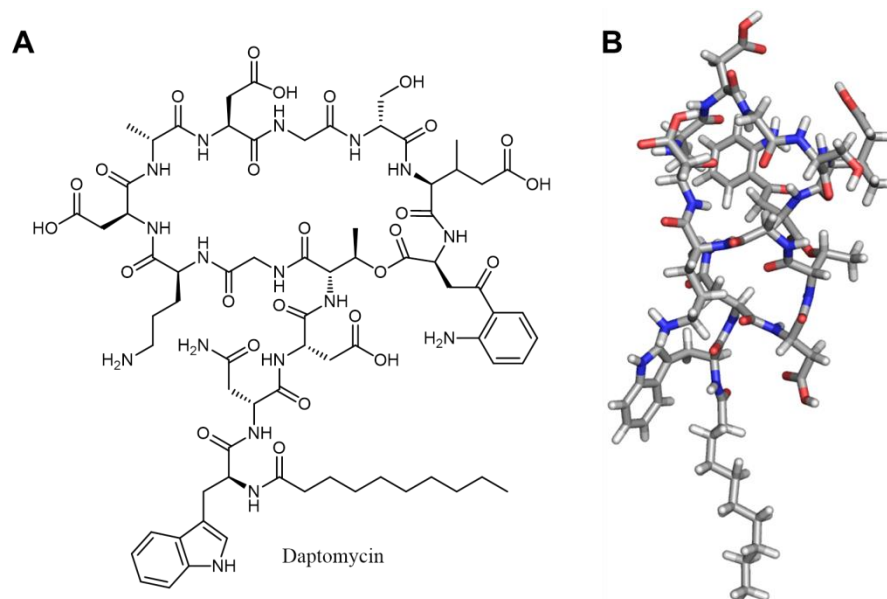


Figure 9. A) Structure of daptomycin from *S. roseosporus*.^[83] B) 3D structure of the same molecule, showing a mostly globular folding of the peptidic part and the membrane-associated fatty acid residue protruding from it. The image was created using PyMol (Version 1.5.0.3 Schrödinger, LLC) with NMR structure data from PDB-entry 1XT7.^[84]

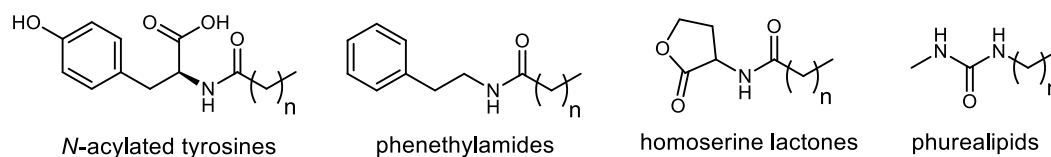
Looking at the structure, not only do we see the incorporation of several *D*-amino acids, but also rather uncommon amino acids such as kynurenine, which is derived from tryptophan, and β -methylated glutamic acid into a cyclic depsipeptide structure.^[83] Another noteworthy feature however is the *N*-acylation which features a decanoyl moiety that protrudes from the otherwise mostly globular structure of the molecule (**Figure 9B**).^[84] This acyl chain readily interacts with the membrane of Gram-positive bacteria, helping to anchor and orient the globular domain correctly in proximity to the phosphate groups of the bacterial target membrane. Ca^{2+} association then helps to locally depolarize the membrane with the help of the four acidic side chains before eventually oligomerization of several peptides causes pore formation. The pores formed in this process cause the leakage of potassium and other electrolytes whose loss eventually leads to the death of the target cell.^[85] Apart from daptomycin there exist many other antibiotic lipopeptides like aspartocin,^[86] tsushimycin,^[87] malleipeptin,^[88] the PAX peptides,^[75] the well-studied polymyxins^[89] and many others.^[84,90] The latter lipopeptides all share the common motive of a cyclic peptide structure with an *N*-acylated exocyclic peptide chain of varying length. By far not all of these are as well understood as daptomycin, a fact that clearly demands further research and

investigation in consideration of the high adaptation rate of pathogens to classic and modern antibiotics.^[91,92]

Apart from this class of rather large NRPs, fatty acids are also incorporated in vastly smaller molecules that in some cases achieve a remarkable degree of bioactivity, clearly proving that size does not always matter. Two such examples are antimicrobial *N*-acylated aromatic amino acid derivatives previously discovered from environmental DNA^[93,94] (**Scheme 2**) and dithiolopyrrolones,^[95] either of which can also be found in entomopathogenic bacteria of the genus *Xenorhabdus*. Another related class of small molecules containing fatty acid residues are phenethylamides (**Scheme 2**) and tryptamides as found in the bacterium *Xenorhabdus doucetiae*.^[96] While little is known about these tryptamides, they have been shown to appear in cocoa plants^[97] and certain phenethylamides have a tyrosinase inhibitory function^[98] and phenethyl-2-acetamide even possesses cytotoxic activity.^[99] Depending on the chain-length of the aforementioned fatty acid phenethylamides and tryptamides significant bioactivity against insect haemocytes (LD₅₀ value as low as 4.3 µg/mL for butyryltryptamide), mouse fibroblast or leukemia cells was observed.^[96] The different susceptibility of the yet unknown targets to phenethylamides shows the great versatility of fatty acid incorporation in small molecules: the length and type of fatty acid incorporated can vary greatly simply by having an amide synthase with great substrate promiscuity in respect to the chosen CoA-thioester. This method allows the production of a vast range of possibly cytotoxic compounds with a single enzyme without the need for rapid evolution of new biosynthetic gene clusters. The same can be said for a range of bacterial but also insect signaling molecules.^[100–102] Among bacteria acyl homoserine lactones (**Scheme 2**) often fulfill this role and the incorporation of fatty acids into smaller or larger peptides allows a tremendous diversification with the alkanoyl chain length and type being strongly strain-dependent.^[103] This again allows the quick diversification of a simple compound class with only minor adjustments to the chain-length specificity of the respective amidation enzyme. As a final example there is the product class of phurealipids (**Scheme 2**), which are produced by entomopathogenic bacteria like *Photorhabdus luminescens*.^[48] The molecule's role has been successfully

elucidated, ultimately showing that it inhibits the juvenile hormone epoxide hydrolase, an enzyme vital for the correct development of insect larvae, which are the hosts of the producing strains.^[104] The alkyl chains attached to the central urea moiety are derived from fatty acids and the chain-length is by far not as variable as with the phenethylamides mentioned above, indicating a high degree of adaptation to the insect host.

Scheme 2. Structures of a few selected secondary metabolites that incorporate fatty acids of different chain-lengths in the order they were mentioned.



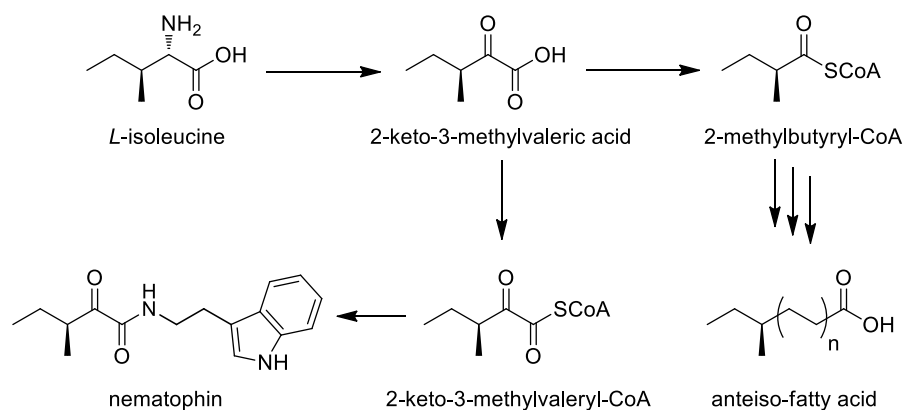
It can thus be summarized that fatty acid incorporation into secondary metabolites has a wide range of applications for the respective producing strains, stretching from membrane association to easily expanded libraries of bioactive metabolites and beyond. Furthermore the required fatty acids are produced in almost any form and length during the elongation and degradation occurring in the primary metabolism described in **chapter 1.2.2**, making these precursors a readily available resource within the organism.

1.3.4 Small molecules with a strong effect

Apart from the two classes of metabolites that either primarily incorporate fatty acids or amino acids, there exists another class of very small bioproducts that can loosely be associated with a very simple NRPS and/or PKS. A simple example for this is nematophin, an α -ketoisocaproyl tryptamide with a strong antimicrobial effect on methicillin resistant *Staphylococcus aureus* (MRSA)^[105,106] Although the isocaproyl moiety is derived from isoleucine, it is also used for the formation of anteiso fatty acids by serving as a starter unit in bacteria like *Myxococcus xanthus* (**Scheme 3**), linking this compound indirectly to fatty acid metabolism (**Chapter 1.2.2**).^[107] A similar biosynthesis can be observed with insecticidal xenocylins,^[108]

which present a close interaction between PKS and amino acid incorporation, leading to yet another potent compound with interesting properties, and yet many more remain to be found.

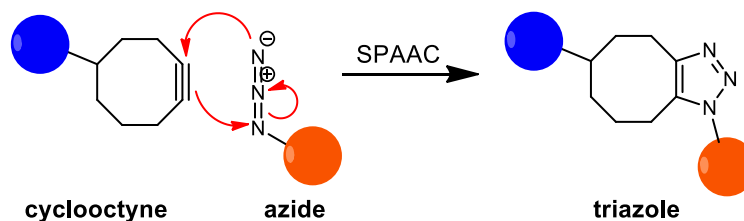
Scheme 3. Biosynthetic conversion of isoleucine to either nematophin or anteiso-fatty acids through 2-keto-3-methylvaleric acid in *Xenorhabdus* spp. (both) or myxobacteria (anteiso-fatty acids).^[35]



1.4 Click-Chemistry – Azides as silent intruders

Although until today click-chemistry is defined loosely as a very efficient and directed reaction of two molecules under easily achieved reaction conditions and without a complicated workup,^[109] the recent years definitely put the Huisgen 1,3-dipolar cycloaddition between an alkyne and an azide^[110] in the center of interest and research.^[111] The applications vary between anorganic^[112] and organic synthesis^[113] to *in vitro* biolabeling^[114] and even further. The true milestone in development and optimization of this technique was however achieved by Bertozzi et al. by the re-discovery of ring-strained cyclooctynes as reaction partners for azides without the need of any possibly cytotoxic copper-catalysts, a process coined the strain-promoted azide-alkyne cycloaddition (SPAAC, **Scheme 4**).^[115,116]

Scheme 4. General mechanism of the strain-promoted alkyne-azide cycloaddition (SPAAC) with octynes, leading to a very stable triazole derivative.



This discovery opened the now very popular field of bioorthogonal chemistry, where two reaction partners (e.g. an alkyne and a cyclooctyne) can react within a live cell without substantially altering or harming it.^[117] This is only possible because in most organisms there is no natural reaction partner for either a cyclooctyne or an azide, nor is the aqueous environment and the mild temperature an obstacle. With the azido group also being a rather small functional group, roughly the size of an ethyl group, not featuring a noteworthy polarity or reactivity, it is the perfect intruder for *in vivo* investigations, only marginally exceeded in smallness by an ethynyl group that requires problematic copper-ions as catalysts to react.^[118] The development of appropriate ring-strained alkynes as easy-to-handle reaction partners is thus an area of vivid research and some key aspects of this development will be brought into the spotlight in this chapter.

1.4.1 The evolution of cyclooctynes for bioorthogonal applications

In 1953 Blomquist et al.^[119] reported the explosive reaction between “cycloöctyne” and phenyl azide and correctly attributed this high reactivity to the ring strain the preferably linear alkyne has in this configuration, a strain that can be significantly reduced by changing the hybridization of the two involved carbons from sp^1 to sp^2 . The potential in this reaction was later acknowledged and elaborated by Bertozzi et al. and a functionalized cyclooctyne termed OCT (**Scheme 5**) was used to perform successful *in vivo* biolabeling experiments^[115] and thus the in-depth development of cyclooctynes for click-chemistry had started. It quickly became clear that there are two major aspects that increase the reactivity of a cyclooctyne

towards an azide: ring strain and electron deficiency. While the former is linked to the favorable change in hybridization mentioned above, the latter has to do with the fact that it is the LUMO of the alkyne that reacts with the HOMO of the azide (**Figure 10**).^[120]

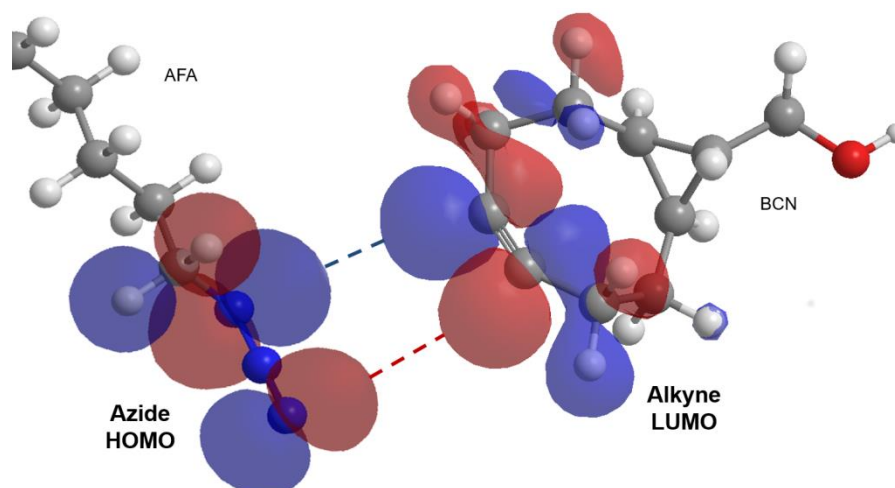
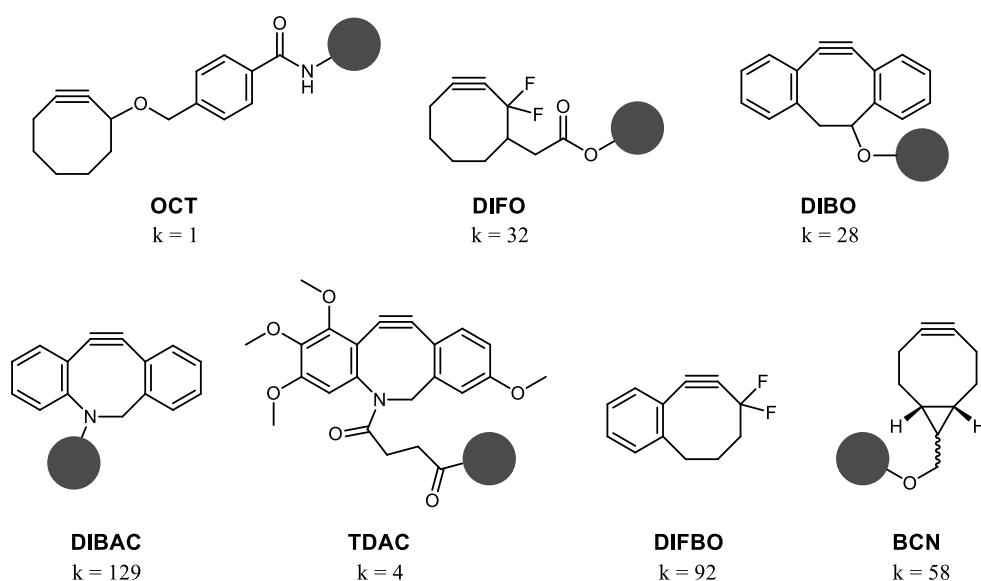


Figure 10. Orbital interaction between the HOMO of an ω -azido fatty acid (AFA) and the LUMO of bicyclononyne (BCN) shortly before the [3+2] cycloadditive click-reaction occurs. The formidable and biologically unique overlap can clearly be seen and explains the efficacy of the reaction.^[120] Picture created using ChemBio3D Ultra (Version 12.0).

A reduction in electron density of the triple bond thus makes the LUMO more easily accessible for the azide and incorporation of fluorine atoms (difluorinated octyne, DIFO, **Scheme 5**) to the α -position of the alkyne indeed increased the reaction rate by a factor of 60.^[121] It also became evident quickly that it is in some cases easier to increase the ring strain through the introduction of more sp^2 centers in the ring structure, reducing the degrees of freedom the ring has to ease the strain. One of the first compounds achieving this feat was dibenzocyclooctyne (DIBO) which had about the same gain in reactivity as DIFO. These effects could of course be combined, as was the case with difluorinated benzocyclooctyne (DIFBO). Another way to increase ring strain is to reduce bond lengths at certain positions to tighten the ring. To achieve this, heteroatoms like nitrogen can be implemented, as is the case with dibenzoazacyclooctyne (DIBAC), which is almost five times more reactive than DIBO.^[111] Many of the compounds named so far are obviously quite lipophilic, a property not always beneficial when working in aqueous

biological environments. This realization led to the development of more amphiphilic substances like tetramethoxydibenzoazacycloctyne (TDAC) which also features a comparably easy synthesis,^[122] an important quality for its applications by biologists. This principle was put into practice with splendor by the development of a reactive, easily synthesized and highly symmetric bicyclononyne (BCN) by van Delft et al.^[123] Although apart from the two obligatory sp carbons in the triple bond all other carbons possess sp³ hybridization, the reaction rate of BCN is still 60 times higher than that of OCT, about which the same assessment of hybridization can be made. The explanation thus lies in the cyclopropane ring, itself a highly strained structure, which drastically constrains flexibility of the whole bicyclic structure. The triumphal progression of this cyclooctyne and its commercial availability are hallmarks of its good design and its use in this work can be seen as a testimony to it.

Scheme 5. Structures and relative reaction rates of several cyclooctynes developed since 2004.^[111,122] The circles reflect different derivifications, including attachment to solid support as in the case of BCN (**chapter 7.3**).



1.5 Aims of this work

The advent of click-chemistry has made it possible to tag and follow the fate of molecules inside the complex environment that a living cell procures as has previously been shown with great success.^[114] This work thus is centered

around new applications of click-chemistry for studies on the metabolism of small molecules like fatty acids and precursors of more complex metabolites such as NRPs. The very simple reaction conditions offered by cyclooctynes in combination with azide-carrying probes led to the implementation of this type of click-reaction for the metabolic studies portrayed in this work. Due to its small size and easy synthetic accessibility the azide was chosen to serve as the bioorthogonal labeling agent that was first introduced at the ω -position of fatty acids to study their metabolism and transport in bacteria. Several cyclooctynes were synthesized and evaluated in the course of this work in order to devise a reliable method for the detection and analysis of biologically modified fatty acids, an approach to fatty acid analysis not undertaken previously.

Due to the very satisfying results obtained from this implementation a more daring series of metabolic studies was commenced. The aim of these latter studies was the detection of metabolites downstream of biochemical pathways of primary and secondary metabolism, ideally to find novel compounds that might otherwise be overseen. Although a common tool for such azide labeling experiments is the ligation to an alkyne-carrying fluorophore^[114] or biotin^[123], these methods were not regarded as ideal for the detection of small amounts of compounds whose structure was not expected to be known beforehand. Instead the alkyne was fixed on a solid support, eventually leading to an azide-enrichment technique that had previously been used for other purposes and with a different structural basis.^[124] This technique was expected to retrieve all azide-containing metabolites that would be produced *in vivo* by bacterial strains known for their wealth of secondary metabolism.

Although it was expected to find certain NRPs that were known previously, the real question was whether it would be possible to find so far unknown compounds that might have been overseen in traditional HPLC-MS or UV screenings. Additionally it was completely unknown what would actually happen to the precursors used in the subsequent feeding experiments. Would the enzymes involved even recognize and process these azidated compounds? Would there be a way to discern actual click-products from artifacts and impurities? With a powerful UPLC-MS system at hand and

fragmentation patterns to be understood these and other questions were eventually answered and so a new tool for the chemical analysis of biological systems can be added to the pool of analytical methods available to science.

2 Manuscripts and publications

2.1 Publication: “ ω -Azido fatty acids as probes to detect fatty acid biosynthesis, degradation, and modification“

Authors: Alexander J. Pérez¹, Helge B. Bode¹

¹Merck Stiftungsprofessur für Molekulare Biotechnologie, Fachbereich Biowissenschaften, Goethe Universität Frankfurt, 60438 Frankfurt am Main, Germany

Published in: Journal of Lipid Research, July 10, 2014, Volume 55, page 1897-1901

Digital Object Identifier: 10.1194/jlr.M047969

For full article and declaration on the contribution of the authors see chapter 7.1.

2.2 Publication: “Click Chemistry for the Simple Determination of Fatty Acid Uptake and Degradation: Revising the Role of Fatty Acid Transporters”

Authors: Alexander J. Pérez¹, Helge B. Bode^{1,2}

¹Merck Stiftungsprofessur für Molekulare Biotechnologie, Fachbereich Biowissenschaften, Goethe Universität Frankfurt, 60438 Frankfurt am Main, Germany

²Buchmann Institute for Molecular Life Sciences (BMLS), Goethe Universität Frankfurt, 60438 Frankfurt am Main, Germany

Published in: ChemBioChem, July 27, 2015, Volume 16, page 1588-1591

Digital Object Identifier: 10.1002/cbic.201500194

For full article and declaration on the contribution of the authors see chapter 7.2.

2.3 Manuscript: “Solid phase enrichment and analysis of azide labeled secondary metabolites – fishing downstream of biochemical pathways”

Authors: Alexander J. Pérez¹, Frank Wesche¹, Hélène Adihou¹, Helge B. Bode^{1,2}

¹Merck Stiftungsprofessur für Molekulare Biotechnologie, Fachbereich Biowissenschaften, Goethe Universität Frankfurt, 60438 Frankfurt am Main, Germany

²Buchmann Institute for Molecular Life Sciences (BMLS), Goethe Universität Frankfurt, 60438 Frankfurt am Main, Germany

Submitted to: Chemistry – A European Journal

For full article and declaration on the contribution of the authors see chapter 7.3.

3 Additional results

Following the good results obtained from the use of azido phenylalanine as presented in **chapter 7.3**, two additional azido amino acids, γ -azido homocysteine (AHA) and δ -azido ornithine (AOR) were evaluated in respect to their behavior in several bacterial strains. The strains investigated were *Xenorhabdus budapestensis*, *Xenorhabdus innexi* and the GxpS overproducing *E. coli* strain presented in the last publication. The XAD extracts were again incubated with the CARR resin to enrich any possible azidated metabolites and then analyzed with HPLC-MS as described before. In the *E. coli* strain, we assumed that AHA could substitute one of the leucine residues of the GameXPepptide, since that position too is prone to variability and the size of AHA is very similar to leucine. The actual experiment did not reveal such incorporation, and little metabolism seemed to have occurred, as the main azide to be detected was AHA and a small amount of apparently propionylated AHA and an even smaller amount of azido-palmitic acid (C₁₆-AFA). The results were more interesting however when either AHA or AOR were fed to *X. budapestensis*. In the case of the feeding of AOR, a significant amount of azido butyric acid (C₄-AFA) and azido valeric acid (C₅-AFA) could be detected along with a small amount of C₁₆-AFA (**Figure 11**). At a retention time of 10.1 minutes there is also a new product ($m/z = 694$) whose fragmentation pattern is indicative of a pentapeptide and is yet to be completely characterized. When feeding AHA to the same strain, the situation found was quite different. Apart from azido propionic acid (C₃-AFA) and its methyl ester, two longer AFAs (C₁₁- and C₁₆-AFA) were identified. The appearance of even and uneven fatty acids from a single precursor is quite interesting, and can be explained by several pathways known in fatty acid biosynthesis.

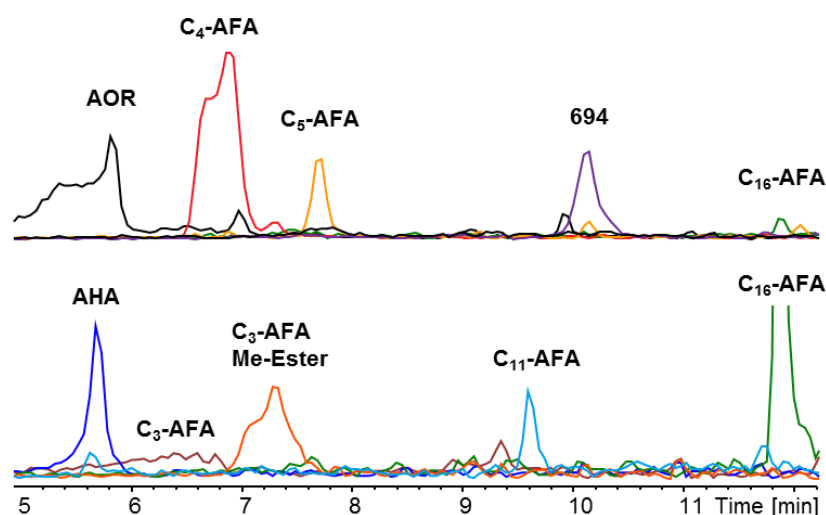
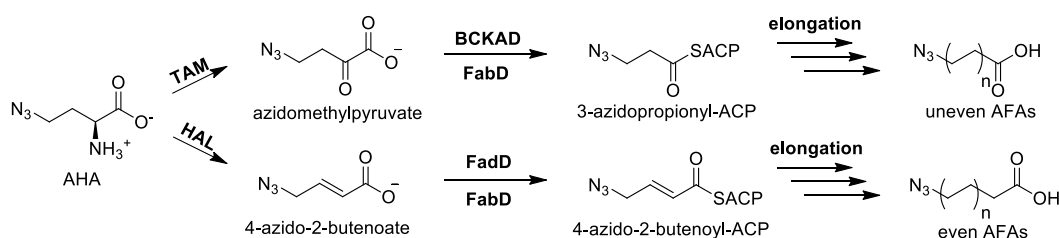


Figure 11. Extracted ion chromatograms of enriched azides from XAD extracts of *X. budapestiensis* after feeding of AOR or AHA respectively.

Depending on whether the azido amino acid first undergoes elimination of ammonia to the corresponding enoate or transamination to the α -keto acid and subsequent oxidative decarboxylation two different starting units can be formed that lead to the observed chain lengths of fatty acids, as explained in detail in **Scheme 6**. While apparently the type of azido amino acid fed leads to different preferences for each pathway, it is interesting to observe that the two compounds provide a high degree of flexibility in bacterial biochemistry, as was observed before for aromatic amino acids (**chapter 7.3**).

Scheme 6. Depiction of the proposed biochemical pathways leading to even and uneven AFAs from a single amino acid precursor. AHA is chosen for this example, although it is apparently valid for AOR too. The pathway on the top follows the pathway known for branched fatty acid biosynthesis as known from *M. xanthus* and other bacteria incorporating such fatty acids.^[35] The process starts with the transamination of AHA by a transaminase (TAM) and subsequent oxidative decarboxylation towards the activated propionyl derivative. The bottom pathway suggests the elimination of ammonia by a histidine-lyase-like protein (HAL) and direct entrance into the fatty acid biosynthesis machinery, just as with the intermediate from the top pathway. The loss of CO_2 in the former pathway leads to AFAs one carbon shorter than those from the latter pathway, explaining the observed fatty acids.



Ever since click chemistry has advanced into the field of biology, the commercial availability of “clickable” compounds has also increased, with several specialized companies appearing in the field. This strongly facilitates the implementation of click-chemistry in research groups that otherwise might feel reluctant to do so and looking at the now great amount of azidated small molecules available that can serve as precursors in metabolic pathways many more experiments of this kind are waiting to be conducted.

4 Discussion

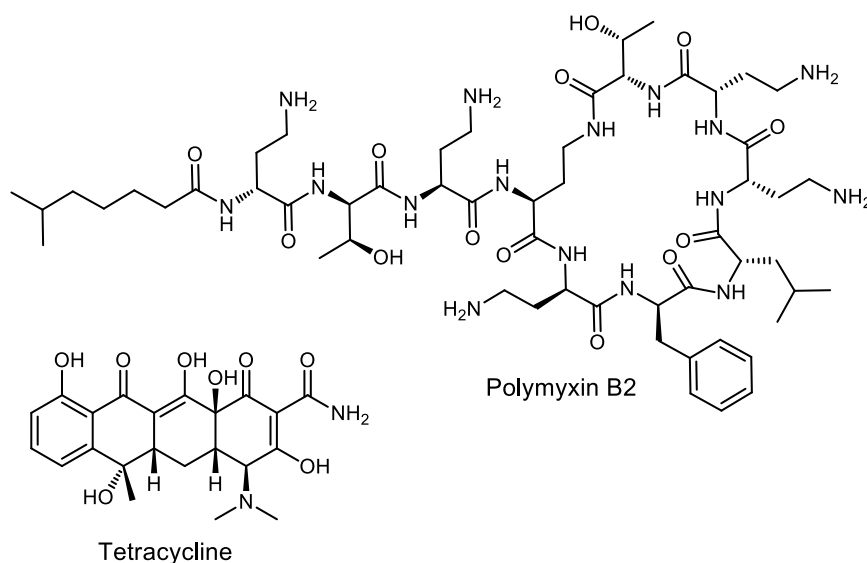
4.1 The true nature of the lipid bilayer – From static to dynamic

As has been described in **chapter 1.2** the membrane basically achieves its primary function as a more or less selective barrier to separate two aqueous environments through the exploitation of a simple physical fact: Oil and water do not mix. For a long time this seemed like a simple-enough fact to accept, and even today it is sometimes accepted as an adamant truth that molecules for which there is no specific transporter might be inhibited from entering a cell.^[36,38] Interestingly, this was thought to be true for fatty acids too, because long-chain fatty acid transporter FadL-deficient mutants were not able to grow on media that contained only fatty acids as an energy and carbon source (for a detailed explanation of the current model of fatty transport see **chapter 1.2.3**).^[9] Against this simple observation stands the experience of hundreds of years of medicine, in which hydrophobic compounds are externally applied (through the epithelium, be it orally, topically or similar) and traverse several layers of eukaryotic membranes without any specific transporters facilitating the passage. If anything, the membrane bilayer works exceptionally well at keeping electrolytes at bay, as this is indeed a crucial ability for all cells to master.^[125,126] Apart from that it is physics at work and so it does not come as a surprise that ω -azido fatty acids (AFAs) could be observed traversing the membranes in *Escherichia coli* and *Sinrorhizobium meliloti* in a notable degree even in the absence of FadL, albeit somewhat slower.^[43] This general mobility of fatty acids has been honored in some cases,^[19] but did not prevent some researchers to stick to the old dogma. The complex nature of life makes many testing systems scientifically flawed and the observation of microorganisms (or any cells for that matter) should indeed be performed under conditions close to their natural environment. This has been successfully achieved in some cases by the addition of proline^[127,128] or trehalose^[129], two compounds commonly found in insect hemolymphs, to growth media for entomopathogenic bacteria. In the case of

the monitoring of fatty acid metabolism, another route is the direct observation of fatty acids *via* click-chemistry assisted derivatization and HPLC-MS analysis. Unlike usual fatty acid methyl ester based chromatography (FAME), this method does not require a gas chromatograph while featuring a high degree of reproducibility and sensitivity.^[130] In combination with other modern liquid-chromatography-based methods for lipid analytics^[42] a powerful tool for lipidome analysis has become available to academia and beyond, offering many possibilities to groups whose access to comprehensive and thorough investigations might have been limited before.

The lipid membrane as such is an ancient component of life and the physics that govern its behavior have hardly changed since its proposed first appearance as a prebiotic chemical reaction product.^[131] In this early stage of life the phosphorylation^[132] (e.g. the nucleotides, FAD, thiamine pyrophosphate) and oxidation (e.g. the many anionic intermediates of the citric acid cycle) of molecules now regarded universal and essential for life lead to an accumulation of such precious molecules inside a cell enveloped by a membrane that indeed is hard to permeate for charged particles.^[133,134] For amphiphilic, lipophilic or even cationic substances on the other hand membrane permeability might actually have been an early way of passive nutrient and resource acquisition.^[134] Even with membranes now being laced with protein channels, receptors and transporters, this permeability has been retained and several antibiotics such as pentacationic polymyxines (**Scheme 7**) make use of that intrinsic weakness after disrupting the LPS-layer of gram-negative bacteria,^[135] while more lipophilic antibiotics like tetracyclines (**Scheme 7**) can directly diffuse into their target cells.^[136] Widespread defense mechanisms thus often include the increase of the hydrophilic character of the membrane, for example by modification of the LPS layer,^[92,136,137] or by the formation of biofilms^[138] in order to reduce the risk of involuntary antibiotic uptake or membrane association.

Scheme 7. Structures of the antibiotics polymyxin B2 and tetracycline showing that molecules with very different polarities can penetrate the membrane without relying on pores or transporters.



In the light of the permeability of several cationic and lipophilic compounds mentioned above, the ligation of anionic CoA to exogenous fatty acids proves itself as a sure-fire way to accumulate a source of energy available in the environment with little effort. The membrane bilayer should thus be regarded as a highly dynamic substance, rather than an infallible barrier, a view that is already finding great acceptance in many,^[136] albeit not all fields of research.^[9,38]

4.2 Click-Chemistry for metabolic analysis – Does it compete?

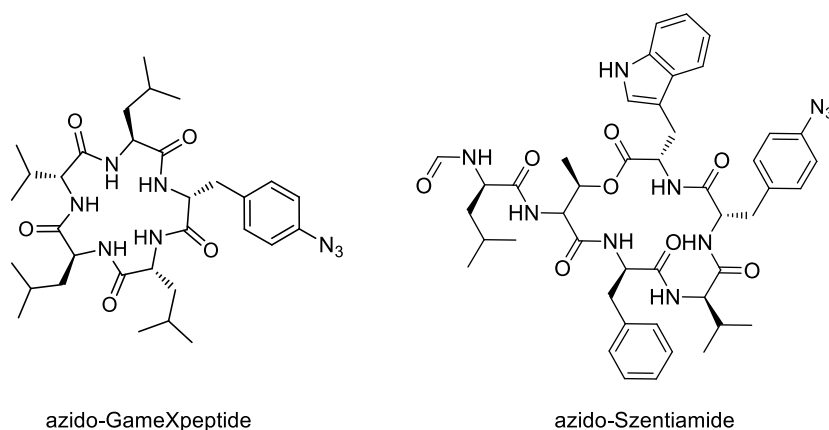
Over time, a large set of methods has been developed to track the fate of small molecules in biological systems. Depending on what is to be observed, the methods include the covalent attachment of fluorophores to probes for bioimaging^[139] or FRET studies^[140] and the ligation of biotin for affinity-binding based retrieval of target macromolecules.^[141] These methods have in common that the modifications introduced to the probe are rather large (e.g. fluorophore + linker \approx 500-1000 Da), often changing the properties of the probe to a degree that will at best change its behavior, or even rendering it completely useless. This effect increases the smaller the probe to be used is,

and thus for rather small molecules (< 500 Da) other methods of labeling are preferred. While radioisotope labeling, in which radioactive elements are incorporated into the probe, offers the smallest possible chemical alteration in combination with a low detection limit through various detection methods,^[142,143] the radioactivity itself, as well as the sometimes difficult synthetic accessibility of the target compounds give this type of labeling a bittersweet taste. Stable isotope labeling is definitely safer and the chemicals are easier to handle, yet since the labeled compounds do not “radiate” their presence or position to the observer, the expected target compound has to be known in order to obtain any meaningful information,^[96] although certain recent techniques are tackling this limitation to some degree.^[144]

It is at this point that azides and terminal alkynes tread into the spotlight, as the small size, unreactive nature and inconspicuous polarity allow the modification of a thus labeled probe at any given time. The use of azides as probes was extensively evaluated in this work and proved that their unobtrusiveness is suited very well for masquerading an artificially labeled compound as a natural one.^[145] The true potential of using azidated compounds unknown to nature hence lies in the fact that it is possible to fool it into accepting such unnatural molecules that we choose and craft, ultimately revealing many aspects of the workings found in nature. This is exemplified by the high degree of metabolization that could be witnessed in feeding experiments of azidated fatty acids, amino acids and derivatives thereof. Prior scientific studies concentrated on binding azide- or alkyne-carrying precursors for *in vivo* metabolization were mostly concerned with protein labeling, either by acylation^[146] or glycosylation.^[114] A third method that was applied to ribosomally produced proteins consisted in complex mutation experiments requiring modified tRNA-synthetases and extensive codon exchanges in the target organism’s genome.^[147–149] Although an application to secondary metabolites was also attempted by Kries et al.^[150], this approach too required genetic modification of the enzyme responsible for the modified amino acid’s incorporation and did not lead to the azidated derivative of the natural product (gramicidin) usually produced by the NRPS in question.

Instead, broad screening experiments with several bacterial strains dared nature to show what it would do with these precursors without any additional directing steps in the setup. While it is easy to imagine that the presence of a not overly polar azido-group at the ω -terminus of a long-chain fatty acid like 16-azidopalmitic acid does not disturb the proteins of the fatty acid degradation pathways^[130] (**chapter 1.2.2**) that are specific only for modifications near the carboxylic terminus, the also observed elongation and degradation of short AFAs showed that even at chain-lengths of only three carbons (3-azidopropionic acid) metabolization occurs like with the unmodified molecules. This observation was bested by the readily occurring metabolization of azido-phenylalanine towards several metabolic modifications known from the phenylalanine and tyrosine catabolism, and especially by the incorporation of several azide-carrying aromatics into larger structures such as GameXpeptide and Szentiamide (**Scheme 8**).

Scheme 8. Structures of azidated cyclic nonribosomal peptides scavenged with CARR after feeding of azidated phenylalanine.



So what can be said about the efficacy of azides as spies for the exploration of an intricate environment as featured by bacterial and possibly even more complex cells? Naturally, the answer depends on the pathway that a specific precursor is to pass through, and the little obstruction caused by azido groups at the terminal position of a fatty acid has been mentioned before.^[130] In other compounds like azido-sugars as implemented by Bertozzi et al., the 4'-hydroxyl-group of xylose was replaced with an azide and did not obstruct the glycosylation of zebrafish proteins with this modified sugar.^[114] When applying this principle to amino acids, it can be regarded as a similar approach when *p*-azido phenylalanine is used: The metabolism of aromatic

amino acids shares many features and enzymes^[55,56], which ultimately also means that they have a certain flexibility in their substrate specificity. The tyrosine aminotransferase TyrB from *E. coli* for example transfers ammonia from phenylalanine, tyrosine or tryptophan to dicarboxylic substrates like oxaloacetate (derived from aspartate) or α -ketoglutarate (derived from glutamate) and *vice versa*.^[151] Taking a closer look at the binding pocket from the same enzyme as found in *Paracoccus denitrificans*^[152] (sequence identity to *Xenorhabdus szentirmaii* homologue is 43%)^[153] it becomes apparent that the *para*-position of the phenyl ring points to the tunnel through which the substrate enters and thus there is plenty of room for an azido-group and possibly even larger modifications^[150] (**Figure 12**). Although this is just a single example, it apparently applies to many other enzymes as well, as the observed multitude of downstream metabolites that were detected prove and as was shown in **chapter 3**, this applies to many other substance classes as well.

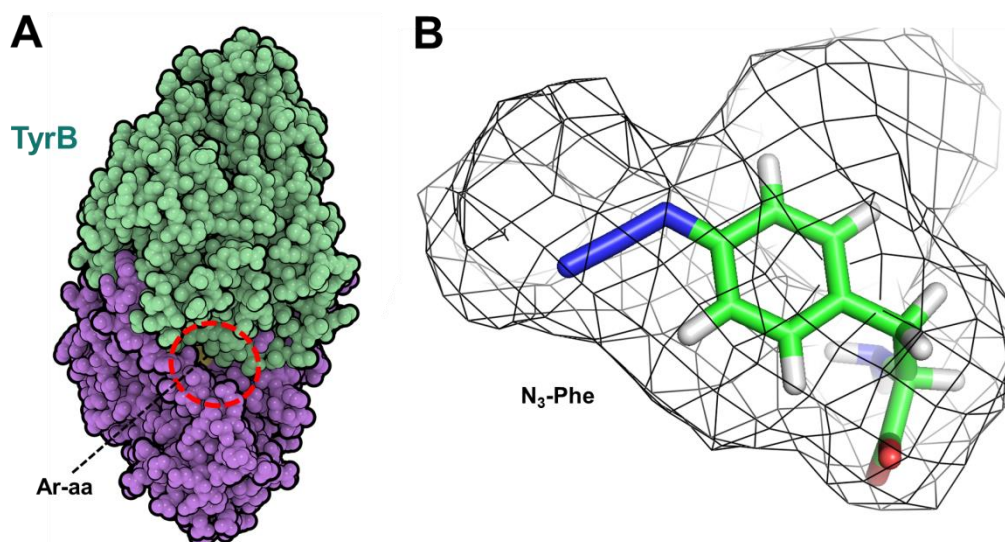


Figure 12. A) Structure of the TyrB dimer, showing the binding pocket (red circle) visible in between the two monomers, with an aromatic amino acid ligand (Ar-aa, yellow) barely visible at the active site. B) Binding pocket (mesh) for aromatic acids in TyrB from *Paracoccus denitrificans* with *p*-azido-*L*-phenylalanine (N₃-Phe, green) bound deep within the enzyme at the active site. It can be seen that the azido-function (blue) has plenty of room in the active site. Docking of substrate performed by the courtesy of Kenan Bozhüyük based on the crystal structure of PDB entry 1AY8^[152] using MOE (Version 2013.08);^[154] the picture was created using PyMol (Version 1.7.4.4 Schrödinger, LLC).

In summary, azides and hence also similarly sized ethynyl or propargyl groups are small enough to not have an overly negative effect on the substrate specificity of many enzymes that are biologically interesting to investigate. Some of the precursors used in this work went through at least four distinct biosynthetic steps, and overall dozens of enzymes were involved in handling and modifying azides. The versatility that click-chemistry offers from that point on are immense, as the probe can then be ligated to:

- fluorophores ^[114,123]
- biotin for affinity separation (with magnetic beads ^[155] or through chromatography with or without fluorescence ^[156])
- radiotherapeutics ^[157]
- a resin for enrichment ^[158] or immunosorbent assays ^[159]
- a cyclooctyne for direct HPLC-MS analyses ^[130]

Many of the compounds required for the above applications are already commercially available and the usage of these methods can thus be expected to increase in the next few years. As can be seen, there are many fancy applications in the biological area alone and the above examples only cover azide-alkyne click chemistry for ligation purposes, an area still so young that many more flabbergasting developments are certain to arise in the near future, not to mention other click-reactions that are also on the rise.^[149]

4.3 New discoveries through innovative searching tools

The discovery of new natural products is an area of research that might have been underestimated for quite some time, with many researchers being contempt at adding small modifications to long-known antibiotics or other therapeutics while underestimating the tremendous adaptive capabilities of microorganisms under constant bombardment by our limited arsenal.^[105,106,160] Nature on the other hand has been tackling the challenges of interspecies warfare since eons and has brought forward a huge set of natural products that are still vastly unknown, yet might be of great

importance if we want to stay a few steps ahead of the pests that ail us. It is here that new tools for the discovery of new natural compounds that easily elude detection by classical methods prove to be far more than just a luxurious scientific excursion.

While the aim of many biological implementations of click-chemistry is focused on trapping and/or visualizing small or large molecules of interest, the idea often is to find a specific, single target, as is the case with the methods portrayed in **chapter 4.2**. A different approach that lied in the focus of this work however consists in the detection of a broad spectrum of molecules derived from a single precursor. By attaching the ring-strained cyclooctyne BCN to a resin that could eventually be cleaved at the disulfide bond of the linker, the cleavable azide-reactive resin (CARR) was born and an enrichment procedure for azides was put into use that promised a very broad applicability, ranging in theory from lipids, to peptides, other secondary metabolites and even proteins. As the method evolved and ripened it became possible to detect and identify compounds whose presence was neither expected nor seen in this form or in the tested strains before. This is especially valid for the nematophin derivatives found in *Xenorhabdus nematophila* and *X. doucetiae*, but also for the *N*-acylated phenylalanine derivatives and benzaldehyde in *Xenorhabdus szentirmaii*.

Methods that achieve such a clean-cut tracking of a class of molecules are rare, and can usually only be achieved by the use of radioactive nuclides as beacons of the precursor to be tracked.^[28] In the area of proteomics, the stable isotope labeling with amino acids (SILAC) has pursued a distantly related tactic, by comparing the masses of proteins that incorporated deuterated or ¹³C-labeled amino acids added to the medium to proteins that did not.^[161] This method however is purely used for quantification and not tracking purposes and much less is it applied to secondary metabolites. In theory however, there lies great potential for a method that automatically scans two bacterial extracts (or other organic extracts for that matter) for mass shifts induced in mass by the feeding of isotope-labeled precursors to a regular medium or regular precursors to a ¹³C-medium. This would allow for tracking any compound that incorporated the isotope-labeled precursor simply by the isotope-specific increase in mass and an automated creation of

corresponding extracted ion chromatograms by HPLC-MS would thus lead to possibly interesting metabolites. To the author's knowledge such a method or software has not been officially published, although research on it is being conducted by Capellades et al. in Spain.^[162,162] Whenever new methods to detect new compounds arise, they are welcome to join the pool already available or in development, and this work hopes to contribute to this endeavor in its own right.

5 Concluding remarks

Starting from the observation at the beginning of this thesis that showed that click-reactions with azidated probes can be put to very practical use without any special functionalization of the alkyne merely by forming an easily protonatable triazole derivative, optimization of this technique soon led to a robust method that is easily accessible even to laboratories not specialized in chemical synthesis.

The second development step of expanding the application and benefits of the [3+2] azide-alkyne cycloaddition towards other compound classes then showed the vastness of possibilities offered by this method, especially by the development and implementation of CARR. The next steps that now await this powerful method revolve around broad screening experiments of many more azidated compounds in as the strains tested so far and additional ones, a consequence already considered in **chapter 3**. Certainly, the true leap forward is constituted by the implementation of this method in other organisms, such as fungi or invertebrates that are also known for a rich secondary metabolome.^[163,164] The future of click-chemistry applications is certain to keep on growing brighter and more diverse, and rarely were the final or most successful applications of a new technique or technology known beforehand to the designers thereof.^[165] Without question, the techniques displayed in this work can be applied to areas where they have so far not been applied yet, or only in a vastly different manner. For this reason, an expansion into the realm of lipidomics and proteomics using CARR does not only seem plausible, but desirable, although the promising results in secondary metabolism give hope to the finding of additional new compounds that one day will find their place among the pharmaceuticals of this time. First steps in this direction have already been conducted by expanding the range of precursors tested in several bacterial strains and the dynamics of azides in small molecular probes remains a topic of high interest for the future endeavors of natural product discovery.

6 References

- [1] Tamura, K., *Journal of biosciences*, (2011) **36**, 921.
- [2] Root-Bernstein, M.; Root-Bernstein, R., *Journal of theoretical biology*, (2015) **367**, 130.
- [3] Forterre, P., *Frontiers in microbiology*, (2015) **6**, 717.
- [4] Artemova, T.; Gerardin, Y.; Dudley, C.; Vega, N. M.; Gore, J., *Molecular systems biology*, (2015) **11**, 822.
- [5] Chen, C.-J.; Huang, Y.-C.; Chiu, C.-H., *The Journal of antimicrobial chemotherapy*, (2015), doi: 10.1093/jac/dkv225.
- [6] Donia, M. S.; Ruffner, D. E.; Cao, S.; Schmidt, E. W., *Chembiochem : a European journal of chemical biology*, (2011) **12**, 1230.
- [7] Russell, M.; Daniel, R.; Hall, A.; Sherringham, J., *J Mol Evol*, (1994) **39**, 231.
- [8] Trifonov, E. N., *J. Biomol. Struct. Dyn.*, (2011) **29**, 259.
- [9] Krol, E.; Becker, A., *Proc. Natl. Acad. Sci. U.S.A.*, (2014) **111**, 10702.
- [10] Hoiczyk, E.; Ring, M. W.; McHugh, C. A.; Schwär, G.; Bode, E.; Krug, D.; Altmeyer, M. O.; Lu, J. Z.; Bode, H. B., *Molecular Microbiology*, (2009) **74**, 497.
- [11] Russell, N. J., *Biochemical Society transactions*, (1983) **11**, 333.
- [12] van Meer, G.; Voelker, D. R.; Feigenson, G. W., *Nat. Rev. Mol. Cell Biol.*, (2008) **9**, 112.
- [13] Chapman, D., *Quart. Rev. Biophys.*, (1975) **8**, 185.
- [14] de la Torre, José R; Christianson, L. M.; Béjà, O.; Suzuki, M. T.; Karl, D. M.; Heidelberg, J.; DeLong, E. F., *Proc. Natl. Acad. Sci. U.S.A.*, (2003) **100**, 12830.
- [15] Vossenberg, Jack L. C. M. van de; Driessen, Arnold J. M.; Konings, W. N., *Extremophiles* **2**, 163.
- [16] Slonczewski, J. L.; Rosen, B. P.; Alger, J. R.; Macnab, R. M., *PNAS*, (1981) **78**, 6271.
- [17] Wilks, J. C.; Slonczewski, J. L., *J. Bacteriol.*, (2007) **189**, 5601.
- [18] Sousa, F. L.; Thiergart, T.; Landan, G.; Nelson-Sathi, S.; Pereira, I. A. C.; Allen, J. F.; Lane, N.; Martin, W. F., *Philosophical transactions of the Royal Society of London. Series B, Biological sciences*, (2013), doi: 10.1098/rstb.2013.0088.

- [19] Paul N Black, Concetta C DiRusso, *Microbiology and Molecular Biology Reviews*, (2003), 454.
- [20] Bos, M. P.; Robert, V.; Tommassen, J., *Annual review of microbiology*, (2007) **61**, 191.
- [21] Remaut, H.; Fronzes, R., *Bacterial Membranes: Structural and Molecular Biology*, (2014), 55, Caister Academic Pr.
- [22] Bishop, R. E.; Gibbons, H. S.; Guina, T.; Trent, M. S.; Miller, S. I.; Raetz, C. R., *The EMBO journal*, (2000) **19**, 5071.
- [23] Kaneda, T., *Microbiological Reviews*, (1991) **55**, 288.
- [24] Rock, C. O.; Jackowski, S., *Biochemical and biophysical research communications*, (2002) **292**, 1155.
- [25] Heath, R. J.; Rock, C. O., *Nat. Prod. Rep.*, (2002) **19**, 581.
- [26] DiRusso, C. C.; Black, P. N.; Weimar, J. D., *Progress in Lipid Research*, (1999) **38**, 129.
- [27] Heath, R. J.; Jackowski, S.; Rock C. O., in *Biochemistry of Lipids, Lipoproteins and Membranes*, 55.
- [28] Huynh, F. K.; Green, M. F.; Koves, T. R.; Hirschey, M. D., *Methods in enzymology*, (2014) **542**, 391.
- [29] Nikaido, H., *Microbiology and Molecular Biology Reviews*, (2003) **67**, 593.
- [30] Venkatesan, R.; Wierenga, R. K., *ACS Chem. Biol.*, (2013) **8**, 1063.
- [31] Spratt, S. K.; Black, P. N.; Ragozzino, M. M.; Nunn, W. D., *Journal of Bacteriology*, (1984) **158**, 535.
- [32] Lodish, H.; Berk, A.; Zipursky, S. L.; Matsudaira, P.; Baltimore, D.; Darnell, J., *Oxidation of Glucose and Fatty Acids to CO₂*, (2000), W. H. Freeman.
- [33] Tarini, M.; Cignoni, P.; Montani, C., *IEEE transactions on visualization and computer graphics*, (2006) **12**, 1237.
- [34] Lukacs, C. M.; Fairman, J. W.; Edwards, T. E.; Lorimer, D., *Crystal structure of Acyl-coA dehydrogenase from Burkholderia thailandensis E264*, (2013).
- [35] Dickschat, J. S.; Bode, H. B.; Kroppenstedt, R. M.; Muller, R.; Schulz, S., *Organic & biomolecular chemistry*, (2005) **3**, 2824.

- [36] Hearn, E. M.; Patel, D. R.; Lepore, B. W.; Indic, M.; van den Berg, B., *Nature*, (2009) **458**, 367.
- [37] van den Berg, B.; Black, P. N.; Clemons Jr., W. M.; Rapoport, T. A., *Crystal structure of the bacterial fatty acid transporter FadL from Escherichia coli*, (2004).
- [38] Black, P. N., *Journal of Bacteriology*, (1988) **170**, 2850.
- [39] van den Berg, B., *ChemBioChem*, (2010) **11**, 1339.
- [40] Parsons, J. B.; Rock, C. O., *Prog. Lipid Res.*, (2013) **52**, 249.
- [41] Kang, Y.; Zarzycki-Siek, J.; Walton, C. B.; Norris, M. H.; Hoang, T. T., *PLoS ONE*, (2010) **5**, e13557.
- [42] Lorenzen, W.; Bozhüyük, Kenan A. J.; Cortina, N. S.; Bode, H. B., *Journal of lipid research*, (2014) **55**, 2620.
- [43] Pérez, A. J.; Bode, H. B., *ChemBioChem*, (2015) **16**, 1588.
- [44] Deshmukh, S. K.; Verekar, S. A.; Bhave, S. V., *Frontiers in microbiology*, (2014) **5**, 715.
- [45] Clardy, J.; Fischbach, M. A.; Walsh, C. T., *Nature biotechnology*, (2006) **24**, 1541.
- [46] Bode, H. B., *Current opinion in chemical biology*, (2009) **13**, 224.
- [47] Reimer, D.; Cowles, K. N.; Proschak, A.; Nollmann, F. I.; Dowling, A. J.; Kaiser, M.; Constant, R. f.; Goodrich - Blair, H.; Bode, H. B., *ChemBioChem*, (2013) **14**, 1991.
- [48] Nollmann, F. I.; Heinrich, A. K.; Brachmann, A. O.; Morisseau, C.; Mukherjee, K.; Casanova - Torres, Á. M.; Strobl, F.; Kleinhans, D.; Kinski, S.; Schultz, K.; Beeton, M. L.; Kaiser, M.; Chu, Y.; Phan Ke, L.; Thanwisai, A.; Bozhüyük, Kenan A. J.; Chantratita, N.; Götz, F.; Waterfield, N. R.; Vilcinskis, A.; Stelzer, Ernst H. K.; Goodrich - Blair, H.; Hammock, B. D.; Bode, H. B., *ChemBioChem*, (2015) **16**, 766.
- [49] Cho, S.; Kim, Y., *Journal of Asia-Pacific Entomology*, (2004) **7**, 195.
- [50] Jansen, R.; Kunze, B.; Reichenbach, H.; Höfle, G., *Liebigs Ann./Recl.*, (1996) **1996**, 285.
- [51] Drew, S. W.; Demain, A. L., *Annual review of microbiology*, (1977) **31**, 343.
- [52] Vaidyanathan, S., *Metabolomics*, (2005) **1**, 17.

- [53] Williams, D. H.; Stone, M. J.; Hauck, P. R.; Rahman, S. K., *J. Nat. Prod.*, (1989) **52**, 1189.
- [54] Vining, L. C., *Gene*, (1992) **115**, 135.
- [55] Boer, L. d.; Harder, W.; Dijkhuizen, L., *Arch. Microbiol.* **149**, 459.
- [56] Sprenger, G. A., *Applied microbiology and biotechnology*, (2007) **75**, 739.
- [57] Zhang, S.; Pohnert, G.; Kongsaree, P.; Wilson, D. B.; Clardy, J.; Ganem, B., *The Journal of biological chemistry*, (1998) **273**, 6248.
- [58] Fitzpatrick, P. F., *Current opinion in structural biology*, (2015) **35**, 1.
- [59] *Yeast*, (2000) **1**, 48.
- [60] Moore, B. S.; Hertweck, C.; Hopke, J. N.; Izumikawa, M.; Kalaitzis, J. A.; Nilsen, G.; O'Hare, T.; Piel, J.; Shipley, P. R.; Xiang, L.; Austin, M. B.; Noel, J. P., *Journal of natural products*, (2002) **65**, 1956.
- [61] Reimer, D.; Nollmann, F. I.; Schultz, K.; Kaiser, M.; Bode, H. B., *Journal of natural products*, (2014) **77**, 1976.
- [62] Zhou, Q.; Dowling, A.; Heide, H.; Wöhnert, J.; Brandt, U.; Baum, J.; Ffrench-Constant, R.; Bode, H. B., *Journal of natural products*, (2012) **75**, 1717.
- [63] Joyce, S. A.; Brachmann, A. O.; Glazer, I.; Lango, L.; Schwär, G.; Clarke, D. J.; Bode, H. B., *Angew. Chem. Int. Ed. Engl.*, (2008) **47**, 1942.
- [64] Kronenwerth, M.; Brachmann, A. O.; Kaiser, M.; Bode, H. B., *ChemBioChem*, (2014) **15**, 2689.
- [65] Buscató, E.; Büttner, D.; Brüggerhoff, A.; Klingler, F.-M.; Weber, J.; Scholz, B.; Zivković, A.; Marschalek, R.; Stark, H.; Steinhilber, D.; Bode, H. B.; Proschak, E., *ChemMedChem*, (2013) **8**, 919.
- [66] Khosla, C.; Herschlag, D.; Cane, D. E.; Walsh, C. T., *Biochemistry*, (2014) **53**, 2875.
- [67] Fischbach, M. A.; Walsh, C. T., *Chemical reviews*, (2006) **106**, 3468.
- [68] Finking, R.; Marahiel, M. A., *Annual review of microbiology*, (2004) **58**, 453.
- [69] Fox, G. E., *Cold Spring Harbor perspectives in biology*, (2010) **2**, a003483.
- [70] Walsh, C. T., *ACS chemical biology*, (2014) **9**, 1653.

- [71] Epand, R. M.; Vogel, H. J., *Biochimica et biophysica acta*, (1999) **1462**, 11.
- [72] Fuchs, S. W.; Sachs, C. C.; Kegler, C.; Nollmann, F. I.; Karas, M.; Bode, H. B., *Anal. Chem.*, (2012) **84**, 6948.
- [73] Trauger, J. W.; Kohli, R. M.; Mootz, H. D.; Marahiel, M. A.; Walsh, C. T., *Nature*, (2000) **407**, 215.
- [74] Bruner, S. D.; Weber, T.; Kohli, R. M.; Schwarzer, D.; Marahiel, M. A.; Walsh, C. T.; Stubbs, M. T., *Structure*, (2002) **10**, 301.
- [75] Fuchs, S. W.; Proschak, A.; Jaskolla, T. W.; Karas, M.; Bode, H. B., *Organic & biomolecular chemistry*, (2011) **9**, 3130.
- [76] Bode, H. B.; Reimer, D.; Fuchs, S. W.; Kirchner, F.; Dauth, C.; Kegler, C.; Lorenzen, W.; Brachmann, A. O.; Grün, P., *Chemistry - A European Journal*, (2012) **18**, 2342.
- [77] Nollmann, F. I.; Dauth, C.; Mulley, G.; Kegler, C.; Kaiser, M.; Waterfield, N. R.; Bode, H. B., *Chembiochem*, (2015) **16**, 205.
- [78] Strieker, M.; Tanović, A.; Marahiel, M. A., *Current opinion in structural biology*, (2010) **20**, 234.
- [79] Bode, H. B.; Brachmann, A. O.; Jadhav, K. B.; Seyfarth, L.; Dauth, C.; Fuchs, S. W.; Kaiser, M.; Waterfield, N. R.; Sack, H.; Heinemann, S. H.; Arndt, H.-D., *Angew. Chem. Int. Ed. Engl.*, (2015) **54**, 10352.
- [80] Imker, H. J.; Krahn, D.; Clerc, J.; Kaiser, M.; Walsh, C. T., *Chemistry & biology*, (2010) **17**, 1077.
- [81] Eliopoulos, G. M.; Willey, S.; Reiszner, E.; Spitzer, P. G.; Caputo, G.; Moellering, R. C., *Antimicrobial agents and chemotherapy*, (1986) **30**, 532.
- [82] Steenbergen, J. N.; Alder, J.; Thorne, G. M.; Tally, F. P., *The Journal of antimicrobial chemotherapy*, (2005) **55**, 283.
- [83] Miao, V.; Coëffet-Legal, M.-F.; Brian, P.; Brost, R.; Penn, J.; Whiting, A.; Martin, S.; Ford, R.; Parr, I.; Bouchard, M.; Silva, C. J.; Wrigley, S. K.; Baltz, R. H., *Microbiology (Reading, England)*, (2005) **151**, 1507.
- [84] Ball, L.-J.; Goult, C. M.; Donarski, J. A.; Micklefield, J.; Ramesh, V., *Organic & biomolecular chemistry*, (2004) **2**, 1872.
- [85] Straus, S. K.; Hancock, R. E. W., *Biochimica et biophysica acta*, (2006) **1758**, 1215.

- [86] Siegel, M. M.; Kong, F.; Feng, X.; Carter, G. T., *Journal of mass spectrometry : JMS*, (2009) **44**, 1684.
- [87] Bunkóczi, G.; Vértesy, L.; Sheldrick, G. M., *Acta crystallographica. Section D, Biological crystallography*, (2005) **61**, 1160.
- [88] Biggins, J. B.; Kang, H.-S.; Ternei, M. A.; DeShazer, D.; Brady, S. F., *Journal of the American Chemical Society*, (2014) **136**, 9484.
- [89] Landman, D.; Georgescu, C.; Martin, D. A.; Quale, J., *Clinical microbiology reviews*, (2008) **21**, 449.
- [90] Khandelia, H.; Ipsen, J. H.; Mouritsen, O. G., *Biochimica et biophysica acta*, (2008) **1778**, 1528.
- [91] Freire-Moran, L.; Aronsson, B.; Manz, C.; Gyssens, I. C.; So, A. D.; Monnet, D. L.; Cars, O., *Drug resistance updates : reviews and commentaries in antimicrobial and anticancer chemotherapy*, (2011) **14**, 118.
- [92] Maria-Neto, S.; Almeida, K. C. de; Macedo, M. L. R.; Franco, O. L., *Biochimica et biophysica acta*, (2015).
- [93] Brady, S. F.; Clardy, J., *Organic letters*, (2005) **7**, 3613.
- [94] Craig, J. W.; Cherry, M. A.; Brady, S. F., *J. Bacteriol.*, (2011) **193**, 5707.
- [95] Li, B.; Wever, W. J.; Walsh, C. T.; Bowers, A. A., *Natural product reports*, (2014) **31**, 905.
- [96] Proschak, A.; Schultz, K.; Herrmann, J.; Dowling, A. J.; Brachmann, A. O.; Ffrench-Constant, R.; Müller, R.; Bode, H. B., *ChemBioChem*, (2011) **12**, 2011.
- [97] Janßen, K.; Matissek, R., *Eur Food Res Technol*, (2002) **214**, 259.
- [98] Le Mellay-Hamon, V.; Criton, M., *Biol. Pharm. Bull.*, (2009) **32**, 301.
- [99] Hwang, S.-Y.; Paik, S.; Park, S.-H.; Kim, H.-S.; Lee, I.-S.; Kim, S.-P.; Baek, W.-K.; Suh, M.-H.; Kwon, T. K.; Park, J.-W.; Park, J.-B.; Lee, J.-J.; Suh, S.-I., *International journal of oncology*, (2003) **22**, 151.
- [100] Waters, C. M.; Bassler, B. L., *Annual review of cell and developmental biology*, (2005) **21**, 319.
- [101] Dubinsky, L.; Jarosz, L. M.; Amara, N.; Krief, P.; Kravchenko, V. V.; Krom, B. P.; Meijler, M. M., *Chem. Commun. (Camb.)*, (2009), 7378.
- [102] Yew, J. Y.; Chung, H., *Progress in Lipid Research*, (2015) **59**, 88.

- [103] Fuqua, C.; Parsek, M. R.; Greenberg, E. P., *Annual review of genetics*, (2001) **35**, 439.
- [104] Jindra, M.; Palli, S. R.; Riddiford, L. M., *Annual review of entomology*, (2013) **58**, 181.
- [105] Li, J.; Chen, G.; Webster, J. M., *Canadian journal of microbiology*, (1997) **43**, 770.
- [106] Kennedy, G.; Viziano, M.; Winders, J. A.; Cavallini, P.; Gevi, M.; Micheli, F.; Rodegher, P.; Seneci, P.; Zumerle, A., *Bioorganic & medicinal chemistry letters*, (2000) **10**, 1751.
- [107] Ware, J. C.; Dworkin, M., *Journal of Bacteriology*, (1973) **115**, 253.
- [108] Proschak, A.; Zhou, Q.; Schöner, T.; Thanwisai, A.; Kresovic, D.; Dowling, A.; Ffrench-Constant, R.; Proschak, E.; Bode, H. B., *ChemBioChem*, (2014) **15**, 369.
- [109] Kolb, H. C.; Finn, M. G.; Sharpless, K. B., *Angew. Chem. Int. Ed. Engl.*, (2001) **40**, 2004.
- [110] Huisgen, R., *Proc. Chem. Soc.*, (1961), 357.
- [111] King, M.; Wagner, A., *Bioconjug. Chem.*, (2014) **25**, 825.
- [112] Wang, J.; Wu, F.; Watkinson, M.; Zhu, J.; Krause, S., *Langmuir : the ACS journal of surfaces and colloids*, (2015).
- [113] Arseneault, M.; Wafer, C.; Morin, J.-F., *Molecules (Basel, Switzerland)*, (2015) **20**, 9263.
- [114] Beahm, B. J.; Dehnert, K. W.; Derr, N. L.; Kuhn, J.; Eberhart, J. K.; Spillmann, D.; Amacher, S. L.; Bertozzi, C. R., *Angew. Chem. Int. Ed. Engl.*, (2014) **53**, 3347.
- [115] Agard, N. J.; Prescher, J. A.; Bertozzi, C. R., *J. Am. Chem. Soc.*, (2004) **126**, 15046.
- [116] Kurpiers, T.; Mootz, H. D., *Angew. Chem. Int. Ed. Engl.*, (2009) **48**, 1729.
- [117] Sletten, E. M.; Bertozzi, C. R., *Angew. Chem. Int. Ed. Engl.*, (2009) **48**, 6974.
- [118] Berg, R.; Straub, B. F., *Beilstein journal of organic chemistry*, (2013) **9**, 2715.
- [119] Blomquist, A. T.; Liu, L. H., *J. Am. Chem. Soc.*, (1953) **75**, 2153.
- [120] Jewett, J. C.; Bertozzi, C. R., *Chem. Soc. Rev.*, (2010) **39**, 1272.

- [121] Baskin, J. M.; Prescher, J. A.; Laughlin, S. T.; Agard, N. J.; Chang, P. V.; Miller, I. A.; Lo, A.; Codelli, J. A.; Bertozzi, C. R., *Proc. Natl. Acad. Sci. U.S.A.*, (2007) **104**, 16793.
- [122] Starke, F.; Walther, M.; Pietsch, H.-J., *Arkivoc*, (2010) **2010**, 350.
- [123] Dommerholt, J.; Schmidt, S.; Temming, R.; Hendriks, L. J. A.; Rutjes, Floris P J T; van Hest, Jan C M; Lefeber, D. J.; Friedl, P.; van Delft, F. L., *Angew. Chem. Int. Ed. Engl.*, (2010) **49**, 9422.
- [124] Nessen, M. A.; Kramer, G.; Back, J.; Baskin, J. M.; Smeenk, L. E. J.; Koning, L. J. de; van Maarseveen, J. H.; Jong, L. de; Bertozzi, C. R.; Hiemstra, H.; Koster, C. G. de, *J. Proteome Res.*, (2009) **8**, 3702.
- [125] Finkelstein, A., *The Journal of General Physiology*, (1976) **68**, 127.
- [126] Paula, S.; Volkov, A. G.; van Hoek, A. N.; Haines, T. H.; Deamer, D. W., *Biophysical Journal*, (1996) **70**, 339.
- [127] Park, H. B.; Crawford, J. M., *Journal of natural products*, (2015) **78**, 1437.
- [128] Gough, N. R., *Science Signaling*, (2010) **3**, ec31-ec31.
- [129] Ill, Floyd L. Inman; Singh, S.; Holmes, L. D., *Indian J Microbiol* **52**, 316.
- [130] Pérez, A. J.; Bode, H. B., *Journal of lipid research*, (2014) **55**, 1897.
- [131] Peretó, J.; López-García, P.; Moreira, D., *Trends in biochemical sciences*, (2004) **29**, 469.
- [132] Schwartz, A. W., *Philosophical Transactions of the Royal Society of London B: Biological Sciences*, (2006) **361**, 1743.
- [133] Gull, M., *Challenges*, (2014) **5**, 193.
- [134] Mansy, S. S., *Cold Spring Harbor perspectives in biology*, (2010) **2**, a002188.
- [135] Vaara, M., *Microbiological Reviews*, (1992) **56**, 395.
- [136] Delcour, A. H., *Biochimica et Biophysica Acta (BBA) - Proteins and Proteomics*, (2009) **1794**, 808.
- [137] Cui, L.; Iwamoto, A.; Lian, J.-Q.; Neoh, H.-m.; Maruyama, T.; Horikawa, Y.; Hiramatsu, K., *Antimicrobial agents and chemotherapy*, (2006) **50**, 428.
- [138] Stewart, P. S.; William Costerton, J., *The Lancet*, (2001) **358**, 135.
- [139] Baker, J. G.; Middleton, R.; Adams, L.; May, L. T.; Briddon, S. J.; Kellam, B.; Hill, S. J., *British journal of pharmacology*, (2010) **159**, 772.

- [140] Zhang, W.-J.; Luo, X.; Liu, Y.-L.; Shao, X.-X.; Wade, J. D.; Bathgate, R. A. D.; Guo, Z.-Y., *Amino acids*, (2012) **43**, 983.
- [141] Norregaard, K.; Andersson, M.; Nielsen, P. E.; Brown, S.; Oddershede, L. B., *Nature protocols*, (2014) **9**, 2206.
- [142] Osborn, J., *Life Science News, Amersham Pharmacia Biotech*, (2000), 1.
- [143] Weinman, E. O.; STRISOWER, E. H.; CHAIKOFF, I. L., *Physiological reviews*, (1957) **37**, 252.
- [144] Ong, S.-E., *Molecular & Cellular Proteomics*, (2002) **1**, 376.
- [145] Sletten, E. M.; Bertozzi, C. R., *Accounts of chemical research*, (2011) **44**, 666.
- [146] Colquhoun, D. R.; Lyashkov, A. E.; Ubaida Mohien, C.; Aquino, V. N.; Bullock, B. T.; Dinglasan, R. R.; Agnew, B. J.; Graham, D. R. M., *Proteomics*, (2015) **15**, 2066.
- [147] Liu, W.; Brock, A.; Chen, S.; Chen, S.; Schultz, P. G., *Nature methods*, (2007) **4**, 239.
- [148] Teramoto, H.; Kojima, K., *Biomacromolecules*, (2014) **15**, 2682.
- [149] Lampkowski, J. S.; Villa, J. K.; Young, T. S.; Young, D. D., *Angew. Chem. Int. Ed. Engl.*, (2015) **54**, 9343.
- [150] Kries, H.; Wachtel, R.; Pabst, A.; Wanner, B.; Niquille, D.; Hilvert, D., *Angew. Chem. Int. Ed. Engl.*, (2014) **53**, 10105.
- [151] Ko, T. P.; Wu, S. P.; Yang, W. Z.; Tsai, H.; Yuan, H. S., *Acta crystallographica. Section D, Biological crystallography*, (1999) **55**, 1474.
- [152] Okamoto, A.; Nakai, Y.; Hayashi, H.; Hirotsu, K.; Kagamiyama, H., *Journal of molecular biology*, (1998) **280**, 443.
- [153] Altschul, S. F.; Gish, W.; Miller, W.; Myers, E. W.; Lipman, D. J., *Journal of molecular biology*, (1990) **215**, 403.
- [154] Chemical Computing Group Inc., *Molecular Operating Environment (MOE)*, (2015), 1010 Sherbooke St. West, Suite #910, Montreal, QC, Canada, H3A 2R7.
- [155] Haun, R. S.; Quick, C. M.; Siegel, E. R.; Raju, I.; Mackintosh, S. G.; Tackett, A. J., *Cancer biology & therapy*, (2015), doi: 10.1080/15384047.2015.1071740.
- [156] Speers, A. E.; Cravatt, B. F., *Chemistry & biology*, (2004) **11**, 535.

- [157] Schultz, M. K.; Parameswarappa, S. G.; Pigge, F. C., *Organic letters*, (2010) **12**, 2398.
- [158] Buncherd, H.; Nessen, M. A.; Nouse, N.; Stelder, S. K.; Roseboom, W.; Dekker, H. L.; Arents, J. C.; Smeenk, L. E.; Wanner, M. J.; van Maarseveen, J. H.; Yang, X.; Lewis, P. J.; Koning, L. J. de; Koster, C. G. de; Jong, L. de, *J Proteomics*, (2012) **75**, 2205.
- [159] Canalle, L. A.; Vong, T.; Adams, P Hans H M; van Delft, F. L.; Raats, J. M. H.; Chirivi, R. G. S.; van Hest, Jan C M, *Biomacromolecules*, (2011) **12**, 3692.
- [160] Uzunović, S.; Bedenić, B.; Budimir, A.; Kamberović, F.; Ibrahimagić, A.; Delić-Bikić, S.; Sivec, S.; Meštrović, T.; Brkić, D. V.; Rijnders, Michelle I. A.; Stobberingh, E. E., *Wiener klinische Wochenschrift*, (2014) **23-24**, 747.
- [161] Chen, X.; Wei, S.; Ji, Y.; Guo, X.; Yang, F., *Proteomics*, (2015) **15**, 3175.
- [162] Metabolomics Society, ed., *GeoRge: Generalizable statistically-oriented R-workflow for isotopic label-tracking experiments*, (2015).
- [163] Noro, J. C.; Kalaitzis, J. A.; Neilan, B. A., *Chemistry & biodiversity*, (2012) **9**, 2077.
- [164] Evans, B. S.; Robinson, S. J.; Kelleher, N. L., *Fungal genetics and biology : FG & B*, (2011) **48**, 49.
- [165] MAIMAN, T. H., *Nature*, (1960) **187**, 493.

7 Attachments

7.1 Publication: “ ω -Azido fatty acids as probes to detect fatty acid biosynthesis, degradation, and modification“

Authors: Alexander J. Pérez¹, Helge B. Bode¹

¹Merck Stiftungsprofessur für Molekulare Biotechnologie, Fachbereich Biowissenschaften, Goethe Universität Frankfurt, 60438 Frankfurt am Main, Germany

Published in: Journal of Lipid Research, July 10, 2014, Volume 55, page 1897-1901

Digital Object Identifier: 10.1194/jlr.M047969

Elaboration of the contributions of each author to the publication in question

Title of the publication: “ ω -Azido fatty acids as probes to detect fatty acid biosynthesis, degradation, and modification“

Project phase	Contribution of the authors
1) Planning and development	HBB: 50%; AJP: 50%
2) Execution of experiments	AJP: 100%
3) Creation of figures and data sheets	HBB: 20%; AJP: 80%
4) Interpretation/Analysis of data	AJP: 100%
5) Abstract/Results/Discussion	HBB: 50%; AJP: 50%

Title: ω -Azido fatty acids as probes to detect fatty acid biosynthesis, degradation and modification

Author names: Alexander J. Pérez, Helge B. Bode*

Affiliations: Merck Stiftungsprofessur für Molekulare Biotechnologie, Fachbereich Biowissenschaften, Goethe Universität Frankfurt, Max-von-Laue-Str. 9, 60438 Frankfurt am Main, Germany

Corresponding author: Prof. Dr. Helge B. Bode, Merck Stiftungsprofessur für Molekulare Biotechnologie, Fachbereich Biowissenschaften, Goethe Universität Frankfurt, Max-von-Laue-Str. 9, 60438 Frankfurt am Main, Germany. E-Mail: h.bode@bio.uni-frankfurt.de Phone: 0049-6979829557. Fax: 0049-6979829527

Disclosure summary: The authors have nothing to disclose

Abstract

Fatty acids (FAs) play a central role in the metabolism of almost all known cellular life forms. Although gas chromatography coupled to mass spectrometry (GC-MS) is regarded as a standard method for FA analysis, other methods as high performance liquid chromatography coupled to mass spectrometry (HPLC-MS) are nowadays widespread but are rarely applied to FA analysis. Here we present azido-FAs as probes that can be used to study FA biosynthesis (elongation, desaturation) or degradation (β -oxidation) upon their uptake, activation and metabolic conversion. These azido-FAs are readily accessible by chemical synthesis and their metabolic products can be easily detected after click-chemistry based derivatization with high sensitivity by HPLC-MS, contributing a powerful tool to FA, and hence, lipid analysis in general.

Keywords: azido fatty acid; click-chemistry; beta-oxidation; fatty acid metabolism; fatty acid biosynthesis; fatty acid desaturation; strained promoted cycloaddition; cyclooctyne; azido-fatty acid-SNAC

Introduction

Fatty acids (FAs) are found in all known living organisms, playing a vital role in cell compartmentalization, energy storage and secondary metabolite production. In bacteria, most FAs are found in the cell membrane as part of the lipid bilayer (1). The actual FA profile of a cell can strongly vary, depending on environmental and developmental conditions, requiring *de novo* biosynthesis, degradation and modification of the FAs involved (2-5). The monitoring of these metabolic pathways is usually conducted by gas chromatography coupled to mass spectrometry (GC-MS) of FA methyl esters or other volatile FA derivatives (6). In spite of its merits, such as high sensibility and direct observability of especially volatile natural products, it is desirable to have also simple and effective methods of FA analysis *via* high performance liquid chromatography coupled to mass spectrometry (HPLC-MS), which today is a widespread tool in analytical chemistry as well. However, HPLC-MS based FA analysis is difficult mainly because of little ionizability and hence little signal strength. Small modifications introduced to certain FAs however can greatly increase ionizability while decreasing lipophilicity, which in turn increases signal resolution on reversed phase HPLC systems (7).

The method we developed for HPLS/MS-based detection of FA intermediates involves two steps: (i) simple preparation of FAs with a terminal azido group (AFAs) that allows most FA modifications to occur, (ii) use of these AFAs as metabolic probes and labeling of the *in vivo* formed derivatives in the corresponding organism with tetramethoxydibenzoazacyclooctyne (TDAC, **1**, Figure 1), a cyclooctyne synthesized originally by Starke *et al.* (8, 9), and (iii) the detection of the clicked compounds by HPLC/MS. Although usually a reporter function such as a fluorophore is linked to the alkyne reagent, no such modifications were needed here, since the formation of an electron-rich triazole ring make it quite susceptible to

protonation and thus detection by mass spectrometry (MS), especially as the molecular mass range of the clicked FAs differs strongly from other lipophilic compounds found in most cells. AFAs are bioorthogonal, do not react with other functional groups other than alkynes, are easily taken up by the cells like other FAs when externally added and can be used to follow the fate of AFAs in a given organisms in real time. Thus AFAs will add to the overall toolbox of lipid analysis in general. Similarly, alkyne modified cholesterol has been used recently to trace cellular cholesterol metabolism and localization (10).

Results and discussion

Prior to the application of AFAs as molecular probes for FA metabolism, a library of eight AFAs of varying chain length was synthesized (**2a-h**, Figure 1A) from the corresponding ω -bromo-fatty acids in a one-step reaction (Scheme S1). TDAC, obtained by a simple three step synthesis (Scheme S2), good click properties and formidable solubility in a wide range of solvents, as it is common to heterocyclic, methoxylated cyclooctynes (11, 12), was then reacted with these AFAs and subsequently analyzed by HPLC-MS (Figure 1). Since 15-bromopentadecanoic acid was not commercially available it was synthesized from pentadecanolide by hydrolysis and subsequent bromination of the resulting 15-hydroxypentadecanoic acid for direct use in the corresponding AFA synthesis (Scheme S3). The results showed tremendous signal amplification by a factor of about 5000 in the extracted ion chromatogram (EIC) of the clicked product as the $[M+H]^+$ ion in comparison to the free AFA (Figure S1A), along with clear differences in retention time according to the chain length of the corresponding AFA (Figure 1B). Due to this strong increase in sensitivity resulting from the formation of the triazole unit a relative quantification also between different TDAC-modified AFAs seems to be reasonable.

Each signal consists of a characteristic double-peak, representing the two regioisomers formed in different amounts in accordance with the findings of Starke *et al.* for **3b/4b**. This regioselectivity corresponds to the different steric demand of each of the transition states (9). It was observed that the more abundant isomers **3a-h** had slightly higher retention times than the less abundant **4a-h**. Analysis of the MS² fragmentation pattern revealed distinct neutral losses for each of the two isomers. In particular, the minor isomer always features a dominant loss of water, followed by loss of the carboxylic group in the form of a dihydroxycarbene, whereas the main isomer predominantly shows only the loss of the latter group (Figure S1B). Thus, by comparing the characteristic fragmentation patterns, retention times and peak shapes, simple identification of fatty acid metabolites becomes possible.

In order to test whether AFAs can be used for the analysis of FA metabolism, β -oxidation was investigated initially. β -Oxidation is the primary FA degradation pathway in most organisms, consisting of desaturation, hydratization, oxidation and finally thiolysis of the resulting CoA-bound 3-keto-FA residue, resulting in the formation of acetyl-CoA and an acyl-CoA residue shortened by two carbon atoms (Figure S2) (13, 14). In most bacteria the basic steps are performed by only three proteins: FadE (desaturation), FadB (hydratization and oxidation) and FadA (thiolysis) (15). Thus, a feeding experiment was conducted in which a long chain AFA was fed to *E. coli* DH10B. Hydrolysis of this culture and derivatisation with TDAC allowed the combined detection of free and (previously) bound FA β -oxidation degradation products clearly showing that ω -azido FAs are tolerated by the β -oxidation machinery. Indeed, C₁₆-AFA (**2h**) was readily degraded in C₂-steps, leading to a degradation product as short as 4-azidobutanoic acid (**2a**) resulting in the detection of **3a/4a** (Figure 2A). Additionally, also the 3-keto and the 3-hydroxy

forms were detectable when high concentrations of the corresponding non-oxidized AFAs were reached (Figure S3). The retention times of these metabolic intermediary products proved to be similar to their saturated counterparts for long chain AFAs, while being slightly lower for short chained AFAs and clearly different from the retention times of C_{n+1} -AFAs which have the same nominal mass as the corresponding C_{n-3} -keto-AFAs.

Next, the degradation of **2h** was analyzed over time in different *E. coli* strains with mutations in *fadA* (JW5578) and *fadE* (JW5020), with *ilvE* (JW5606) as a control. The *fadA* mutant supposedly lacked the ability to conduct the final thiolysis step, whereas the *fadE* mutant lacked the acyl-CoA dehydrogenase. In the control strain (with a defect in leucine degradation not influencing FA metabolism) signals correlated to C_{14} - and C_{12} -AFA (**2i** and **2f**, respectively) showed a maximum at 2.3 and 2.8 h after the addition of **2h**, respectively, and also shorter degradation products could be observed (Figure 2B). Notably, analysis of the *fadA* mutant showed no difference to the *ilvE* control strain (not shown), indicating the functional complementation of the *fadA* mutation, while the *fadE* mutant showed no degradation activity at all (Figure S4) (16). The decrease in concentration of **2h** in the latter experiment might be attributed to absorption on the glass wall of the cultivation flasks or micelle formation in the medium. Similarly, C_{15} -AFA (**2g**) was also fed to the *E. coli* wildtype and degradation products of uneven carbon chain length could be observed as expected (Figure S5). This also proved that AFA incorporation and degradation is not dependent on a specific chain length, but occurs with several long chain AFAs furthermore indicating the broad applicability of AFAs for degradation studies.

Next, FA biosynthesis was studied, generally requiring the condensation of a given FA thioester with malonyl-ACP leading to an elongation in C₂-steps in a fashion reverse to FA degradation (Figure S2). Therefore acyl-ACP-mimicking S-azidoacyl-N-acetylcysteamines (azidoacyl-SNACs) of five or six carbons in acyl chain length were synthesized (**5a** and **5b**, respectively; see SI) and fed to the *E. coli fadE* mutant and to the wildtype (DH10B) as control. The wildtype showed only trace amounts of **3g** and **3k** (Figure 3A), whereas elongated AFA derivatives up to C₁₅-AFA (**3g**) could be observed in the *fadE* mutant during the first 12 h after the addition of **5a** (Figure 3B). No elongation could be observed when C₆-azidoacyl-SNAC (**5b**) was fed (not shown), which implies that **5a** more closely resembles the natural FA and is well tolerated by the FA biosynthesis machinery.

Besides FA degradation and biosynthesis also FA modification can be studied using the described approach: *Psychrobacter urativorans*, formerly known as *Micrococcus cryophilus*, is a Gram-negative psychrophilic bacterium found in cold habitats that possesses a simple membrane FA composition, consisting mostly of Δ⁹-unsaturated palmitoleate and oleate residues (17, 18). When adapting to temperature changes in the range of 0-20°C, *P. urativorans* changes its FA profile by varying the ratio of the two main FA residues in the membrane (19, 20). Feeding C₁₆-AFA (**2g**) to a culture of *P. urativorans* at 16°C followed by the subsequent detection of a mono-unsaturated FA with slightly reduced retention time (**3m/4m**, Figure 4) confirming that indeed a desaturase is involved in this process.

Materials and Methods

General experimental procedures

Solvents and reagents were obtained from Sigma-Aldrich (München, Germany). TDAC was synthesized as by the procedure described by Starke *et al.* (9) and can be obtained from the authors of this work. Alternative cyclooctynes, such as dibenzocyclooctyne-amine, with comparable structures can be obtained commercially from Sigma-Aldrich and mostly share the abilities of the cyclooctyne chosen in this work. Silica chromatographic purification was performed on a Biotage SP1™ Flash Purification System (Biotage, Uppsala, Sweden), using 40+M, 25+M or 12+M KP-Sil Cartridges (Biotage, Uppsala, Sweden) in combination with an UV detector. ^1H , ^1H - ^1H -COSY, ^1H - ^{13}C -HSQC and ^1H - ^{13}C -HMBC NMR spectra for the synthesis products were recorded on a Bruker AV500 (500 MHz), AV400 (400 MHz) or AM250 (250 MHz) spectrometer using CDCl_3 or CD_3CN as solvent and internal standard, using the chemical shifts described by Gottlieb *et al.* (21) with the exception of the ^{13}C -shift of CDCl_3 which was set to 77.00 ppm. ^1H -NMR: CHCl_3 : $\delta = 7.24$ ppm; CH_3CN : $\delta = 1.96$ ppm; ^{13}C -NMR: CDCl_3 : $\delta = 77.00$ ppm; CD_3CN : $\delta = 118.26$ ppm. ESI HPLC MS analysis was performed with a Dionex UltiMate 3000 system coupled to a Bruker AmaZon X mass spectrometer and an Acquity UPLC BEH C18 1.7 μm RP column (Waters) using a MeCN/0.1 % formic acid in H_2O gradient ranging from 5 to 95 % in 22 min. at a flow rate of 0.6 mL/min (22). High resolution mass spectra were obtained from a MALDI LTQ Orbitrap XL (Thermo Fisher Scientific, Inc., Waltham, MA), equipped with a laser at 337 nm. A 4-chloro- α -cyanocinnamic acid matrix was used, and the sum formulas and according masses were internally calibrated using fluorescein (monoisotopic mass = 332.068473) as a standard (23).

Bacterial strains and culture conditions

All *Escherichia coli* strains used in this study were grown on solid and liquid Luria-Bertani (LB, pH 7.0) medium at 30 °C and 180 rpm on a rotary shaker. The mutants and controls obtained from the Coli Genetic Stock Center were grown in the presence of kanamycin (40 µg/mL). *Psychrobacter urativorans* (ATCC 15174) was obtained from the German Collection of Microorganisms and Cell Cultures (DSMZ) and grown on solid and liquid Oxoid nutrient broth (DSMZ medium 948) at 16 °C on a rotary shaker at 210 rpm.

Feeding experiments for observation of fatty acid degradation and desaturation

The feeding experiments for the observation of the degradation of fatty acids were conducted with 16-azidoheptadecanoic acid. The compound was fed at a final concentration of 1 mmol/L to a culture of *fadE*, *fadA* and *ilvE* respectively. Cultures were grown in 250 mL Erlenmeyer flasks containing 30 mL of LB medium. Inoculation was performed from a preculture that was incubated overnight. The OD was set to 0.1 and the culture was incubated at 30 °C and 180 rpm for 3h before feeding ensued and samples of 1 mL were taken. The samples were frozen in liquid nitrogen and freeze-dried before adding 1 mL 1 M NaOH and heated to 80 °C for 4h. Thereafter the now clear solution was acidified with 190 µL of 6 M HCl and 1 mL of Hexane was added. After vigorous stirring the samples were centrifuged for 5 minutes at 4000 rpm (3220 g) and 700 µL of the supernatant were removed, dried and taken up in 500 µL of Acetonitrile, after which 40 µL of a 10 mM solution of the pre-purified raw product of **1** was added. The reaction was allowed to occur at room temperature for 24h before HPLC-MS analysis. The experiments with *P. urativorans* were conducted in the same fashion under different incubation conditions as described above.

Feeding experiments for fatty acid elongation observation

The feeding experiments for the observation of the elongation of fatty acids were either conducted with *S*-(5-azidopentanoyl)-*N*-acetylcysteamine or *S*-(6-azidohexanoyl)-*N*-acetylcysteamine respectively. The compounds were fed at a final concentration of 2 mmol/L to a culture of *fadE*, *fadA* and DH10B. Cultures were grown in 100 mL Erlenmeyer flasks containing 10 mL of LB medium, including kanamycin in the concentration mentioned above in the case of *fadE* and *fadA*. Inoculation was performed from a preculture that was incubated over night. The OD was set to 0.1 and the culture was incubated at 30 °C and 180 rpm for 2h before feeding ensued and samples of 700 µL were taken. To these samples 200 µL 4 M NaOH and heated to 90 °C for 1 h. Thereafter the now clear solution was acidified with 200 µL of 6 M HCl and 800 µL of Hexane were added. After vigorous stirring the samples were centrifuged for 5 minutes at 13300 rpm (17000 g) and 600 µL of the supernatant were removed, dried and taken up in 100 µL of Acetonitrile, after which 10 µL of a 0.1 M solution of the pre-purified raw product of **1** was added. The reaction was allowed to occur at 50 °C for 1h before HPLC-MS analysis.

Summary

The use of AFAs in combination with modern and easy to synthesize cyclooctynes such as TDAC has shown to be a viable method for the analysis of FA metabolism, ranging from biosynthesis to degradation and desaturation. Since no degradation products smaller than 4-azidobutanoic acid (**2a**) have been detected, it can be assumed that **2a** cannot be degraded. This might lead to increased availability of labeled FAs even after prolonged metabolisation as compared to completely degradable isotope labels (24). The azido label forms an easily detectable triazole ring after reacting with a cyclooctyne and is readily introduced into the desired target

compound, thus allowing a wide range of applications in a time resolved manner at low cost and high sensitivity. Our method can easily be applied to study also FA uptake or FA activation, which can be coupled to FA β -oxidation and can be detected by our approach. Moreover, it can also be applied not only to FA but lipid metabolism in general. For the latter, simply leaving out the hydrolytic step during sample preparation would enable the detection of acylcarnitines or CoA derivatives as well as other lipid species carrying the respective AFA not only in bacteria but all organisms including mammals in which lipid metabolism needs to be studied.

Acknowledgements

This work was supported by an European Research Council starting grant under grant agreement no. 311477.

References

1. Spector, A. A. 1999. Essentiality of fatty acids. *Lipids*, **34** Suppl: S1-3.
2. Aguilar, P., D. Mendoza. 2006. Control of fatty acid desaturation: a mechanism conserved from bacteria to humans. *Mol. Microbiol.* **62**: 1507-1514.

3. Di Pasqua, R., N. Hoskins, G. Betts, G. Mauriello. 2006. Changes in membrane fatty acids composition of microbial cells induced by addition of thymol, carvacrol, limonene, cinnamaldehyde, and eugenol in the growing media. *J. Agric. Food Chem.* **54**: 2745-2749.
4. Russell, N. J. 1984. Mechanisms of thermal adaptation in bacteria: blueprints for survival. *TIBS*, **9**: 108-112.
5. Ingram, L. 1976. Adaptation of membrane lipids to alcohols. *J. Bacteriol.* **125**: 670-678.
6. Griffiths W. J. 2003. Tandem mass spectrometry in the study of fatty acids, bile acids, and steroids. *Mass Spectrom. Rev.* **22**: 81-152.
7. Hang, H. C., J. P. Wilson, G. Charron. 2011. Bioorthogonal chemical reporters for analyzing protein lipidation and lipid trafficking. *Acc. Chem. Res.* **44**: 699-708.
8. Jewett, J. C., C. R. Bertozzi. 2010. Cu-free click cycloaddition reactions in chemical biology. *Chem. Soc. Rev.* **39**: 1272-1279.
9. Starke, F., M. Walther. H. Pietzsch. 2010. A novel dibenzoazacyclooctyne precursor in regioselective copper-free click chemistry. An innovative 3-step synthesis. *ARKIVOC XI*: 350-359.
10. Hofmann, K., C. Thiele, H. F. Schött, A. Gaebler, M. Schoene, Y. Kiver, S. Friedrichs, D. Lütjohann, L. Kuerschner. 2014. A novel alkyne cholesterol to trace cellular cholesterol metabolism and localization. *J. Lipid Res.* **55**: 583-591.
11. Sletten, E. M., C. R. Bertozzi. 2008. A Hydrophilic Azacyclooctyne for Cu-Free Click Chemistry. *Org. Lett.* **10**: 3097-3099.

12. van Geel, R., G. J. M. Pruijin, F. L. van Delft, W. C. Boelens. 2012. Preventing thiol-yne addition improves the specificity of strain-promoted azide-alkyne cycloaddition. *Bioconjugate Chem.* **23**: 392-398.
13. Heath R. J., C. O. Rock. 2002. The Claisen condensation in biology. *Nat. Prod. Rep.* **19**: 581-596.
14. Parsons J. B., C. O. Rock. 2013. Bacterial lipids: metabolism and membrane homeostasis *Prog. Lipid Res.* **52**: 249-276.
15. Campbell J. W., J. E. Cronan Jr. 2002. The Enigmatic *Escherichia coli* *fadE* Gene Is *yafH*. *J. Bacteriol.* **184**: 3759-3764.
16. Campbell J. W., R. M. Morgan-Kiss, J. E. Cronan Jr. 2003. A new *Escherichia coli* metabolic competency: growth on fatty acids by a novel anaerobic beta-oxidation pathway. *Mol. Microbiol.* **47**: 793-805.
17. Russell, N. J. 1983. Adaptation to temperature in bacterial membranes. *Biochem. Soc. Trans.* **11**: 333-335.
18. Li Y.; D. Dietrich, R. D. Schmid, B. He, P. Ouyang, V. B. Urlacher. 2008. Identification and functional expression of a Delta9-fatty acid desaturase from *Psychrobacter urativorans* in *Escherichia coli*. *Lipids* **43**: 207-213.
19. Russell, N. J. 1971. Alteration in fatty acid chain length in *Micrococcus cryophilus* grown at different temperatures. *Biochim. Biophys. Acta* **231**: 254-256.
20. Sandercock, S., N. J. Russell. 1980. The Elongation of Exogenous Fatty Acids and the Control of Phospholipid Acyl Chain Length in *Micrococcus cryophilus*. *Biochem. J.* **188**: 585-592.
21. Gottlieb H. E., V. Kotlyar, A. Nudelman. 1997. NMR Chemical Shifts of Common Laboratory Solvents as Trace Impurities. *J. Org. Chem.* **62**: 7512-7515.

22. Reimer D., K. M. Pos, M. Thines, P. Grün, H. B. Bode. 2011. A natural prodrug activation mechanism in nonribosomal peptide synthesis. *Nat. Chem. Biol.* **7**: 888-890.
23. Fuchs S. W., C. C. Sachs, C. Kegler, F. I. Nollmann, M. Karas, H. B. Bode. 2012. Neutral Loss Fragmentation Pattern Based Screening for Arginine-Rich Natural Products in *Xenorhabdus* and *Photorhabdus*. *Anal. Chem.* **84**: 6948-6955.
24. Weinman, E. O., E. H. Strisower, L. L. Chaikoff. 1957. Conversion of Fatty Acids to Carbohydrate: Application of Isotopes to this Problem and Role of the Krebs Cycle as a Synthetic Pathway. *Physiol. Rev.* **37**: 252-272.

Figure legends

Fig. 1. (A) Reaction of TDAC with various AFAs resulting in two regioisomers per AFA. Several AFAs (**2i-1**) were only produced *in vivo* and henceforth detected as their clicked products (**3i-1** and **4i-1**). (B) EICs of the click product of TDAC with the eight synthesized AFAs. Where visible, the smaller peak arises from **4a-h** and the larger one from **3a-h**.

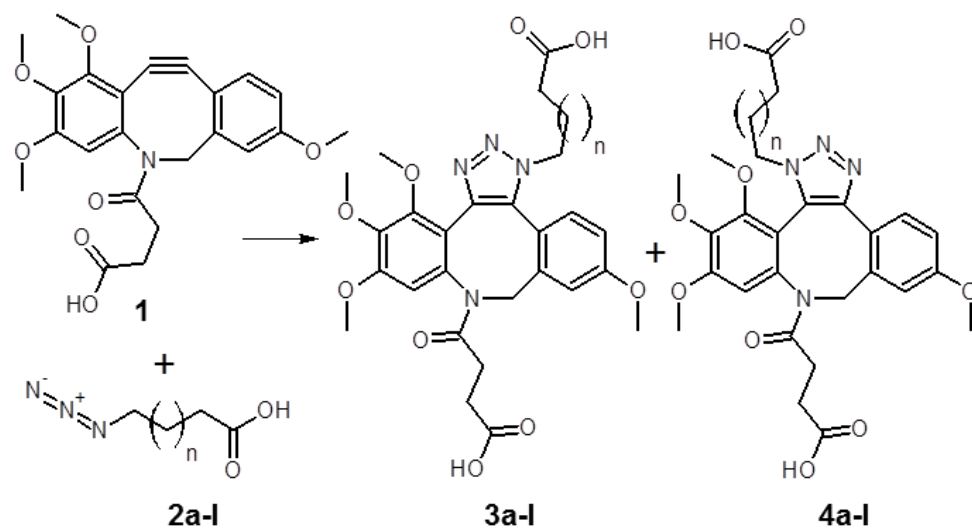
Fig. 2. (A) EICs of click-labeled degradation products of **2h** 12h after initial feeding at 1 mM. The same amount of **2h** was fed again right before the sample was taken. **3h/4h** = TDAC-C₁₆-AFA, **3l/4l** = TDAC-C₁₄-AFA, **3f/4f** = TDAC-C₁₂-AFA, **3d/4d** = TDAC-C₁₀-AFA, **3i/4i** = TDAC-C₈-AFA, **3c/4c** = TDAC-C₆-AFA, **3a/4a** = TDAC-C₄-AFA. (B) Relative peak area (in % relative to the amount of **3h+4h**) of **2h** degradation products when fed to *ilvE*-mutant. Increasing amounts of C₁₄- and C₁₂-AFA can be seen 1h after feeding, followed by further degradation products.

Fig. 3: (A) EICs of clicked uneven AFAs immediately after and 24h after feeding of **5a** (detected as **3b/4a**) to *fadE* mutant. The other EICs prove the production of C₉- (**3j**), C₁₁- (**3e**), C₁₃- (**3k/4k**) and C₁₅-AFA (**3g/4g**). Even after 24h the wildtype (DH10B) only shows minimal production of C₁₃- (**3k**) and C₁₅-AFA (**3g**). (B) Relative peak areas (in % relative to the area of **3b+4b**) of various AFAs from the feeding experiment with the *fadE* mutant. C₁₅-AFA (as click product **3g**) can clearly be seen as emerging main product of FA elongation. Production of C₇-AFA could not be detected due to signal overlap with an impurity in the TDAC reagent.

Fig. 4. Desaturase activity shown in *P. urativorans*. The EIC of the clicked AFAs shows that C₁₆-AFA (shown as click products **3h** and **4h**) is converted to the monodesaturated C_{16:1}-AFA (shown as click products **3m** and **4m**, with the regiochemistry assumed to be the same as with **3a-l** and **4a-l** respectively).

Figure 1

A



	n	2a-l	3a-l	4a-l
Synthesized	1	2a	3a	4a
	2	2b	3b	4b
	3	2c	3c	4c
	7	2d	3d	4d
	8	2e	3e	4e
	9	2f	3f	4f
	12	2g	3g	4g
	13	2h	3h	4h
Detected	5	2i	3i	4i
	6	2j	3j	4j
	10	2k	3k	4k
	11	2l	3l	4l

B

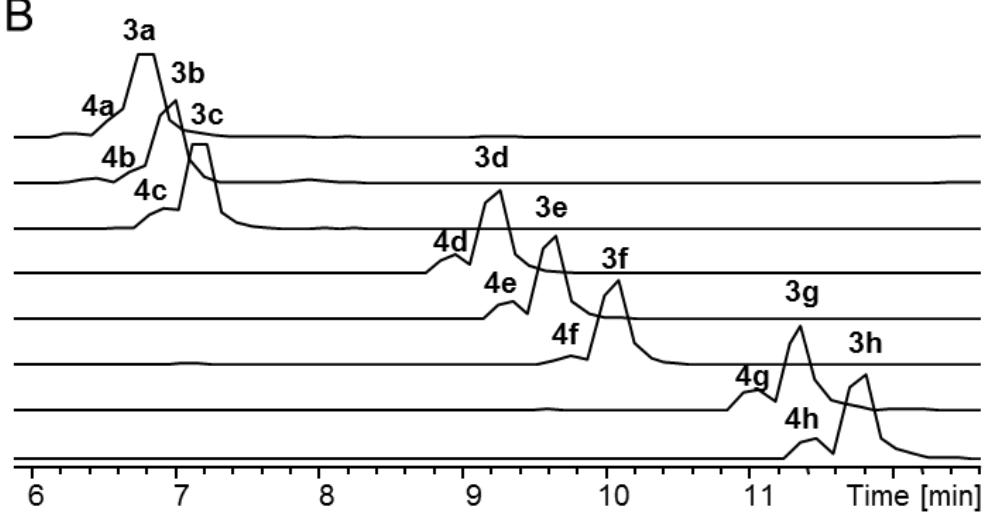


Figure 2

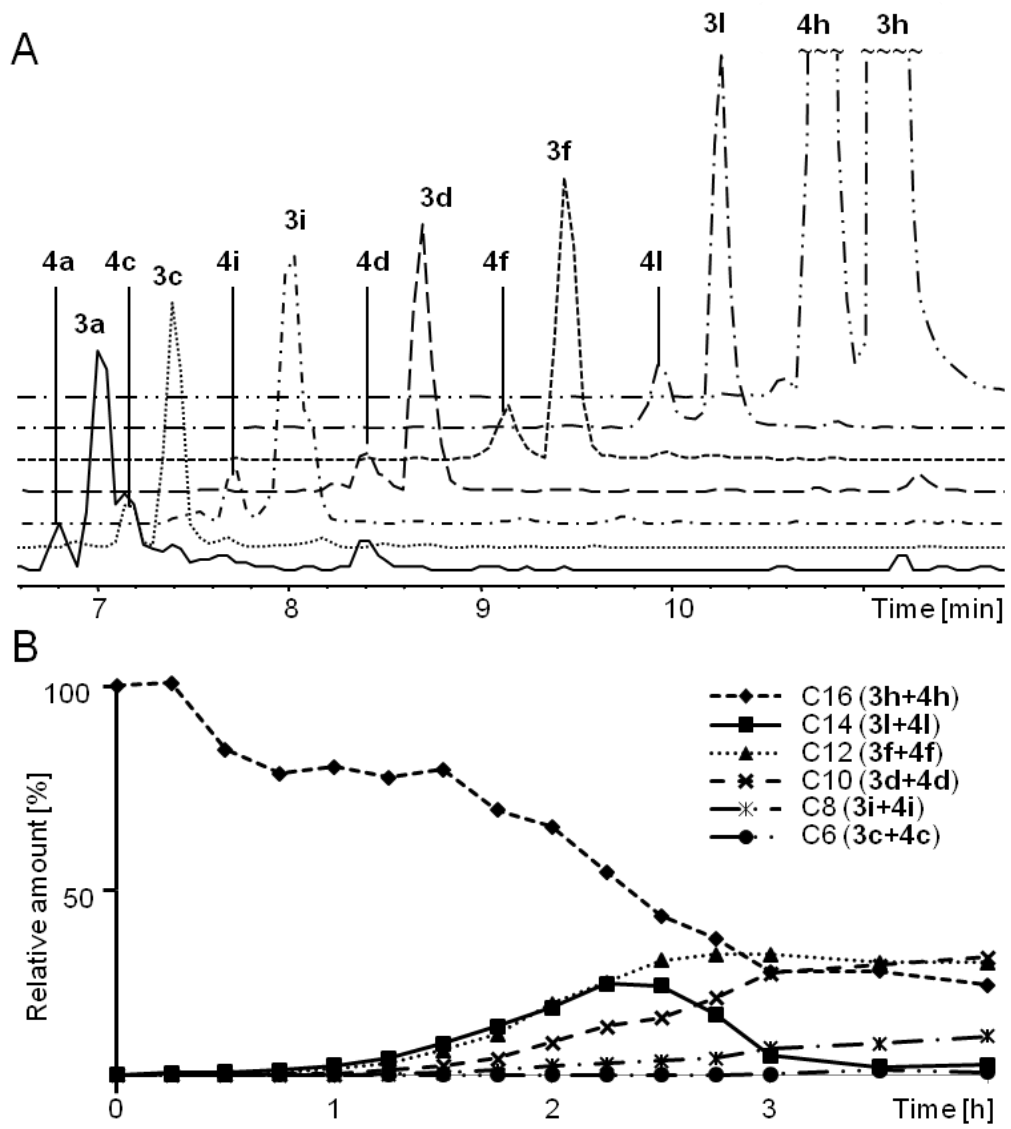


Figure 3

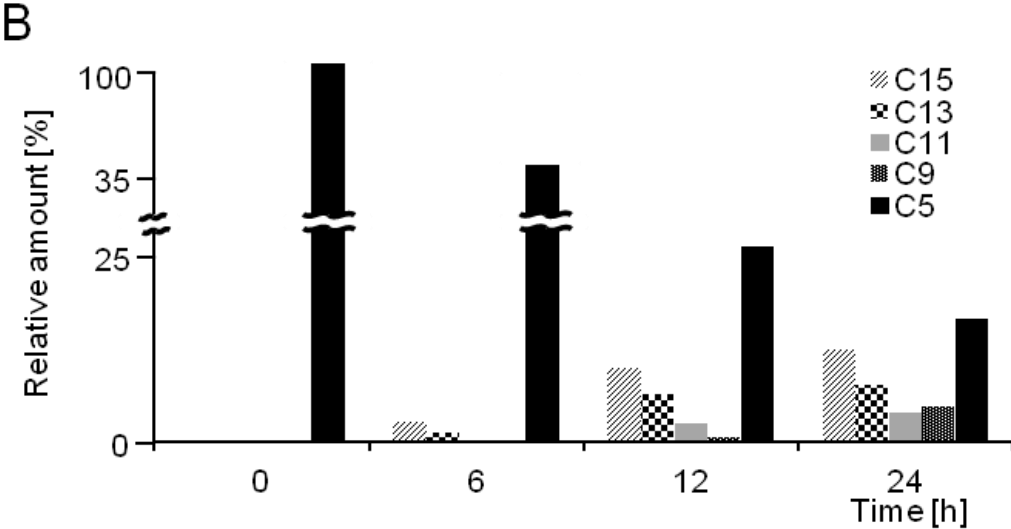
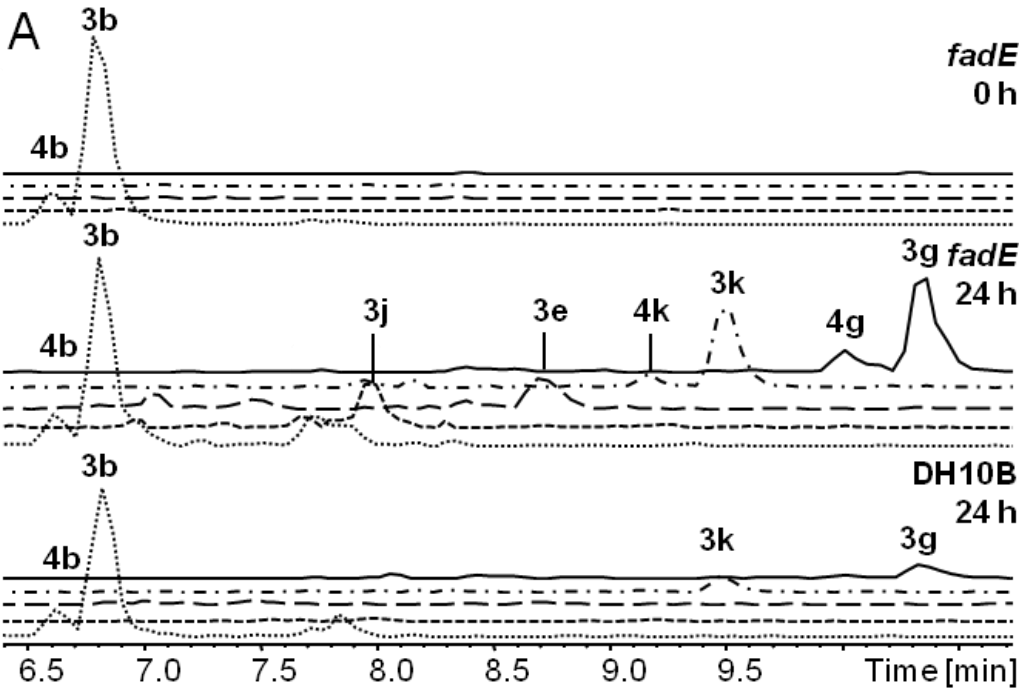
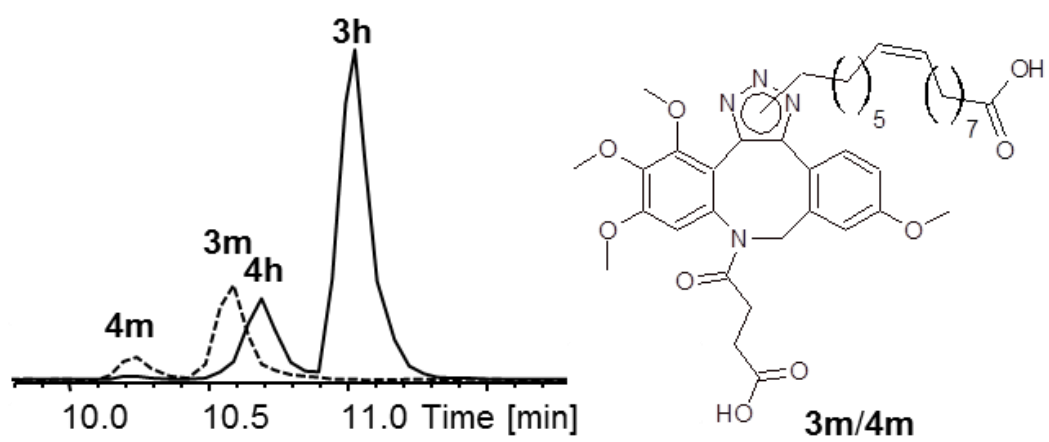


Figure 4



Analysis of fatty acid metabolism using Click- Chemistry and HPLC-MS

Alexander J. Pérez and Helge B. Bode

-Supporting Information-

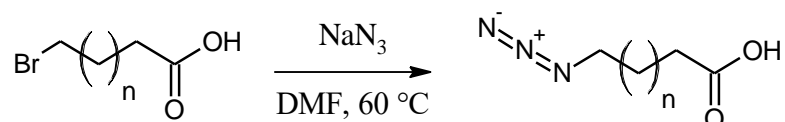
Contents

Experimental section	Page S2
Supplementary figures	Page S9
NMR spectra	Page S13

Experimental section

General procedure for the synthesis of azido fatty acids (2a,b,c,d,e,f,h)

Scheme S1. Synthesis of azido fatty acids.



All azido fatty acids were synthesized in the same way with slightly differing starting amounts. The general procedure of the reaction of the corresponding bromide with 3 equivalents of sodium azide is exemplified for the synthesis of 16-azidohexanoic acid (**1h**):

16-Azidohexadecanoic acid (**2h**)

To a solution of 16-bromohexadecanoic acid (1.5 g, 4.47 mmol) in 10 mL dry DMF, sodium azide (872 mg, 13.4 mmol, 3 eq.) was added and stirred for 44h at 60 °C. Subsequently the solvent was evaporated and 50 mL of aqueous HCl were added. The raw product was extracted three times with 30 mL of EtOAc, the organic fractions were combined and dried over Na_2SO_4 . Purification was conducted by column chromatography on silica, eluting with Hexane to Hexane/EtOAc (1:1), giving the product as a white solid (1.06 g, 3.55 mmol, 79%). ^1H NMR (500 MHz, CDCl_3) δ = 1.15 -1.43 (m, 22H), 1.49-1.69 (m, 4H), 2.33 (t, J = 7.5 Hz, 2H), 3.23 (t, J = 6.9 Hz); ^{13}C NMR (500 MHz, CDCl_3) δ = 24.7, 26.7, 28.1, 29.0, 29.1, 29.2, 29.4, 29.5, 29.5, 29.6, 29.6, 29.6, 29.6, 34.0, 51.5, 180.0.

12-Azidododecanoic acid (**2f**)

Yield: 723 mg, 3.0 mmol, 84%. ^1H NMR (250 MHz, CDCl_3) δ = 1.15-1.41 (m, 14H), 1.49-1.69 (m, 4H), 2.32 (t, J = 7.5 Hz, 2H), 3.23 (t, J = 6.9 Hz); ^{13}C NMR (250 MHz, CDCl_3) δ = 24.6, 26.7, 28.8, 29.0, 29.1, 29.2, 29.3, 29.4, 29.4, 34.0, 51.5, 180.2.

11-Azidoundecanoic acid (2e)

Yield: 462 mg, 2.03 mmol, 54%. ^1H NMR (250 MHz, CDCl_3) δ = 1.19-1.41 (m, 12H), 1.48-1.68 (m, 4H), 2.31 (t, J = 7.5 Hz, 2H), 3.21 (t, J = 6.9 Hz), 11.52 (s, 1H); ^{13}C NMR (250 MHz, CDCl_3) δ = 24.6, 26.4, 28.8, 29.0, 29.0, 29.1, 29.2, 29.3, 34.0, 51.4, 180.2.

10-Azidodecanoic acid (2d)

Yield: 608 mg, 2.85 mmol, 72%. ^1H NMR (250 MHz, CDCl_3) δ = 1.15-1.38 (m, 10H), 1.45-1.64 (m, 4H), 2.28 (t, J = 7.5 Hz, 2H), 3.19 (t, J = 6.9 Hz); ^{13}C NMR (250 MHz, CDCl_3) δ = 24.4, 26.5, 28.6, 28.8, 28.9, 28.9, 29.0, 33.9, 51.4, 180.2.

6-Azidohexanoic acid (2c)

Yield: 856 mg, 5.46 mmol, 71%. ^1H NMR (250 MHz, CDCl_3) δ = 1.32-1.45 (m, 2H), 1.49-1.71 (m, 4H), 3.32 (t, J = 7.3 Hz, 2H), 3.23 (t, J = 6.8 Hz, 2H); ^{13}C NMR (250 MHz, CDCl_3) δ = 24.0, 26.0, 28.4, 33.7, 51.0, 179.9.

5-Azidopentanoic acid (2b)

Yield: 332 mg, 3.1 mmol, 37%. ^1H NMR (250 MHz, CDCl_3) δ = 1.51-1.76 (m, 4H), 2.36 (t, J = 7.1 Hz, 2H), 3.26 (t, J = 6.4 Hz, 2H), 11.05 (s, 1H); ^{13}C NMR (250 MHz, CDCl_3) δ = 21.7, 28.0, 33.3, 50.9, 179.6.

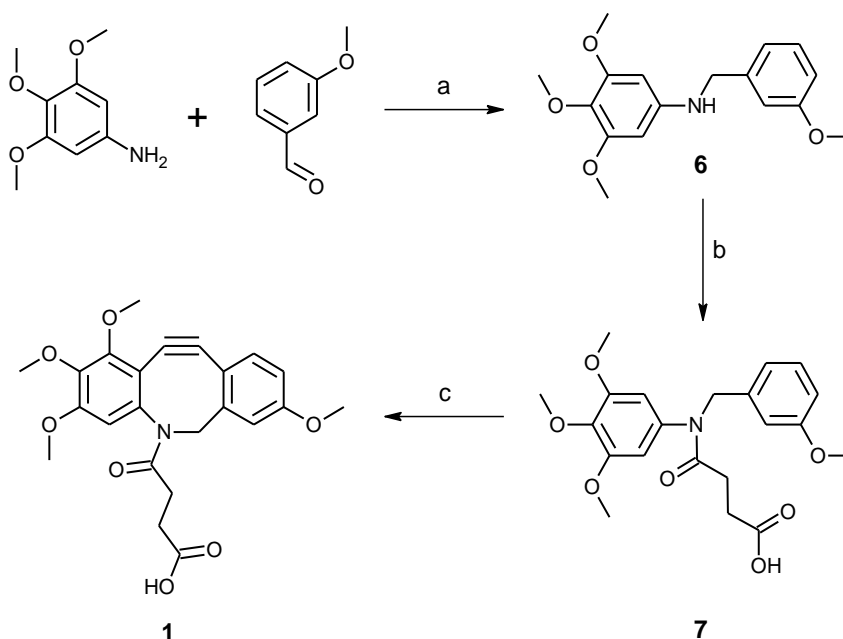
4-Azidobutanoic acid (2a)

Purification gave 34 mg of a mixture of γ -butyrolactone and **2a** with a ^1H NMR integral ratio of 31% to 69%. The mixture was used directly for the formation of **3a/4a**. ^1H NMR (250 MHz, CDCl_3) δ = 1.88 (quin, J = 6.9 Hz, 2H), 2.44 (t, J = 7.3 Hz, 2H), 3.34 (t, J = 6.7 Hz, 2H); ^{13}C NMR (250 MHz, CDCl_3) δ = 23.9, 30.8, 50.4, 178.3.

γ -Butyrolactone: ^1H NMR (250 MHz, CDCl_3) δ = 2.15-2.31 (m, 2H), 2.43-2.52 (m, 2H), 4.32 (t, J = 7.0 Hz, 2H); ^{13}C NMR (250 MHz, CDCl_3) δ = 22.1, 27.8, 68.6, 178.0.

Synthesis of the TDAC

Scheme S2. Three step synthesis of TDAC.



Three step synthesis of TDAC. (a) 1. MeOH, RT, 5h, 2. NaBH_4 (1.7 eq.), 0 °C, 30 min. (b) Succinic anhydride (2 eq.), NEt_3 (1.5 eq.), DMAP (0.1 eq.), DCM, RT, 20h. (c) 1. Tetrachlorocyclopropene (1.01 eq.), AlCl_3 (3.8 eq.), DCM, -78 °C, 3h, 2. hv, MeCN, 24h.

3,4,5-Trimethoxy-N-(3-methoxybenzyl)aniline (6)

3,4,5-Trimethoxyaniline (3.0 g, 16.4 mmol, 1 eq) and 3-methoxybenzaldehyde (2.0 mL, 16.4 mmol, 1 eq) were stirred for 3.5h in dry Methanol, before the solution was cooled to 0° C and sodium borohydride (930 mg, 24.6 mmol, 1.3 eq) was added carefully. When gas formation ceased after 30 min of stirring at room temperature, the reaction was quenched by addition of 40 mL 1M NaOH and extracted three times with 50 mL of Et_2O . The organic phases were combined, washed with brine, dried

over Na_2SO_4 and the solvents evaporated, giving the product as a yellow solid (4.63 g, 15.3 mmol, 93%). ^1H NMR (250 MHz, CDCl_3) δ = 3.73(s, 3H), 3.75 (s, 3H), 3.77 (s, 3H), 4.24 (s, 2H), 5.85 (s, 2H), 6.79 (ddd, J = 8.4 Hz, 2.5 Hz, 0.9 Hz, 1H), 7.24 (t, J = 7.8 Hz, 1H); ^{13}C NMR (250 MHz, CDCl_3) δ = 48.8, 55.1, 55.8, 60.9, 90.6, 112.6, 113.1, 119.7, 129.6, 130.2, 141.0, 144.9, 153.9, 159.9.

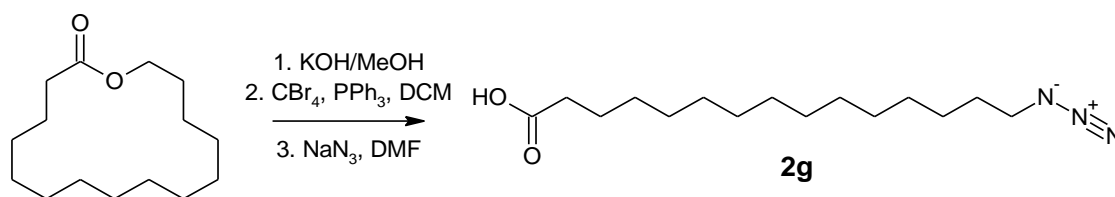
4-((3-Methoxybenzyl)(3,4,5-trimethoxyphenyl)amino)-4-oxobutanoic acid (7)

To a solution of **6** (4.49 g, 14.8 mmol) and succinic anhydride (2.96 g, 29.6 mmol, 2 eq) in dry DCM 4-(dimethylamino)-pyridine (180 mg, 1.5 mmol, 0.1 eq) and triethylamine (3.1 mL, 22.2 mmol, 1.5 eq) were added and stirred at room temperature. The solution turned dark after 1h and the reaction was quenched by the addition of 60 mL of 1M NaOH after 24h. After 15 fore minutes of stirring, the solution turned to a brownish color, after which the solution was acidified with 50 mL of 1.8 M HCl and extracted twice with 50 mL CHCl_3 . The combined organic phases were washed with brine, dried over Na_2SO_4 . After evaporation of the solvents the product was purified by column chromatography on silica, eluting with Hexane to Hexane/EtOAc (1:1), giving the product as a brown solid (5.06 g, 12.6 mmol, 85%). ^1H -NMR(400 MHz, CDCl_3): δ = 2.43 (t, J = 6.4 Hz, 2H), 2.66 (t, J = 6.4 Hz, 2H), 3.68(m, 6H), 3.73 (s, 3H), 3.82 (s, 3H), 4.79 (s, 2H), 6.17 (s, 2H), 6.74-6.79 (m, 3H), 7.16 (t, J = 7.9 Hz, 1H); ^{13}C NMR (250 MHz, CDCl_3) δ = 29.0, 29.5, 53.1, 55.2, 56.1, 60.8, 105.7, 113.2, 114.3, 121.3, 129.3, 137.1, 137.9, 138.9, 153.5, 159.6, 171.7, 177.3.

Oxo(1,2,3,8-tetramethoxy-11,12-didehydrodibenzo[b,f]azocin-5(6H)-yl)butanoic acid (1)

7 (4.91 g, 12.2 mmol) was dissolved in 80 mL of dry DCM and cooled to -80 °C while a portion of aluminium chloride (1.79 g, 13.4 mmol, 1.1 eq) was suspended in a separate flask in dry DCM and tetrachlorocyclopropane (1.49 mL, 12.3 mmol, 1.01 eq) was added. The suspension was diluted with 20 mL of dry DCM and stirred for 10 minutes. Aluminium chloride (4.41 g, 33.1 mmol, 2.7 eq) was added at -80 °C to the solution of **2** before the activated tetrachlorocyclopropane suspension was added by syringe, leading to gas formation. After 3h the reaction mixture was allowed to slowly reach room temperature and stirring was continued for 12h. The reaction was quenched carefully at 0°C by addition of 130 mL of 1M HCl. The clear solution was extracted three times with 50 mL CHCl₃ and the combined organic phases washed with brine, dried over Na₂SO₄ and the solvents evaporated. The raw product was purified by column chromatography on silica, eluting with CHCl₃ to CHCl₃/MeOH (9:1), giving the cyclopropenone precursor as 1.4 g of a green solid, consisting of a mixture of isomers. The precursor was subsequently dissolved in 31 mL ACN and irradiated with UV light for 24h to give the desired cyclooctyne. The progress of the quantitative photoreaction was monitored by HPLC-MS. ¹H-NMR (400 MHz, CD₃CN): δ = 2.27-2.36 (m, 2H), 2.36-2.46 (m, 2H), 3.69 (d, J = 13.9 Hz, 1H), 3.84 (s, 3H), 3.85 (s, 3H), 3.87 (s, 3H), 4.07 (s, 3H), 5.00 (d, J = 13.9 Hz, 1H), 6.89 (dd, J = 8.5 Hz, 2.6 Hz, 1H), 7.04 (s, 1H), 7.19 (d, J = 8.4 Hz, 1H), 7.22 (d, J = 2.6 Hz, 1H); ¹³C NMR (400 MHz, CD₃CN) δ = 29.8, 30.1, 56.2, 56.5, 57.1, 61.5, 61.5, 105.4, 109.1, 111.0, 113.5, 115.6, 116.2, 119.7, 127.1, 141.9, 148.1, 151.0, 151.2, 154.6, 160.2, 172.9, 174.2. ESI-MS: *m/z* = 426.1 [M+H]⁺, 448.1 [M+Na]⁺, 872.8 [2M+Na]⁺. MALDI-HR-MS: calculated for C₂₃H₂₃NO₇ 425.14690, found 425.14674 as [M]⁺.

Scheme S3. Synthesis of 15-azidopentadecanoic acid by hydrolysis of pentadecanolide, subsequent bromination of the hydroxy fatty acid and final azidation.

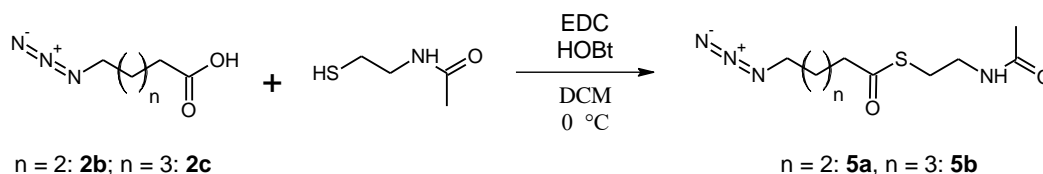


15-Azidopentadecanoic acid (2g)

Pentadecanolide (4.0 g, 16.6 mmol) was dissolved in a mixture of 200 mL MeOH and 20 mL H₂O to which potassium hydroxide (3.7 g, 66.6 mmol, 4 eq) were added. The solution was stirred for 72h, after which it was acidified with 70 mL of 1M HCl and extracted 5 times with 50 mL EtOAc. The organic fractions were combined, dried over Na₂SO₄ and the solvent evaporated, giving 4.14 g of a white solid which consisted almost entirely of the hydrolysis product as confirmed by TLC. A part of the raw product (1.0 g, 3.87 mmol) and triphenylphosphine (1.05 g, 4.0 mmol, 1.05 eq) were then dissolved in 20 mL dry DCM before tetrabromomethane (1.33 g, 4.0 mmol, 1.05 eq) was added. The reaction mixture was stirred at room temperature for 46h before the mixture was diluted with 10 mL H₂O and 20 mL of citric acid solution (20%) were added. The bromination product was extracted three times with 30 mL EtOAc and once with 30 mL of Et₂O. The combined organic phases were dried over Na₂SO₄ and the solvents evaporated, giving the bromination product as a white solid (977 mg, 3.04 mmol, 1 eq). NMR analysis showed sufficient product purity for direct use in the following substitution step. The bromide was dissolved in 10 mL dry DMF, then sodium azide (593 mg, 9.1 mmol) was added and stirred for 6h at 60 °C. Subsequently the solvent was evaporated and 30 mL of aqueous HCl were added. The raw final product was extracted from the aqueous phase three times with 30 mL of EtOAc, the organic fractions were combined and dried over Na₂SO₄. Purification was conducted by column chromatography on silica, eluting with Hexane to Hexane/EtOAc (1:1), giving the product as a white solid (295 mg, 0.92 mmol, 6%). ¹H NMR (500 MHz, CDCl₃) δ = 1.17-1.39 (m, 20H), 1.53-1.65 (m, 4H), 2.32 (t, J = 7.6 Hz, 2H), 3.23 (t, J = 7.0 Hz, 2H); ¹³C NMR (500 MHz, CDCl₃)

$\delta = 24.7, 26.7, 28.8, 29.0, 29.1, 29.2, 29.4, 29.5, 29.5, 29.6, 29.6, 34.0, 51.5, 180.0.$

General procedure for the synthesis of azido fatty acid SNAC esters



The two azidoacyl-SNACs were synthesized in the same way with equal molar quantities. The general procedure of the reaction of the corresponding AFA with NAC is exemplified for the synthesis of *S*-(5-Azidopentanoyl)-*N*-acetylcysteamine (**5a**):

S-(5-Azidopentanoyl)-*N*-acetylcysteamine (**5a**)

To a solution of **2b** (200 mg, 1.27 mmol, 1 eq.) in 10 mL of dry DCM 1-ethyl-3-(3-dimethylaminopropyl)carbodiimide hydrochloride (280 mg, 1.46 mmol, 1.15 eq.) and hydroxybenzotriazole (172 mg, 1.27 mmol, 1 eq.) were added at 0 °C, before *N*-acetylcysteamine (212 mg, 1.78 mmol, 1.4 eq.) was added by syringe. After stirring for 1h the reaction mixture was allowed to reach room temperature and was stirred for another 3h. The reaction was quenched by addition of 20 mL of 1M HCl and the product was extracted three times with DCM. The combined organic phases were dried over Na₂SO₄, the solvents were evaporated and the raw product was purified by column chromatography on silica, eluting with Hexane to Hexane/EtOAc (1:1), giving **5a** as colorless liquid (102 mg, 0.42 mmol, 42%). ¹H-NMR (400 MHz, CDCl₃): $\delta = 1.53$ (tt, $J = 8.2$ Hz, 6.9 Hz, 2H), 1.70 (tt, $J = 7.8$ Hz, 7.0 Hz, 2H), 1.91 (s, 3H), 2.56 (t, $J = 7.3$ Hz, 2H), 2.97 (t, $J = 6.5$ Hz, 2H), 3.24 (t, $J = 6.7$ Hz, 2H), 3.36 (q, $J = 6.3$ Hz, 2H), 6.10 (br, 1H); ¹³C NMR (400 MHz, CDCl₃) $\delta = 22.6, 23.0, 27.9, 28.4, 39.4, 43.2, 50.8, 170.3, 199.1.$

S-(6-Azidohexanoyl)-*N*-acetylcysteamine (**5b**)

Yield: 127 mg, 0.49 mmol, 39%. $^1\text{H-NMR}$ (400 MHz, CDCl_3): δ = 1.30-1.38 (m, 2H), 1.53 (quin. J = 7.0, 2H), 1.62 (quin., J = 7.6 Hz, 2H), 1.90 (s, 3H), 2.51 (t, J = 7.4 Hz, 2H), 2.95 (t, J = 6.5 Hz, 2H), 3.20 (t, J = 6.8 Hz, 2H), 3.34 (q, J = 6.4 Hz, 2H), 6.24 (br, 1H); $^{13}\text{C NMR}$ (400 MHz, CDCl_3) δ = 22.9, 24.9, 25.8, 28.3, 28.3, 39.4, 43.6, 51.0, 170.4, 199.4.

Supplementary figures

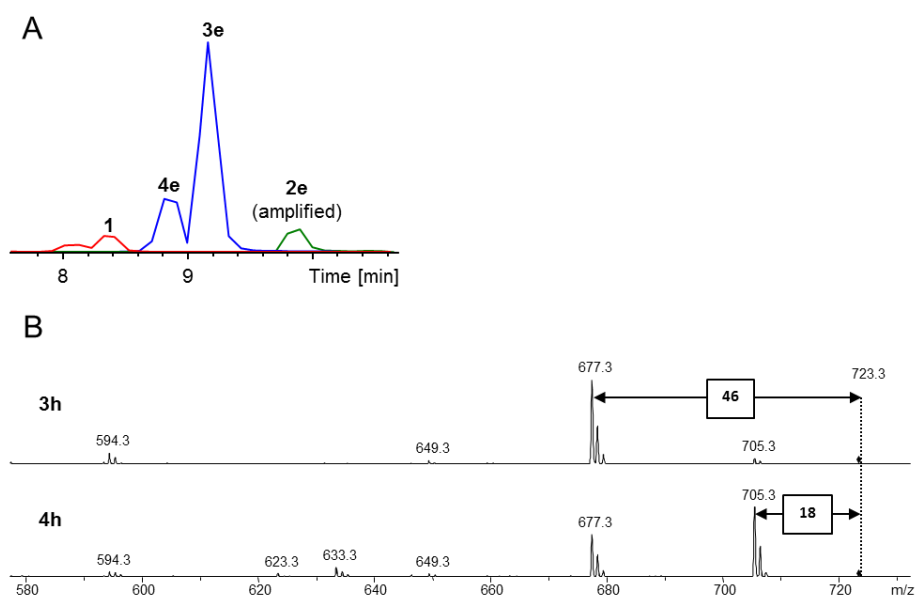


Figure S1. (A) EIC of reactants **1** (as $[M+H]^+$) and **2e** (as $[M-H]^-$, peak amplified 1000-fold for better visibility) in comparison with the EIC of the clicked product (**3e/4e**) after the reaction, showing a significant increase in signal strength. (B) MS² Fragmentation pattern of click products **3h** and **4h**: m/z $[M+H]^+ = 723.3$.

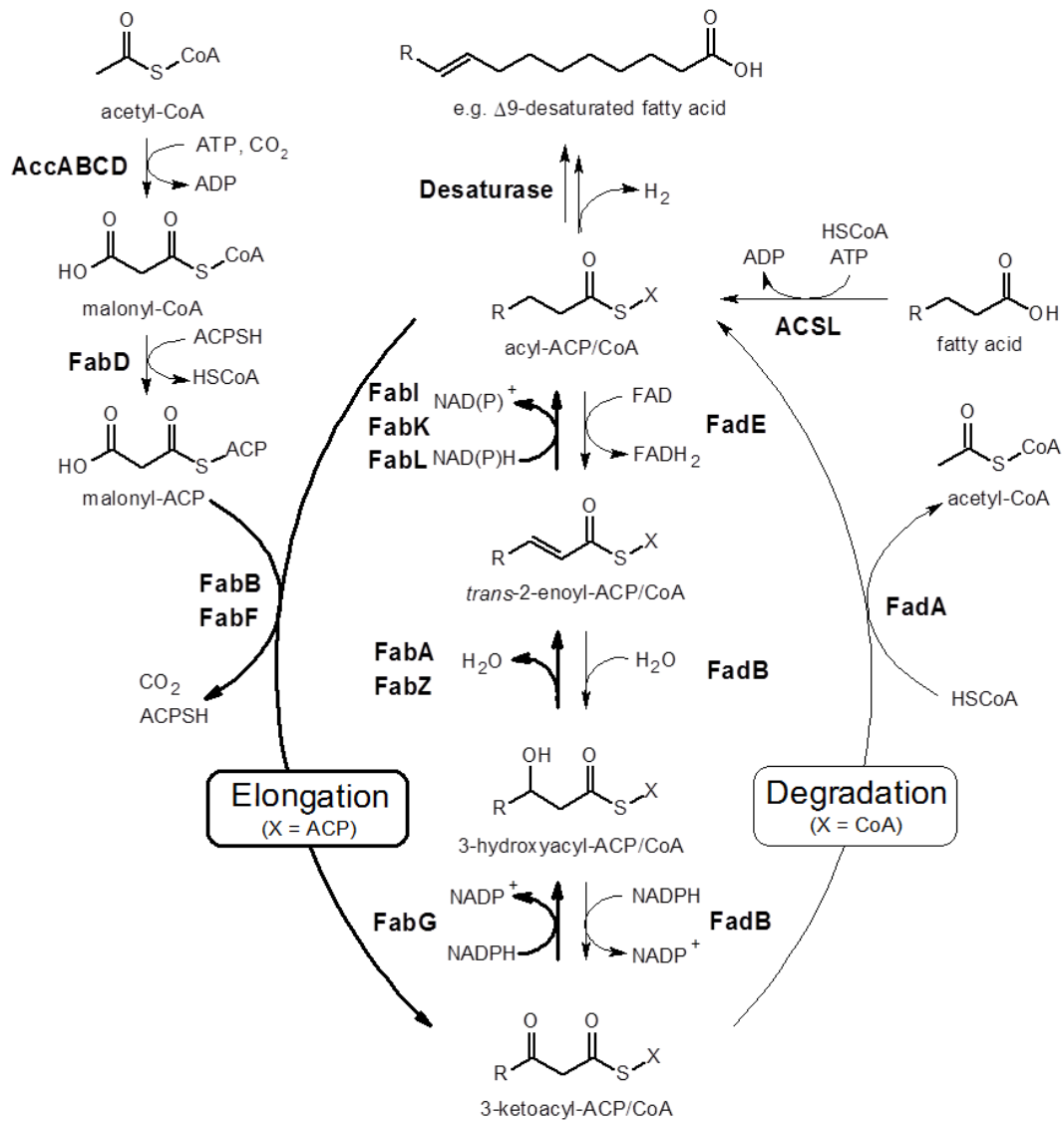
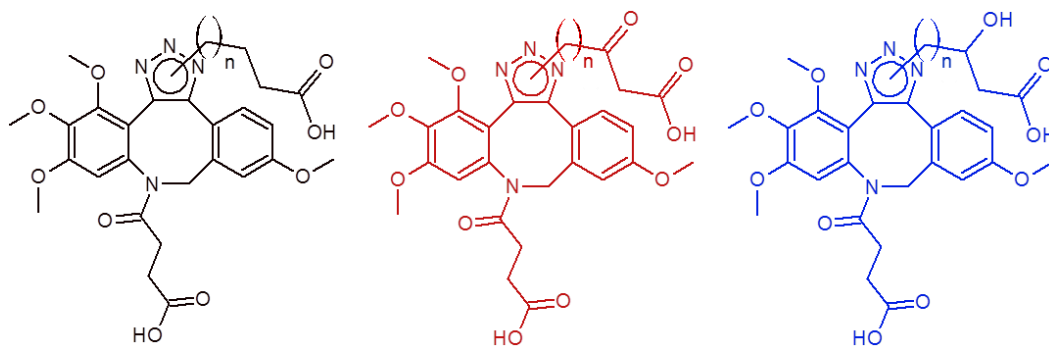


Figure S2. Central steps of fatty acid elongation and degradation in *E. coli*.



	3/4d,f,i,l	8a-d	9a-d
n			
5	3/4i	8a	9a
7	3/4d	8b	9b
9	3/4f	8c	9c
11	3/4l	8d	9d

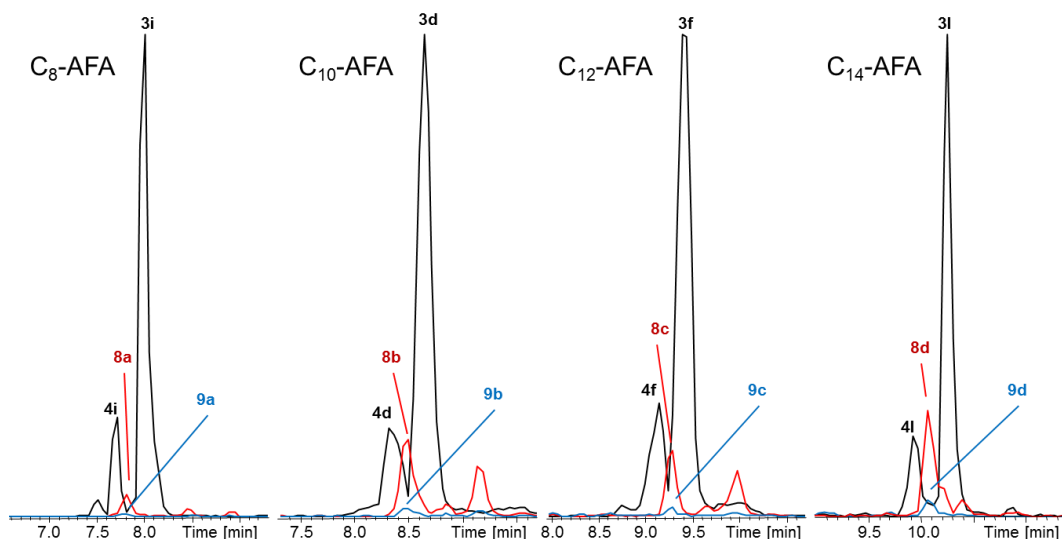


Figure S3. EICs of various clicked degradation products of **2h**. 3-Keto-AFAs (detected as **8a-d**, red) and to a lesser degree 3-hydroxy-AFAs (detected as **9a-d**, blue) can be detected at high concentration of the corresponding AFAs **2i**, **2d**, **2f** and **2l**. Either of the two regioisomers is assumed to attribute to the detected masses.

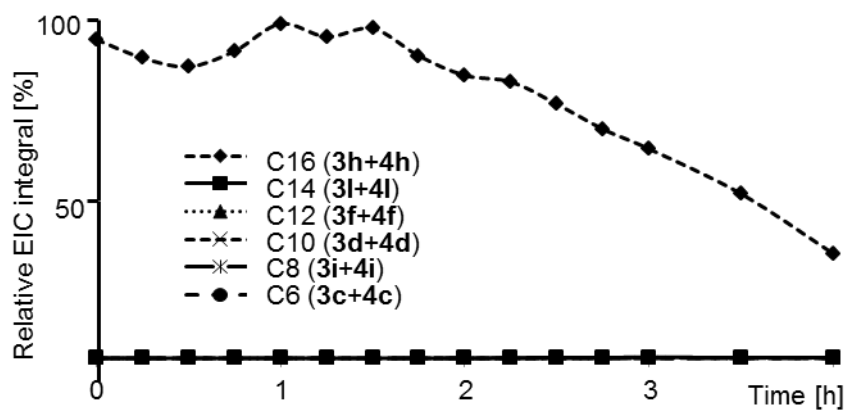


Figure S4. Relative abundance of 2h degradation products when fed to *fadE*-mutant. All degradation products remain below detectable levels due to inhibition of FA degradation.

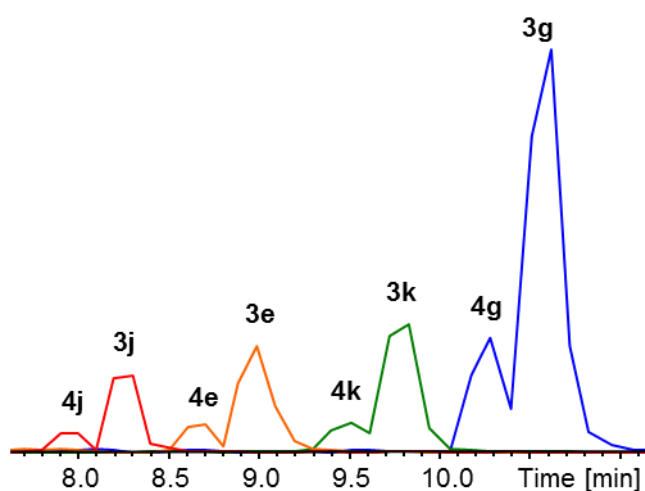
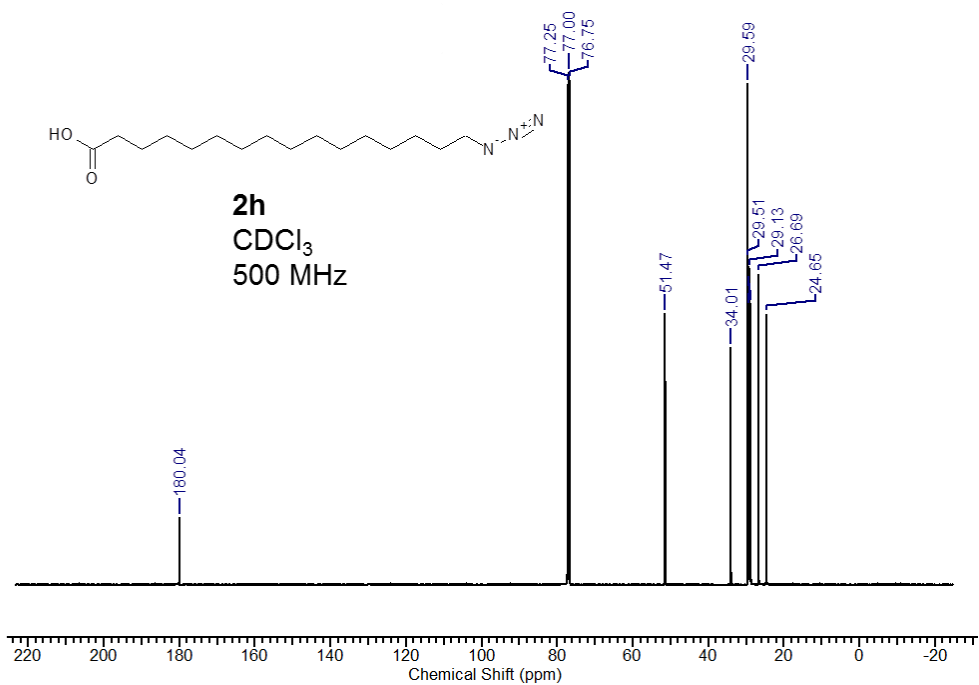
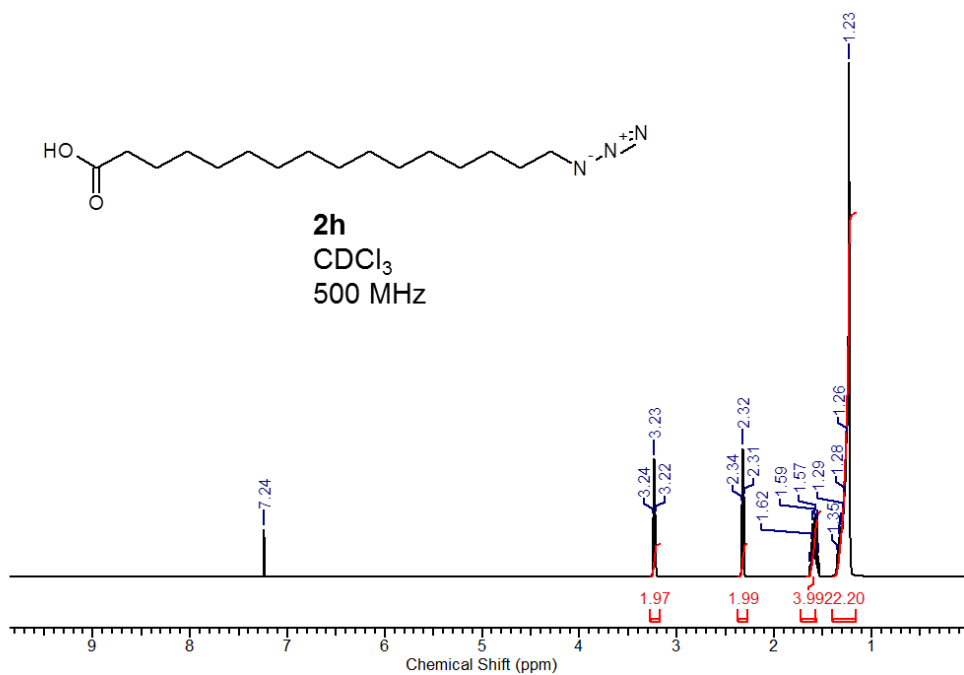
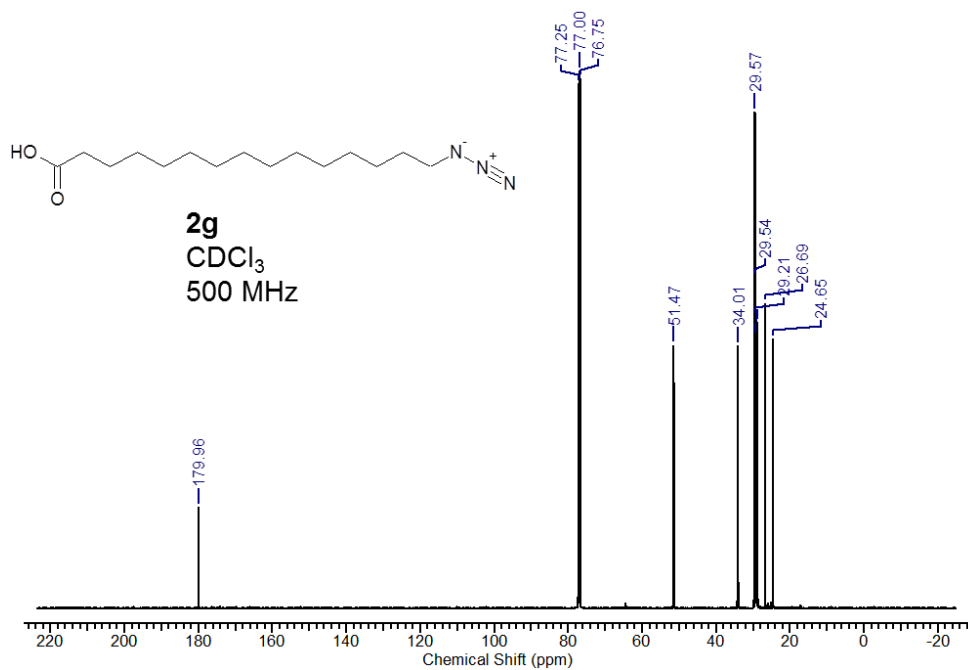
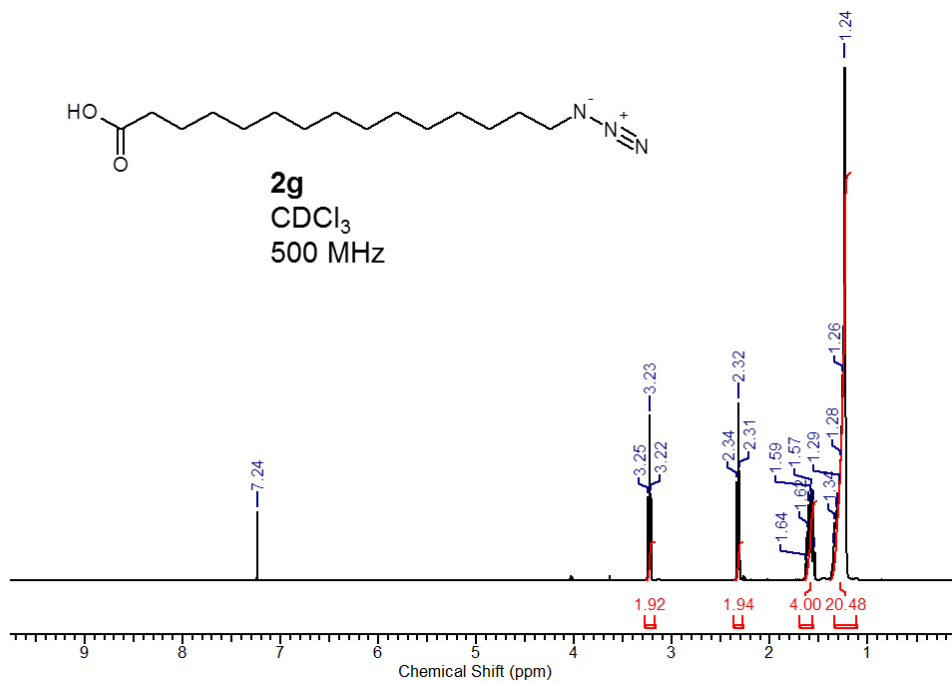
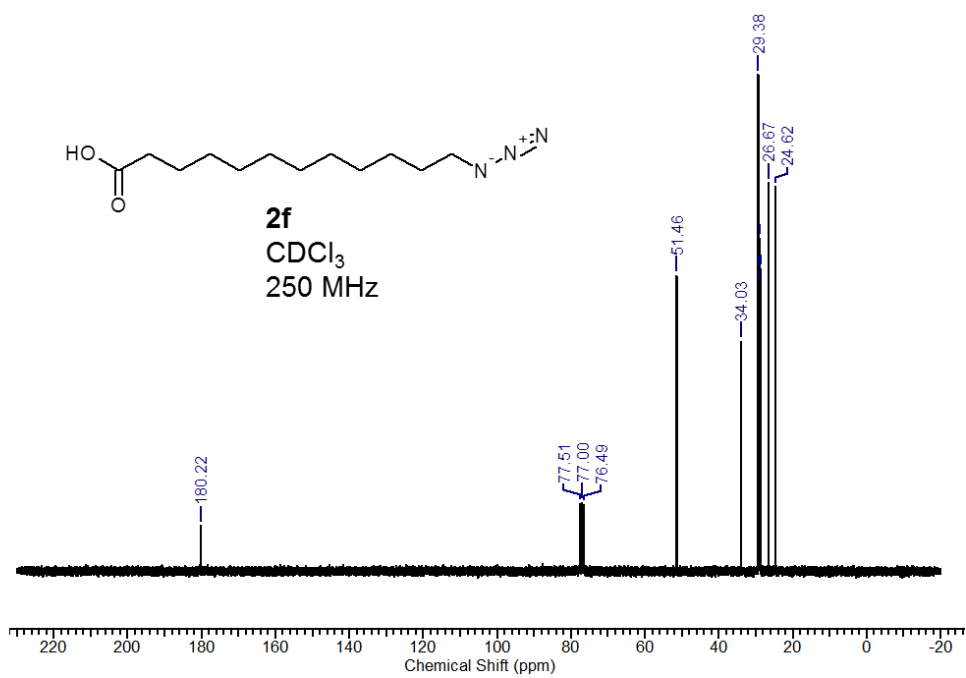
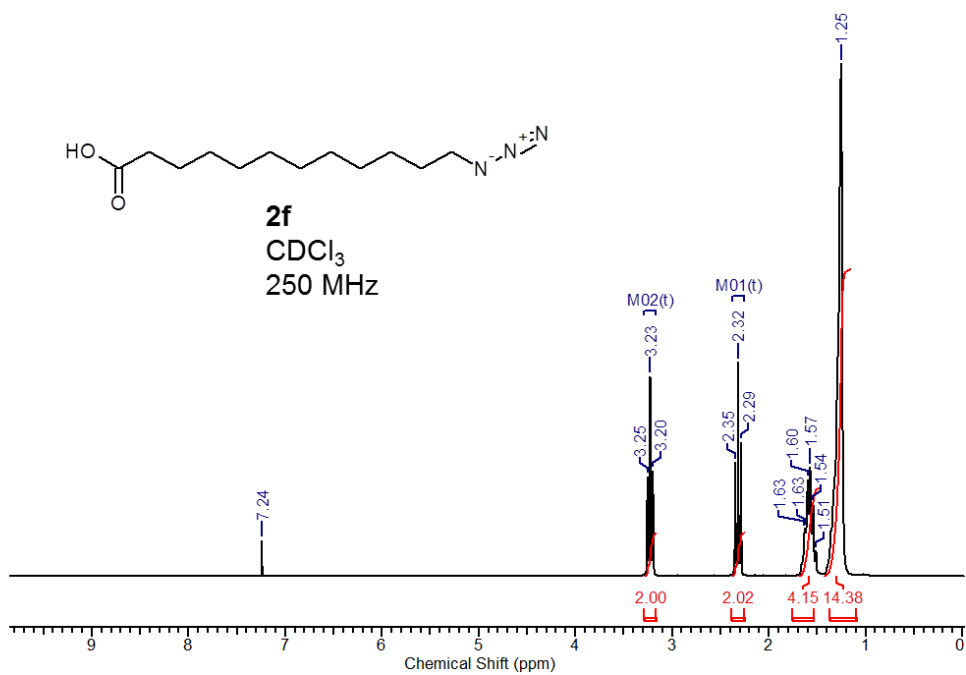


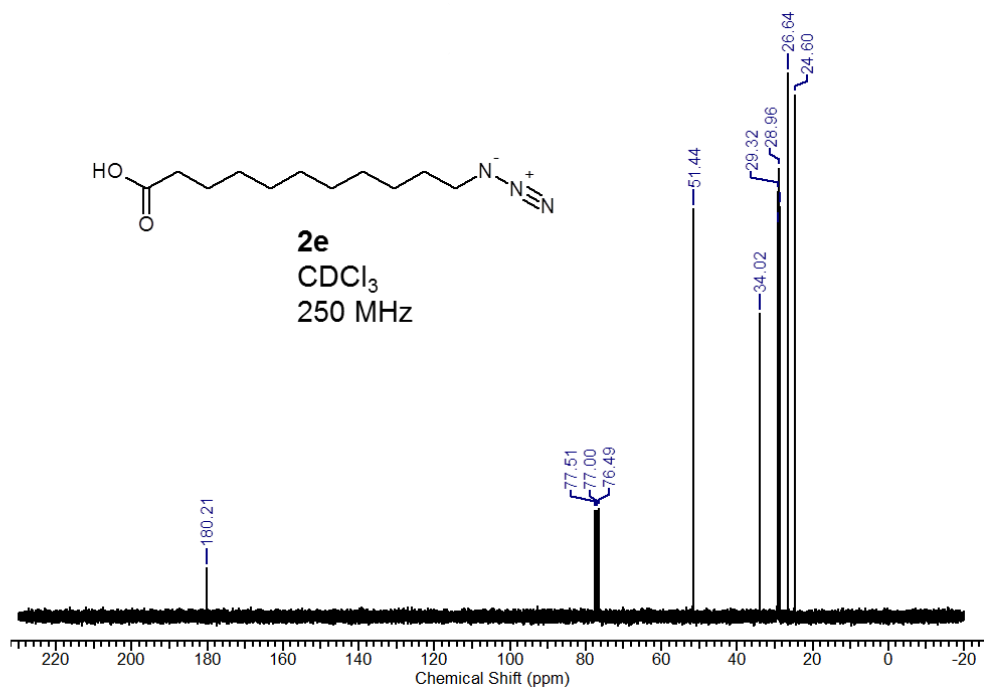
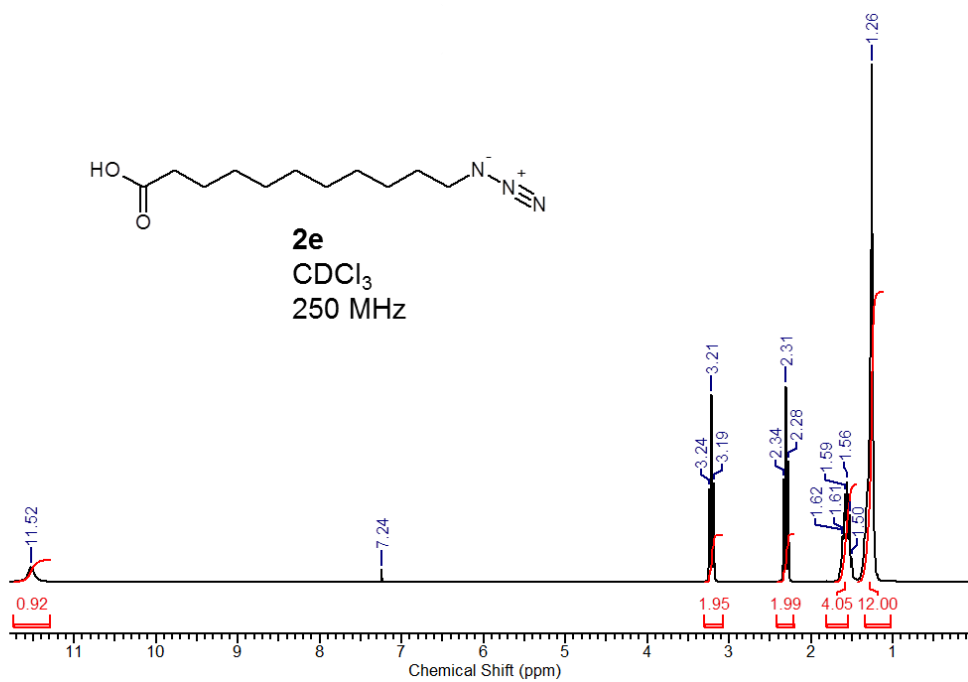
Figure S5. EICs of various clicked degradation products of **2g** (blue) 2h after feeding it to *E. coli* DH10B wildtype, indicating the formation of C₁₃- (green), C₁₁- (orange) and C₉-AFA (red).

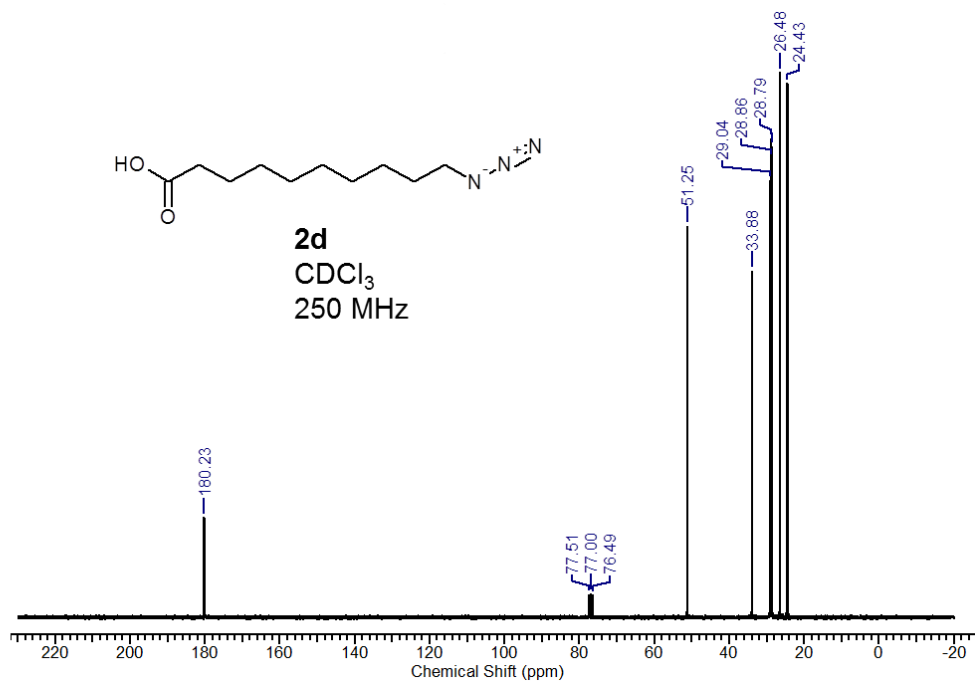
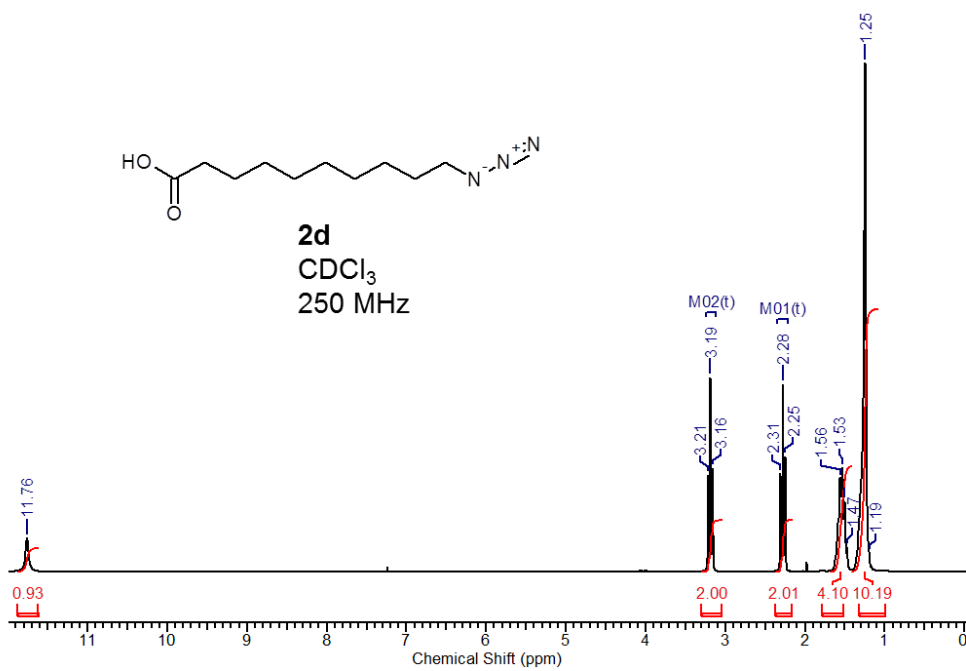
NMR Spectra

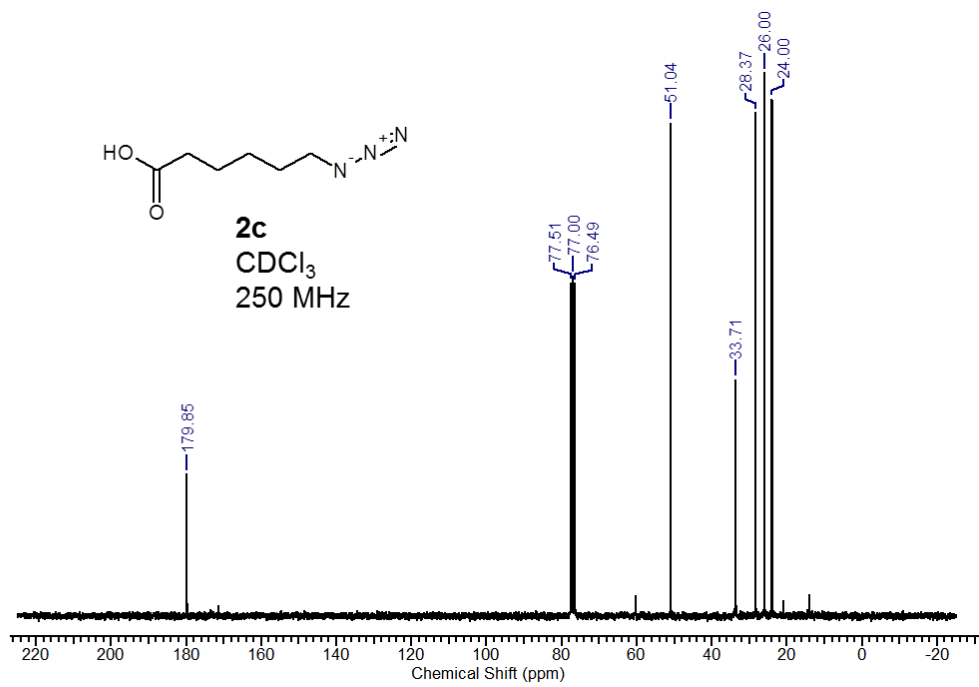
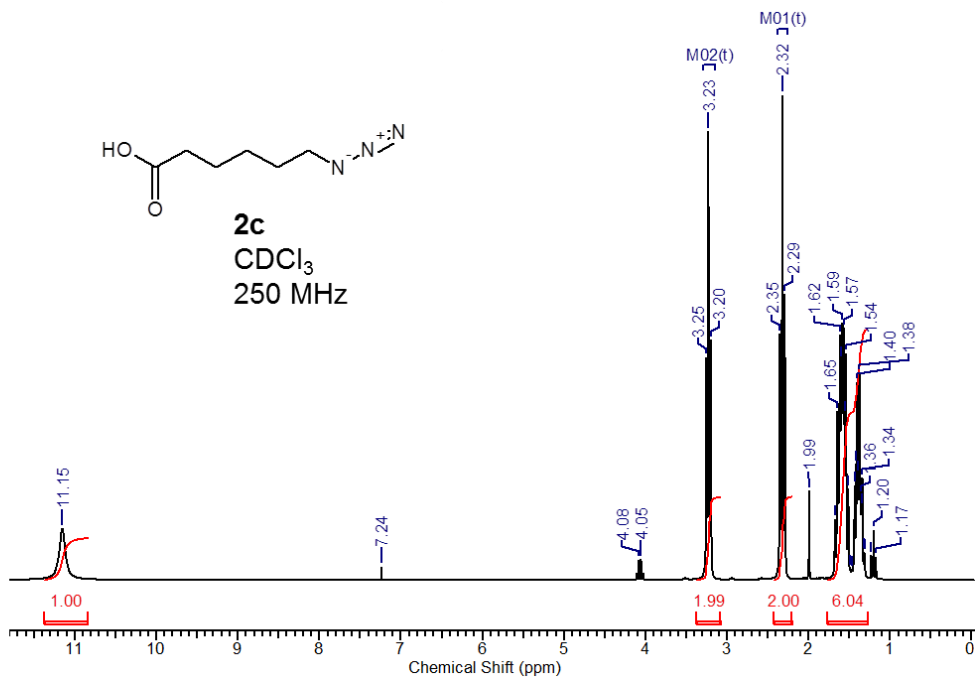


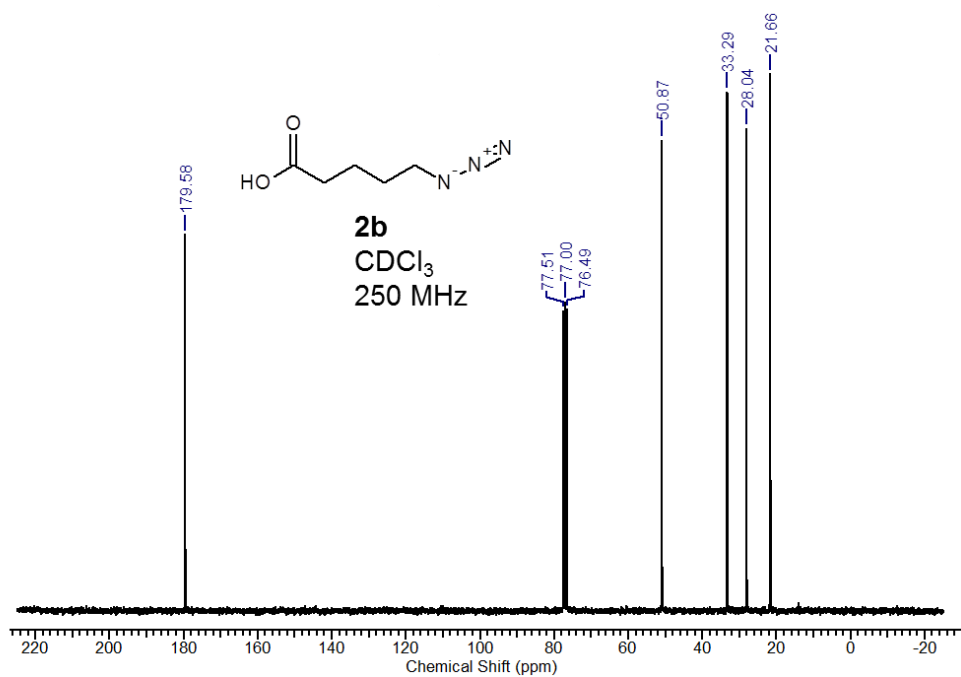
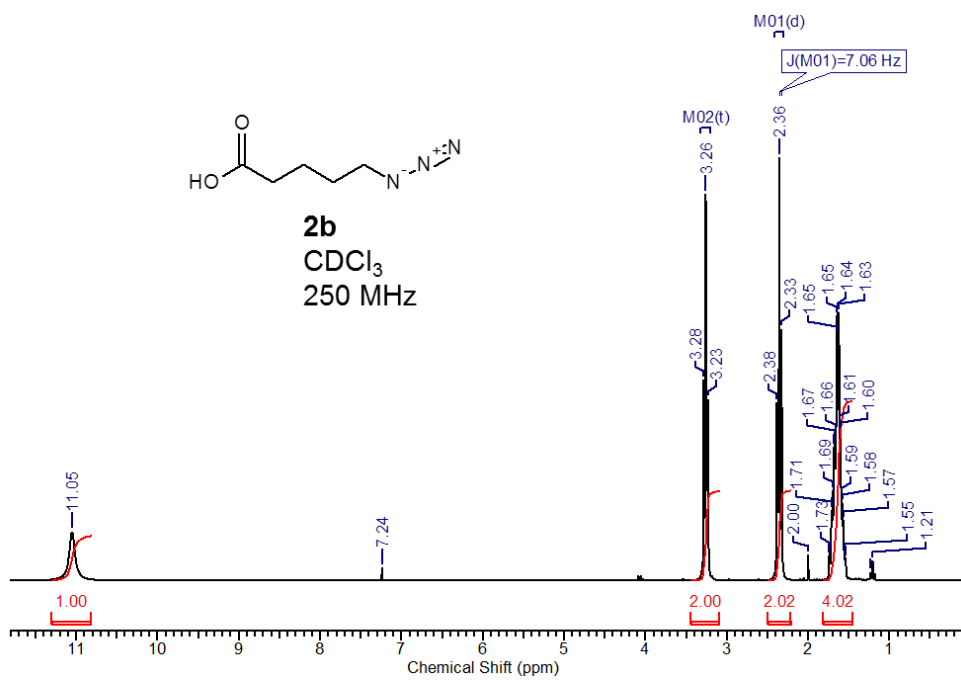


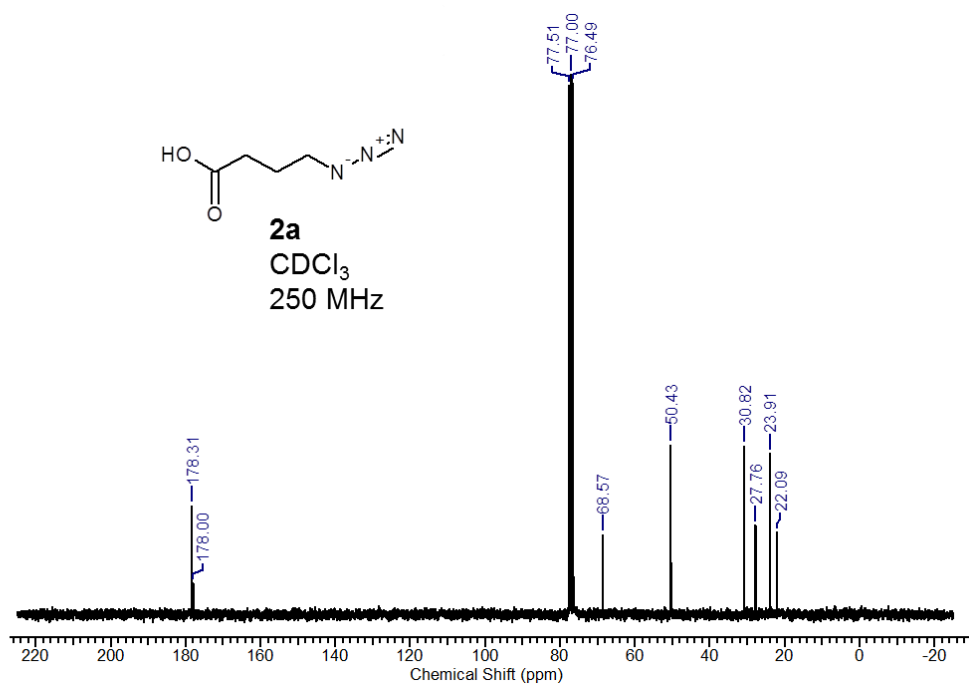
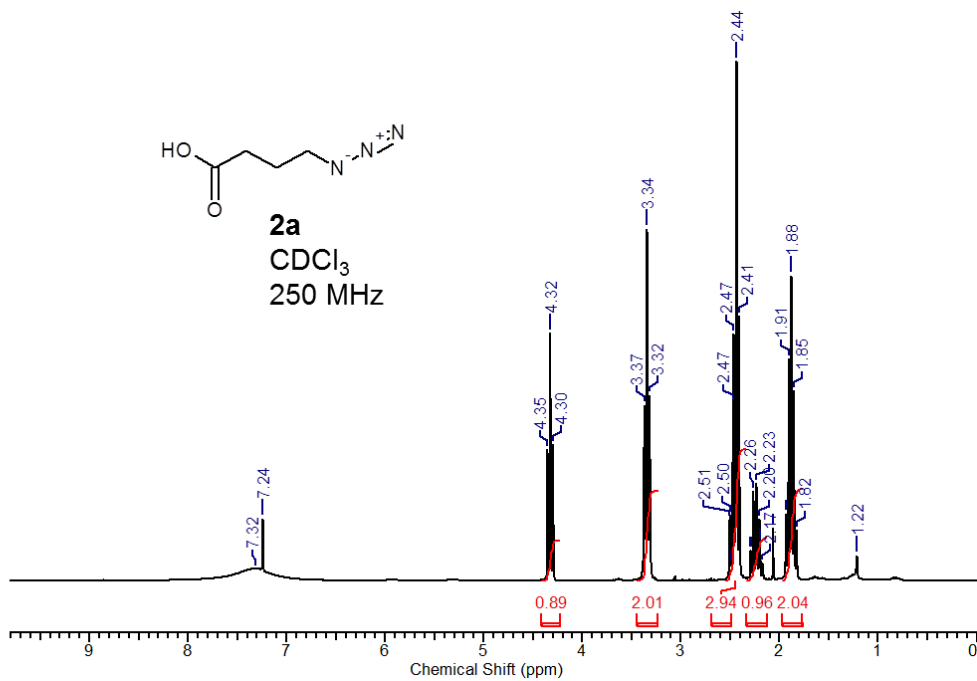


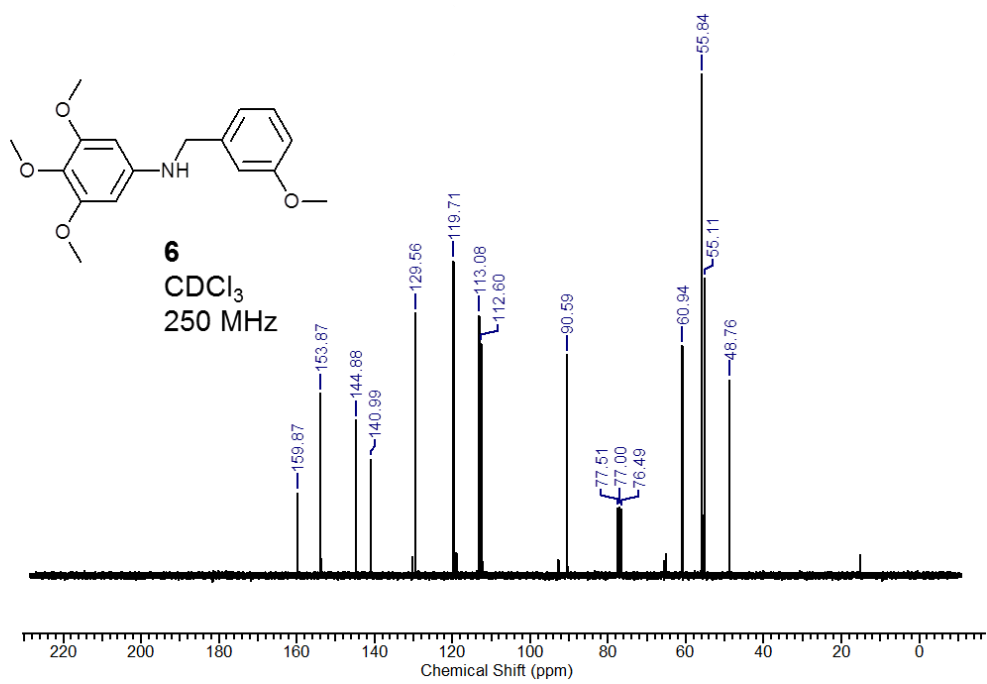
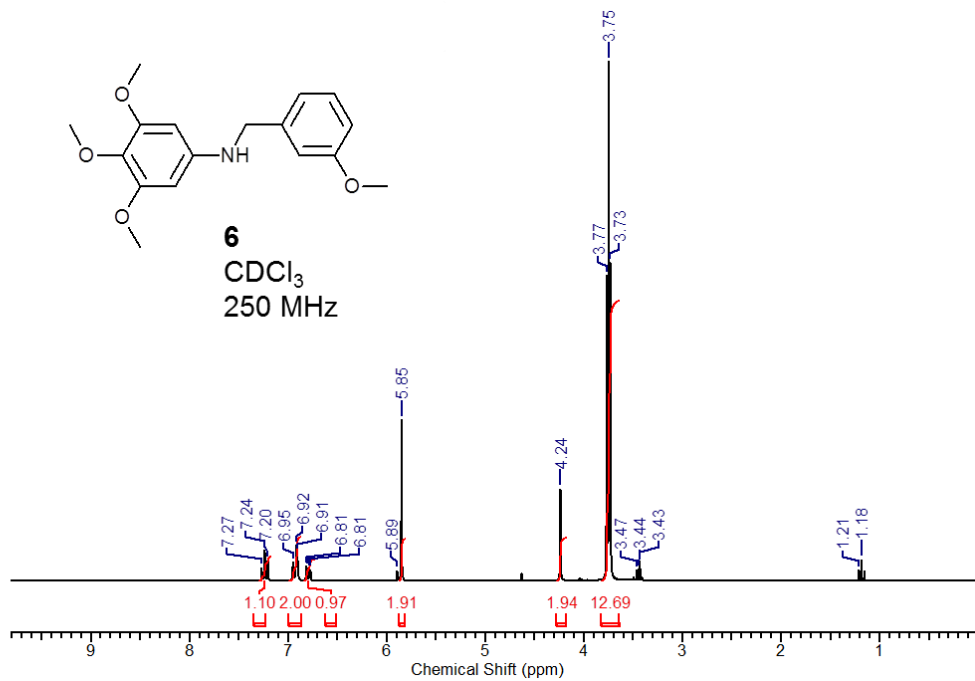


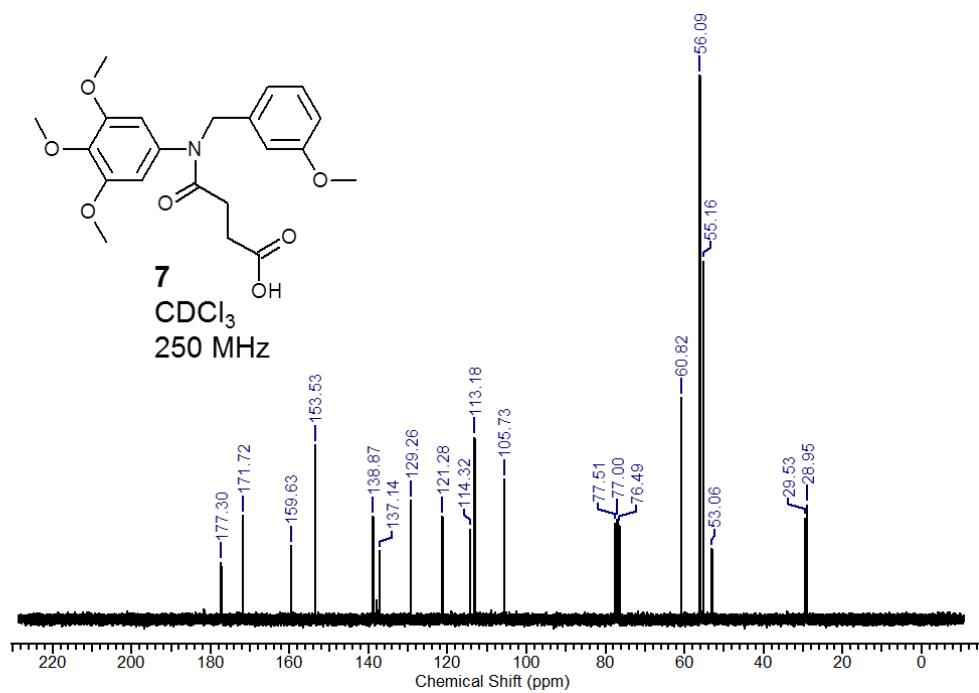
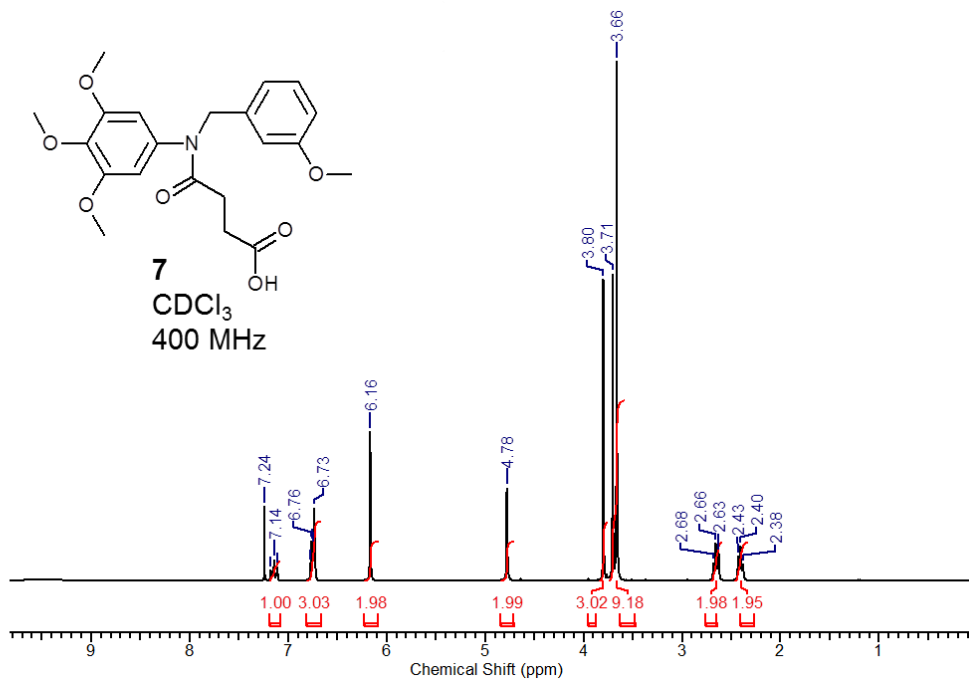


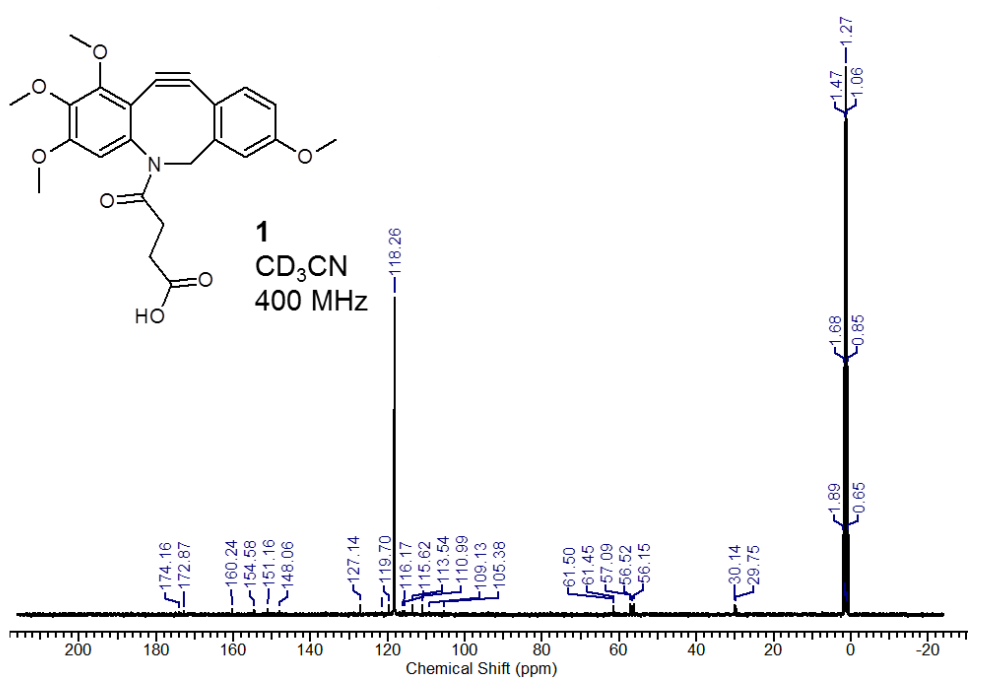
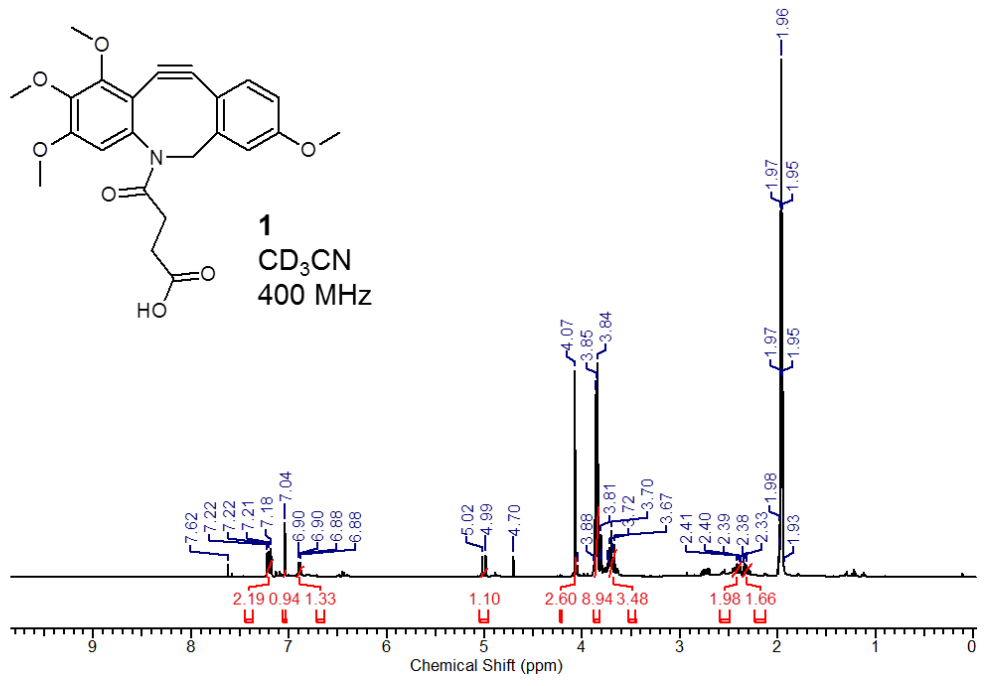


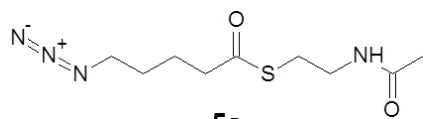




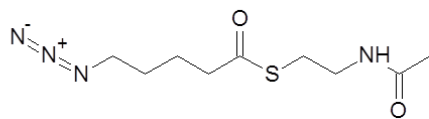
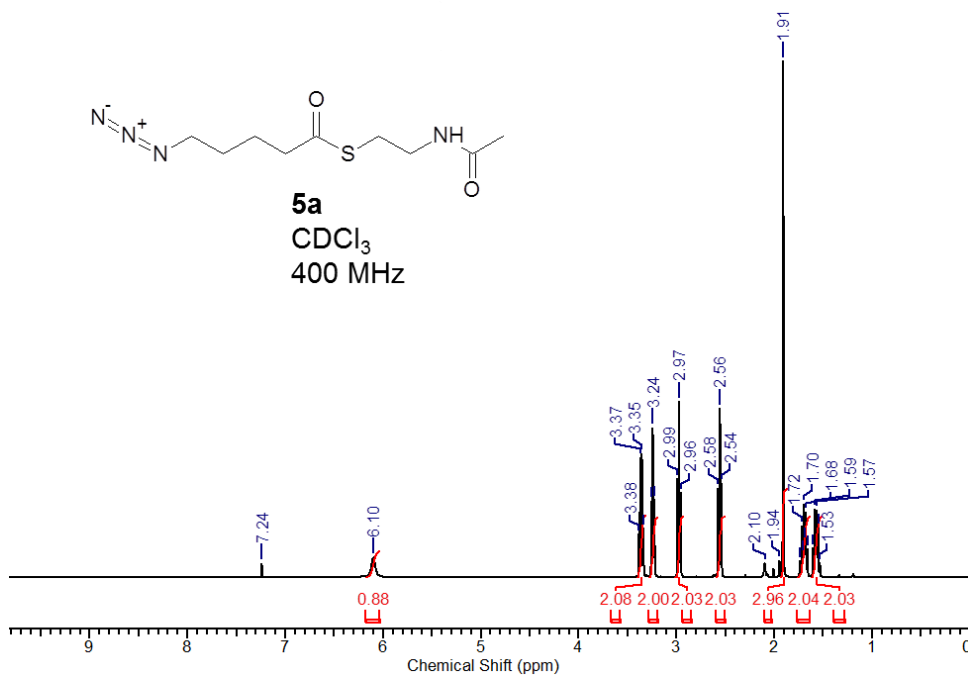




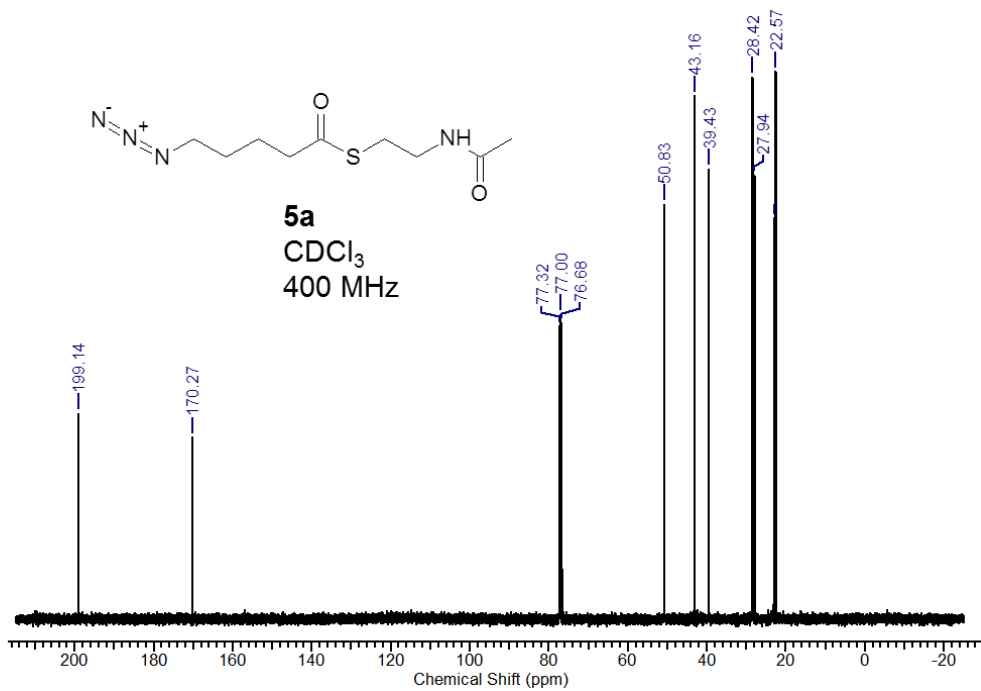


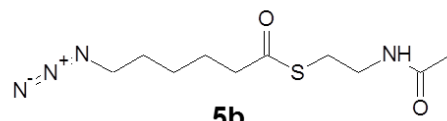


5a
CDCl₃
400 MHz

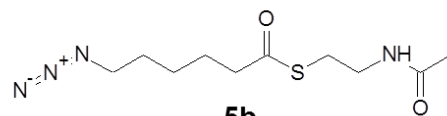
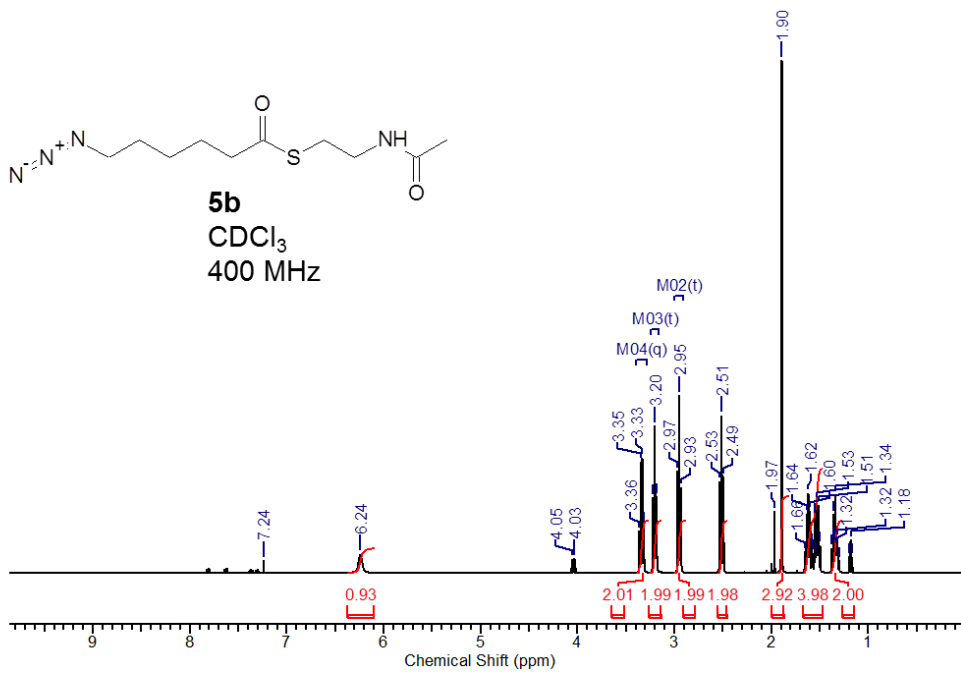


5a
CDCl₃
400 MHz

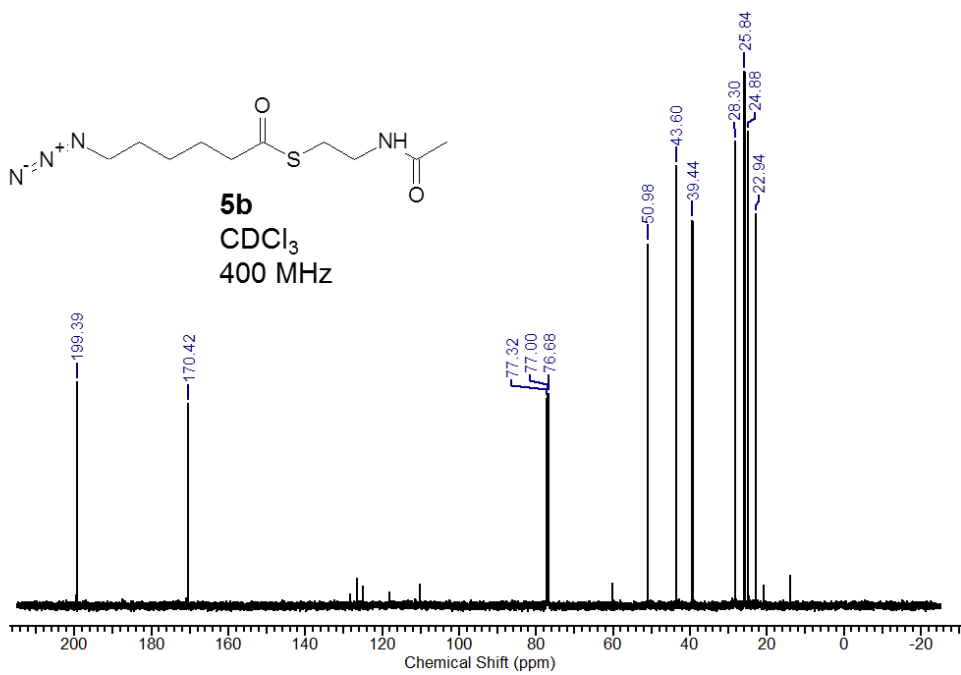




5b
CDCl₃
400 MHz



5b
CDCl₃
400 MHz



7.2 Publication: “Click Chemistry for the Simple Determination of Fatty Acid Uptake and Degradation: Revising the Role of Fatty Acid Transporters”

Authors: Alexander J. Pérez¹, Helge B. Bode^{1,2}

¹Merck Stiftungsprofessur für Molekulare Biotechnologie, Fachbereich Biowissenschaften, Goethe Universität Frankfurt, 60438 Frankfurt am Main, Germany

²Buchmann Institute for Molecular Life Sciences (BMLS), Goethe Universität Frankfurt, 60438 Frankfurt am Main, Germany

Published in: ChemBioChem, July 27, 2015, Volume 16, page 1588-1591

Digital Object Identifier: 10.1002/cbic.201500194

Elaboration of the contributions of each author to the publication in question

Title of the publication: “Click Chemistry for the Simple Determination of Fatty Acid Uptake and Degradation: Revising the Role of Fatty Acid Transporters”

Project phase	Contribution of the authors
1) Planning and development	AJP: 70%; HBB: 30%
2) Execution of experiments	AJP: 100%
3) Creation of figures and data sheets	AJP: 100%
4) Interpretation/Analysis of data	AJP: 70%; HBB: 30%
5) Abstract/Results/Discussion	AJP: 70%; HBB: 30%

“Click-chemistry” for the simple determination of fatty acid uptake and degradation - Revising fatty acid transporters

Alexander J. Pérez^[a] and Helge B. Bode^{*[a][b]}

[a] A. Pérez, Prof. Dr. H. B. Bode

Merck Stiftungsprofessur für Molekulare Biotechnologie, Fachbereich Biowissenschaften, Goethe Universität, Max-von-Laue-Straße 9, 60438 Frankfurt am Main (Germany)
E-mail: h.bode@bio.uni-frankfurt.de

[b] Prof. Dr. H. B. Bode

Buchmann Institute for Molecular Life Sciences (BMLS), Goethe Universität, Max-von-Laue-Straße 15, 60438 Frankfurt am Main (Germany)

Supporting information for this article is given via a link at the end of the document.

Abstract: Fatty acids (FAs) comprise a wide area of functions among all living organisms, ranging from structural roles to energy production and secondary metabolite biosynthesis. Due to their high energy content, the acquisition of exogenous FAs is a central feature of metabolism for which several biological systems are known, although their precise role is not yet entirely clear. In this work we investigated the role of CoA-ligase FadD and FA transporter FadL in different bacterial strains using an improved version of click-chemistry assisted labeling of azido-FAs. The high sensitivity associated with this method allows for a direct and precise assessment of FA metabolism, being far better suited than mere growth experiments. Our results show that while FA activation is indeed essential for their degradation, FA transport can also be independent of transporters like FadL.

Keywords: fatty acid transport, fatty acid activation, fatty acid metabolism, azido fatty acids, bioorthogonal labeling.

Fatty acids (FAs) have several different roles among all living organisms, extending far beyond energy production or the assembly of the well-known and vital lipid bilayer. One of the most recent observations is that FAs are the major carbon source for dNTP biosynthesis in endothelial cells during vessel sprouting and angiogenesis and thus also tumor growth in mammals^[1]. Additionally, many bacteria make extended use of FAs by incorporating them into various different secondary metabolites, such as acylated nonribosomal peptides, pyrones or stilbenes^[2]. In all of these cases transport of exogenous FAs into the cell as well as activation of the rather unreactive carboxylic head group is important if not vital, e.g. when FAs constitute the sole carbon source. In *Escherichia coli* there are two proteins involved in FA acquisition^[3]: FadL, a passive and unselective FA transporter located in the outer membrane, and FadD, a CoA-ligase which activates fatty acids under ATP consumption. The Coenzyme A thioesters thus formed can then enter several different biochemical pathways, including oxidative degradation and polyketide or nonribosomal peptide synthesis^[4].

Using the method of azide labeling previously reported, it is possible to follow these pathways in a very direct fashion^[5]. The method employed in this work involves the derivatisation of azido fatty acids (AFAs) from hydrolyzed cell-pellet extracts with a bicyclononyne (BCN, **1**, Scheme 1) and subsequent analysis by HPLC-MS. The use of BCN^[6], rather than the previously used dibenzoazacyclooctyne derivative (TDAC, **2**, Fig. S1)^[7] not only leads to better peak shapes, but also features a more straightforward synthesis, easier purification and isolation of single diastereomers whose click adducts form physically identical enantiomers (Scheme S1).

First, BCN was tested as a suitable derivatisation agent for AFAs. For this end 16-azidoheptadecanoic acid (**3**) was directly reacted with BCN in methanol and in acetonitrile at room temperature for 24 h, leading to the expected click adduct **3a** in each case. Furthermore a chromatographic analysis of the reaction products of **3** with pure *exo*-BCN in comparison to a mixture of *exo*- and *endo*-BCN was performed, revealing that there is little notable difference in retention time nor are any further byproducts visible (Fig. S2). This shows that the synthetic procedure can be simplified if desired,

although in this work pure *exo*-BCN was used. *Endo*-BCN can also be obtained directly from Sigma-Aldrich.

We then investigated the role of FadD and FadL in the uptake and subsequent degradation of AFAs with our model organism *E. coli* (wildtype strain MG1655). For this end, mutant strains lacking either *fadD* (BW25113 Δ *fadD*) or *fadL* (BW25113 Δ *fadL*) were compared in their ability to produce a C₁₄-AFA (**4**) from externally provided C₁₆-AFA (**3**) via the β -oxidative degradation pathway (Fig. S3)^[4]. Assuming that FAs cannot easily permeate the bacterial membranes and that FA activation is crucial for β -oxidation, no or at least a decreased production of AFA degradation products should be expected in either deletion strains^{[9][10]}, whereas it should be well visible in the wildtype as shown in our previous work^[5].

The feeding experiment clearly showed that FadD is essential for the processing of long chain FAs (LCFAs), as no degradation products could be observed in the Δ *fadD* mutant four hours after the addition of **3** to the culture (Fig. 2). This is in close accordance with previous findings that showed the dependence of *Pseudomonas aeruginosa* on FadD homologues for survival on media with FAs as the sole carbon source, although β -oxidation was then only shown indirectly via growth experiments^[8]. The influence of FadL on the process is more subtle, as a delay in FA degradation of roughly one hour can be observed in Δ *fadL* mutants compared to the wildtype. This result suggests that AFA transport into the cell does not necessarily require a transporter like FadL, but may occur through diffusion. This is made especially likely under the consideration of the low pH in intermembrane space of Gram-negative bacteria^[11], which facilitates protonation of FA carboxylate moieties caught in the outer membrane and subsequent diffusion to the inner membrane where no FA transporter is known to be located^[12]. Furthermore the findings of Hearn et al.^[13] strongly reinforce the notion that FAs generally are freer to move within and between membranes than earlier models would suggest, which is in great accordance with our results.

To get a better picture of the influence of FadL on FA uptake, AFA degradation was monitored in various *Sinorhizobium meliloti* mutants lacking the genomic *fadL* gene^[14]. Instead the mutants expressed FadL proteins from

Agrobacterium tumefaciens (At), *Mesorhizobium loti* (Ml), wildtype *S. meliloti* (Sm) and a FadL deletion mutant (Sm Δ FadL) as control respectively. These mutants have previously been compared regarding their growth on minimal media with oleic or palmitic acid as the sole carbon source, showing that the *S. meliloti* wildtype is unable to grow under these conditions and its FadL thus is most likely not involved in transport of these FAs^[153]. To support this theory, the mutants were fed with **3** under normal growth conditions and the amount of oxidation product **4** was measured (via derivatisation to **4a**) 6 h after feeding taking into account the slower growth rate of *S. meliloti* in comparison to *E. coli* (Fig. 3). As was expected from the FadL deletion experiment in *E. coli*, all tested strains showed degradation activity, including the deletion mutant, although certain differences in efficacy could be observed. The greatest amounts of **4** could be detected with At and Ml, closely followed by Sm while, as expected, the least production level was observed with the FadL deletion strain Sm Δ FadL. This suggests differently accentuated contributions of FadL to the FA degradation process whereas previously merely a broad chain length tolerance was reported^[15].

After showing that AFA uptake and degradation is possible in a complete medium, the sinorhizobial strains were subjected to a growth experiment under minimal medium conditions with FAs as the sole carbon source. As it had been previously shown that growth on palmitic acid minimal medium is possible for at least some of the strains^[14], their growth was compared under the same conditions but with AFA **3** or stearic acid as carbon sources, which has about the same length as **3**. Since the solubility of both **3** and stearic acid are very low compared to the more soluble oleic acid tested previously, the experiment was conducted on an opaque agar emulsion and the resulting clearing of the growing bacteria by FA consumption was observed 8 days after plating. As predicted by the cycloaddition-based assay, all strains, including the FadL deletion mutant, were able to grow on AFA minimal medium with only little observable differences. Interestingly, no growth at all was observed on stearic acid minimal medium (Fig. S5), although it is still observable to some degree with palmitic acid, as has been shown previously^[14].

It thus appears that not only do FadL from different strains exhibit different chain length specificities, but that membrane permeability of different FAs greatly differs, as can be concluded from the differences in growth of FadL deletion mutants on different carbon sources. An AFA with its slightly polar end group instead of a non-polar alkyl chain might interact better with the charged outer membrane^[8], facilitating its uptake compared to standard FAs. Although this observation can be regarded as a disadvantage of AFAs as tools for studying FA transport, our data (Fig. 2 and 3) show that they can still be used to determine the FadL contribution to FA uptake. Even more subtle differences in FA metabolism, such as depicted in Fig. 3, can be accessed.

Our experiments confirmed that CoA ligation, as performed by FadD, is an essential key step in the FA degradation pathway in Gram-negative bacteria. It is known however that some organisms express more than one FadD homologue with varying substrate specificity and thus are less prone to FA degradation obstruction by a single knockout^[16], as is known for *P. aeruginosa*^[8]. The role of FadL however is less clear-cut, with FA degradation occurring irrespectively of the type or even actual presence of FadL but instead seems to be depend on the FA nature. We thus suggest that FadL merely facilitates AFA migration through the outer membrane, hence boosting AFA consumption within the cell. It was shown previously that FadL also plays a role in the transport of signaling molecules such as acylhomoserine lactones^[13]. Thus, the general role of FadL might be the facilitation of lipophilic signals, as there is no chemical driving force to direct their transport into the cell. For FAs FadD fulfills such a role via their conversion into FA-CoA-thioesters.

As FadL mutants generally grow very slowly or not at all on FA containing minimal media it makes the effect of *fadL* mutation difficult and time consuming to analyze via growth experiments. Here the big advantage of our approach is the very fast (5 hours compared to 8 days) and precise determination of differences in FA uptake and degradation when compared to an analysis of cell growth alone, since the latter fails to detect FA degradation directly under normal growing conditions^[17]. Even radioisotope feeding experiments have, to our knowledge, been only conducted under unnatural growing conditions^[18] for reasons unclear to the authors.

Experimental Section

General experimental procedures

Solvents and reagents were obtained from Sigma-Aldrich (München, Germany). Silica gel based chromatographic purification was performed on a Biotage SP1™ Flash Purification System (Biotage, Uppsala, Sweden), using 40+M KP-Sil cartridges (Biotage, Uppsala, Sweden) in combination with an UV detector. ¹H and ¹³C NMR spectra for the synthesis products were recorded on a BrukerAV500 (500 MHz) or AV400 (400 MHz) spectrometer using CDCl₃ as solvent and internal standard. ¹H-NMR: CHCl₃: δ = 7.24 ppm; ¹³C-NMR: CDCl₃: δ = 77.00 ppm. ESI HPLC MS analysis was performed with a DionexUltiMate 3000 system coupled to a Bruker AmaZon X mass spectrometer using a MeCN/0.1 % formic acid in H₂O gradient ranging from 5 to 95 % in 22 min. at a flow rate of 0.6 mL/min.

Analytical procedure

For determination of AFA **3** degradation the extracted ion chromatogram (EIC) peak of its first degradation product C₁₄-AFA-BCN adduct **4a** ([M+H]⁺ = 420) was monitored. Excess **3a** was not monitored, although its presence could always be detected.

Strains and cultivation conditions

E. coli MG1655 wildtype, as well as mutants BW25113Δ*fadD* and BW25113Δ*fadL* used in this study were obtained from the Keio collection^[19] and grown on solid and liquid Luria-Bertani (LB, pH 7.0) medium at 30°C and 180 rpm on a rotary shaker. For plasmid selection kanamycin (40 µg/mL) and/or chloramphenicol (34 µg/mL) were added, respectively. *S. meliloti* strains were described earlier^[14] and were grown in tryptone yeast (TY, pH 7.0) medium with kanamycin (200 µg/mL), gentamicin (40 µg/mL) and IPTG (100 µM) at 30°C and 180 rpm on a rotary shaker.

Azido fatty acid degradation experiments

The feeding experiments for the observation of FA degradation activity were conducted by the addition of 16-azidohexanoic acid (**3**) at a final concentration of either 1 mM or 0.1 mM to each culture, respectively.

Inoculation was performed from a preculture that was incubated overnight. The optical density (OD₆₀₀) was set to 0.1 and the cultures were grown in 100 mL Erlenmeyer flasks containing 15 mL of Luria-Bertani (LB, pH 7.0) or tryptone yeast (TY, pH 7.0) medium respectively at 30 °C and 180 rpm on a rotary shaker for 2 h before feeding ensued. At the given times, culture samples of 1 mL were centrifuged at 17.000 g for 5 min in a 2 mL reaction tube and the supernatant was discarded. Cell pellets were then lysed by the addition of 500 µL of 1M NaOH at 90°C for 60 min. The lysate was acidified by the addition of 90 µL of 6M HCl and 800 µL of hexane were added. The sample was mixed, centrifuged as before and 500 µL of the organic layer were collected in a 1.5 mL reaction tube. After evaporation of the solvent the extract was dissolved in 200 µL of a 1 mM solution of **1** in ACN and stirred for 24 h at 30 °C. 100 µL of the solution were then used for HPLC-MS analysis.

Growth on MOPS-buffered minimal medium plates

For growth experiments of *S. meliloti fadL* mutants the strains were grown on carbon-free agar solutions based on MOPS minimal medium^[20] complimented with IPTG (500 µM) for *fadL* induction and Brij 58 (0.5%) for better solubility of fatty acids. Carbon sources stearic acid and 16-azidopalmitic acid were added at a final concentration of 5 mM each, while mannitol was added at 3 g/L. On each plate 2 µL of bacterial suspension in 0.9% NaCl with a measured OD₆₀₀ of 1 were spotted and photographed after 2 or 8 days respectively.

Acknowledgements

Work in the Bode lab was supported by an European Research Council starting grant under grant agreement number 311477. The authors are grateful to Elizaveta Krol and Anke Becker from the University of Marburg for supplying *Sinorhizobium meliloti* strains and for the conduction of the growth experiments in minimal medium.

References

- [1] S. Schoors, U. Bruning, R. Missiaen, K. C. S. Queiroz, G. Borgers, I. Elia, A. Zecchin, A. R. Cantelmo, S. Christen, J. Goveia, W. Heggemont, L. Godde, S. Vinckier, P. P. van Veldhoven, G. Eelen, L. Schoonjans, H. Gerhardt, M. Dewerchin, M. Baes, K. de Bock, B. Ghesquière, S. Y. Lunt, S. Fendt, P. Carmeliet. *Nature* **2015**, *520*, 192-197.
- [2] a) D. Reimer, K. M. Pos, M. Thines, P. Grün, H. B. Bode. *Nat. Chem. Biol.* **2011**, *7*, 888-890; b) A. O. Brachmann, S. Brameyer, D. Kresovic, I. Hitkova, Y. Kopp, C. Manske, K. Schubert, H. B. Bode, R. Heermann. *Nat. Chem. Biol.* **2013**, *9*, 573-578; c) S. W. Fuchs, K. A. J. Bozhüyük, D. Kresovic, F. Grundmann, V. Dill, A. O. Brachmann, N. R. Waterfield, H. B. Bode. *Angew. Chem. Int. Ed.* **2013**, *52*, 4108-4112.
- [3] a) B. van den Berg. *Curr. Opin. Struct. Biol.* **2005**, *15*, 401-407; b) C. C. DiRusso, P. N. Black, *J. Biol. Chem.* **2004**, *279*, 49563-49566.
- [4] C. C. DiRusso, P. N. Black, J. D. Weimar. *Prog. Lipid Res.* **1999**, *38*, 129-197.
- [5] A. J. Pérez, H. B. Bode, *J. Lipid. Res.* **2014**, *55*, 1897-1901.
- [6] J. Dommerholt, S. Schmidt, R. Temming, L. J. A. Hendriks, F. P. J. T. Rutjes, J. C. M. van Hest, D. J. Lefeber, P. Friedl, F. L. van Delft, *Angew. Chem. Int. Ed.* **2010**, *49*, 9422-9425.
- [7] F. Starke, M. Walther, H. Pietzsch, *ARKIVOC*, **2010**, *XI*, 350-359.
- [8] H. Nikaido. *Microbiol. Mol. Biol. Rev.* **2003**, *67*, 593-656.
- [9] J. Zarzycki-Siek, M. H. Norris, Y. Kang, Z. Sun, A. P. Bluhm, I. A. McMillan, T. T. Hoang. *PLoS one*, **2013**, *8*, e64554.
- [10] A. Pech-Canul, J. Nogales, A. Miranda-Molina, L. Álvarez, O. Geiger, M. J. Soto, I. M. López-Lara, *J. Bacteriol.* **2011**, *193*, 6295-6304.
- [11] P. N. Black, C. C. DiRusso. *Microbiol. Mol. Biol. Rev.* **2003**, *67*, 454-472.
- [12] E. M. Hearn, D. R. Patel, B. W. Lepore, M. Indic, B. van der Berg. *Nature* **2009**, *458*, 367-370.

- [13] D. G. Mashek, L. O. Li, R. A. Coleman. *Future Lipidol.* **2007**, 2, 465-476.
- [14] E. Krol, A. Becker, *Proc. Natl. Acad. Sci. USA*, **2014**, 111, 10702-10707.
- [15] W. D. Nunn, R. W. Colburn, P. N. Black. *J. Biol. Chem.* **1986**, 261, 167-171.
- [16] Y. Kang, J. Zarzycki-Siek, C. B. Walton, M. H. Norris, T. T. Hoang. *PLoS One*, **2010**, 5, e13557.
- [17] a) G. B. Kumar, P. N. Black, *J. Biol. Chem.* **1993**, 268, 15469-15476; b) P. N. Black, *J. Bacteriol.* **1988**, 170, 2850-2854,
- [18] C. O. Rock, S. Jackowski, *J. Biol. Chem.* **1985**, 260, 12720-12724.
- [19] T. Baba, T. Ara, M. Hasegawa, Y. Takai, Y. Okumura. *Mol. Syst. Biol.* **2006**, 2, 1-11.
- [20] F. C. Neidhardt, P. L. Bloch, D. F. Smith. *J Bacteriol.* **1974**, 119, 736-747.

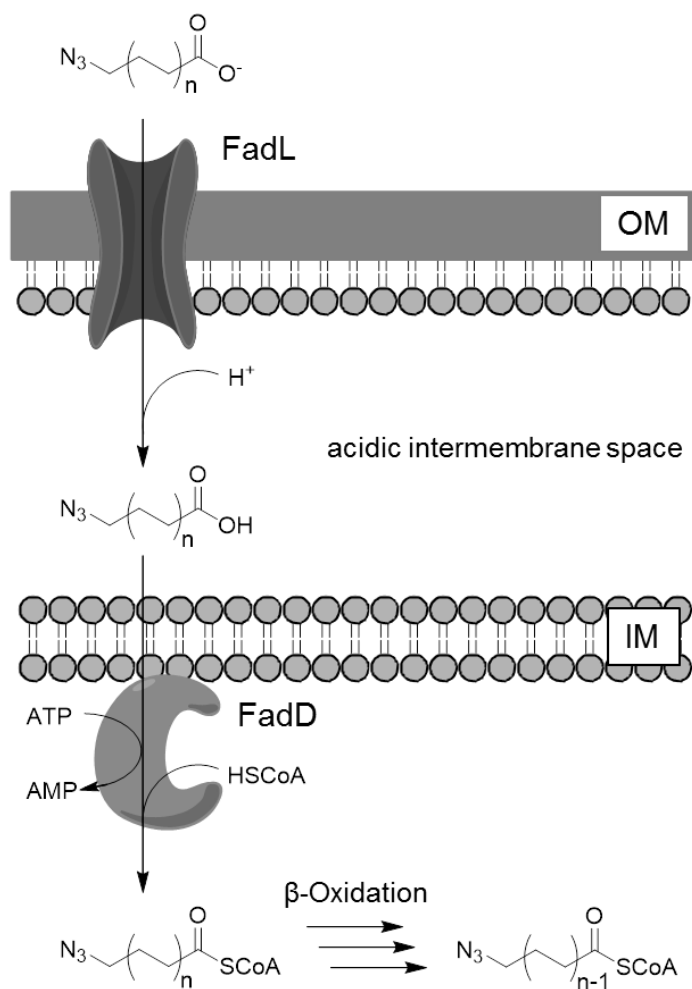
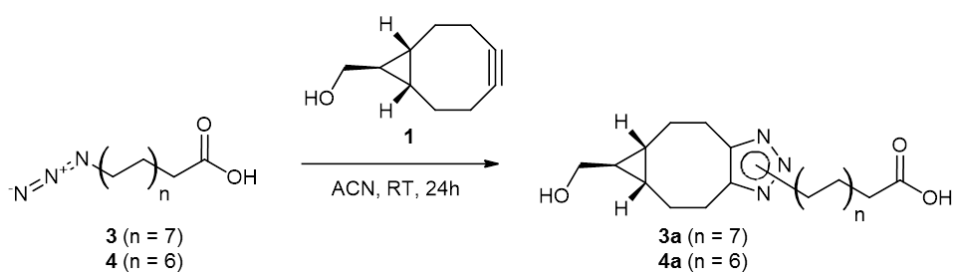


Figure 1. Established model of fatty acid transport through the outer membrane (OM) with the help of FadL and subsequent activation by inner membrane (IM) associated FadD in Gram-negative bacteria^[8] shown for the azido fatty acids used in this work. Oxidative degradation by C_2H_4 steps is shown for the activated CoA-thioesters that are formed *in vivo*.



Scheme 1. *In vitro* derivatisation of AFAs with BCN.

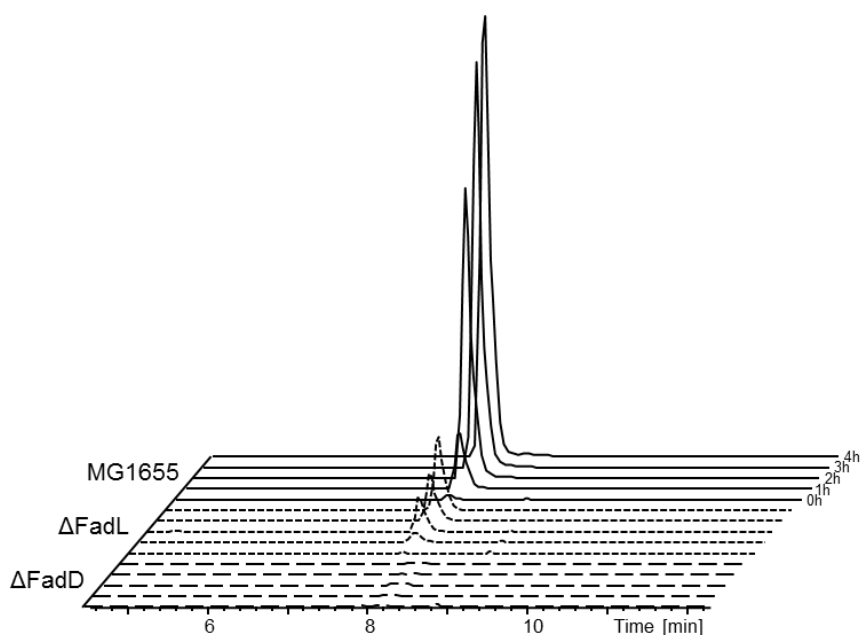


Figure 2. Extracted ion chromatograms of derivatized AFA degradation product **4a** ($m/z = 420$) at different time points after feeding of **3** at a concentration of 0.1 mM to the wildtype (MG1655) and Δ FadL mutant. The Δ FadD mutant was grown with a higher starting concentration of 1 mM of **3**. While deletion of *fadL* significantly slows down degradation of external AFA in comparison to the wildtype (MG1655), deletion of *fadD* completely prevents AFA degradation even at higher substrate concentration.

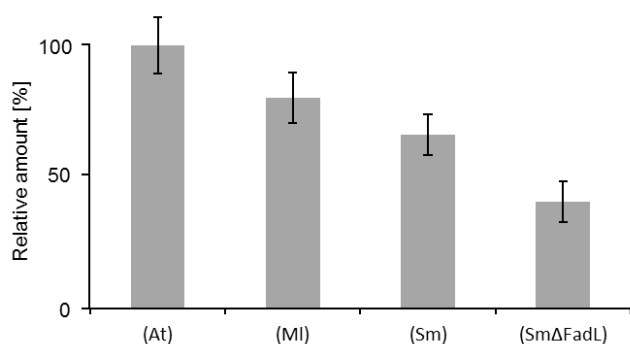


Figure 3. Amounts of **4a** after 5 h of feeding **3** at a concentration of 1 mM to various *S. melliloti* FadL strains relative to the strongest producer, At. A dominant production of oxidation product can be observed in the At mutant, alongside with little, yet readily observable oxidation products in complete absence of FadL (Sm Δ FadL, Fig. S4).

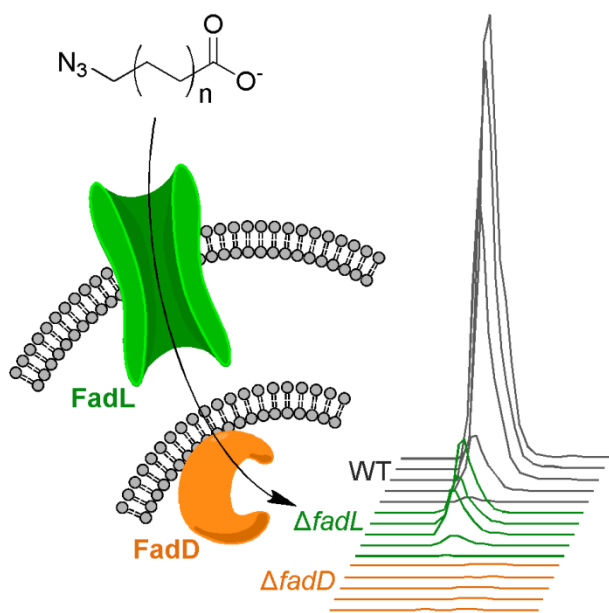


Table of Contents Text: No way to hide – Click-chemistry-based fatty acid analysis helps to shed light on the behaviour of bacterial fatty acid transport associated proteins FadD and FadL under natural growing conditions, casting doubt upon the essentiality of FadL for fatty acid transport through the membrane.

The role of the fatty acid transport associated proteins FadD and FadL for fatty acid uptake and degradation

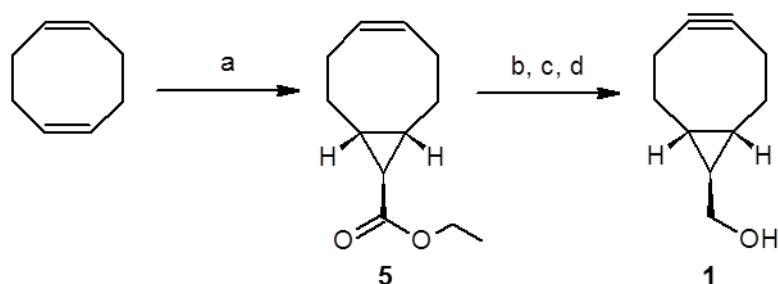
Alexander J. Pérez, Helge B. Bode

-Supporting Information-

Contents

Synthetic procedures	Page S2
Supplementary figures	Page S4

Synthetic procedures



Scheme S1: Synthesis of BCN from cyclooctadiene: (a) DCM, N₂CHCOOEt (0.125 eq.), 0 °C → RT, 40 h. (b) Et₂O, LiAlH₄ (2 eq.), 0 °C → RT, 20 h. (c) DCM, Br₂ (1 eq.), RT, 30 min. (d) THF, K^tBuO (4 eq.), 0 °C → RT, 18 h.

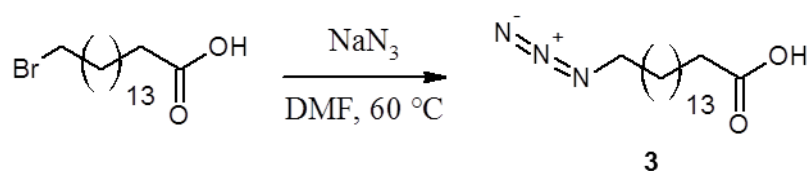
(1R,8S,9R,Z)-Ethylbicyclo[6.1.0]non-4-ene-9-carboxylate (5)

To a solution of 1,5-cyclooctadiene (22.3 mL, 181 mmol) and Rh₂(OAc)₄ (100 mg, 0.23 mmol) in dry DCM (10 mL) a solution of ethyl diazoacetate (2.38 mL, 22.6 mmol) in DCM (10 mL) was added over 1 h at 0°C. The reaction mixture was then stirred at RT for another 40 h, after which DCM and excess octadiene were evaporated. Progress of the evaporation was monitored by the weight of the remaining residues and TLC. The raw product was purified by column chromatography on silica (EtOAc/hexane, 1:25), yielding the *exo*-form (**5**) as the main product (1.74 g, 39%). ¹H NMR (CDCl₃, 500 MHz): δ = 5.67-5.61 (m, 2H), 4.12 (q, J = 7.2 Hz, 2H), 2.35-2.6 (m, 2H), 2.24-2.16 (m, 2H), 2.13-2.05 (m, 2H), 1.60-1.53 (m, 2H), 1.53-1.44 (m, 2H), 1.25 (t, J = 7.1 Hz, 3H), 1.19 (t, J = 4.6 Hz, 1H). ¹³C NMR (CDCl₃, 500 MHz): δ = 174.4, 129.9, 60.2, 28.2, 27.9, 27.7, 28.6, 14.3.

(1R,8S,9R)-Bicyclo[6.1.0]non-4-yn-9-ylmethanol (1)

A solution of **5** (1.1 g, 5.7 mmol) in dry Et₂O (10 mL) was added dropwise to a suspension of LiAlH₄ (437 mg, 11.5 mmol) in dry Et₂O (30 mL) at 0°C. After 10 min the reaction mixture was allowed to reach RT and stirred for 20 h. After cooling again to 0°C water (3 mL) was added and the mixture was stirred for 10 minutes after which the precipitate had turned white. The organic phase was decanted onto Na₂SO₄ (2 g), filtered and washed

thoroughly with Et₂O. The solvent was evaporated. Without further purification the alcohol was dissolved in DCM (10 mL) and a solution of Br₂ (292 μL, 5.7 mmol) in DCM (10 mL) was added dropwise until the yellow color persisted. Excess bromine was reduced with a 3 mL of sat. Na₂SO₃ and extracted with DCM (3 x 30 mL). The organic layer was dried over Na₂SO₄ and the solvent was evaporated, yielding the raw dibromide (1.0 g). Without further purification the dibromide was dissolved in THF (20 mL) and a suspension of excess K^tBuO (1.4 g, 12.8 mmol) in THF (10 mL) was added at 0°C. The reaction mixture was heated to reflux for 3 h and then stirred for another 18 h at RT. The reaction was quenched by the addition of sat. NH₄Cl (10 mL) and the product was extracted with Et₂O (2 x 20 mL) and DCM (2 x 20 mL). The organic phase was dried over Na₂SO₄ and the solvents were evaporated. The residue was purified by column chromatography on silica (EtOAc/hexane, 1:3) to afford **1** (110 mg, 0.74 mmol, 13% over 3 steps) as a colorless oil. ¹H NMR (CDCl₃, 400 MHz): δ = 2.55 (d, J = 6.4 Hz, 2H), 2.44-2.38 (m, 2H), 2.32-2.23 (m, 2H), 2.19-2.11 (m, 2H), 1.44-1.33 (m, 2H), 0.73-0.63 (m, 3H). ¹³C NMR (CDCl₃, 500 MHz): δ = 98.9, 67.1, 33.4, 27.3, 22.6, 21.4.



Scheme S2: Synthesis of 16-azidohexadecanoic acid from the corresponding bromide.

16-Azidohexadecanoic acid (**3**)

To a solution of 16-bromohexadecanoic acid (1.5 g, 4.47 mmol) in 10 mL dry DMF, sodium azide (872 mg, 13.4 mmol, 3 eq.) was added and stirred for 44h at 60 °C. Subsequently the solvent was evaporated and 50 mL of aqueous HCl were added. The raw product was extracted three times with 30 mL of EtOAc, the organic fractions were combined and dried over Na₂SO₄. Purification was conducted by column chromatography on silica, eluting with Hexane to Hexane/EtOAc (1:1), giving the product as a white solid (1.06 g, 3.55 mmol, 79%). ¹H NMR (500 MHz, CDCl₃) δ = 1.15 -1.43 (m, 22H), 1.49-

1.69 (m, 4H), 2.33 (t, J = 7.5 Hz, 2H), 3.23 (t, J = 6.9 Hz); ^{13}C NMR (500 MHz, CDCl_3) δ = 24.7, 26.7, 28.1, 29.0, 29.1, 29.2, 29.4, 29.5, 29.5, 29.6, 29.6, 29.6, 29.6, 34.0, 51.5, 180.0.

Supplementary Figures

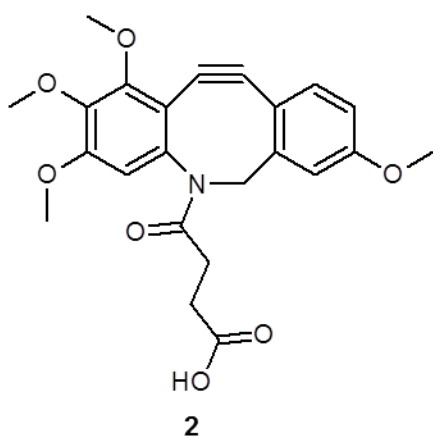


Figure S1: Structure of previously used tetramethoxydibenzoazacyclooctyne (TDAC, **2**)

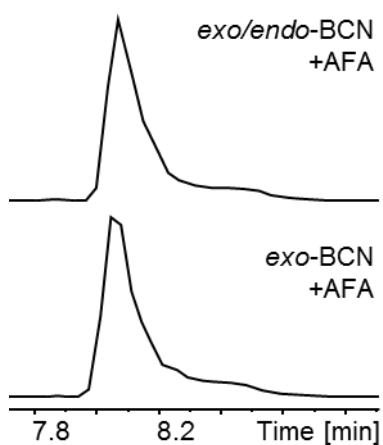


Figure S2: Comparison of the EICs of the reaction product of **4** with *exo*-BCN (top) and an *exo/endo* mixture of BCN (bottom). Peak shapes are very similar, and no difference in fragmentation could be observed.

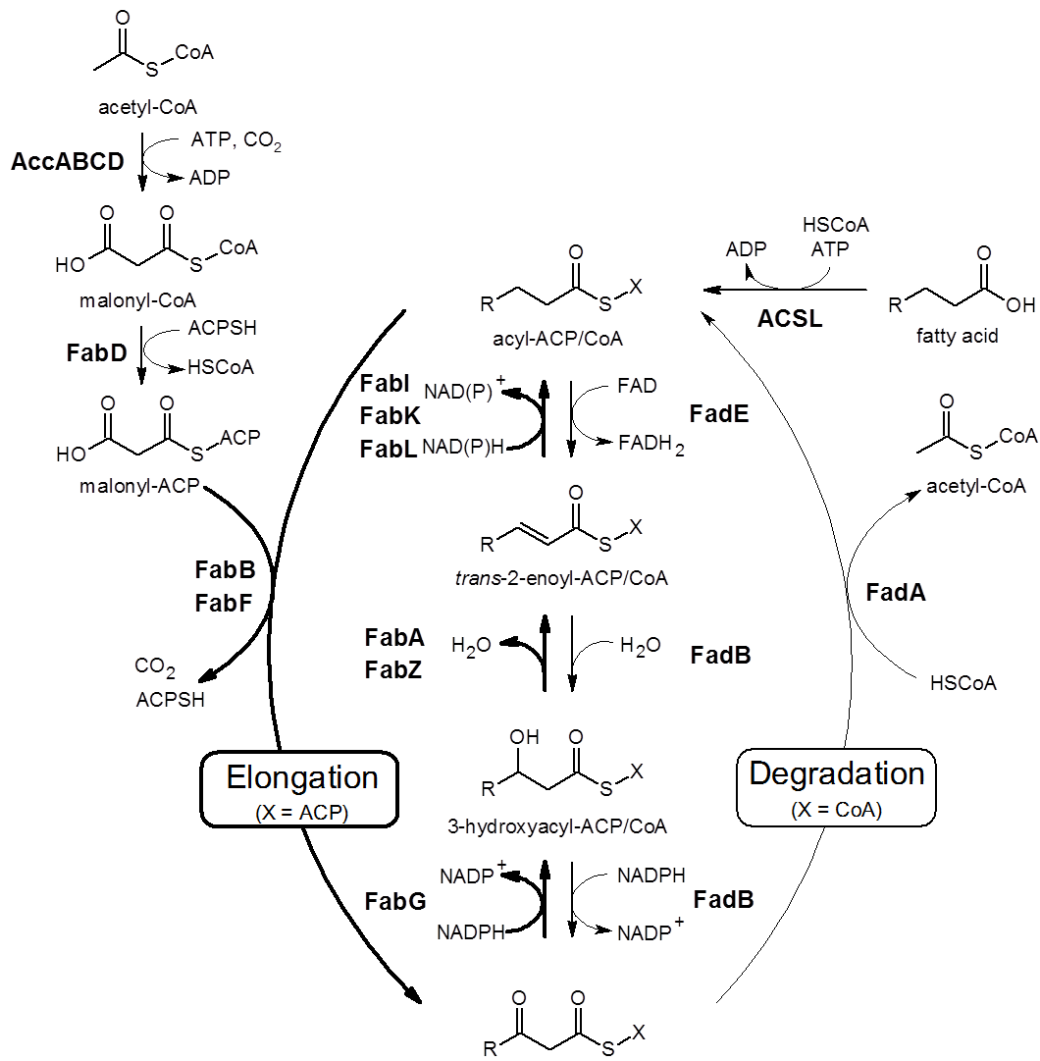


Figure S3: Central steps of fatty acid elongation and degradation in *E. coli*.

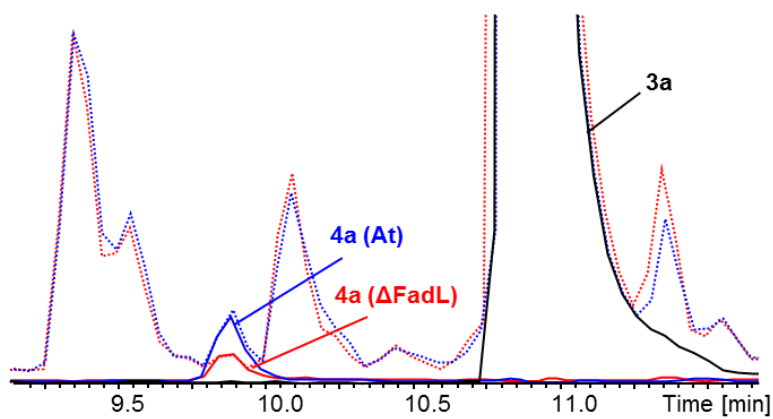


Figure S4: Base peak chromatograms of the At strain (blue) and the FadL-deficient Sm Δ FadL (red) mutant (dotted lines) with the corresponding EICs of the derivatized degradation product of **3**. The base peak chromatograms only differ in the amount of degradation product, making compareability of the peak integrals evident. EIC of undegraded AFA cycloaddition adduct **3a** is shown in black.

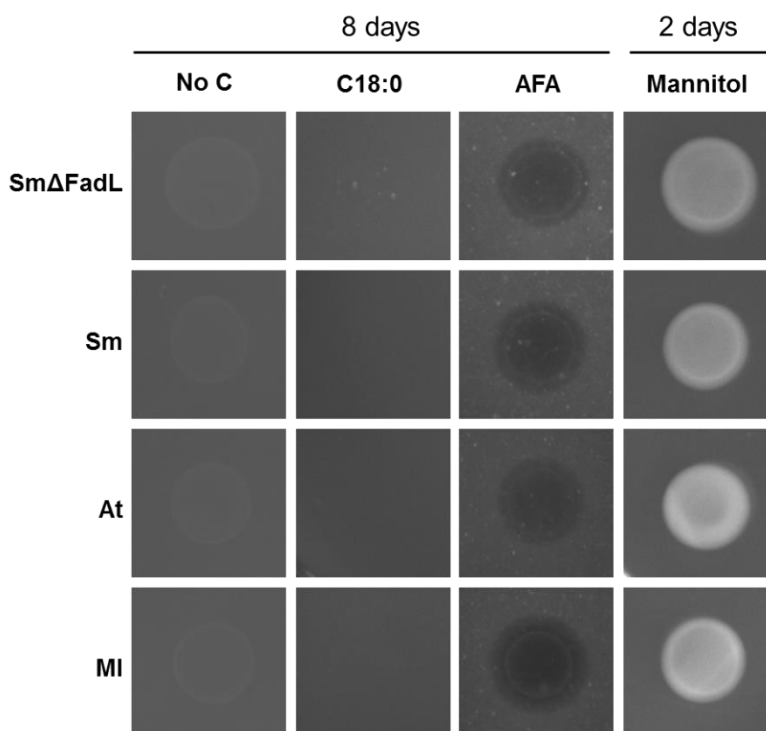


Figure S5: Growth of *S. meliloti* strains on minimal medium with either no carbon source (No C), stearic acid (C18:0) or 16-azidopalmitic acid (AFA) and mannitol as a positive control. Lack of any growth can be seen in the negative control as well as with stearic acid, whereas clearing of the opaque background can be seen when FA consumption occurs (AFA). The positive control on the other hand shows strong bacterial growth after only two days.

7.3 Manuscript: “Solid phase enrichment and analysis of azide labeled secondary metabolites – fishing downstream of biochemical pathways”

Authors: Alexander J. Pérez¹, Frank Wesche¹, Hélène Adihou¹, Helge B. Bode^{1,2}

¹Merck Stiftungsprofessur für Molekulare Biotechnologie, Fachbereich Biowissenschaften, Goethe Universität Frankfurt, 60438 Frankfurt am Main, Germany

²Buchmann Institute for Molecular Life Sciences (BMLS), Goethe Universität Frankfurt, 60438 Frankfurt am Main, Germany

Submitted to: Chemistry – A European Journal

Elaboration of the contributions of each author to the publication in question

Title of the manuscript: “Solid phase enrichment and analysis of azide labeled secondary metabolites – fishing downstream of biochemical pathways”

Project phase	Contribution of the authors
1) Planning and development	AJP: 70%, HBB: 20%, HA: 10%
2) Execution of experiments	AJP: all experiments except: HA: synthesis of N ₃ -PEA, FW: synthesis of N ₃ -Phe resin and N ₃ -szentiamide
3) Creation of figures and data sheets	AJP: 100%
4) Interpretation/Analysis of data	AJP: 90%; HBB: 10%
5) Abstract/Results/Discussion	AJP: 80%; HBB: 20%

Solid phase enrichment and analysis of azide labeled natural products – fishing downstream of biochemical pathways

Alexander J. Pérez,[†] Frank Wesche,[†] H el ene Adihou,[†] Helge B. Bode^{†,§,*}

[†]Merck Stiftungsprofessur f ur Molekulare Biotechnologie, Fachbereich Biowissenschaften, Goethe Universit at Frank-furt, Max-von-Laue-Str. 9, 60438 Frankfurt am Main, Germany

[§]Buchmann Institute for Molecular Life Sciences (BMLS), Goethe Universit at Frankfurt, Max-von-Laue-Str. 15, 60438 Frankfurt am Main, Germany

ABSTRACT: Many methods have been devised over the decades to trace precursors of specific molecules in cellular environments e.g. for biosynthesis studies. The advent of click-chemistry now allows the powerful combination of tracing and at the same time sieving the highly complex metabolome for compounds derived from simple or com-plex starting materials, especially when the click-reaction takes place on a solid support. While the principle of solid phase click-reactions has already been successfully applied for selective protein and peptide enrichment, the successful enrichment of much smaller primary and secondary metab-olites that constitute a large structural diversity and undergo many different biosynthetic steps has not been shown so far. For bacterial secondary metabolism a far larger toler-ance for “clickable” precursors was observed than in ribo-somal proteinogenesis, thus making this method a surpris-ingly valuable tool for the tracking and discovery of com-pounds within the cellular biochemical network. The imple-mentation of this method led to the identification of several new compounds from the bacterial genera Photorhabdus and Xenorhabdus, clearly proving its power.

INTRODUCTION

Specialized metabolites are small molecules with many different roles, ranging from nutrient acquisition (siderophores)^[1] and cell-to-cell signaling to weapons of interspecies warfare (antibiotics)^[2] and beyond. The structural

and biosynthetic nature of such compounds is just as diverse as the roles they fulfill, with several metabolites being peptides (ribosomally or non-ribosomally produced), polyketides or peptide-polyketide hybrids.^[3] While the precise role of several of these molecules is still unknown, identification of new compounds and their subsequent characterization are the basis in the assignment of their function and the subsequent development of new therapeutics.^[4]

Over the decades, a considerable amount of tools have been developed and applied in the fast and reliable identification of new metabolites. Among these are MS methods^[5], also coupled with stable isotope feeding experiments to unravel the structure of unknown compounds.^[6] With all of these methods having their very own limitations, it is highly favorable to have as many different methods available as possible. With the emergence of easily applicable click chemistry^[7], especially the bioorthogonal ring-strain-promoted cycloaddition as developed by Bertozzi *et al.*^[8], a door has been opened towards new approaches on the tracing and identification of potentially interesting compounds.

Here we describe an easily synthesized cleavable azide reactive resin (CARR, **1**, Figure 1, top) capable of reacting with and thus specifically absorbing a broad range of azides gained from *in vivo* metabolization and incorporation of previously fed precursor molecules. Methanolic XAD extracts of azide-supplemented bacterial cultures are incubated with the resin and subsequent cleavage of the cycloaddition products under mild conditions resulted in the rapid identification of several natural products showing the incorporated azides. Subsequent HPLC-MS analysis allows the rapid identification of these natural products among them several novel natural products that would otherwise have been easily overseen (Figure 1, bottom).

RESULTS AND DISCUSSION

Synthesis of the CARR resin. For the synthesis of the cleavable azide reactive resin (CARR, **1**, Figure 1) a PEGA resin was used as basis since it is both suited for polar molecules like peptides but also for small hydrophobic compounds^[9]. Furthermore functional group accessibility is retained in polar and amphiphilic solvents such as water, methanol or acetonitrile. The amino

moiety of the resin was succinylated and then derivatized with a cystamine linker, allowing for a reductive cleavage of the disulfide bond later on under mild conditions. Finally a reactive carbonate ester of BCN^[10] (**2**, Scheme S1) was used to attach the alkyne to the resin (Scheme S2). The BCN was used as an *endo/exo* mixture, as it had been previously shown that the chemical properties and retention times of each stereoisomer are almost indistinguishable.^[11] The resin was incubated with XAD extracts of cultures that were grown for 3 days after feeding each azide compound at 5 mM final concentration. For disulfide bond cleavage tris-(2-carboxyethyl)-phosphine (TCEP), dissolved in a 1:5:10 mixture of PBS/chloroform/methanol at pH 7, was used as a reducing agent, affording high reactivity and a broad solubility margin for peptides and lipids alike.

CARR enrichment of azido-fatty acids and natural products derived thereof. The resin was first tested with a fatty acid (FA) extract from a culture of *Myxococcus xanthus*, a bacterium that is known to possess a complex lipidome.^[12] As expected, after feeding of 15-azidopentadecanoic acid (**3i**) over 3 days, β -oxidation products could be detected directly from the base peak chromatogram of the sample, but also elongation products up to 19-azidononadecanoic acid (**3l**) were observed (Figures S1-2). The presence of this unusual FA might indicate the activity of a fatty acid elongase in *M. xanthus*.

Starting from there, azido fatty acids (AFAs) of varying chain length were fed to strains that are known for a rich production of secondary metabolites, such as the genera *Xenorhabdus* and *Photorhabdus*. *Xenorhabdus doucetiae* for example is known to produce simple amides formed from phenethylamine (PEA) and a variety of FAs^[13], indicating a great substrate tolerance concerning the fatty acyl residue. Thus a feeding experiment with three different AFAs (**3b**, **3c** and **3d**) was conducted, resulting in the production of several phenethylamides (Figure 2 and S3). Interestingly, not only was C₁₀-AFA (**3d**) degraded in C₂H₄-steps to yield **5f**, **5d** and **5b**, but the shorter AFAs were also elongated, including unsaturated variants **7a**, **7b** and **7c** with a chain length of 10, 12 and 14 carbons in the case of feeding of **3c** (Figure

S4). In spite of the already very short chain length, β -oxidation products of **3b** and **3c** were also observed, leading to **5a** and **5b** respectively. This was confirmed by cultivation of *X. doucetiae* with C₆-AFA (**3b**) in ¹³C-medium, showing incorporation of 8 carbons for the direct amidation product **5d**, and 8+2m ¹³C-carbons (two additional carbons for each elongation cycle m) for AFA elongation products **5f** (m = 1), **5h** (m = 2) and **5j** (m = 3) where m is the number of elongation cycles performed on the AFA prior to their incorporation (Figure S3). Additionally, elongation products were also observed with 10+2m ¹³C-carbons requiring four elongation cycles (m = 4, Figure S5). This might be explained by an initial degradation step of **3c** to **3a** (C₆-AFA to C₄-AFA, m = 1) prior to elongation and final amidation, resulting in the same final length of the amides observed (m = 4-1 = 3). FA biosynthesis and thus elongation usually requires ligation of the starter acyl chain to the phosphopantetheinyl moiety of an acyl carrier protein (ACP), whereas degradation is performed with the FA activated as CoA-thioester^[14]. The finding of 10+2m ¹³C-carbons in elongated amides thus shows that a transesterification of the CoA-thioester of **3a** to ACP must have occurred via a FabD-like protein. Since iso-branched fatty acids, such as produced by *X. doucetiae* and *M. xanthus* require special starting units like isovaleryl-CoA^[15], short-chain AFAs too might be activated as CoA-thioesters before entering the elongation cycle, finally resulting in the production of the respective ACP-bound intermediates used in the biosynthesis of the phenethylamides that might use ACP- or CoA-bound acyl intermediates.

In *P. luminescens* a long chain AFA **3j** was fed, resulting in the detection of several β -oxidation products, along with a signal that could be linked to an azido phurealipid derivative^[16] (**10c**, Figure 2 and S6). Upon feeding the shorter AFA **3i**, similar signals for **9b** and **9d** could be observed, while feeding of the short AFA **3c** resulted in the formation of the elongated FA **4h** and also in the formation of phurealipid **9a** and **9c** (Table S1). N-Methylation of these lipids was confirmed via the MS fragmentation pattern that showed the neutral loss of methylamine and methylisocyanate (Figure S7). These results show that the chain length tolerance for the incorporation of AFAs is more narrow compared to phenethylamides, which correlates well with previous findings^[16] showing the incorporation of C₉ to C₁₄ alkyl chains in

phurealipids. Since in our case **10a** and **10d** were only detected in trace amounts, it can be concluded that the preferred chain length for AFAs in this case is C₉ and C₁₀ (**9b** and **9c**), which is in accordance with the main natural products when the azide group is regarded as equivalent to the size of an ethyl group rather than a propyl group due to the higher rigidity of the azido group.

CARR enrichment of p-azidophenethylamine and natural products derived thereof. Following the good results gained with phenethylamides from *X. doucetiae*, *p*-azidophenethylamine (azido-PEA, **11a**) was synthesized^[17] and fed to the same strain, expecting to find similar products but labeled on the other end of the linear molecules. Instead, large amounts of azidophenylacetic acid (**12a**) were found, along with the corresponding phenethylamide **13a** (Figure S8A). To further elaborate the biochemical pathways involved in the conversion of PEA to phenylacetic acid (PAA, **12c**) an isotope labeling experiment was conducted (Figure S9). Extracts of cultures grown in ¹³C-medium led to a mass shift of 16 relative to the natural compound's mass of $m/z = 420$ [M+H]⁺, as was expected for the incorporation of 16 carbons into **13c**. Addition of PAA to this culture led to the incorporation of eight ¹²C carbons, whereas addition of PEA led to the incorporation of 8 and 16 ¹²C carbons, showing that PEA can easily be converted to PAA but not vice versa (Figure S9). Thus, it can be concluded that azido-PEA is not a suitable substrate for the unknown amide synthase but is readily converted into azido-PAA via transamination and oxidation (Figure 3).

Azido-PEA was also fed to cultures of *Xenorhabdus nematophila*, which is known to incorporate PEA into rhabdopeptides^[18] and xenortides^[19]. While it quickly became evident that azido-PEA was not incorporated into any rhabdopeptide, the expected adduct mass for the dimethylated tripeptide xenortide A (**14a**) was indeed found and confirmed by HR ESI-MS and its fragmentation pattern (Figures 3, S8B and S10). Again azido-PAA was found as a byproduct of PEA metabolism, apparently without further incorporation into other compounds. Two additional signals could be linked to a derivative

of nematophin (**15b**, Figure 3), a branched α -ketoisocaproyl tryptamides^[20] and to a homologous α -ketoisovaleryl derivative thereof (**16b**, Figure 3, S8B and S11). Although no PEA derivatives of nematophin are known, the presence of the azido-function might allow the incorporation of this slightly larger PEA analogue. Interestingly, compound **15a** was also found in *X. doucetiae* after feeding of azido-PEA, even though it was previously unknown that nematophin is produced by this strain. Careful HPLC-MS analysis of the raw XAD extract of *X. doucetiae* then indeed showed the presence of nematophin (Figure S12).

CARR enrichment of *p*-azidophenylalanine and natural products derived thereof. Next, the tolerance for the incorporation of azido-phenylalanine (azido-Phe, **17a**) was investigated. A certain degree of ambiguity/promiscuity in the incorporation of aromatic amino acids is known for compounds such as the taxllaid peptides^[21] and GameXPeptides^[22]. Taxllaid-producing *Xenorhabdus indica* was thus incubated with commercially available **17a** at 5 mM for three days, after which a single product was detected that was identified as azido-PAA (**12a**) not showing the expected incorporation into peptide natural products. However, additional metabolic steps must have occurred: transamination of azido-Phe to azidophenylpyruvic acid (**18a**, found only in miniscule amounts), followed by decarboxylation and eventually oxidation of a putative aldehyde (Figure S13A). Since the formation of **11a** was never observed, we deem it unlikely that an alternate pathway consisting of the transformation of **17a** to **11a**, transamination and subsequent oxidation took place. Interestingly, most enzymes showed a good substrate tolerance of the azido-group. However, consecutive degradation to acetyl-CoA and succinyl-CoA derivatives that have been shown to follow in the catabolic pathways of PAA in many bacteria have not been detected.^[23] In order to differentiate between the two possible pathways of azido-Phe degradation *Escherichia coli* was incubated with azido-Phe and the culture broth was analyzed for azido-phenylpyruvic acid and azidophenylacetaldehyde. While azido-phenylpyruvic acid could be found and identified in notable amounts already 24h after feeding azido-Phe at 5 mM, the aldehyde could not be found during this experiment (Figure

S13B). When **17a** was fed to *X. doucetiae* the formation of phenethylamide **13a** could be observed (Figure S13C), just as after the feeding of **11a** previously, suggesting that **17a** was first converted to **12a** via **18a** as has been shown to occur in other strains.

When azido-Phe was fed to *Xenorhabdus szentirmaii* many azido-derivatives of the phenylalanine catabolism described above were found^[23] (**18a**, **12a**, Figure S14). Additionally, a new signal was identified that could be attributed to azidobenzaldehyde (**19a**, detected as **19b** in Figure S15). The closest precursor of **19a** might be azidophenylpyruvic acid (**18a**) as it was described from *Lactobacillus plantarum*.^[24] Eluting at a similar retention time as **12b**, the oxidized form of aldehyde **19a**, azido-benzoic acid (**20a**), could also be detected (Figure 3, S14). Although produced only in small amounts after the regular 3 days of incubation, the amounts were significantly higher after 5 days (not shown), which is to be expected if the product is formed directly from **19a**. While it is known that *Streptomyces maritimus* produces benzoyl-CoA from phenylalanine via cinnamic acid^[25], it is unlikely that this pathway takes place in *X. szentirmaii*, since cinnamic acid was not detected, suggesting a direct oxidation of the abundant aldehyde **19a** instead (Figure 3). Considering the versatility of phenylalanine metabolism in *X. szentirmaii*, azidobenzoic acid (**20a**) was fed to the strain in a separate experiment to search for possible downstream metabolites via the CARR incubation method. A single product was observed, which could be assigned to the ethyl ester of said acid (**21b**, Figure 3 and S14) as it was confirmed by chemical synthesis followed by CARR enrichment (Figure S16A) and fragmentation pattern (Figure S16B). The formation of a benzoic acid ester is interesting in so far that production of such compounds is primarily a specialty of plants.^[26]

At a Rt between 9.8-11.1 min, four additional new products could be seen (**22b-25b**, Figure 3, S14 and S15) after addition of azido-Phe (**17a**). The fragmentation pattern showed the formation of positively charged **17a** from all of these compounds in their underivatized form and the sum formulas gained from HR-MS (Table S1) indicated that the first two derivatized products (**22b-23b**) were *N*-acylation products of **17a**, with octanoyl (**22b**) and *iso*-nonanoyl (**23b**) sidechains for the first two signals, as was confirmed by growth experiments in ¹³C-medium (Figure S17B). The incorporation of an iso-

branched FA was confirmed via the feeding of D₉-Leucin, leading to the expected mass-shift for **23a** and **25a** in the crude extract, while feeding of D₃-Methionine showed no mass shift (Figure S17A), excluding the possibility of S-adenosylmethionine derived *N*- or *C*-methylation for these compounds. To confirm the general structure of these compounds, **22a** was synthesized on solid support, reacted with CARR and analyzed under the same conditions as the natural products, showing identical retention time and MS²-fragmentation for **22b** (Figure S17C). The mass increase of 16 suggested the incorporation of an additional oxygen atom in **24b** and **25b**. An in-dept investigation of the fragmentation pattern of compounds **22b** and **24b** revealed that the mass shift is caused by a heavier acyl chain (Figure S18) suggesting the presence of β-hydroxy acyl or other oxygen-carrying moieties in these two structures and Figure 3 shows one possible structure for compounds **24a** and **25a**. At a retention time of 10.6 min, a small peak linked to the expected szentiamide^[27] derivative (**26a**, Figure 3) was also detected and the compound was identified via HR-MS (Table S1), its fragmentation pattern (Figure S19) and chemical synthesis (Figure S15). As could be deduced from the *m/z* ratio of **26b** and its fragmentation pattern, **17a** was incorporated instead of tyrosine, indicating that it is favorable when the natural amino acid to be substituted is larger than phenylalanine, just as was the case with nematophin (**11a** instead of tryptamin) due to the sterical demand of the azido group.

When **17a** was fed to *P. luminescens*, a small amount of PAA could be detected, along with a large amount of *p*-azidocinnamic acid (**27b**, Figure 3, Figure S20, S21A). *P. luminescens* is known to produce cinnamic acid for incorporation into Isopropylstilbene^[28] (IPS) and possibly other secondary metabolites. However, no azido-labeled IPS was detected, and as previous experiments had shown that *p*-chlorocinnamic acid is not incorporated into this compound class, while *m*-chlorocinnamic is^[29], it is likely that no *p*-substituted cinnamic acid derivatives might be used as IPS precursors. The second largest peak had a fragmentation pattern quite alike the acylated phenylalanine structures found in *X. szentirmaii*. HR-MS and the fragmentation pattern (**28b**, Table S1, Figure S21B) revealed that indeed this compound is azido-phenylalanine acylated with cinnamic acid, as was further

confirmed by solid phase peptide synthesis of **28a** and by repetition of the experiment with a $\Delta stlB$ mutant lacking the CoA-ligase needed for activation of cinnamic acid (Figure S21A).^[28] Finally, a small signal was discovered at a higher retention time as GameXPeptide A^[22,30] (**29b**), with **17a** being incorporated instead of the phenylalanine. The structure was confirmed via HR-MS (Table S1), the fragmentation pattern (Figure S21C) and via repetition of the feeding experiment with a *gxpS*-overexpressing *E. coli* strain as described previously^[31] where compound **29b** was detected as major compound (Figure S21A).

CONCLUSION

The combination of feeding of azide-labeled precursors with CARR can be regarded as a special form of precursor directed biosynthesis.^[32] Its advantage is the enrichment step that allows the detection of even minute amounts of compounds from complex mixtures. Thus, it has become an easy task to investigate the fate of small molecules from complex mixtures, yet this has not been conducted for the area of secondary metabolites until now.^[33] As was previously shown for FA analysis^[11,34], derivatized azides sport an excellent protonizability that makes LC/MS analysis especially simple since otherwise neutral or negatively charged compounds become well visible within a single analytic run (Figure S14). Our results also show that azido groups introduced into an amino or fatty acids are readily partaking in primary and secondary metabolism, allowing for an easy recovery of downstream products and their subsequent analysis. Similarly, the described approach can be expanded to other functional groups allowing the detection and enrichment of complimentary functions.^[35] An additional benefit of the described procedure might be a possible scale-up thus allowing the collection of sufficient amounts for a preparative purification of yet unidentified compounds. In this work, it could be shown that even small-scale analytical procedures such as liquid chromatography, high resolution mass spectrometry and MS²-fragmentation are already sufficient to shed light on the fate of compounds whose metabolic fate is at best surmised.

MATERIAL AND METHODS

General experimental procedures

Solvents and reagents were obtained from Sigma-Aldrich (München, Germany). Silica gel based chromatographic purification was performed on a Biotage SP1™ Flash Purification System (Biotage, Uppsala, Sweden), using 40+M KP-Sil cartridges (Biotage, Uppsala, Sweden) in combination with an UV detector. ¹H and ¹³C NMR spectra for the synthetic products were recorded on a Bruker AV500 (500 MHz), AV400 (400 MHz) or AV300 (300 MHz) spectrometer using CDCl₃ or D₆-DMSO as solvent and internal standard. ¹H-NMR: CHCl₃: δ = 7.27 ppm or D₆-DMSO: δ = 2.50 ppm; ¹³C-NMR: CDCl₃: δ = 77.00 ppm or D₆-DMSO: δ = 39.51. ESI HPLC MS analysis was performed with a Dionex UltiMate 3000 system coupled to a Bruker AmaZon X mass spectrometer using a MeCN/0.1 % formic acid in H₂O gradient ranging from 5 to 95 % in 16 min. at a flow rate of 0.6 mL/min. High resolution mass spectra were obtained from a Dionex Ultimate 3000 RSLC coupled to a Bruker micrOTOF-Q II equipped with an ESI source set to positive ionization mode. HR-HPLC settings were identical to those described above, although the column bed was 100 mm in length and the gradient length was set to 20 min. The mass spectrometer was calibrated using a sodium formate calibrant solution (10 mM). MS data were acquired within the mass range of $m/z = 100-1500$.^[12a] Alternatively, in some cases high resolution measurements were carried out using a MALDI LTQ Orbitrap XL (Thermo Fisher Scientific, Inc., Waltham, MA), equipped with a laser at 337 nm and a resolution of 100000. A 4-chloro- α -cyanocinnamic acid matrix was used, and the sum formulas and according masses were internally calibrated using des-Arg¹-Bradkynin ($m/z = 904.46811224$ [M+H]⁺) from Calibration Mixture 1 (SCIEX, Peptide Mass Standards Kit for Calibration of AB SCIEX MALDI-TOF™ Instruments) as a standard.^[6b]

Strains and cultivation conditions

All strains used in this work with the exception of *M. xanthus* were grown on solid and liquid Luria-Bertani (LB, pH 7.0) medium at 30°C and 180 rpm on a

rotary shaker. The *Photorhabdus* Δ *stilB* mutant was prepared according to the procedure described by Joyce et al.^[28] and needed no selection marker. The *E. coli* DH10B::*mtaA gxpS* overexpression mutant was grown with the addition of 100 mg/L ampicillin.^[31] *M. xanthus* was grown on solid and liquid CTT medium^[36] at 30°C and 180 rpm on a rotary shaker. The strains used were *Myxococcus xanthus* DK1622, *Escherichia coli* DH10B, *Xenorhabdus doucetiae* DSM17909, *Xenorhabdus nematophila* HGB081, *Xenorhabdus indica* DSM17382, *Xenorhabdus szentirmaii* DSM16338 and *Photorhabdus luminescens* TTO1.

Preparation of XAD extracts

10 mL of the corresponding cultures were inoculated at an optical density (OD₆₀₀) of 0.5 from overnight precultures and fed with the respective compounds at a final concentration of 5 mM. 2 vol.% of Amberlite XAD-16 beads were added and the cultures were cultivated at 30°C on a rotary shaker at 180 rpm for 72 h if not stated otherwise. The supernatant was then removed and the XAD was eluted with 10 mL of MeOH for 1 h. The solution was filtered, the solvent was evaporated and then dissolved in 1 mL of MeOH.

Azide enrichment procedure

3 mg of DMF-wet CARR (**2**) were placed inside a syringe for solid-phase peptide synthesis which was then filled with 500 μ L of the respective methanolic XAD extract after washing the resin thoroughly with MeOH and DCM. The suspension was heated to 55°C for 1h and then stirred over night. Excess extract was then removed and the resin was washed extensively with MeOH and DCM, after which the resin was incubated with 1 mL of a phosphate-buffered (pH = 7) 5 mM solution of tris(2-carboxyethyl)phosphine (TCEP) in PBS/CHCl₃/MeOH (1:5:10) for 1 h, after which the resulting solution was collected and evaporated. The cleavage products were then dissolved in 200 μ L of ACN and analyzed directly by HPLC/MS.

Acknowledgements

Work in the Bode lab was supported by an European Research Council starting grant under grant agreement number 311477. Special thanks are expressed towards our former interns Martin Brineck and Gina Grammbitter for helping with the resin synthesis and its first tests.

Keywords: click chemistry • azide enrichment • bioorthogonal chemistry • metabolic labeling • natural product identification

- [1] Saha, R.; Saha, N., Donofrio, R. S.; Bestervelt, L. L. *J. Basic Microbiol.* **2013**, *53*, 303-317.
- [2] Clardy, J.; Fischbach, M. A.; Walsh, C. T. *Nat. Biotechnol.* **2006**, *24*, 1541-1550.
- [3] Wenzel, S. C.; Müller, R. *Curr. Opin. Chem. Biol.* **2005**, *9*, 447-458.
- [4] Newman, D. J.; Cragg, G. M. *J. Nat. Prod.* **2007**, *70*, 461-477.
- [5] Kersten, R. D.; Yang, Y.; Xu, Y.; Cimermancic, P.; Nam, S.; Fenical, W.; Fischbach, M. A.; Moore, B. S.; Dorrestein, P. C. *Nat. Chem. Biol.* **2011**, *7*, 794-802.
- [6] (a) Bode, H. B.; Reimer, D.; Fuchs, S. W.; Kirchner, F.; Dauth, C.; Kegler, C.; Lorenzen, W.; Brachmann, A. O.; Grün, P. *Chem. Eur. J.* **2012**, *18*, 2342-2348. (b) Fuchs, S. W.; Sachs, C. C.; Kegler, C. Nollmann, F. I.; Karas, M.; Bode, H. B. *Anal. Chem.* **2012**, *84*, 6948-6955.
- [7] Moses, J. E.; Moorhouse, A. D. *Chem. Soc. Rev.* **2007**, *36*, 1249-1262.
- [8] Jewett, J. C.; Bertozzi, C. R. *Chem. Soc. Rev.* **2010**, *39*, 1272-1279.
- [9] Meldal, M.; Auzanneau, F.; Hindsgaul, O.; Palcic, M. M. *J. Chem. Soc., Chem. Commun.* **1994**, 1849-1850.
- [10] Dommerholt, J.; Schmidt, S.; Temming, R.; Hendriks, L. J. A.; Rutjes, F. P. J. T.; van Hest, J. C. M.; Lefeber, D. J.; Friedl, P.; van Delft, F. L. *Angew. Chem. Int. Ed.* **2010**, *49*, 9422-9425.
- [11] Pérez, A. J.; Bode, H. B. *ChemBioChem* **2015**, *16*, 1588-1591.

- [12] (a) Lorenzen, W.; Bozhüyük, K. A.; Cortina, N. S.; Bode, H. B. *J. Lipid Res.* **2014**, *55*, 2620-2633. (b) Ahrendt, T.; Wolff, H.; Bode, H. B. *App. Environ. Microbiol.* **2015**, doi: 10.1128/AEM.01537-15
- [13] Proschak, A.; Schulz, K.; Herrmann, J.; Dowling, A. J.; Brachmann, A. O.; ffrench-Constant, R.; Müller, R.; Bode, H. B. *ChemBioChem* **2011**, *12*, 2011-2015.
- [14] Parsons, J. B.; Rock, C. O. *Prog. Lipid Res.* **2013**, *52*, 249-276.
- [15] Dickschat, J. S.; Bode, H. B.; Kroppenstedt, R. M.; Müller, R.; Schulz, S. *Org. Biomol. Chem.* **2005**, *3*, 2824-2831.
- [16] Nollmann, F. I.; Heinrich, A. K.; Brachmann, A. O.; Morisseau, C.; Mukherjee, K.; Casanova-Torres, A. M.; Strobl, F.; Kleinhans, D.; Kinski, S.; Schultz, K.; Beeton, M. L.; Kaiser, M.; Chu, Y.; Phan Ke, L.; Thanwisai, A.; Bozhüyük, K. A. J.; Chantratita, N.; Götz, F.; Waterfield, N. R.; Vilcinskas, A.; Stelzer, E. H. K.; Goodrich-Blair, H.; Hammock, B. D.; Bode, H. B. *ChemBioChem* **2015**, *16*, 766-771.
- [17] (a) Hausler, N. E.; Devine, S. M.; McRobb, F. M.; Warfe, L.; Pouton, C. W.; Haynes, J. M.; Bottle, S. E.; White, P. J.; Scammells, P. J. *J. Med. Chem.* **2012**, *55*, 3521-3534. (b) Goddard-Borger, E. D.; Stick, R. V. *Org. Lett.*, **2007**, *9*, 3797-3800.
- [18] Reimer, D.; Cowles, K. N.; Proschak, A.; Nollmann, F. I.; Dowling, A. J.; Kaiser, M.; ffrench-Constant, R.; Goodrich-Blair, H.; Bode, H. B. *ChemBioChem* **2013**, *14*, 1991-1997.
- [19] Reimer, D.; Nollmann, F. I.; Schultz, K.; Kaiser, M.; Bode, H. B. *J. Nat. Prod.* **2014**, *77*, 1976-1980.
- [20] Li, J.; Chen, G.; Webster, J. M. *Can. J. Microbiol.* **1997**, *43*, 770-773.
- [21] Kronenwerth, M.; Bozhüyük, K. A. J.; Kahnt, A. S.; Steinhilber, D.; Gaudriault, S.; Kaiser, M.; Bode, H. B. *Chemistry* **2014**, *20*, 17478-17487.
- [22] Nollmann, F. I.; Dauth, C.; Mulley, G.; Kegler, C.; Kaiser, M.; Waterfield, N. R.; Bode, H. B. *ChemBioChem* **2015**, *16*, 205-208.

- [23] Teufel, R., Mascaraque, V., Ismail, W.; Voss, J. M.; Perera, Eisenreich, W.; Haehnel, W.; Fuchs, G. *PNAS* **2010**, *107*, 14390-14395.
- [24] Nierop Groot, M. N.; de Bont, J. A. M. *Appl. Environ. Microbiol.* **1998**, *64*, 3009-3013.
- [25] Moore, B. S.; Hertweck, C.; Hopke, J. N.; Izumikawa, M.; Kalaitzis, J. A.; Nilsen, G.; O'Hare, T.; Piel, J.; Shipley, P. R.; Xiang, L.; Austin, M. B.; Noel, J. P. *J. Nat. Prod.* **2002**, *65*, 1956-1962.
- [26] (a) Widhalm, J. R.; Dudareva, N. *Mol. Plant* **2015**, *8*, 83-97. (b) Dudareva, N.; Murfitt, L. M.; Mann, C. J.; Gorenstein, N.; Kolosova, N.; Kish, C. M.; Bonham, C.; Wood, K. *Plant Cell* **2000**, *12*, 949-961.
- [27] Ohlendorf, B.; Simon, S.; Wiese, J.; Imhoff, J. F. *Nat. Prod. Commun.* **2011**, *6*, 1247-1250.
- [28] Joyce, S. A.; Brachmann, A. O.; Glazer, I.; Lango, L.; Schwär, G.; Clarke, D. J.; Bode, H. B. *Angew. Chem. Int. Ed.* **2008**, *47*, 1942-1945.
- [29] Kronenwert, M.; Brachmann, A. O.; Kaiser, M.; Bode, H. B. *ChemBioChem*, **2014**, *15*, 2689-2691.
- [30] Bode, H. B.; Reimer, D.; Fuchs, S. W.; Kirchner, F.; Dauth, C.; Kegler, C.; Lorenzen, W.; Brachmann, A. O.; Grün, P. *Chem. Eur. J.* **2012**, *18*, 2342-2348.
- [31] Schimming, O.; Fleischhacker, F.; Nollmann, F. I.; Bode, H. B. *ChemBioChem* **2014**, *15*, 1290-1294.
- [32] Sun, H.; Liu, Z.; Zhao, H.; Ang, E. L. *Drug. Des. Devel. Ther.* **2015**, *9*, 823-833.
- [33] (a) Nessen, M. A.; Kramer, G; Back, J.; Baskin, J. M.; Smeenk, L. E. J.; de Koning, L. J.; van Maarseveen, J. H.; de Jong, L.; Bertozzi, C. R.; Hiemstra, H.; de Koster, C. G. *J. Proteome Res.* **2009**, *8*, 3702-3711. (b) Temming, R. P.; van Scherpenzeel, M.; te Brinke, E.; Schoffelen, S.; Gloerich, J.; Lefeber, D. J.; van Delft, F. L. *Bioorg. Med. Chem.* **2012**, *20*, 655-661.
- [34] Pérez, A. J.; Bode, H. B. *J. Lipid. Res.* **2014**, *55*, 1897-1901.

[35] Deb Roy, A.; Grüşchow, S.; Cairns, N.; Goss, R. J. *J. Am. Chem. Soc.* **2010**, *132*, 12243-12245.

[36] Hodgkin, J.; Kaiser, D. *Proc. Natl. Acad. Sci. USA* **1977**, *74*, 2938-2942.

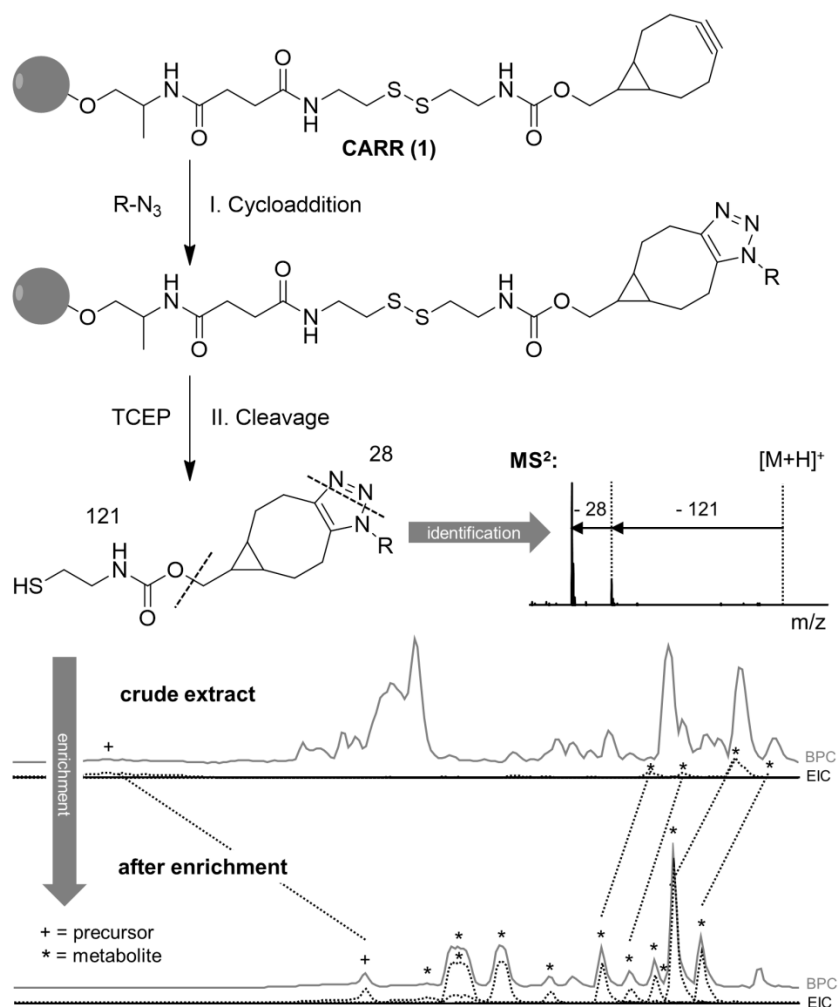


Figure 1. Principle of azide enrichment and product identification. After an azide (R-N₃) is covalently bound to the resin via an azide-alkyne cycloaddition, the compound is cleaved off the resin and analyzed via HPLC-MS. The characteristic fragmentation pattern of the derivatized azide allows the differentiation of true cycloaddition products from possible artifacts. The exemplary base peak chromatograms (grey) at the bottom demonstrate the production of a large number of metabolites (*) from a single precursor (+). The strength of this method to selectively enrich azide-bearing compounds that would otherwise be easily overlooked is made clear by the fact that almost each peak in the base peak chromatogram (BPC, grey) corresponds to the extracted ion chromatogram (EIC, black, dotted lines) of a metabolite of the precursor after enrichment, while most of the metabolites were almost undetectable in the crude extract. A detailed description of these particular chromatograms can be found in the supplementary information.

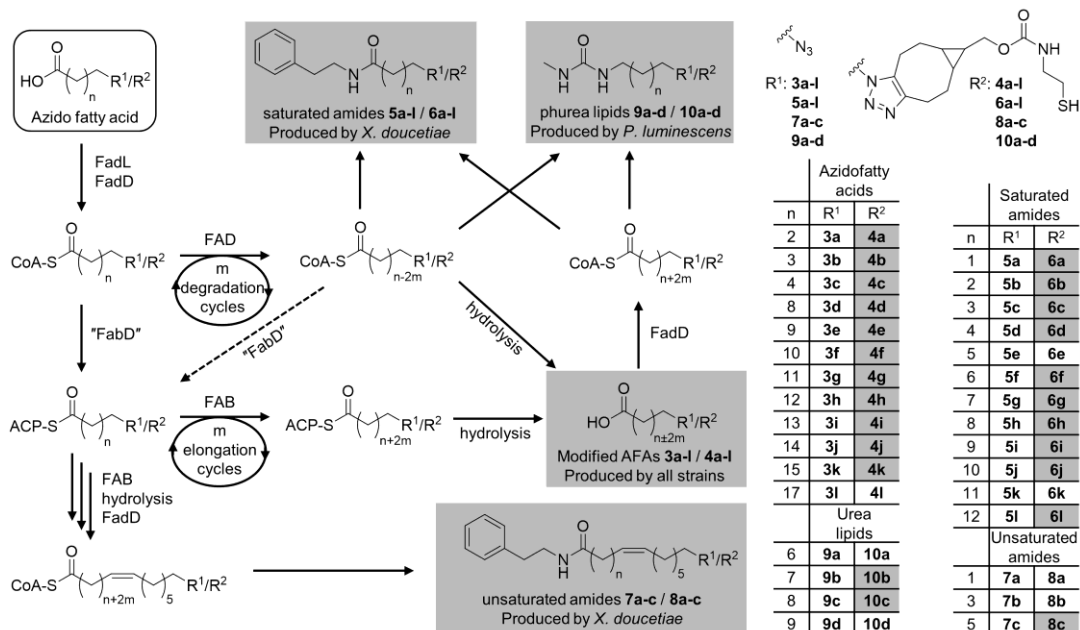


Figure 2. Metabolization of AFAs (framed) to various compounds (R^1) and their derivatized analogues (R^2) as found in the bacterial strains *Xenorhabdus doucetiae* (amides), *Photorhabdus luminescens* (phurealipids) and *Myxococcus xanthus* (long fatty acids), showing important degradation (FAD) and elongation (FAB) cycles (m = number of C_2H_4 addition or removal cycles) as well as the natural products they are eventually incorporated into. The dashed arrow indicates the case where degradation was proven to occur prior to elongation (Figure S5). Cycloaddition products that were verified via HR-MS (Table S1) are highlighted in grey in the table to the right. A detailed account of each feeding experiment can be found in supplementary Figures S1, S3 and S6.

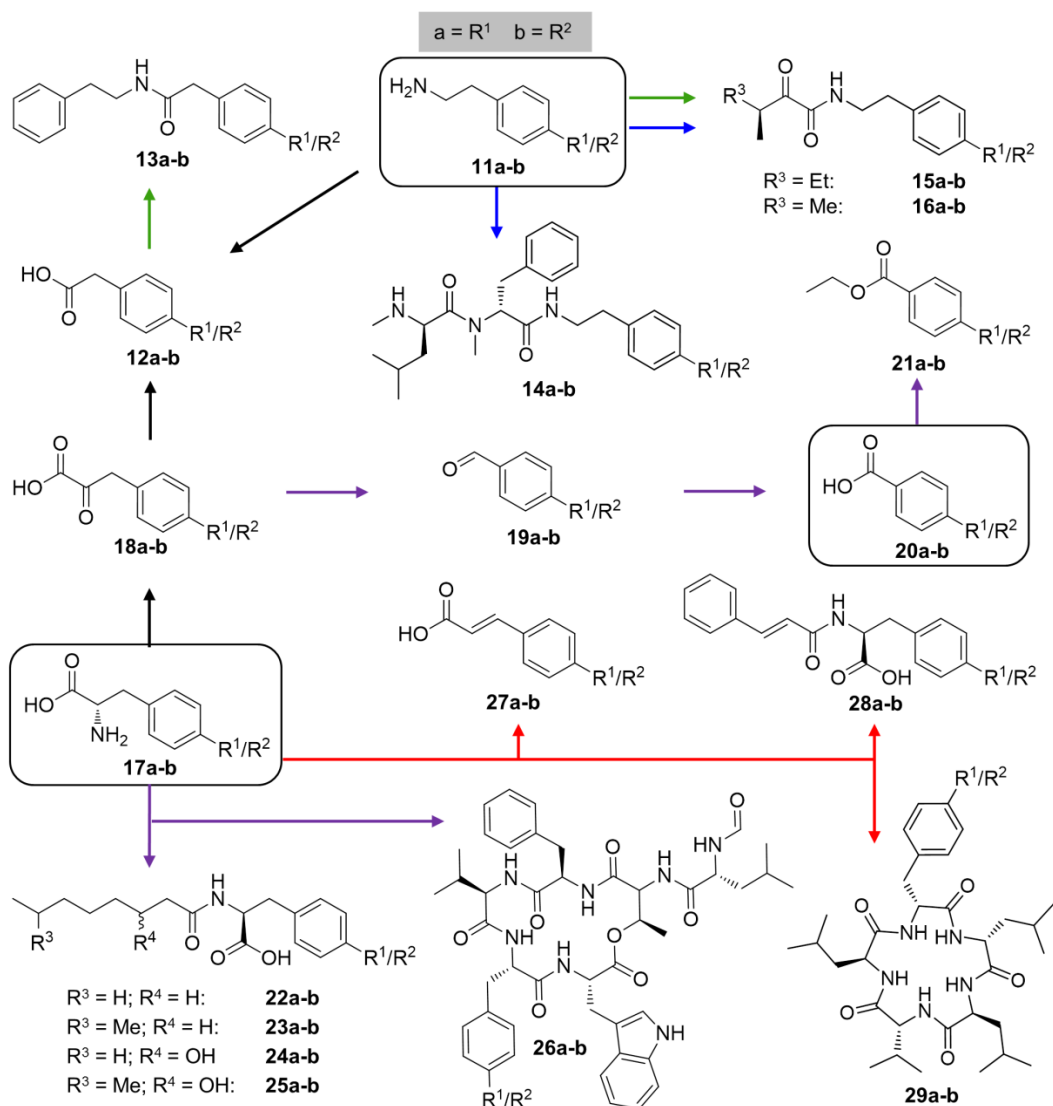


Figure 3. Metabolic pathways as observed in feeding experiments in various *Xenorhabdus* strains and one *Photorhabdus* strain. The substances that were fed (**11a**, **16a** and **23a**) are framed. Conversions seen in all accordingly fed strains are shown with black arrows, while colored arrows show conversions seen in only one particular strain: *P. luminescens* (red), *X. nematophila* (blue), *X. doucetiae* (green), *X. szentirmaii* (purple). *X. indica* only took part in general pathways and is thus not shown explicitly. A detailed account of each feeding experiment can be found in supplementary figures S8, S13, S14 and S20.

Solid phase enrichment and analysis of azide labeled secondary metabolites – fishing downstream of biochemical pathways

Alexander J. Pérez, Frank Wesche, H  l  ne Adihou, Helge B. Bode

-Supporting Information-

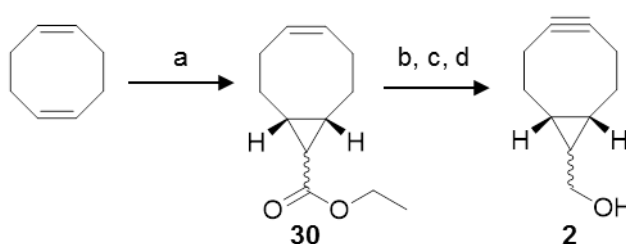
Contents

Synthetic procedures	Page S2
Supplementary tables	Page S11
Supplementary figures	Page S12
NMR Spectra	Page S29
References	Page S33

Synthetic procedures

BCN (**2**) and its activated form (**31**) were prepared basically as described by van Delft et al.¹ with minor changes to the equivalents and prepurification method used for ester **30**. Azidofatty acids **3b**, **3c**, **3d**, **3i** and **3j** were prepared as described previously from the corresponding ω -bromo fatty acids.²

Synthesis of BCN (**2**)



Scheme S1: Synthesis of BCN from cyclooctadiene: (a) DCM, $\text{N}_2\text{CHCOOEt}$ (0.125 eq.), $0\text{ }^\circ\text{C} \rightarrow \text{RT}$, 40 h. (b) Et_2O , LiAlH_4 (2 eq.), $0\text{ }^\circ\text{C} \rightarrow \text{RT}$, 20 h. (c) DCM, Br_2 (1 eq.), RT, 30 min. (d) THF, K^tBuO (4 eq.), $0\text{ }^\circ\text{C} \rightarrow \text{RT}$, 18 h.

(1*R*,8*S*,9 ξ ,*Z*)-Ethylbicyclo[6.1.0]non-4-ene-9-carboxylate (**30**)

To a green solution of 1,5-cyclooctadiene (43.3 mL, 351 mmol, 8 eq.) and $\text{Rh}_2(\text{OAc})_4$ (100 mg, 0.23 mmol, 0.5 mol%) in dry DCM (20 mL) a solution of ethyl diazoacetate (5 g, 44 mmol, 1 eq.) in DCM (20 mL) was added over 1 h at $0\text{ }^\circ\text{C}$ after which the solution had turned dark green. The reaction mixture was then stirred at RT for another 40 h, after which DCM and excess octadiene were evaporated. Progress of the evaporation was monitored by the weight of the remaining residues and TLC. The raw product was purified by column chromatography on silica (EtOAc/hexane, 1:6), yielding the product as a mixture of *exo*- and *endo*-forms (5.75 g, 67%).

endo-**30**: ^1H NMR (CDCl_3 , 500 MHz): δ = 5.64-5.57 (m, 2H), 4.10 (q, J = 7.17 Hz, 2H), 2.50-2.45 (m, 2H), 2.20-2.13 (m, 2H), 2.09-2.00 (m, 2H), 1.83-1.78 (m, 2H), 1.68 (t, J = 8.8 Hz, 1H), 1.39-1.34 (m, 2H), 1.27 (t, J = 7.1 Hz, 3H).

^{13}C NMR (CDCl_3 , 300 MHz): δ = 172.4, 129.3, 59.7, 26.9, 24.1, 22.6, 21.2, 14.2.

exo-**30**: ^1H NMR (CDCl_3 , 500 MHz): δ = 5.67-5.61 (m, 2H), 4.12 (q, J = 7.2 Hz, 2H), 2.35-2.6 (m, 2H), 2.24-2.16 (m, 2H), 2.13-2.05 (m, 2H), 1.60-1.53 (m, 2H), 1.53-1.44 (m, 2H), 1.25 (t, J = 7.1 Hz, 3H), 1.18 (t, J = 4.6 Hz, 1H). ^{13}C NMR (CDCl_3 , 300 MHz): δ = 174.6, 129.8, 60.2, 28.1, 27.8, 27.7, 26.5, 14.1.

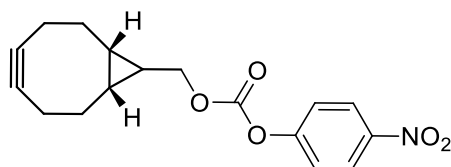
(1*R*,8*S*,9*ξ*)-Bicyclo[6.1.0]non-4-yn-9-ylmethanol (BCN, 2)

A solution of **30** (5.75 g, 29.6 mmol, 1 eq.) in dry Et_2O (40 mL) was added dropwise to a suspension of LiAlH_4 (2.25 g, 59 mmol, 2 eq.) in dry Et_2O (140 mL) at 0°C . After 10 min the reaction mixture was allowed to reach RT and stirred for 20 h. After cooling again to 0°C water (15 mL) was added and the mixture was stirred for 10 minutes after which the precipitate had turned white. The organic phase was decanted onto Na_2SO_4 (4 g), filtered and washed thoroughly with Et_2O . The solvent was evaporated. Without further purification the alcohol was dissolved in DCM (50 mL) and a solution of Br_2 (21.5 mL, 29.3 mmol, 1 eq.) in DCM (10 mL) was added dropwise until the yellow color persisted. Excess bromine was reduced with 5 mL of sat. Na_2SO_3 and extracted with DCM (3 x 30 mL). The organic layer was dried over Na_2SO_4 and the solvent was evaporated, yielding the raw dibromide (7.65 g). Without further purification the dibromide was dissolved in dry THF (20 mL) and a suspension of K^tBuO (10 g, 89.3 mmol, 3 eq.) in THF (10 mL) was added at 0°C . The reaction mixture was heated to reflux for 3 h and then stirred for 18h at RT. The reaction was quenched by the addition of sat. NH_4Cl (10 mL) and the product was extracted with Et_2O (2 x 20 mL) and DCM (2 x 20 mL). The organic phase was dried over Na_2SO_4 and the solvents were evaporated. The residue was purified by column chromatography on silica ($\text{EtOAc}/\text{hexane}$, 1:3) to afford **2** (1.11 g, 7.4 mmol, 25% over 3 steps) as a light yellow oil.

endo-**2**: ^1H NMR (CDCl_3 , 400 MHz): δ = 3.71 (d, J = 7.8 Hz, 2H), 2.33-2.19 (m, 6H), 1.66-1.53 (m, 2H), 1.43-1.31 (m, 1H), 0.97-0.89 (m, 2H). ^{13}C NMR (CDCl_3 , 400 MHz): δ = 98.8, 59.8, 29.0, 21.5, 21.4, 19.9.

exo-**2**: ^1H NMR (CDCl_3 , 400 MHz): δ = 3.54 (d, J = 6.4 Hz, 2H), 2.44-2.38 (m, 2H), 2.32-2.23 (m, 2H), 2.19-2.11 (m, 2H), 1.44-1.33 (m, 2H), 0.73-0.63 (m, 3H). ^{13}C NMR (CDCl_3 , 500 MHz): δ = 98.8, 67.0, 33.4, 27.2, 22.5, 21.4.

(1*R*,8*S*,9*ξ*)-Bicyclo[6.1.0]non-4-yn-9-ylmethyl (4-nitrophenyl) carbonate (31)

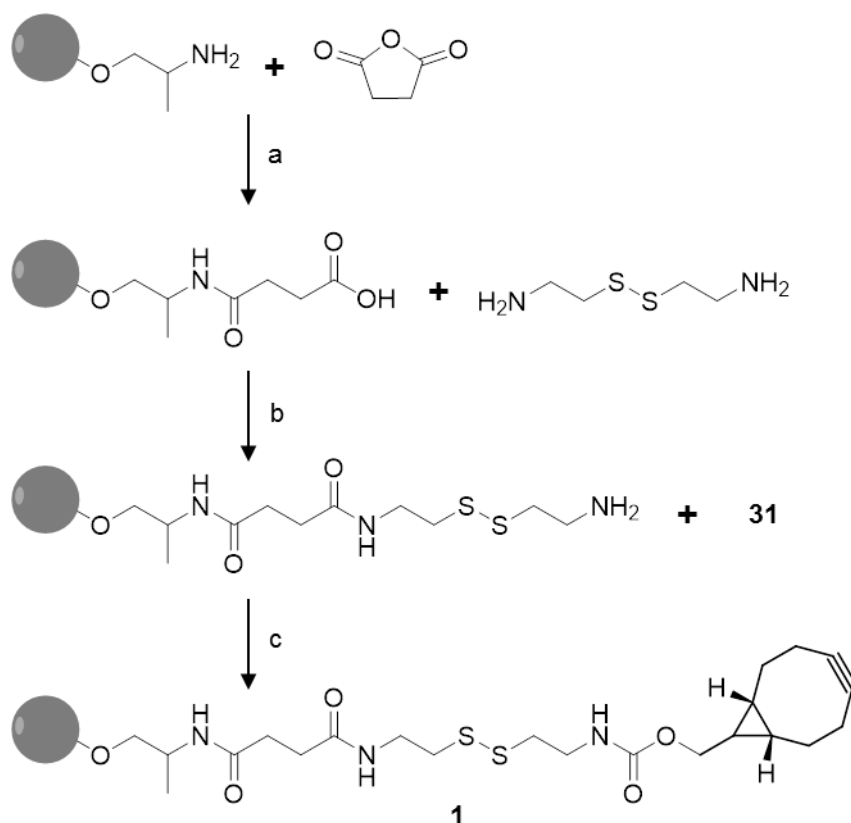


To a solution of a 1:2 *endo/exo*-mixture of **1** (369 mg, 2.45 mmol, 1 eq) and pyridine (494 μL , 6.1 mmol, 2.5 eq.) in 40 mL of dry DCM 4-nitrophenyl chloroformate (618 mg, 3.07 mmol, 1.2 eq.) were added under nitrogen atmosphere and stirred at RT. After 30 min the reaction was quenched with 30 mL of sat. NH_4Cl and extracted with 3 x 30 mL of DCM. The organic layer was dried over Na_2SO_4 and the solvent was evaporated. Purification by column chromatography (Hex/EtOAc; 0 \rightarrow 25%) yielded 415 mg (1.32 mol, 54%) of **31** as a white solid.

endo-**31**: ^1H NMR (CDCl_3 , 400 MHz): δ = 8.29 (J = 9.0 Hz, 2H), 7.39 (J = 8.9 Hz, 2H), 4.41 (J = 8.2 Hz, 2H), 2.38-2.24 (m, 6H), 1.68-1.57 (m, 2H), 1.57-1.47 (m, 1H), 1.12-1.01 (m, 2H). ^{13}C NMR (CDCl_3 , 400 MHz): δ = 155.6, 152.5, 145.3, 125.3, 121.7, 98.7, 68.0, 29.0, 21.3, 20.5, 17.2

exo-**31**: ^1H NMR (CDCl_3 , 400 MHz): δ = 8.29 (J = 9.0 Hz, 2H), 7.39 (J = 8.9 Hz, 2H), 4.23 (J = 6.6 Hz, 2H), 2.50-2.41 (m, 2H), 2.38-2.24 (m, 2H), 2.24-2.14 (m, 2H), 1.47-1.36 (m, 2H), 0.92-0.80 (m, 3H). ^{13}C NMR (CDCl_3 , 400 MHz): δ = 155.6, 152.6, 145.3, 125.3, 121.8, 98.6, 73.9, 33.1, 23.2, 23.0, 21.3.

Synthesis of cleavable azide reactive resin (CARR, 1)



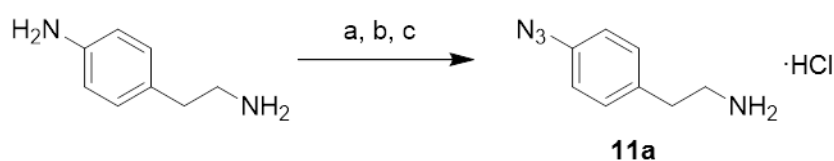
Scheme S2. Solid phase synthesis of CARR: a) DMAP, pyridine, RT, 20h; b) EDC·HCl, HOBt, DBU, DIPEA, RT, 3d; c) **31**, DIPEA, RT, 20h.

Step a: 1.36 g (0.1 mmol) of PEGA resin were washed with DMF and incubated with a solution of *p*-(dimethylamino)-pyridin (DMAP, 12 mg, 0.1 mmol, 1 eq.), succinic anhydride (250 mg, 2.5 mmol, 25 eq.) and pyridine (32 μ L, 0.4 mmol, 4 eq.) in 2 mL of DMF at RT over night. The resin was washed extensively with DMF and DCM. An ensuing Kaiser test was negative, showing that the reaction was quantitative.

Step b: The succinylated resin from the previous step (0.1 mmol) was incubated with a solution of *N*-(3-dimethylaminopropyl)-*N*'-ethylcarbodiimide hydrochloride (EDC·HCl, 23 mg, 0.12 mmol, 1.2 eq.), 4-hydroxy-*H*-benzotriazole (HOBt, 18 mg, 0.12 mmol, 1.2 eq.), cystamine dihydrochloride (45 mg, 0.2 mmol, 2 eq.), 1,8-Diazabicyclo[5.4.0]undec-7-ene (DBU, 38 mg, 0.25 mmol, 2.5 eq.) and diisopropylethylamine (DIPEA, 34 μ L, 0.2 mmol, 2 eq.) in 3 mL DMF at RT over three days. The resin was washed extensively with DMF and DCM. An ensuing Kaiser test was positive.

Step c: 300 mg (20 μ mol) of cystamidated resin from the previous step were incubated with a solution of **31** (9 mg, 30 μ mol, 1.5 eq.) and DIPEA (7 μ L, 38 μ mol, 1.9 eq.) in 800 μ L of DMF over night at RT. The resulting yellow solution was washed off extensively with DMF, yielding the target resin **1**.

p-Azidophenethylamine (**11a**)



Scheme S3. Synthesis of azidophenylethylamine (**11a**): a) Boc_2O , 10°C, DCM. b) Imidazole-1-sulfonyl azide hydrogen sulfate, $\text{CuSO}_4 \cdot 5\text{H}_2\text{O}$, K_2CO_3 , MeOH, RT c) 2 M HCl, Et_2O .

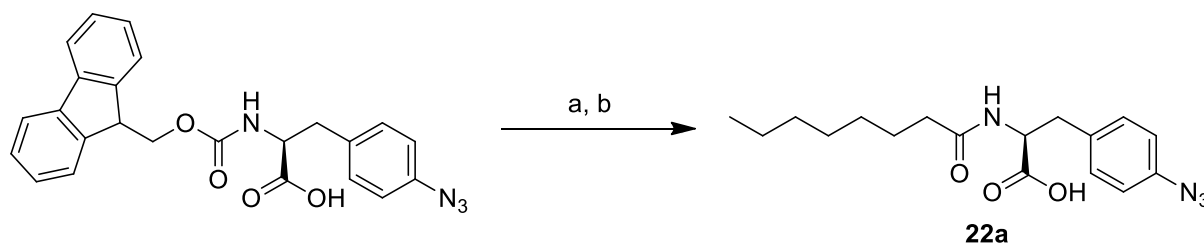
Step a: To a solution of 4-(2-Aminoethyl)aniline (120 mg, 0.88 mmol, 1 eq.) in 12 mL of DCM Boc_2O (173 mg, 0.81 mmol, 0.92 eq.) was slowly added at -10 °C. The mixture was stirred for 1 h at 0°C and the reaction process was monitored by TLC (R_f : 0.46 in PET/EtOAc 1:1). 8 mL of H_2O were added and organic phase was separated, washed with 2 x 8 mL H_2O and 2 x 8 mL brine, dried over Na_2SO_4 and the solvent was evaporated. The product was obtained as an orange solid (145 mg, 75%) and was used without further purification.³

Step b: To a solution of the protected amine (124 mg, 0.52 mmol, 1 eq.) in 2 mL of MeOH imidazole-1-sulfonyl azide hydrogen sulfate (170 mg, 0.62 mmol, 1.2 eq.), $\text{CuSO}_4 \cdot 5\text{H}_2\text{O}$ (1.3 mg, 5 μ mol, 1%) and K_2CO_3 (140 mg, 1.04 mmol, 2 eq.) were added. The suspension was stirred over night at RT. After addition of 8 mL of H_2O and 15 mL of EtOAc the organic layer was extracted and washed with 2 x 8 mL sat. NaHCO_3 and with 8 mL brine. After drying over Na_2SO_4 the solvent was evaporated, yielding the product as a brown solid (140 mg, quant.). The product was used without further purification.⁴

Step c: The resulting azide (100 mg, 0.38 mmol) in was dissolved in 2M HCl (10 ml) at 0°C in a falcon tube and the mixture was stirred at room temperature overnight. The suspension was centrifuged and the precipitated

was washed twice with Et₂O, and then dried. The brown powder (75 mg, quant.) was obtained as the hydrochloride and pure enough to be used without further purification. ¹H NMR (D₆-DMSO, 400 MHz): δ = 8.19-8.08 (3H, bs), 7.37-7.33 (2H, m), 7.14-7.10 (2H, m), 3.08-2.98 (2H, m), 2.96-2.89 (2H, m). ¹³C NMR (D₆-DMSO, 400 MHz): δ = 137.9, 134.4, 130.4, 119.4, 39.9, 32.3.

***N*-Octanoyl-*p*-azidophenylalanin (**22a**)**



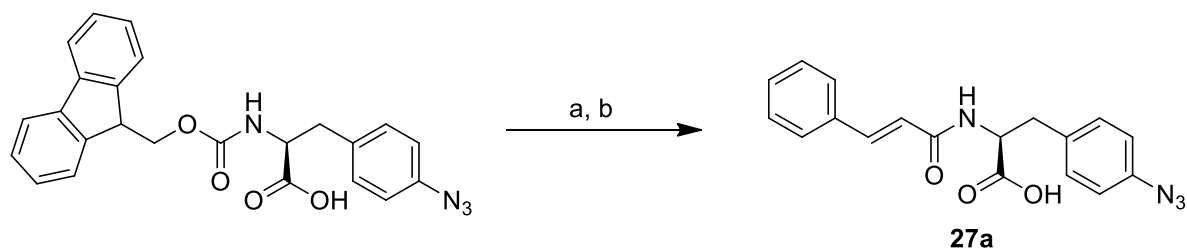
Scheme S4. Synthetic procedure for acylated azidophenylalanine **22a** on solid support, starting from commercially available Fmoc-protected azidophenylalanine: a) 2-chlorotrityl resin, DIPEA, RT, DCM, then 20% piperidine; b) octanoic acid, HATU, HOAt, DIPEA, RT, DMF.

Step a: 62.4 mg (0.1 mmol, 1 eq.) of 2-chlorotrityl resin (1.6 mmol/g) was brought in a plastic reactor vessel equipped with a teflon frit. The resin was washed with DCM, dry DCM and activated with 21.7 μL (0.3 mmol, 3 eq.) thionyl chloride in 1.5 mL dry DCM for 1 h and washed afterwards several times with dry DCM. 51.4 mg (0.12 mmol, 1.2 eq.) of Fmoc-L-Phe(4-N₃)-OH, 81.5 μL (0.48 mmol, 4.8 eq.) of DIPEA in 0.6 mL dry DCM were added to the resin and stirred overnight. At the end of this time the resin was washed with DCM, and stirred additional with DCM/MeOH/DIPEA (17/2/1) for 30 min to inactivate the left free binding sites and washed again with DCM. Afterwards the Fmoc protecting group was removed with 20% piperidine in NMP (three times 5 min) and washed again several times with DCM. Loading was estimated to be 70% through Fmoc loading.

Step b: 5 mg (5 μmol) of the loaded resin from the previous step were washed with DMF and incubated with a solution of octanoic acid (4 μL, 25 μmol, 5 eq.), HATU (10 mg, 25 μmol, 5 eq.), HOAt (4 mg, 25 μmol, 5 eq.) and DIPEA (9 μL, 50 μmol, 10 eq.) in 200 μL of DMF for 20 h at 40 °C. The resin was then washed several times with DMF and DCM, after which the product

was cleaved off with a mixture of TFA/TIS/H₂O (95:2.5:2.5) and the solvents were evaporated. The crude product **22a** (1 mg) was then used for analysis without further purification. HR-ESI-MS data for this compound can be found in Table S1.

***N*-Cinnamoyl-*p*-azidophenylalanine (**27a**)**

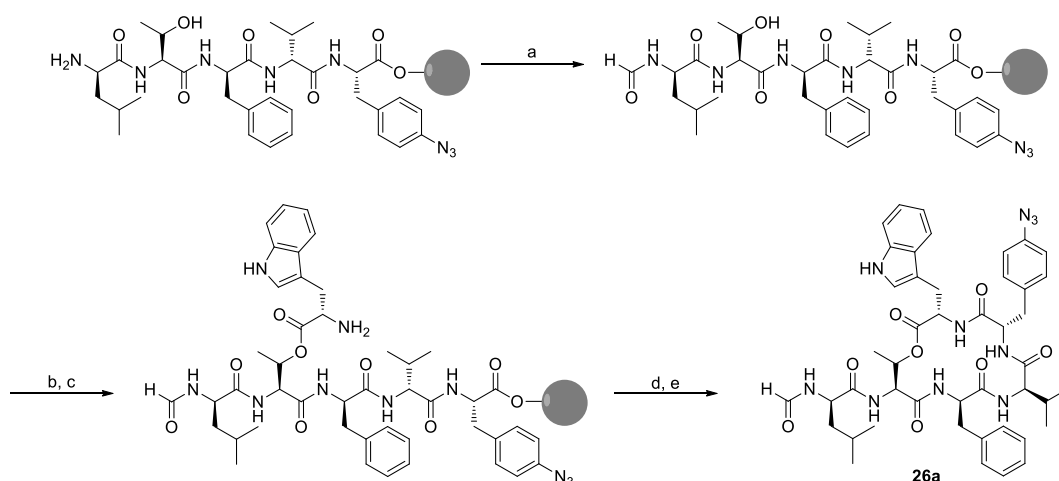


Scheme S5. Synthetic procedure for acylated azidophenylalanine **27a** on solid support, starting from commercially available Fmoc-protected azidophenylalanine: a) 2-chlorotrityl resin, DIPEA, RT, DCM, then 20% piperidine; b) cinnamic acid chloride, DIPEA, RT, DMF.

Step a: see synthesis of **22a** above.

Step b: 5 mg (5 μ mol) of the loaded resin from the previous step were washed with DMF and incubated with a solution of cinnamic acid chloride (4 mg, 25 μ mol, 5 eq.) and DIPEA (9 μ L, 50 μ mol, 10 eq.) in 200 μ L of DMF for 20 h at 40 °C. The resin was then washed several times with DMF and DCM, after which the product was cleaved off with a mixture of TFA/TIS/H₂O (95:2.5:2.5) and the solvents were evaporated. The crude product **27a** (1 mg) was then used for analysis without further purification. HR-ESI-MS data for this compound can be found in Table S1.

Azido-szentiamide (26a)



Scheme S6. a) pPNF, NMM, DMF, 4 °C, 18 h; b) Fmoc-Trp-OH, DIC, DMAP, THF; c) 3*5 min 20% piperidine in NMP; d) 3*15 min 20 % HFIP in DCM; e) EDC-HCl, oxyma pure, 75 °C, 25 W, 20 min.

Solid Phase Peptide Synthesis: The linear sequence was synthesised on the preloaded 2-chlorotrityl resin (see step a in synthesis of **22a** above) on a 25 μmol scale with a Syro Wave peptide synthesizer (Biotage, Uppsala, Sweden) by using standard 9-fluorenylmethoxycarbonyl/*tert*-butyl (Fmoc/*t*-Bu) chemistry. Therefore the resin was placed in a plastic reactor vessel with a teflon frit and an amount of 6 eq. of amino acid derivatives (different suppliers, $c = 0.2\text{mol/L}$) was activated *in situ* at room temperature with 6 eq. of *O*-(6-Chlorobenzotriazol-1-yl)-*N,N,N',N'*-tetramethyluronium hexafluorophosphate (HCTU, $c = 0.6\text{ mol/L}$) in dimethylformamide (DMF) in the presence of 12 eq. *N,N*-diisopropylethylamine (DIPEA, $c = 2.4\text{ mol/L}$) in *N*-methylpyrrolidone (NMP). Fmoc-protecting groups were removed with a solution of 40% piperidine in NMP (v/v%) for 5 min and the deprotection step was repeated for another 10 min with 20% piperidine in NMP (v/v%).

Step a: For the formylation of the free *N*-terminus a mixture of *para*-nitrophenyl formate (pPNF, 5 eq., 15.3 μL) and *N*-methylmorpholine (NMM, 3 eq. 8.2 μL ,) in 2 mL DMF was added to the peptidyl resin and incubated at 4 °C over night. Afterwards the resin was washed with DMF (5x) and DCM (5x). Small scale cleavage and LC-MS analysis confirmed formylation of the *N*-terminus.

Step b and c: The resin was first dried and then washed with dry THF (3x) under nitrogen atmosphere. Fmoc-Trp-OH (10 eq. 250 μmol , 106.6 mg) was dissolved in dry THF at 0 °C and diisopropylcarbodiimide (DIC, 10 eq., 250 μmol , 38.7 μL) and the mixture was pre-activated at this temperature for 20 min. Thereafter the resin and the prepared amino acid mixture were transferred to an Eppendorf tube and 4-(*N,N*-dimethylamino)pyridine (DMAP, 1 eq., 3.0 mg) dissolved in 0.2 mL dry THF was added. The Eppendorf tube was placed in a thermoshaker and was shaken for 24 h at 37 °C. Then the beads were transferred again to the plastic reactor vessel and subsequently the resin was washed with DMF (5x) and DCM (5x). Small scale cleavage and LC-MS analysis confirmed ester bond formation. Additionally no epimerization could be observed. Fmoc-protection group was removed with a solution of 20% piperidine in NMP (v/v%) for 5 min and the deprotection step was repeated twice. The fractions were used for determination of the Fmoc-loading by measuring the optical density at 301 nm ($E = 7800 \text{ L/mol}\cdot\text{cm}$). A loading of 16.3 μmol was calculated.

Step d and e: The branched peptide was cleaved from the dried resin with 0.5 mL of 20 % hexafluoroisopropanol (HFIP) in DCM (v/v%) for 15 min. This procedure was repeated two more times (2*15 min). The combined filtrates were dried to obtain the crude peptide. Thereafter the peptide was cyclized microwave assisted (20 min, 25 W, 75 °C) in mixture of EDC HCl (2 eq., 6.3 mg) and ethyl(hydroxyimino)cynoacetate (oxyma pure, 2 eq., 4.7 mg) in 10.2 mL DMF ($c = 1.6 \text{ mmol/L}$). LC-MS analysis confirmed complete cyclization. The solvent was evaporated and the crude peptide dissolved in MeOH in order to purify it by small sized flash chromatography (silica gel, 1:1 \rightarrow 1:3 \rightarrow 0:1 *n*-hexane/EtOAc (v/v%)). The purity was determined by RP-HPLC. 5.8 mg of peptide **29a** were isolated (27% overall yield based on the initial resin loading) HR-ESI-MS data for this compound can be found in Table S1.

Supplementary Tables

Table S1. Verification of substance sum formulas via high resolution mass spectrometry. Compounds where no high resolution masses could be obtained are labeled with an asterisk (*) and their structures were verified via their substance-specific fragmentation patterns.

Cmpd.	Compound class/name	Calculated mass [M+H]	Detected mass [M+H]	Δ ppm
4a	Fatty acid	383.1748	383.1756	2.1
4b	Fatty acid	397.1904	397.1890	3.5
4c	Fatty acid	411.2061	411.2060	0.2
4d	Fatty acid	467.2687	467.2696	1.9
4e	Fatty acid	481.2834	481.2826	3.5
4f	Fatty acid	495.3000	495.2977	4.6
4g	Fatty acid	509.3156	509.3139	3.3
4h	Fatty acid	420.3221	420.3208	3.1
4i	Fatty acid	537.3469	537.3451	3.3
4j	Fatty acid	448.3534	448.3543	2.0
4k	Fatty acid	565.3782	565.3765	3.0
4l	Fatty acid	593.4095	593.4*	-
6a	Phenethylamide	572.2377	572.2357	3.5
6b	Phenethylamide	486.2533	486.2522	2.3
6c	Phenethylamide	500.2695	500.2698	0.6
6d	Phenethylamide	514.2852	514.2850	0.4
6f	Phenethylamide	542.3165	542.3167	0.4
6g	Phenethylamide	556.3321	556.3316	0.9
6h	Phenethylamide	570.3478	570.3459	3.3
6i	Phenethylamide	584.3629	584.3600	5.0
6j	Phenethylamide	598.3791	598.3818	4.5
6l	Phenethylamide	626.4104	626.4101	0.5
8a	Phenethylamide	568.3316	568.3*	-
8b	Phenethylamide	596.3629	569.4*	-
8c	Phenethylamide	624.3942	624.3930	1.9
10a	Phurea lipid	481.2955	481.3*	-
10b	Phurea lipid	495.3112	495.3105	1.4
10c	Phurea lipid	509.3268	509.3261	1.4
10d	Phurea lipid	523.3425	523.3*	-
11b	Phenethylamine	416.2115	416.2*	-
12b	Phenylacetic acid	431.1748	431.1740	1.9
13b	Phenethylamide	534.2533	534.2524	1.7
14b	Xenortide	704.3958	704.3934	3.4
15b	Nematophin	528.2645	528.2628	3.2
16b	Nematophin	514.2483	514.2*	-
17b	Phenylalanin	460.2013	460.2021	1.7
18b	Phenylpyruvic acid	459.1697	459.1701	0.9
19b	Benzaldehyde	401.1642	401.1646	1.0
20b	Benzoic acid	417.1591	417.1587	1.0
21b	Ethyl benzoate	445.1899	445.1898	0.2
22b	Acylated phenylalanin	586.3058	586.3054	0.7
23b	Acylated phenylalanin	600.3214	600.3212	0.3
24b	Acylated phenylalanin	602.3007	602.3*	-
25b	Acylated phenylalanin	616.3163	616.3*	-
26b	Szentiamide	1116.5335	1116.5290	4.0
27b	Cinnamic acid	443.1748	443.1769	4.7
28b	Cinnamoylated Phe	590.2432	590.2431	0.2
29b	GameXPeptide	880.5113	880.5117	0.5
32	Fatty acid methyl ester	425.2218	425.2233	3.5
33	Ac-Phe methyl ester	600.3214	600.3224	1.7
34	Methyl benzoate	431.1741	431.1763	4.9

Supplementary figures

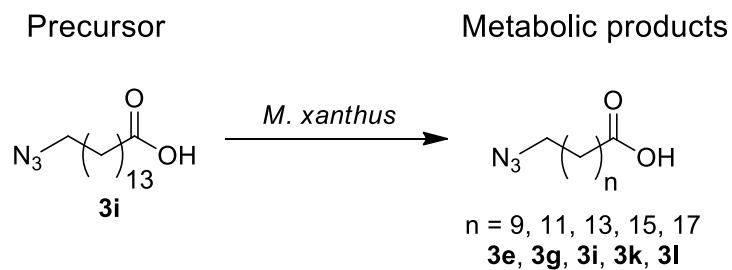


Figure S1. Degraded and elongated AFAs obtained after feeding of C₁₅-AFA (**3i**) to *M. xanthus*.

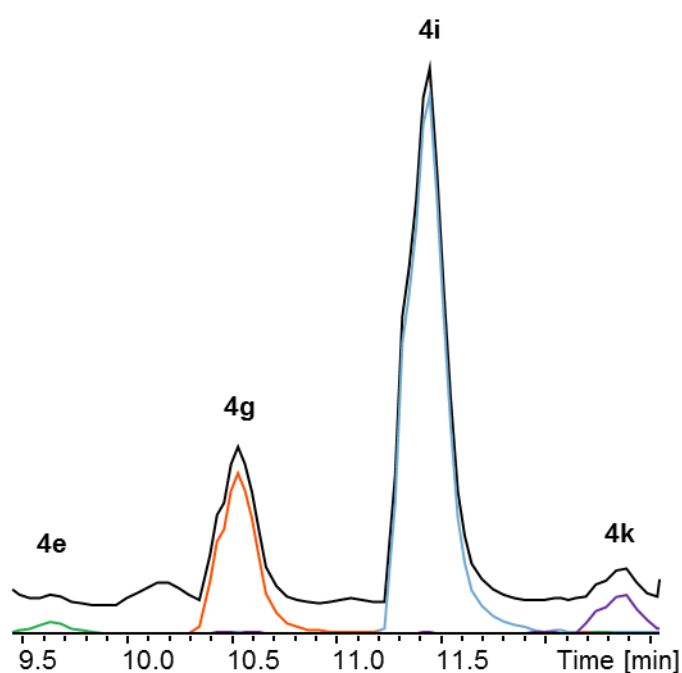


Figure S2. Base peak chromatogram (black) and superimposed extracted ion chromatograms of azide-enriched extract from *M. xanthus* 3 d after feeding of **3i** (seen as **4i**, light blue). Degraded fatty acid adducts **4e** (green) and **4g** (orange) can be seen as well as elongation product **4k** (purple). Elongation product **4l** was only seen in small amounts and is not depicted here.

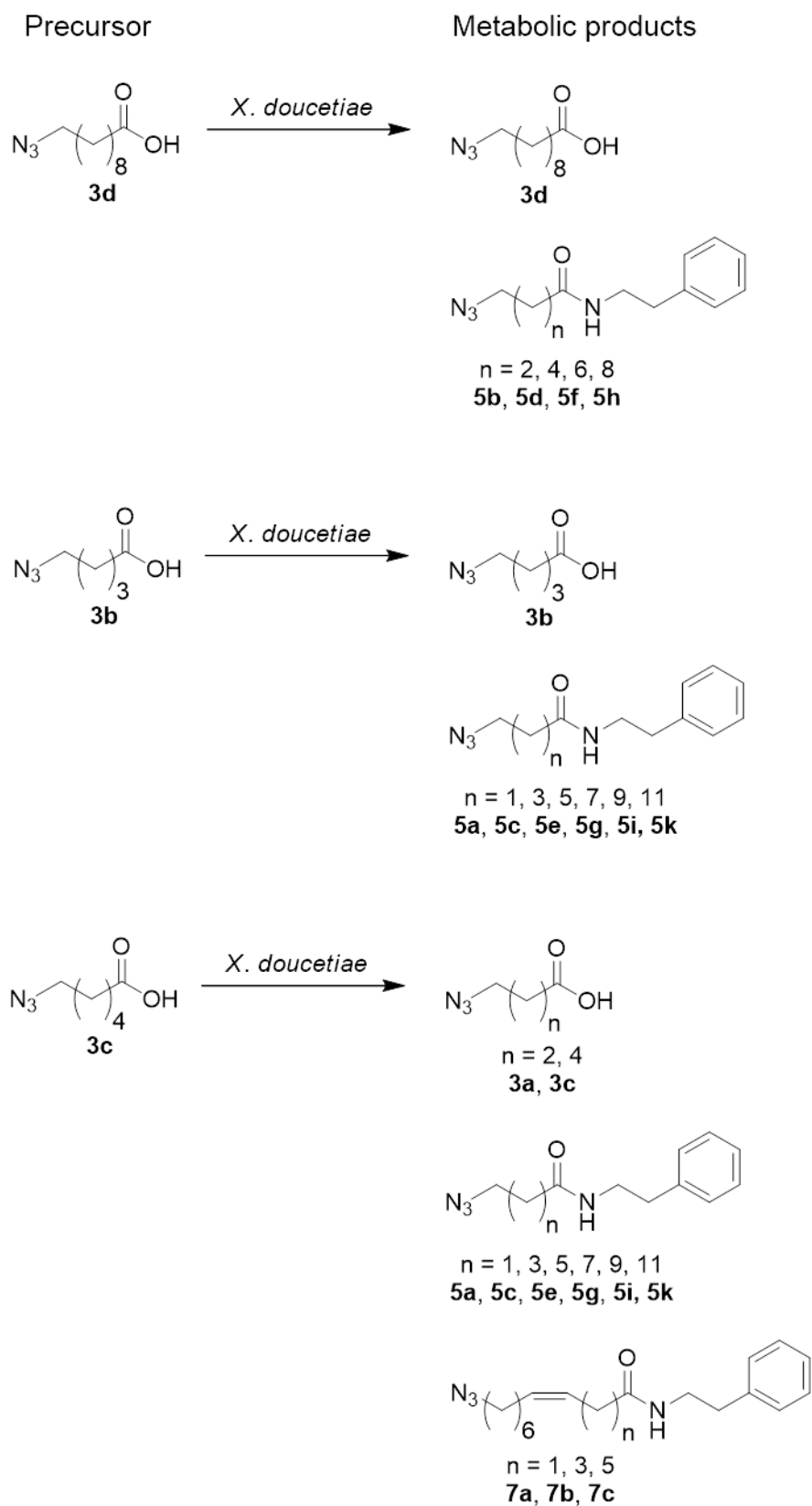


Figure S3. AFAs and phenethylamides obtained after feeding of C₅- (**3b**) C₆- (**3c**) or C₁₀-AFA (**3d**) to *X. doucetiae*.

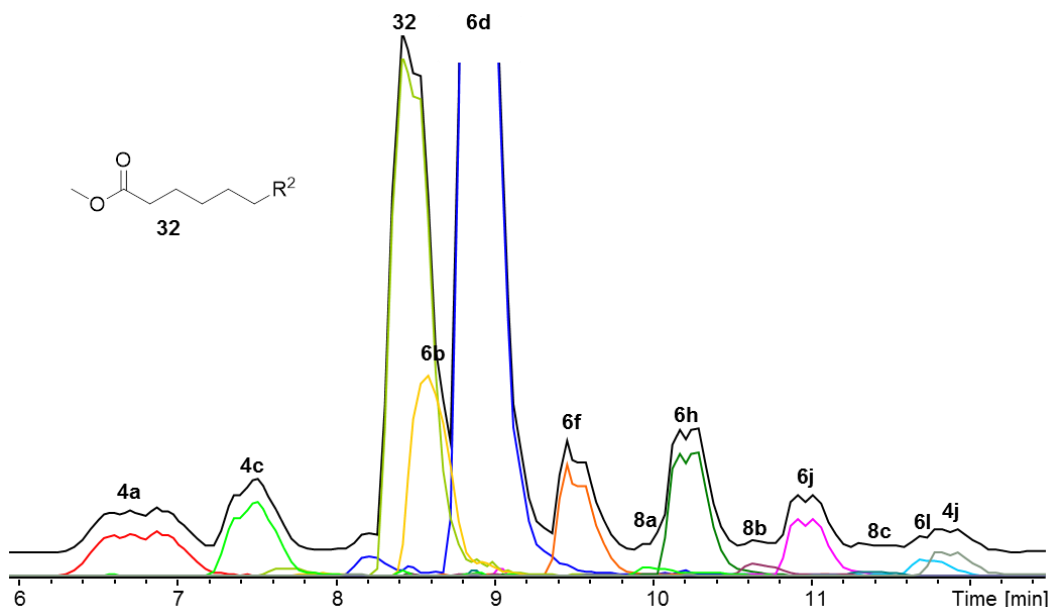


Figure S4. Base peak chromatogram (black) and superimposed extracted ion chromatograms of azide-enriched extract from *X. doucetiae* 3 d after feeding of **3c** (seen as **4c**, light green). Apart from several phenylethylamides, the AFA that was fed, its elongation product **4j** and its degradation product **4a** could be detected. Due to the administration of **3c** as a methanolic solution, some AFA was detected as its methyl ester (**32**), as could easily be confirmed by a neutral fragmentation loss of MeOH (not shown).

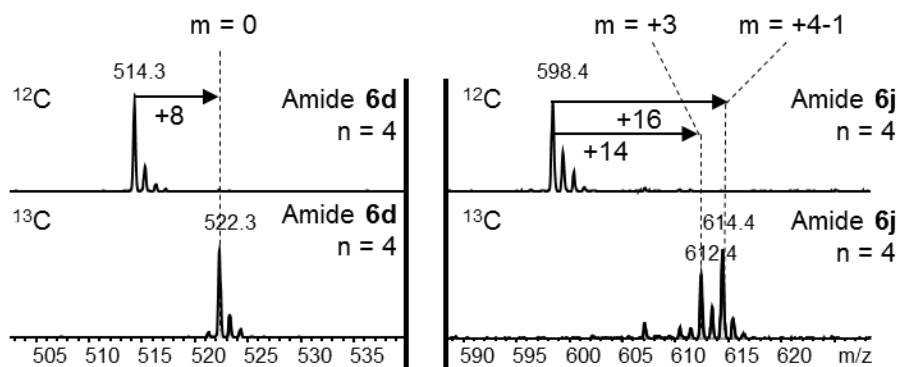


Figure S5. Isotope labeling experiment showing the differing incorporation of ^{13}C -atoms into PEAs after feeding of C_6 -AFA (**3c**, $n = 4$). In the case of direct incorporation of the added fatty acid ($m = 0$), a mass shift of 8 is observed for **6d**. Depending on whether elongation of the AFA started directly or after a single degradation step, a long acyl chain PEA like **6j** is found with either 14 or 16 ^{13}C -atoms according to $m = 3$ or 4 respectively, leading to the shifts shown for these two exemplary compounds.

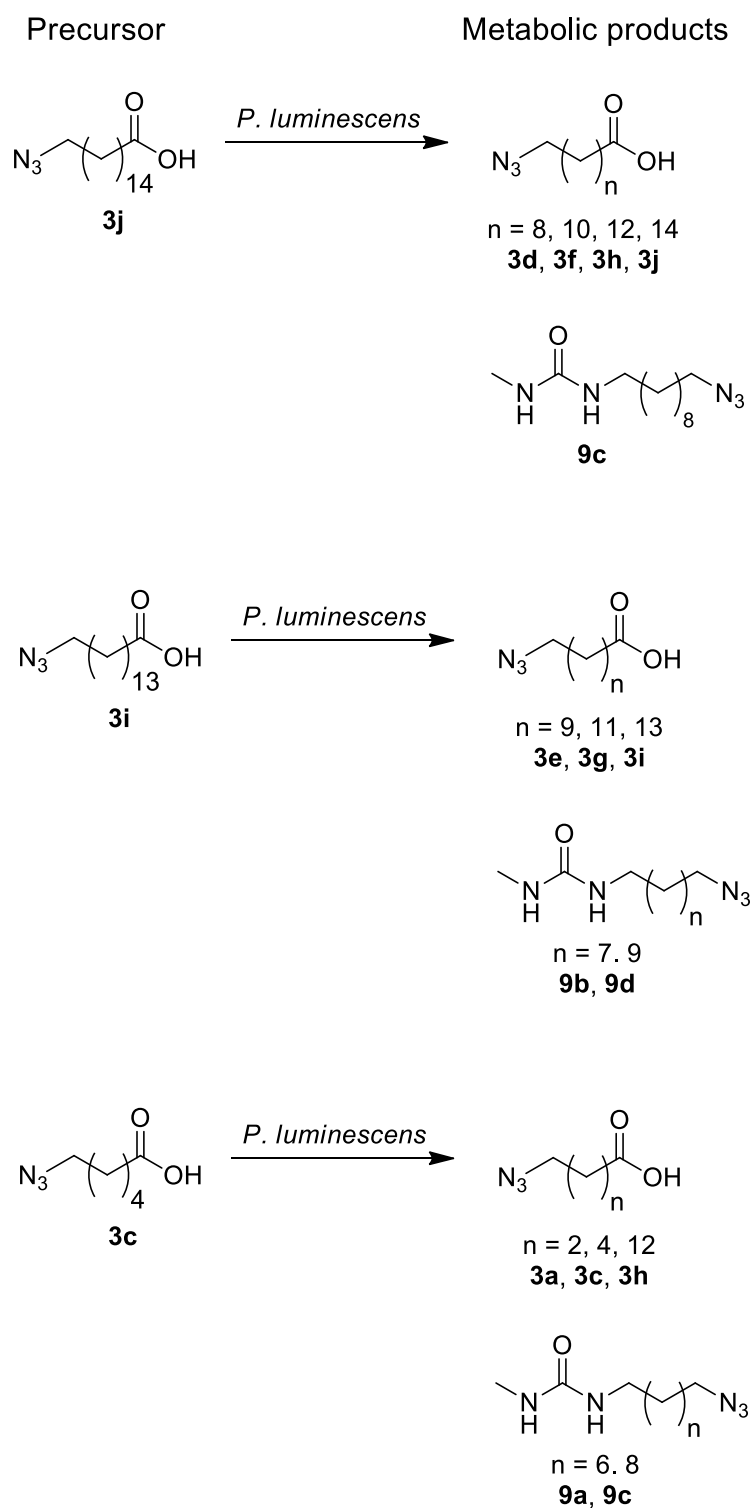


Figure S6. AFAs and phurea lipids obtained after feeding of C₆- (**3c**), C₁₅- (**3i**) or C₁₆-AFA (**3j**) to *P. luminescens*.

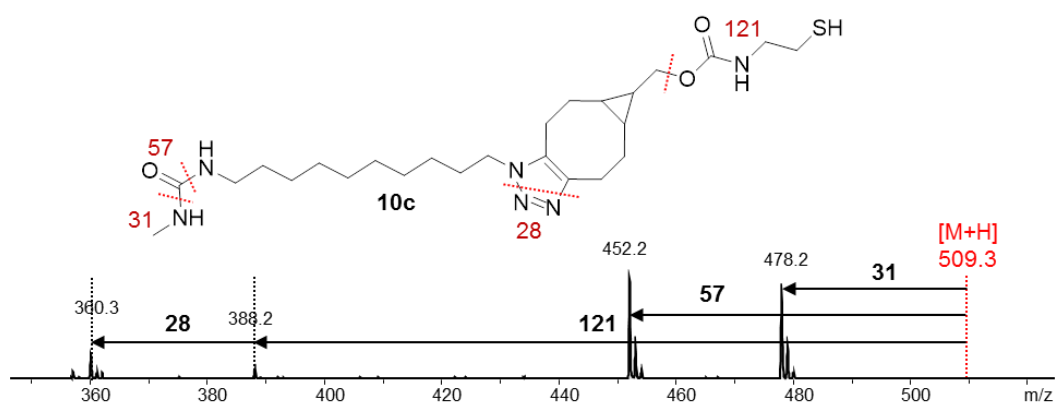


Figure S7. Exemplary MS² spectrum of derivatized urea lipid **10c**. Apart from the common neutral mass losses at the BCN residue (121 and 149), strong signals indicate the loss of methylamine (-31) and methylisocyanate (-57).

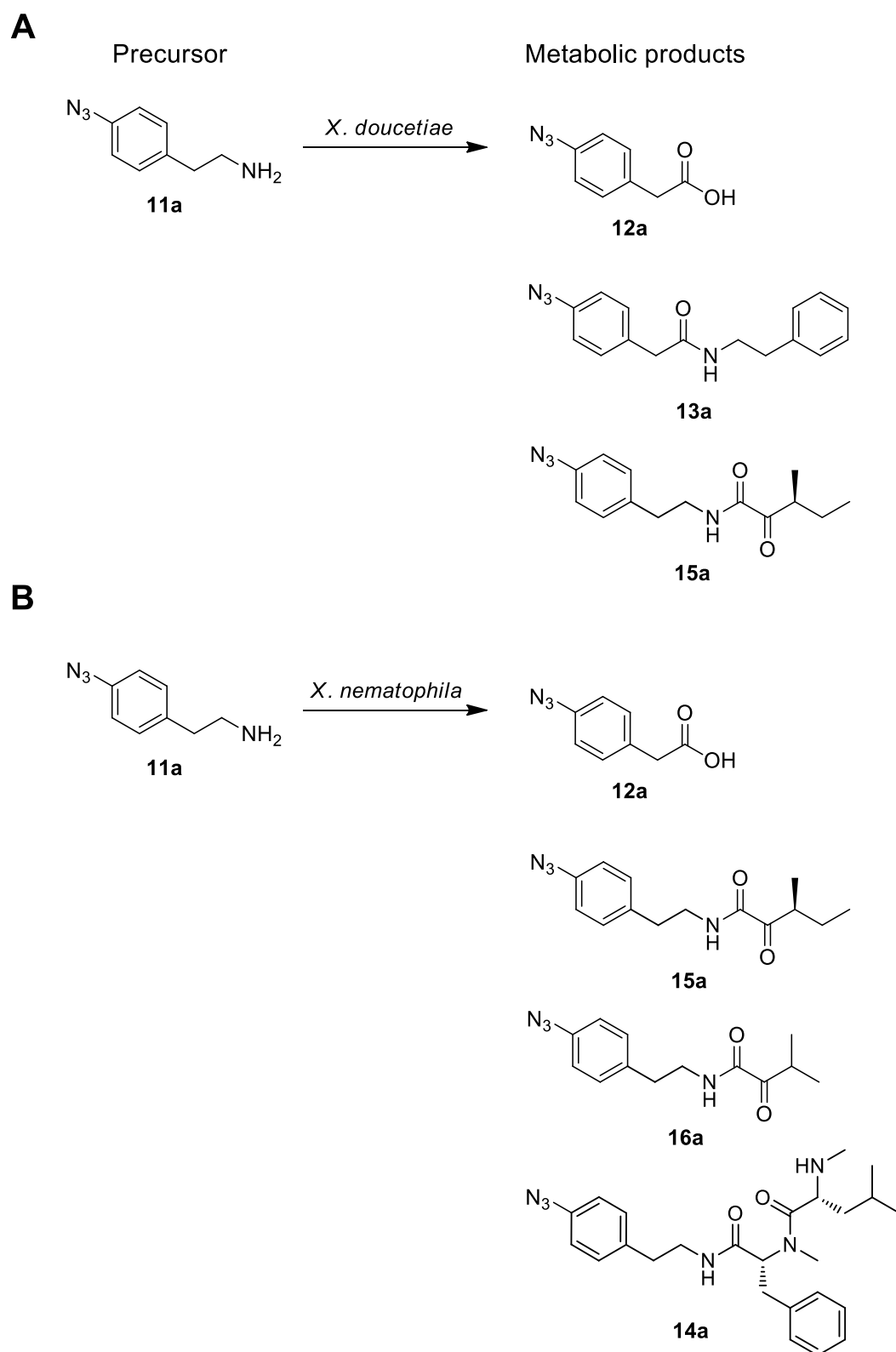


Figure S8. Results of feeding azido-phenethylamine (**11a**) to *Xenorhabdus doucetiae* (A) or *Xenorhabdus nematophila* (B). While some basic metabolism is shared, each strain produces special peptides, such as phenethylamide **13a** or xonortide (**14a**).

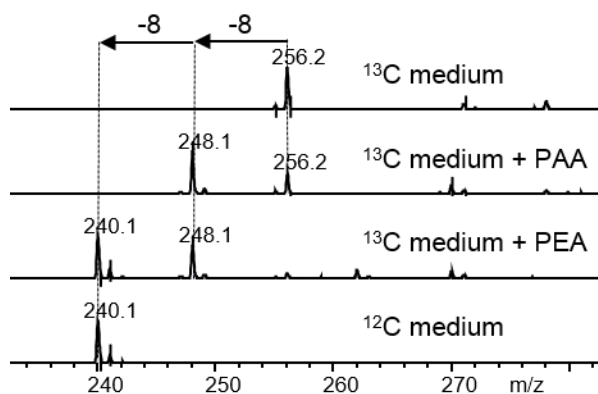


Figure S9. Incorporation of ^{13}C atoms from fed precursors phenylacetic acid (PAA) and phenethylamine (PEA) into *N*-phenethylamide, proving the conversion of PEA into PAA but not vice versa in *X. doucetiae*.

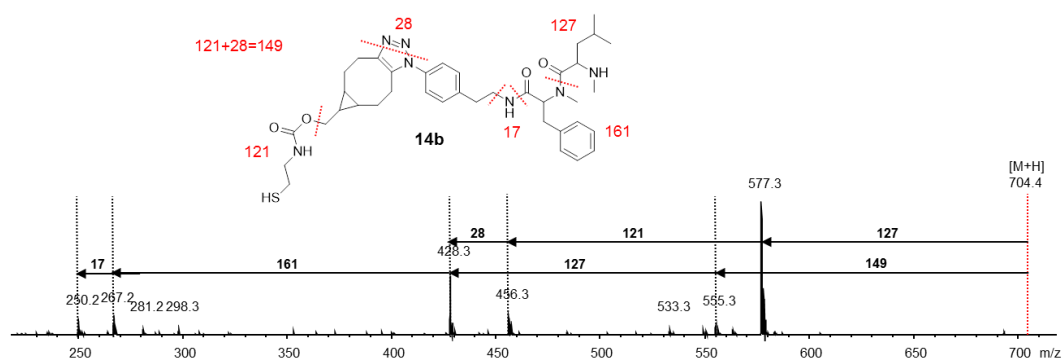


Figure S10. MS^2 spectrum of derivatized Xenortide A (**14b**, m/z 704 $[\text{M}+\text{H}]^+$), as detected via the CARR enrichment method. The fragmentation pattern clearly shows the losses of methylated leucine (127), phenylalanine (161) and ammonia, starting either from the mother ion ($m/z = 704$ $[\text{M}+\text{H}]^+$) or immediately after the formation of the de-carbamated and de-nitrogenated form ($m/z = 555$ $[\text{M}+\text{H}]^+$).

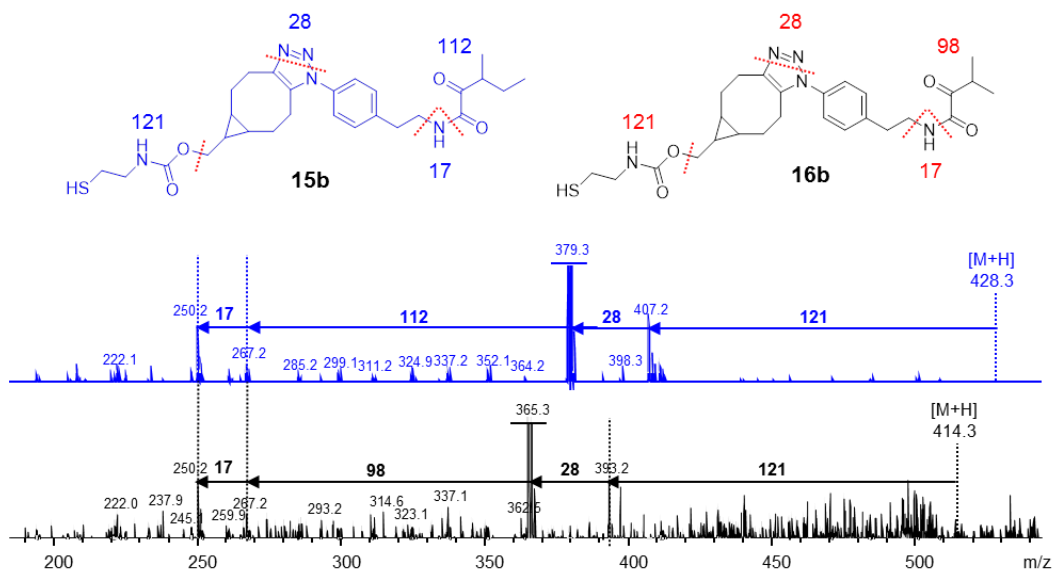


Figure S11. MS² spectrum of derivatized Nematophin (**15b**, $m/z = 428$ [M+H]⁺) and its valine-derivative (**16b**, $m/z = 414$ [M+H]⁺) as detected via the CARR enrichment method. Neutral losses of the two different moieties (98/112) can be seen as well as ensuing ammonia loss (-17). As is often observed after reaction with CARR, most of these molecule-specific fragmentations occur after the common loss of the carbamate and nitrogen function.

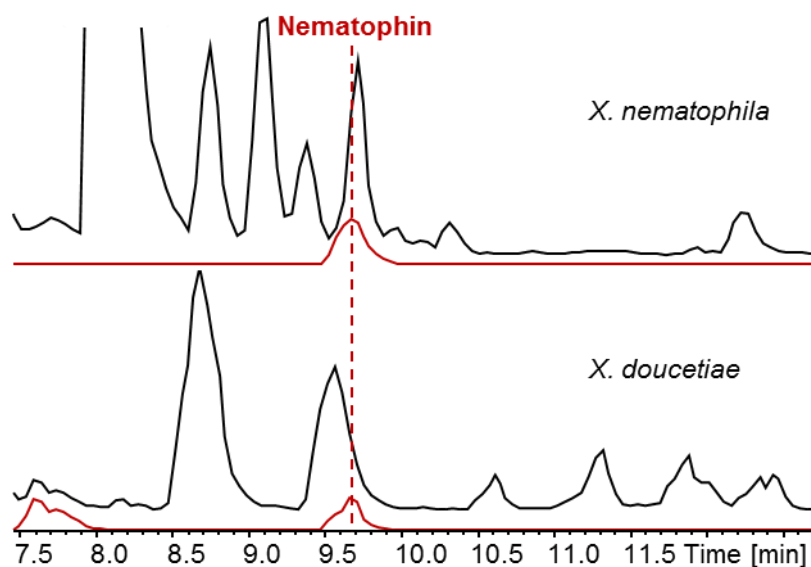


Figure S12. Raw XAD extracts from *X. nematophila* (top) and *X. doucetiae* (bottom) with the superimposed extracted ion chromatogram of protonated nematophin ($m/z = 273$ [M+H]⁺), showing the presence of this compound in both strains.

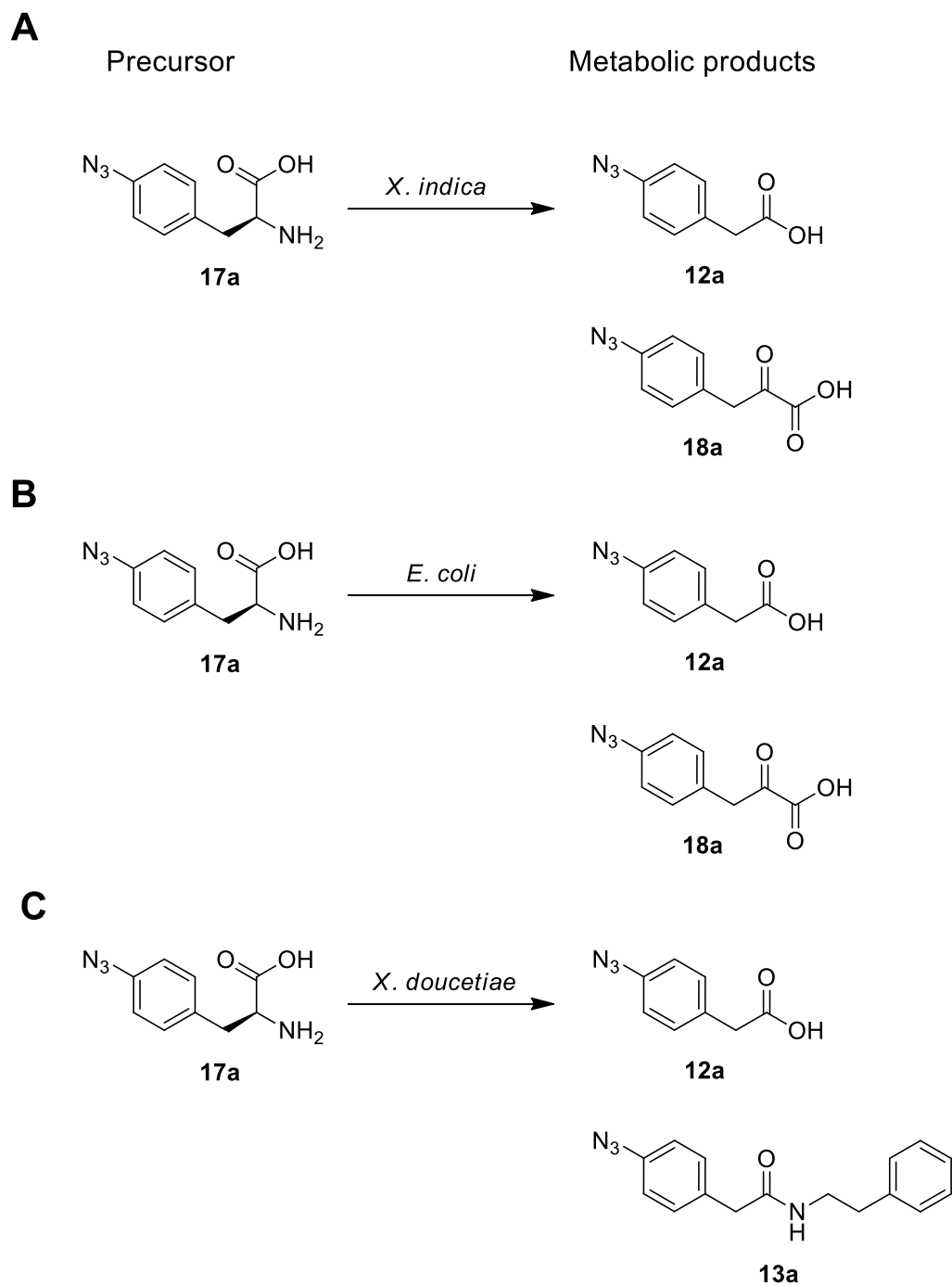


Figure S13. Results of feeding azido-phenylalanin (**17a**) to *Xenorhabdus indica* (A) *Escherichia coli* (B) or *Xenorhabdus doucetiae* (C). As expected all strains share the formation of azido-phenylacetic acid (**12a**), which is only processed further in *X. doucetiae*.

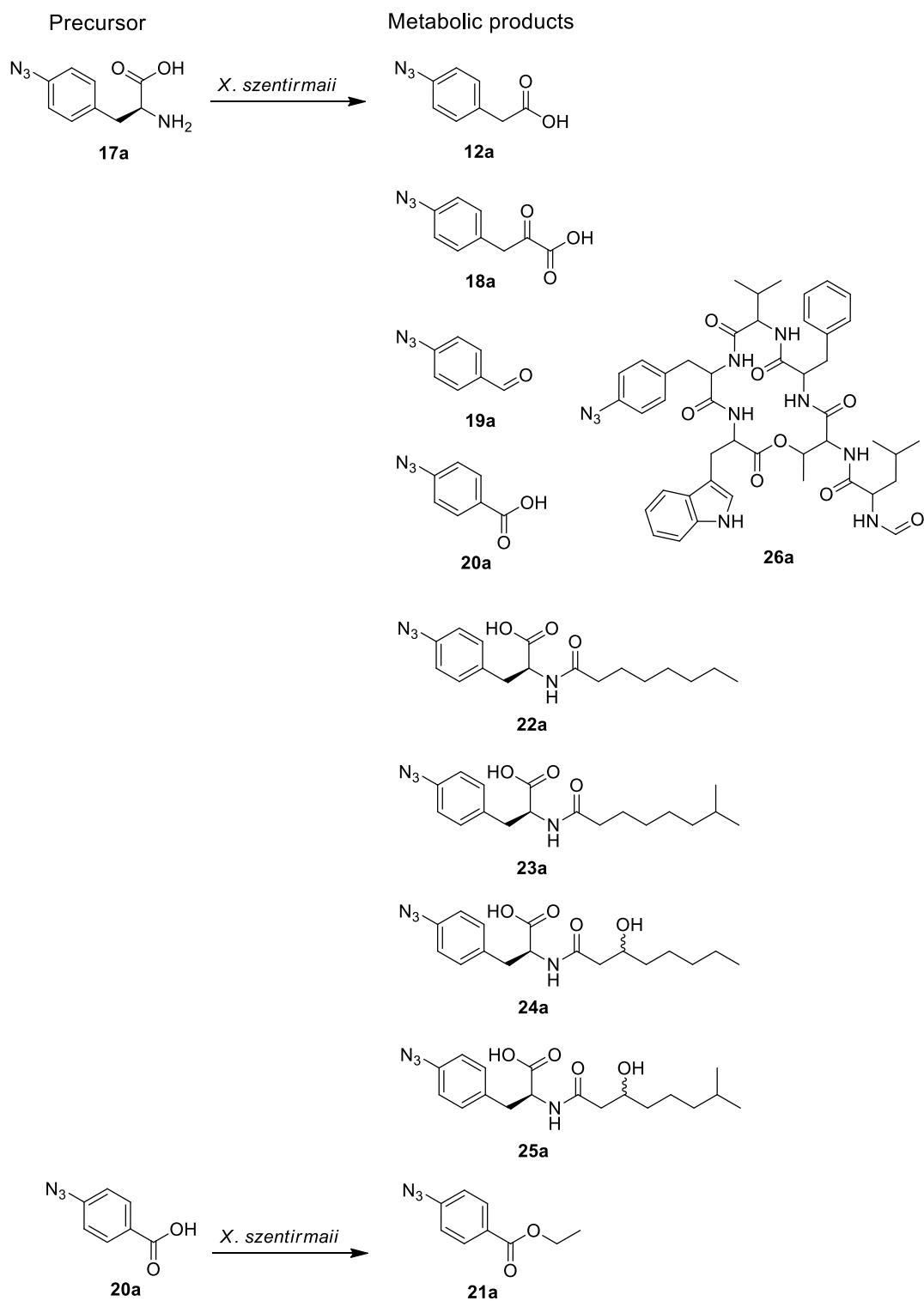


Figure S14. Results of feeding azido-phenylalanin (**17a**) to *Xenorhabdus szentirmai*, showing a broad diversity of metabolites. At the bottom are shown the results of feeding azido-benzoic acid (**20a**), resulting in its esterification.

After azide enrichment

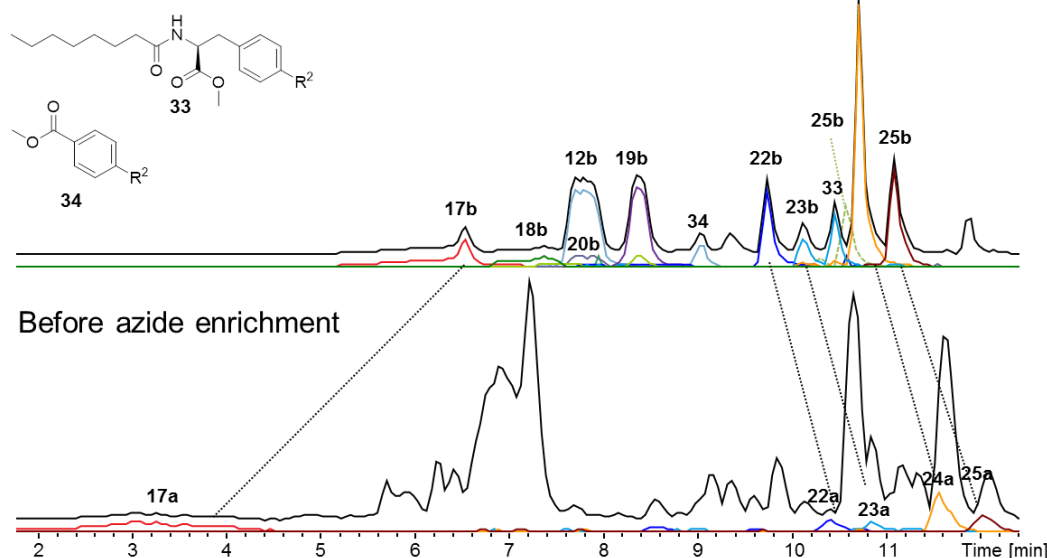


Figure S15. Top: Base peak chromatogram (black) and superimposed extracted ion chromatograms of azide-enriched extract from *X. szentirmaii* 3 d after feeding of **17a** (seen as **17b**). With increasing retention time phenylpyruvic acid (**18b**), phenylacetic acid (**12b**) and benzaldehyde (**19b**) follow. Acylation products of **16a** are seen at a later retention time (**22b**, **23b**, **24b**, **25b**). Products **33** and **34** were later identified as methyl esters of **20b** and **21b**. Fragmentation analysis and ¹³C-cultivation experiments then showed that the methylation resulted from the presence of MeOH during the enrichment procedure. Szentiamide (**26b**) is shown as a superposition from the synthesized product after enrichment. The actual peak from the biological extract is too small to be seen in this representation. Bottom: Base peak chromatogram (black) of the same raw extract before enrichment. It can clearly be seen that not all compounds that the enrichment procedure revealed can be seen before derivatization. This is partly due to their poor ionizability (**19a**) or decreased tendency to accept protons (**12a** and **18a**).

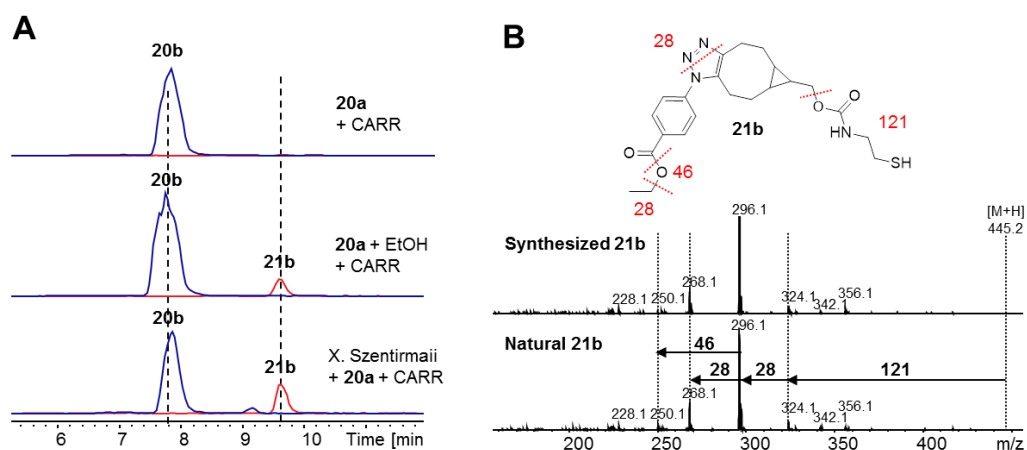


Figure S16. A) Extracted ion chromatograms of **20b** (blue) and its ethyl ester **21b** (red) compared to the azide extraction experiment conducted with the pure compound (**20a**, top), the partially esterified compound (**21a**, middle) and the bacterial extract (bottom). B) MS² Fragmentation pattern of derivatized ethyl benzoate (**21b**, $m/z = 445$ [M+H]⁺), showing typical ethylene (-28) and ethanol (-46) loss starting from the common fragment of 296.

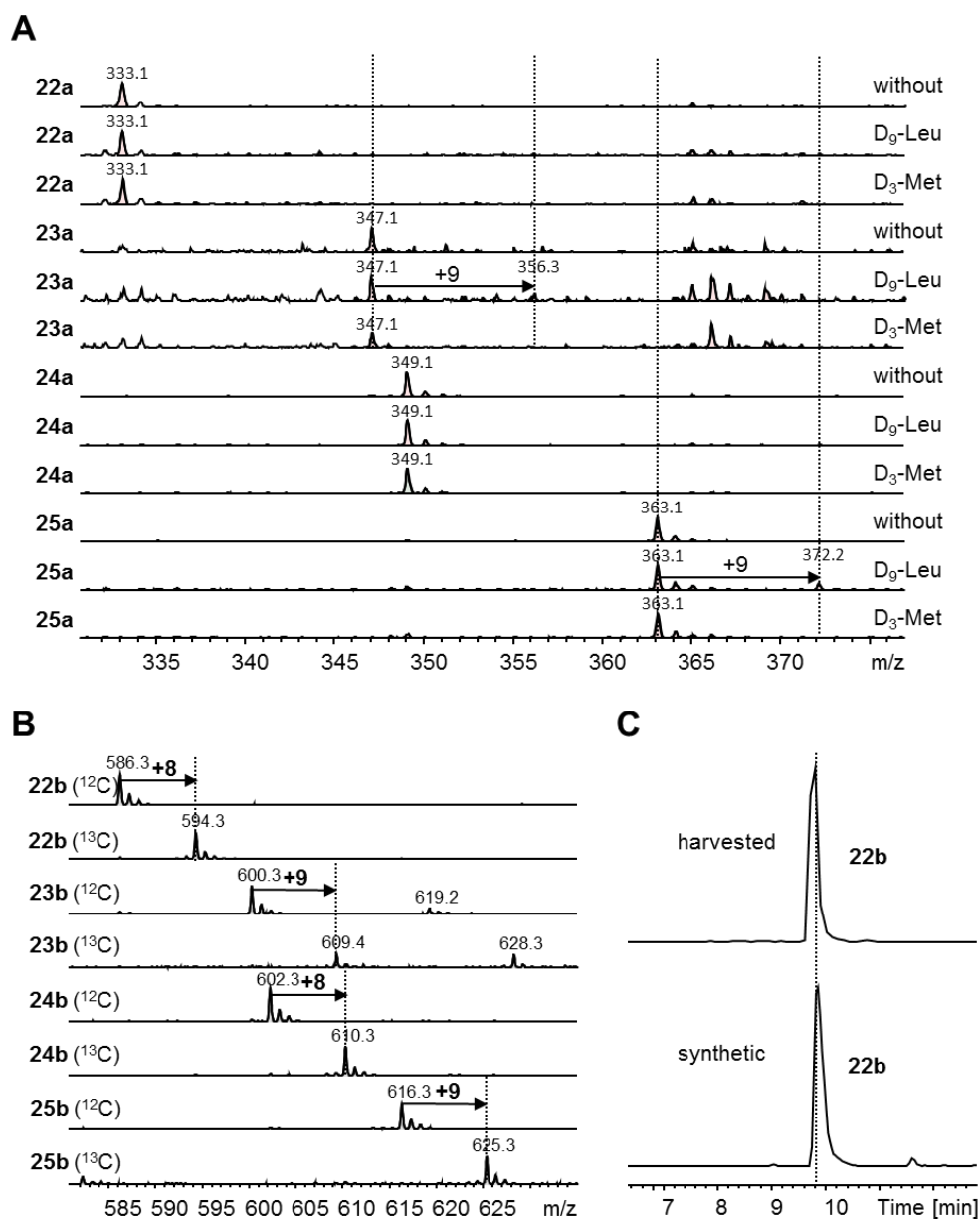


Figure S17. Analysis of acylated phenylalanine derivatives via feeding experiments and synthesis. A) Feeding experiments with deuterated amino acids in *X. szentirmaii* showing the incorporation of D₉-leucin into substances **22a** and **25a**. B) Feeding experiment in ¹³C media, showing the incorporation of 8 or 9 carbons into the acyl chain of **22b/24b** and **23b/25b** respectively. C) Comparison of retention times of synthetic **22b** (bottom, base peak chromatogram) to the compound enriched from the culture extract of *X. szentirmaii* (top, extracted ion chromatogram),

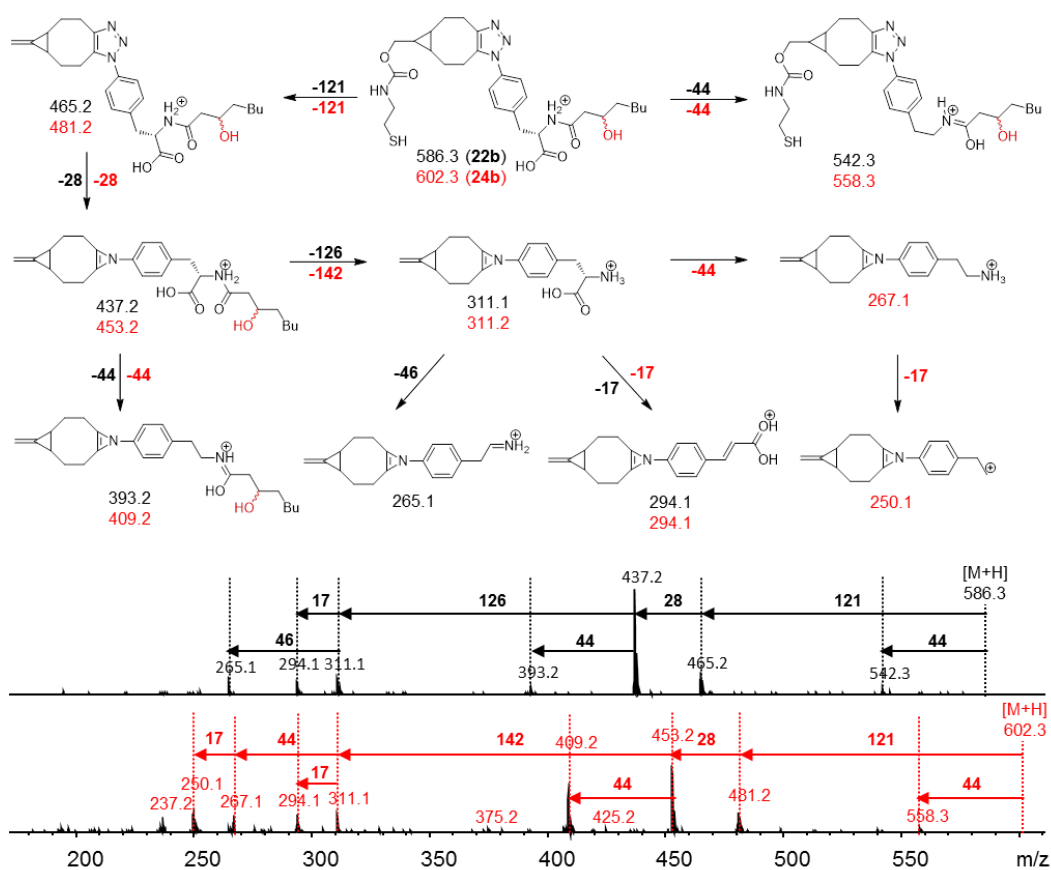


Figure S18. Fragmentation pathways of acylated azido-phenylalanin derivatives **22b** and **24b**. It can clearly be seen that the fragments coincide once the acyl chain is lost, proving that the difference in both compounds originates from an hydroxyl function in the acyl chain. Since β -hydroxy fatty acids are a common intermediate of β -oxidation and are incorporated into several other known non-ribosomal peptides⁵ the hydroxyl function is proposed to be located at this position. Although the increased retention time suggests a more lipophilic modification, intramolecular hydrogen bonding and resulting sterical changes can explain the observed effect.

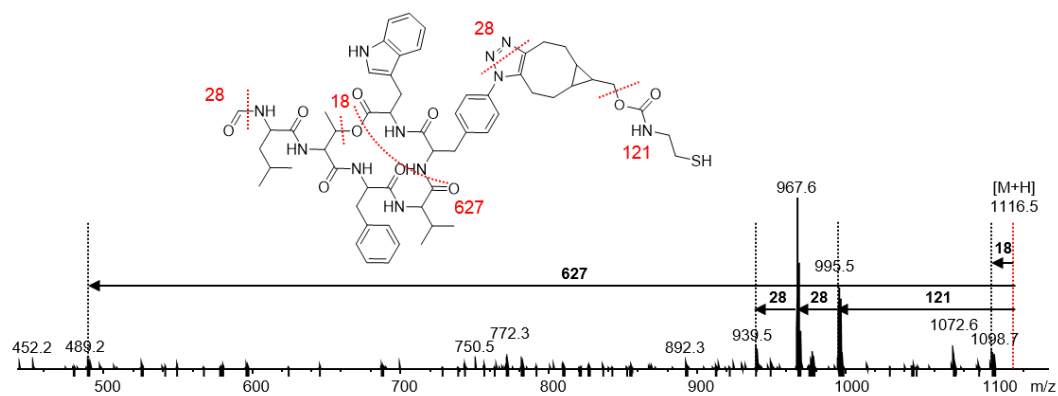
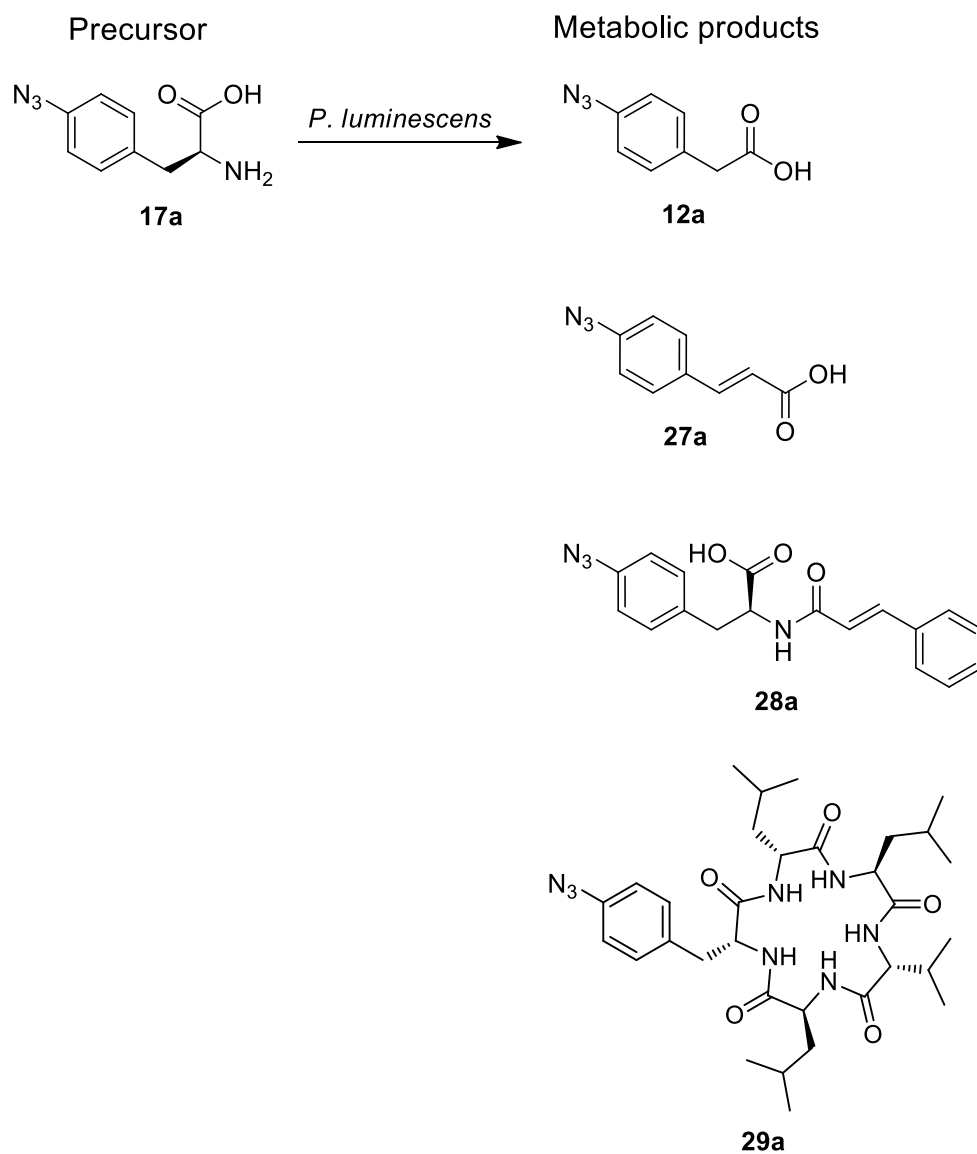


Figure S19. Fragmentation pattern of derivatized szentiamide (**26b**, $m/z = 1116.5 [M+H]^+$). The origin of the lost water molecule (-18) is a suggestion, other origins, such as the carbonyl functions are also possible. The loss of the tetrapeptidic moiety (-627) is furthermore highly indicative of szentiamide, since it is a dominant neutral loss in the natural compound, as is carbonyl loss (-28) from the formylated *N*-terminus.



Scheme S20. Results of feeding azido-phenylalanin (**17a**) to *Photorhabdus luminescens*, showing the unique production of cinnamic acid (**27a**), cinnamoylated phenylalanine (**28a**) and GameXPepptide A (**29a**), apart from common catabolic product **12a**.

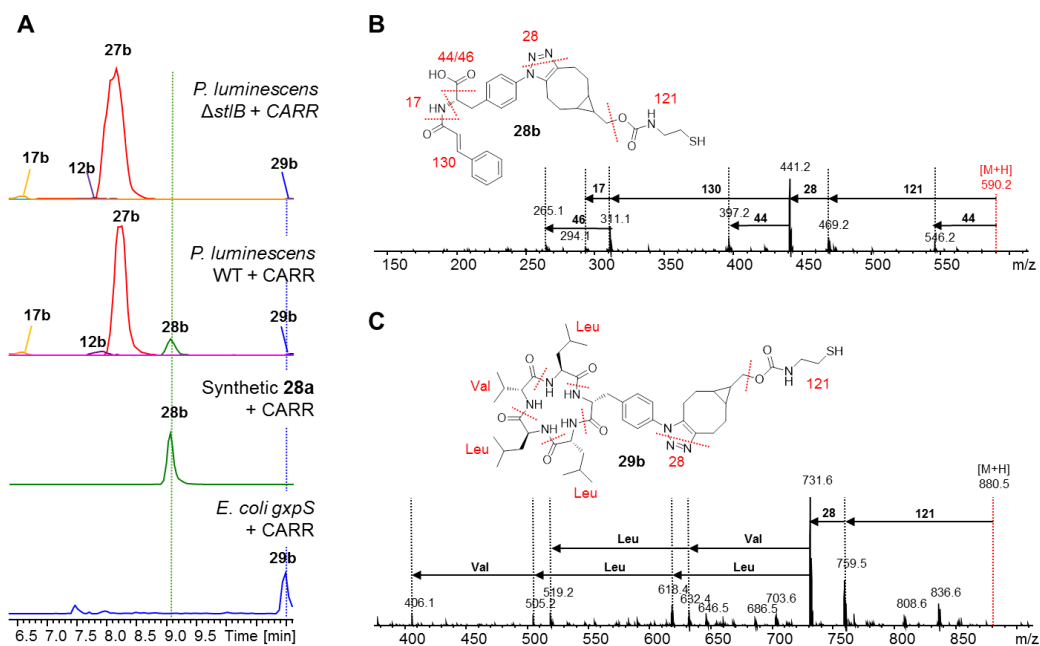
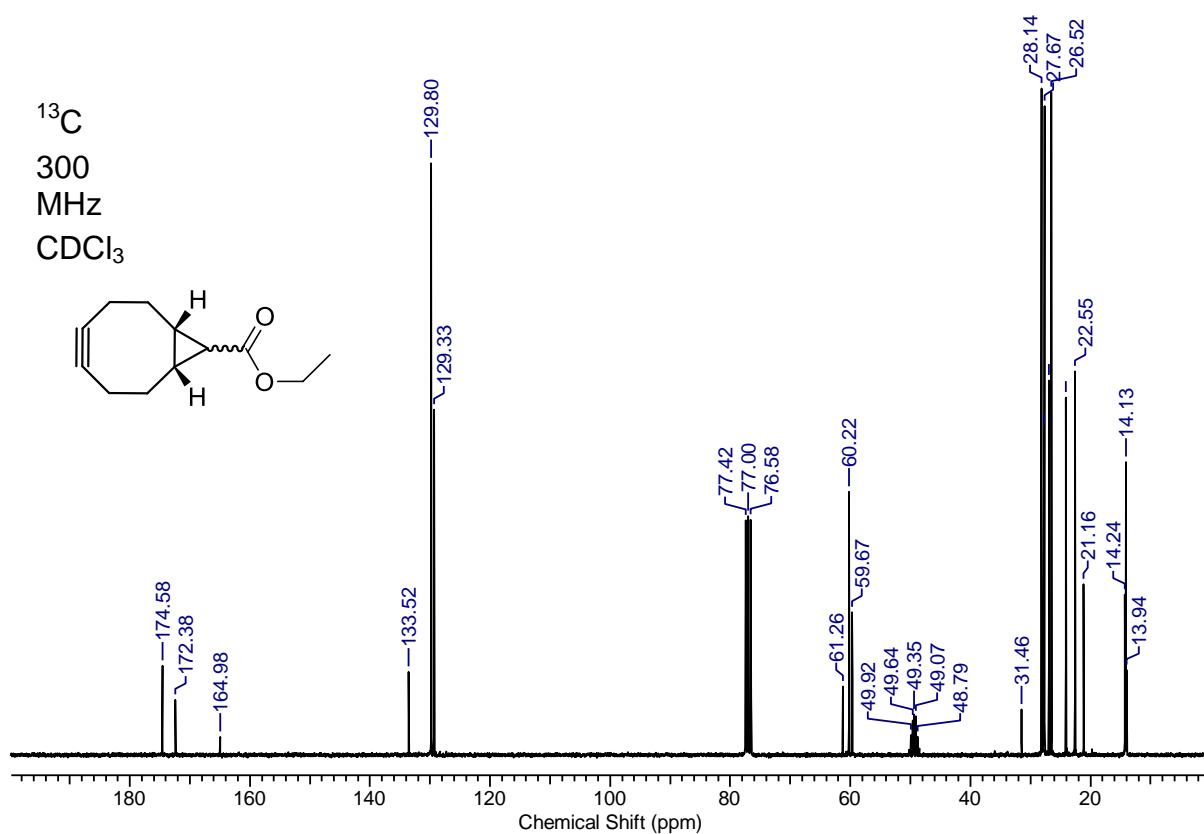
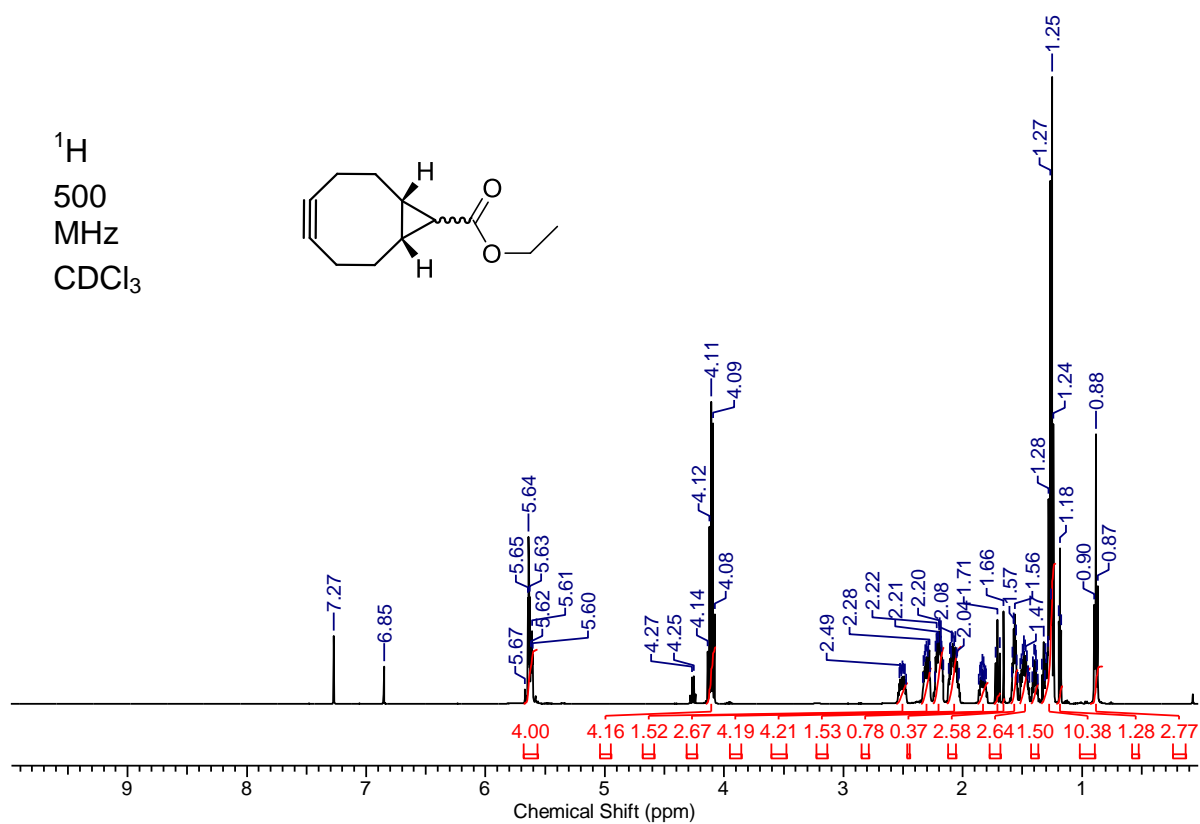


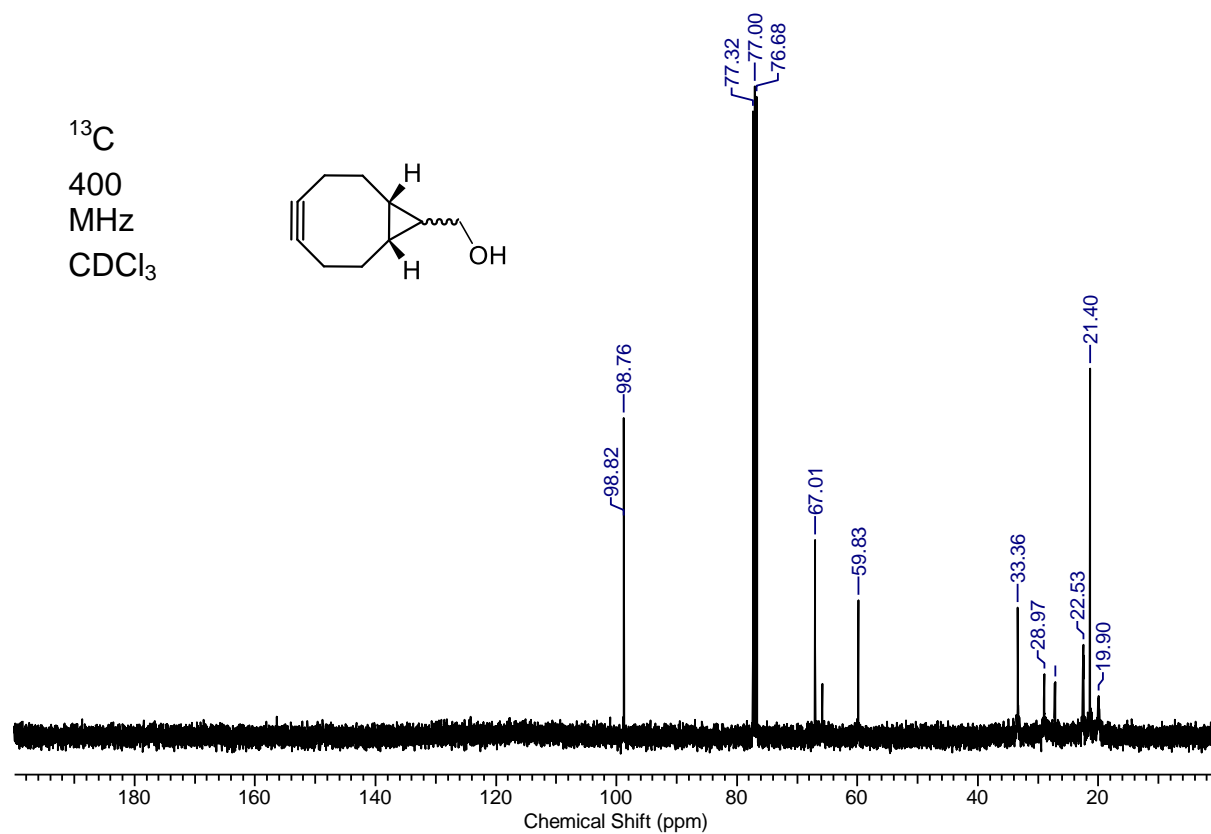
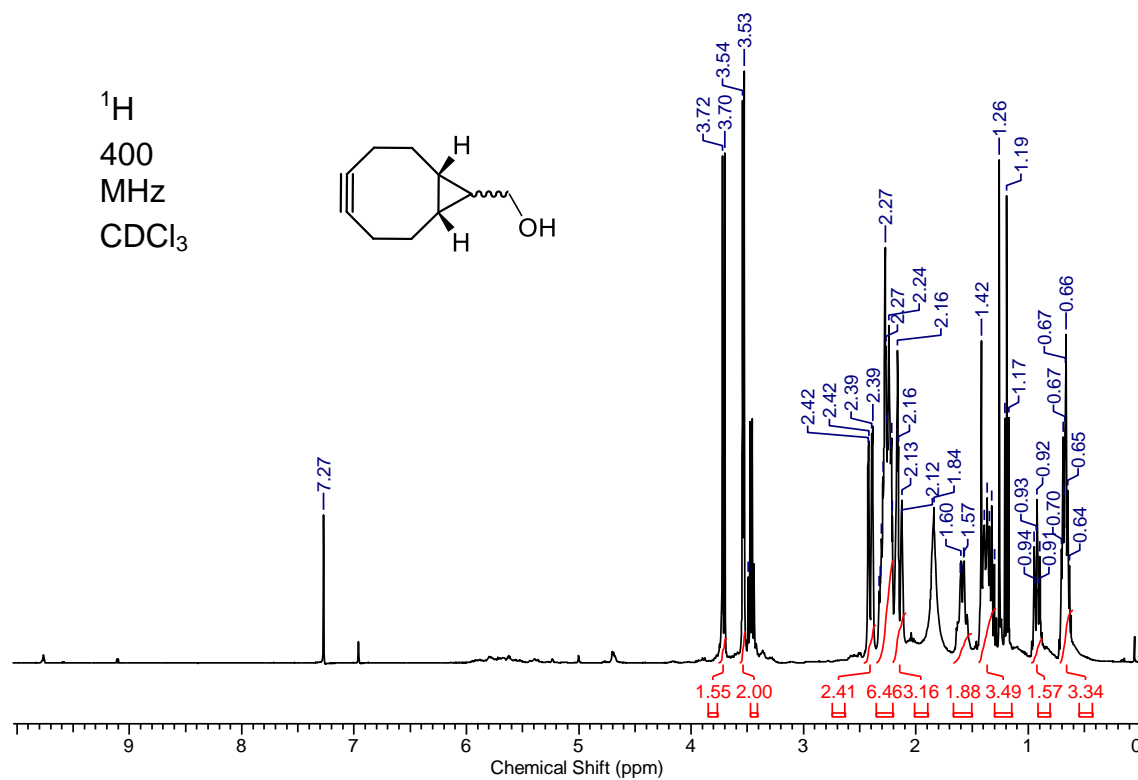
Figure S21. A) Extracted ion chromatograms of extracts of *P. luminescens* wildtype (WT) in comparison with the according StlB (cinnamic acid CoA-ligase) deficient mutant ($\Delta stlB$) after feeding of **17a** and enrichment with the CARR procedure. Most importantly cinnamic acid derivative **27b** can be seen in each case, whereas compound **28b** is only seen in the wildtype, indicating that cinnamoyl-CoA production is essential for the acylation of **17a** as expected. Compound **28a** (green) was later synthesized and derivatized and the retention time of the resulting **28b** was shown to be equivalent to the natural compound. The EIC of compound **29b** (blue) as seen in the *gxpS* overexpressing *E. coli* strain is shown at the bottom. B) Fragmentation pattern of derivatized cinnamoylated azido-phenylalanine (**28b**, $m/z = 590.2$ $[M+H]^+$), showing a very similar fragmentation to compounds **22b-25b**, as explained in Scheme S11. C) Fragmentation pattern of derivatized azido-GameXPeptide (**29b**, $m/z = 880.6$ $[M+H]^+$), showing that amino acid loss happens almost exactly as in the natural product, right after the common losses of carbamate (-121) and nitrogen (-28) have occurred, making 731.6 the precursor for main peptide fragmentation. The observed neutral losses are in accordance with previous studies].⁶

NMR Spectra

(1*R*,8*S*,9 ξ ,*Z*)-Ethylbicyclo[6.1.0]non-4-ene-9-carboxylate (30)

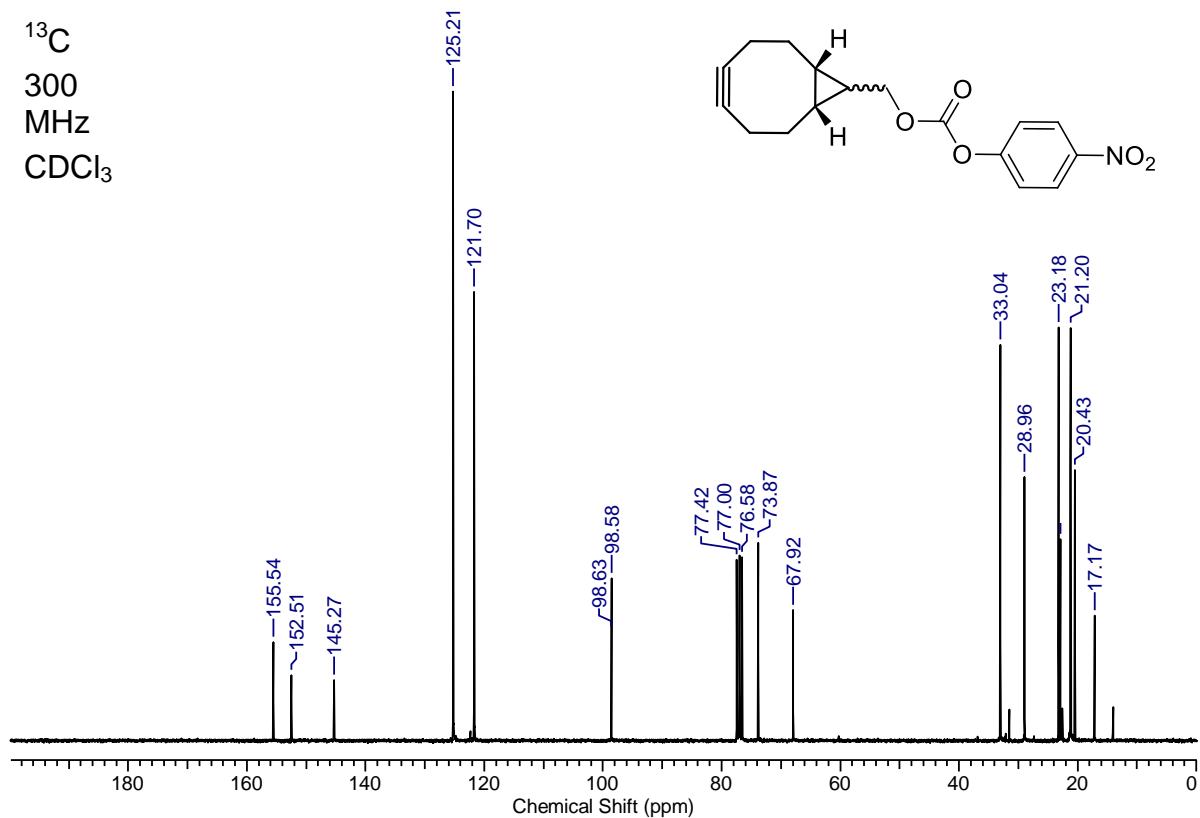
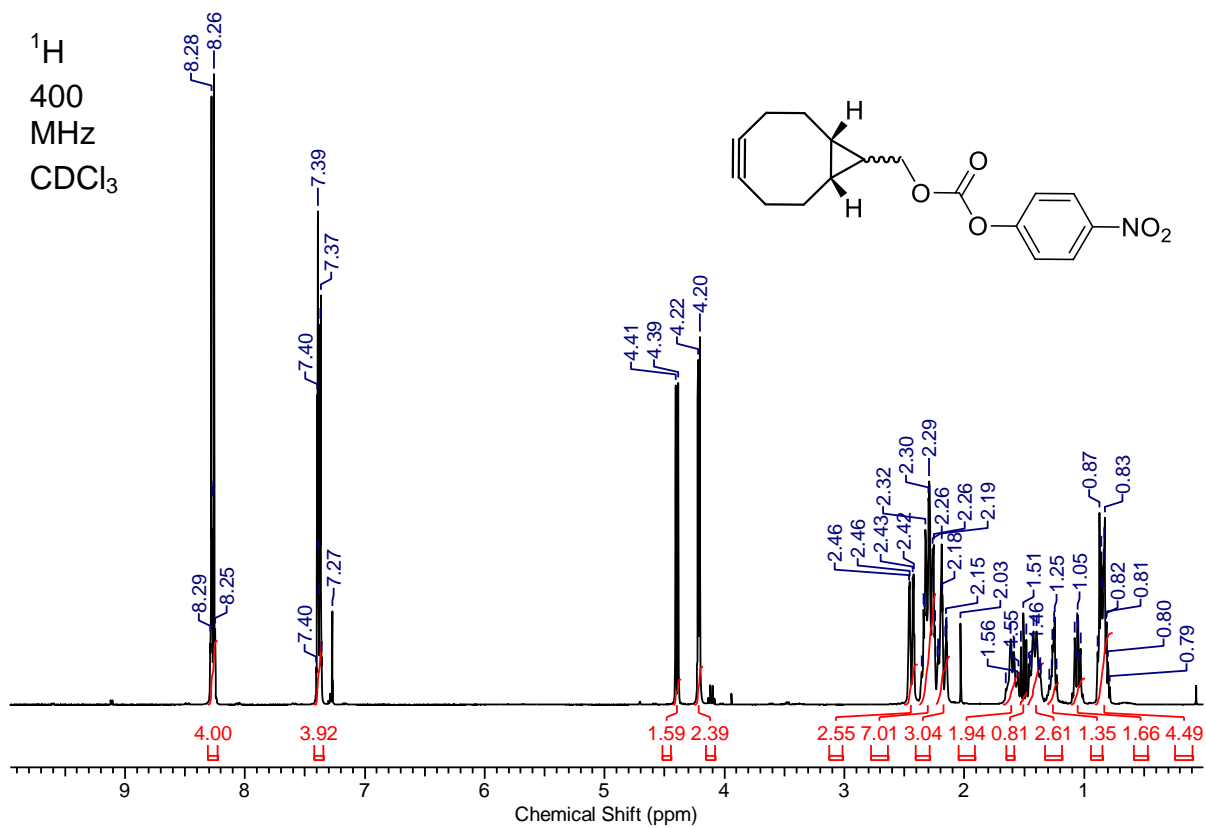


(1*R*,8*S*,9*ξ*)-Bicyclo[6.1.0]non-4-yn-9-ylmethanol (BCN, 2)

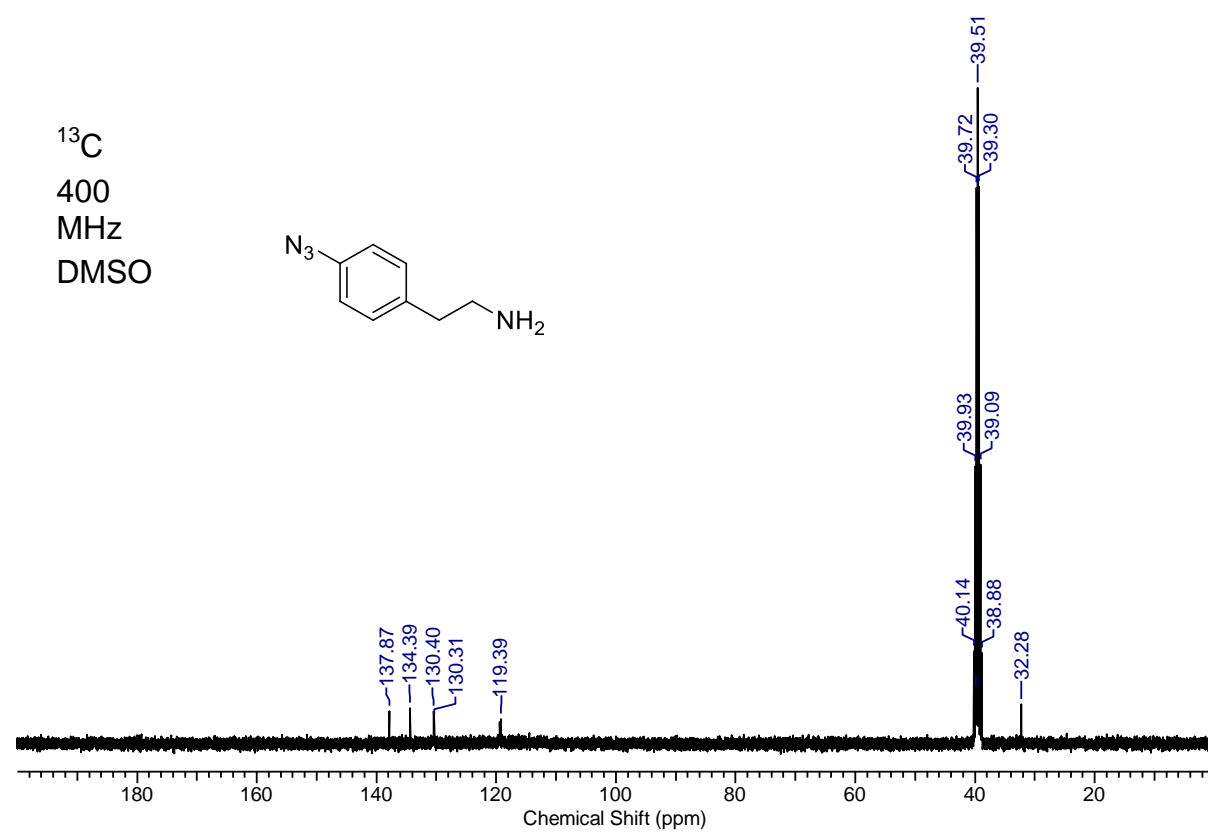
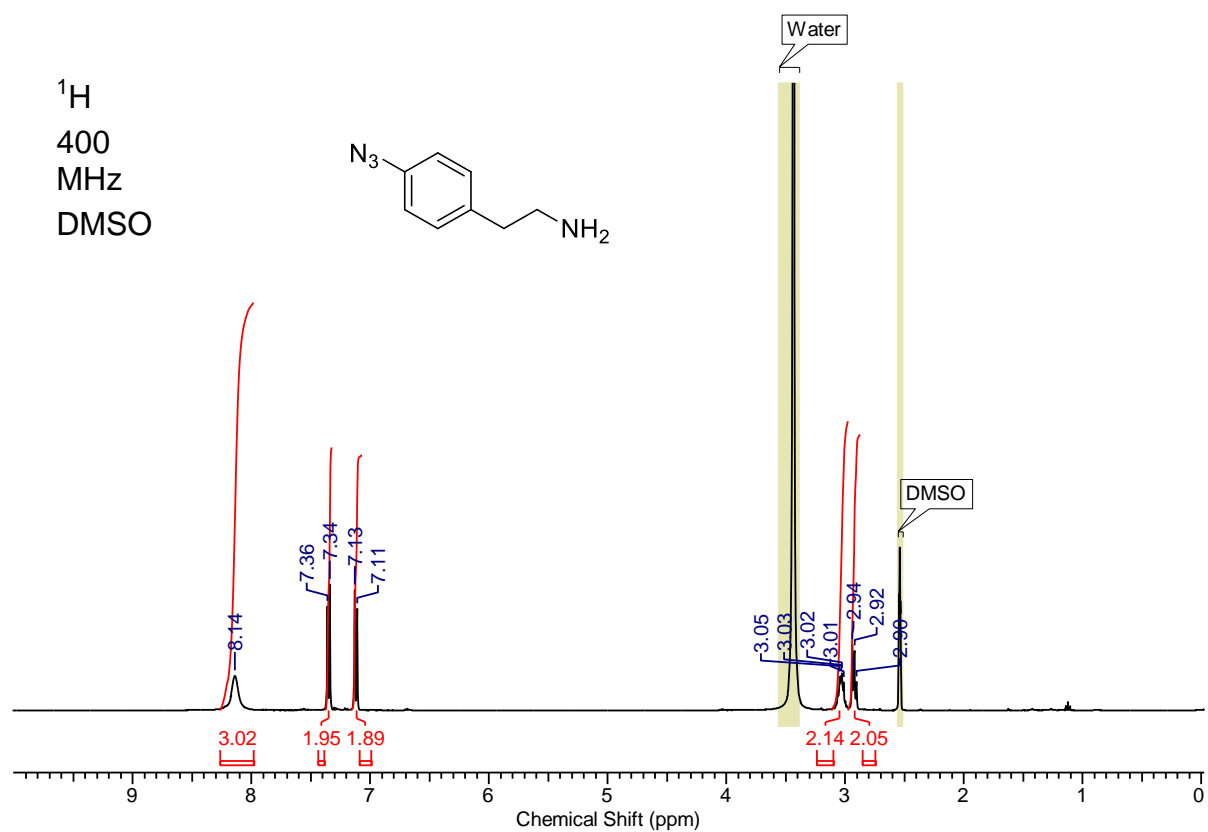


(1*R*,8*S*,9*ξ*)-Bicyclo[6.1.0]non-4-yn-9-ylmethyl (4-nitrophenyl) carbonate

(31)



p-Azidophenethylamine (11a)



References

- (1) Dommerholt, J.; Schmidt, S.; Temming, R.; Hendriks, L. J. A.; Rutjes, F. P. J. T.; van Hest, J. C. M.; Lefeber, D. J.; Friedl, P.; van Delft, F. L. *Angew. Chem. Int. Ed.* **2010**, *49*, 9422-9425.
- (2) Pérez, A. J.; Bode, H. B. *J. Lipid. Res.* **2014**, *55*, 1897-1901.
- (3) Hausler, N. E.; Devine, S. M.; McRobb, F. M.; Warfe, L.; Pouton, C. W.; Haynes, J. M.; Bottle, S. E.; White, P. J.; Scammells, P. J. *J. Med. Chem.* **2012**, *55*, 3521-3534.
- (4) Goddard-Borger, E. D.; Stick, R. V. *Org. Lett.*, **2007**, *9*, 3797-3800.
- (5) Fuchs, S. W.; Proschak, A.; Jaskolla, T. W.; Karas, M.; Bode, H. B. *Org. Biomol. Chem.* **2011**, *9*, 3130-3132.
- (6) Bode, H. B.; Reimer, D.; Fuchs, S. W.; Kirchner, F.; Dauth, C.; Kegler, C.; Lorenzen, W.; Brachmann, A. O.; Grün, P. *Chem. Eur. J.* **2012**, *18*, 2342-2348.

8 Curriculum vitae

Alexander José Pérez

Date of birth: 12th of August 1985

Place of birth: Nürnberg

Citizenship: German

Contact: Thomas-Mann-Straße 18

60439 Frankfurt am Main

Germany

+49-(0)69 15625446

alex@famps.de

Education and Studies

- 03/2012-09/2015 **Promotion** at the institute for molecular biosciences in the group of professor Dr. Helge B. Bode at the Goethe-university, Frankfurt, Germany. Thesis: *“Tracking of bacterial metabolism with azidated precursors and click-chemistry”*
- 12/2011 **Diploma in chemistry**
- 05/2011-12/2011 **Diploma thesis** with the major subject of the synthesis of deuterated and alkynylated lipids for biological applications at the Goethe-university, Frankfurt, Germany. Thesis: *“Synthesis of lipid derivatives for the investigation of the E- or C-signal in the fruiting body formation of Myxococcus xanthus”*
- 10/2004-12/2011 **Studies in chemistry** at the Goethe-university, Frankfurt, Germany.
- 08/1991-06/2004 **Abitur and school education** at the Kopernikusschule, Freigericht, Germany and the Gründauschule, Langenselbold, Germany.

9 List of Publications

A. J. Pérez, H. B. Bode. ω -Azido fatty acids as probes to detect fatty acid biosynthesis, degradation, and modification. *Journal of Lipid Research* **2014**, 55, 1987-1901.

A. J. Pérez, H. B. Bode. "Click Chemistry" for the Simple Determination of Fatty Acid Uptake and Degradation: Revising the Role of Fatty Acid Transporters. *ChemBioChem* **2015**, 16, 1588-1591.

10 Record of conferences

Bioorthogonal Chemistry - Meeting of the Biochemistry Division

16.07.-18.07.2014

Berlin, Germany

Contribution: poster & oral poster presentation with the title *“Investigations of fatty acid metabolism with copper-free click chemistry”*

VAAM Workshop – On The Biology Of Bacteria Producing Natural Products

04.09.-06.09.2015

Frankfurt am Main, Germany

Contribution: lecture with the title *“Fishing downstream of biochemical pathways – solid phase click chemistry for metabolic studies and natural product discovery”*

11 Versicherung

Ich erkläre hiermit, dass ich die vorgelegte Dissertation selbstständig angefertigt und mich anderer Hilfsmittel als der in ihr angegebenen nicht bedient habe, insbesondere, dass alle Entlehnungen aus anderen Schriften mit Angabe der betreffenden Schrift gekennzeichnet sind.

Frankfurt am Main, den

Alexander J. Pérez